PREPARATION OF COMBINED ANNEALING AND ENZYMATIC TREATMENT OF TAPIOCA AND RICE STARCHES AND THE UTILIZATION

PRAKAN LEERAPONGNUN

A THESIS SUBMITTED IN PARTIAL FULFILLMENT
OF THE REQUIREMENTS FOR
THE DEGREE OF MASTER OF SCIENCE (BIOTECHNOLOGY)
FACULTY OF GRADUATE STUDIES
MAHIDOL UNIVERSITY
2005

ISBN 974-04-6099-2

Thesis
Entitled

PREPARATION OF COMBINED ANNEALING AND ENZYMATIC TREATMENT OF TAPIOCA AND RICE STARCHES AND THE UTILIZATION

.....
Mr. Prakan leerapongnun
Candidate

.....
Assoc. Prof. Saiyavit Varavinit,
Dr.Ing (Chemical Engineering)
Major-Advisor

.....
Assoc. Prof. Manop Suphantharika,
Ph.D.(Biochemical Engineering)
Co-Advisor

.....
Assoc. Prof. Sujin Shobsngob
Ph.D.(Chemistry)
Co-Advisor

.....
Assoc. Prof. Rassmidara Hoonsawat,
Ph.D.
Dean
Faculty of Graduate Studies

.....
Assoc. Prof. Manop Suphantharika,
Ph.D.(Biochemical Engineering)
Chair
Master of Science Programme
in Biotechnology
Faculty of Science

Thesis
Entitled

PREPARATION OF COMBINED ANNEALING AND ENZYMATIC TREATMENT OF TAPIOCA AND RICE STARCHES AND THE UTILIZATION

was submitted to the Faculty of Graduate Studies, Mahidol University
For the degree of Master of Science (Biotechnology)
on
May 17, 2005

.....
Mr. Prakan leerapongnun
Candidate

.....
Assoc. Prof. Saiyavit Varavinit,
Dr. Ing (Chemical Engineering)
Chair

.....
Assoc. Prof. Manop Suphantharika,
Ph.D.(Biochemical Engineering)
Member

.....
Lect. Benjawan Thumthanaruk,
Ph.D.(Food Science and Technology)
Member

.....
Assoc. Prof. Sujin Shobsngob,
Ph.D.(Chemistry)
Member

.....
Assoc. Prof. Rassmidara Hoonsawat,
Ph.D.
Dean
Faculty of Graduate Studies
Mahidol University

.....
Prof. Amaret Bhumiratana,
Ph.D.
Dean
Faculty of Science
Mahidol University

ACKNOWLEDGEMENTS

I would like to express my sincere gratitude and appreciation to my advisor, Assoc. Prof. Dr. Saiyavit Varavinit for his helpful guidance, continuous comments, discussion, encouragement and support throughout this study. All his kindness and courtesy will be long remembered with respect.

My sincerely gratitude is also given to all members of the advisory committee, Assoc. Prof. Dr. Manop Suphantharika and Assoc. Prof. Sujin Shobsngob for their valuable suggestion, expert comments, generosity in contributing time and criticisms with kindness about the work of my thesis. Moreover, I am thankful for Dr. Benjawan Thumthanaruk for her helpful comments and suggestion on this study.

I am thankful to Cho Heng Rice Vermicelli Factory Co. Ltd., Nakornpathom, Thailand for supporting materials (starches, megazyme starch damage kit and enzyme termamyl) and instruments (particle size analyzer, differential scanning calorimeter) that used in these experiments. I am also very grateful to all members in Q. C. section of Cho Heng Rice Vermicelli Factory Co. Ltd., Nakornpathom, Thailand for providing tremendous support and help in the research study.

I am particularly grateful to all members of the room BT 210, BT 204 and also Mr. Pimon Jumnong for their helps, friendship and encouragement and also to my all fellows in the Department of Biotechnology, Faculty of Science for their helps and providing facilities during my study.

I would like to special express my gratitude and deepest appreciation to my parent and members in my family, for their love, sincere, intention encouragement understanding support throughout my life.

“This work was partially supported by Ministry of Education, Commission of Higher Education”, subproject “Graduate Study and research in Agricultural Biotechnology”.

Prakan Leerapongnun

PREPARATION OF COMBINED ANNEALING AND ENZYMATIC TREATMENT OF TAPIOCA AND RICE STARCHES AND THE UTILIZATION

PRAKAN LEERAPONGNUN 4536147 SCBT/M

M.Sc.(BIOTECHNOLOGY)

THESIS ADVISORS: SAIYAVIT VARAVINIT, Dr. Ing., MANOP SUPHANTHARIKA, Ph.D, SUJIN SHOBSNGOB, Ph.D., BENJAWAN THUMTHANARUK, Ph.D.

ABSTRACT

Annealing of 25% (w/w) the slurry of native tapioca and rice starches and subsequence treatment with thermostable alpha-amylase were prepared by heating tapioca and rice starches with stirring in a water bath at 60 ^{o}C for 90 min and 70 ^{o}C for 150 min, respectively. It was followed by the addition of 0.5% (v/w) thermostable alpha-amylase (Thermamyl, Novo, Denmark) at the maintained temperature with the reaction times of 15, 30 and 60 min. The reaction products were subjected to spray drier to obtain anneal - enzyme hydrolyzed tapioca (SANET) and rice (SANER) starches in the form of spherical agglomerate granules. SANET and SANER were compared the properties with those of the spray dried annealed tapioca (SANT-H) and rice (SANR-H) starches without the enzyme treatment, with those of tapioca (SANT-L) and rice (SANR-L) starches only annealing at lower temperature (55 ^{o}C and 65 ^{o}C, respectively), and the native spray dried tapioca (SNT) and rice starches (SNR). It was found from DSC that by annealing alone at higher temperature caused the increasing of To, Tp and Tc with significant reduction of gelatinization enthalpy (ΔH) for rice starch. However, the damaged starches were found from both starches after annealing. By the addition of thermostable alpha-amylase after the annealing provided the increasing of To, Tp and Tc with dramatic reduction of ΔH together with the increasing of damaged starch. However, annealing at lower temperature for both starches provided the increasing of To, Tp and Tc with no significant change of ΔH but slightly increased in damaged starch in comparison with the native starches. It was accounted for the occurring of partial gelatinization of starches during annealing at the temperature near to the onset temperature. The onset temperature was the temperature that starches gelatinized. However, for this case would be explained that the onset temperature was the mean of the onset temperatures of all starch molecules. It should be many molecules exhibited lower and higher than the recorded onset temperature from the DSC. Then many starch molecules with lower onset temperature would be gelatinized in the case of the annealing temperature was closed to the onset temperature. Enzyme treatment of the annealed starch could facilitate the gelatinization of starches by the decreasing of ΔH and the increasing of damaged starches. For annealing at lower temperature provided no significant change of ΔH while slightly change in the damaged starch. All types of starch were subjected to tablet compression and compared the tablet properties among the type of starch. It was found that SANET and SANER exhibited the best tablet properties, i.e., high tablet hardness. The improving of crushing strength was possibly responded from the presence of maltose or low molecular weight oligosaccharide that derived from the enzymatic hydrolyzed starch granules which influence the increasing of damaged starch in both SANET and SANER with respected to their spray dry native starches. It was very good chance for SANET and SANER to be very good direct compression tablet filler for the pharmaceutical industries.

KEY WORDS:TAPIOCA STARCH/ RICE STARCH/ ANNEALING/ THERMOSTABLE α-AMYLASE/ TABLET FILLER/ GELATINIZATION CHARACTERISTICS

p. 182 ISBN 974-04-6099-2

การเตรียมแป้งมันสำปะหลังและแป้งข้าวเจ้าจากการแอนนีลร่วมกับการใช้เอนไซม์และการใช้ประโยชน์ (PREPARATION OF COMBINED ANNEALING AND ENZYMATIC TREATMENT OF TAPIOCA AND RICE STARCHES AND THE UTILIZATION)

ปราการ ลีรพงศ์นันต์ 4536147 SCBT/M

วท.ม. (เทคโนโลยีชีวภาพ)

คณะกรรมการควบคุมวิทยานิพนธ์ : ไสยวิชญ์ วรวินิต, Dr. Ing., มานพ สุพรรณธริกา, Ph.D., สุจินต์ ชอบสงบ, Ph.D., เบญจวรรณ ธรรมธนารักษ์, Ph.D.

บทคัดย่อ

ผลิตภัณฑ์แป้งแอนนีล (Annealed) มันสำปะหลังและแป้งข้าวเจ้าย่อยด้วยเอนไซม์พ่นแห้งเตรียมได้จากการผสมน้ำแป้งมันสำปะหลังและแป้งข้าวเจ้าความเข้มข้น 25 เปอร์เซ็นต์ (กรัมแป้งต่อกรัมน้ำ) แล้วจึงให้ความร้อนขณะกวนด้วยอุณหภูมิ 60 องศาเซลเซียส 90 นาทีและ 70 องศาเซลเซียส 150 นาที ในอ่างควบคุมความร้อน ตามลำดับ หลังจากนั้นจึงเติม 0.5 เปอร์เซ็นต์ของเอนไซม์อะมิเลสที่ทนต่อความร้อนที่อุณหภูมิดังกล่าวแล้วทำปฏิกิริยาต่อไปด้วยเวลา 15, 30 และ 60 นาที จากนั้นจึงนำผลิตภัณฑ์ที่ได้นี้ผ่านการพ่นแห้งจะได้แป้งที่เกาะกลุ่มลักษณะทรงกลม ทั้งนี้ในการทดลองนี้ได้ทำการศึกษาควบคู่ไปกับแป้งแอนนีลมันสำปะหลังและข้าวเจ้าที่อุณหภูมิสูง (60 และ 70 องศาเซลเซียส ตามลำดับ) พ่นแห้งโดยปราศจากการเติมเอนไซม์และแป้งแอนนีลมันสำปะหลังและข้าวเจ้าที่อุณหภูมิสูง (55 และ 65 องศาเซลเซียส ตามลำดับ) พ่นแห้ง รวมถึงแป้งมันสำปะหลังและข้าวเจ้าพ่นแห้ง จากการประมวลผลการเปลี่ยนแปลงรูปแบบความร้อนจากเครื่อง DSC พบว่า การแอนนีลที่อุณหภูมิสูงมีผลต่อการเพิ่มอุณหภูมิที่เริ่มเกิดความสุก (T_o), อุณหภูมิที่เกิดความสุกสูงสุด (T_p) และอุณหภูมิจุดสิ้นสุดของการทำให้เกิดการสุก (T_c) โดยในกรณีของแป้งข้าวเจ้าพลังงานที่ใช้ในการเกิดเป็นเจลของแป้ง (ΔH) มีการลดลงอย่างมีนัยสำคัญ อย่างไรก็ตาม พบว่าจะเกิดเม็ดแป้งที่ถูกทำลายหรือแป้งสุก (Damaged starch) ในแป้งทั้ง 2 ชนิดหลังจากการแอนนีล การเติมเอนไซม์อัลฟ่าอะมิเลสที่ทนต่อความร้อนหลังจากการแอนนีลจะมีผลทำให้ค่าของ T_o, T_p และ T_c เพิ่มขึ้นเช่นเดียวกัน ในขณะเดียวกันก็ลดค่าของ ΔH ลงไปอย่างมาก รวมถึงมีการเพิ่มขึ้นในส่วนของการเกิดเม็ดแป้งที่ถูกทำลายอีกด้วย อย่างไรก็ตาม การแอนนีลที่อุณหภูมิต่ำของแป้งทั้ง 2 ชนิดจะเพิ่มค่า T_o, T_p และ T_c แต่ไม่พบการเปลี่ยนแปลงอย่างมีนัยสำคัญของ ΔH ขณะที่เกิดการเพิ่มของเม็ดแป้งที่ถูกทำลายเล็กน้อย เมื่อเทียบกับแป้งที่ไม่ผ่านการดัดแปร ซึ่งทั้งหมดนี้ก็เนื่องจากการเกิดการสุกบางส่วน (Partial gelatinization) ของแป้งในระหว่างการแอนนีลแป้งที่อุณหภูมิใกล้กับ T_o นั่นเอง ซึ่ง T_o นั้นเป็นอุณหภูมิที่เม็ดแป้งจะเริ่มเกิดการสุก เพราะฉะนั้นในกรณีนี้ สามารถอธิบายได้ว่า T_o ที่บันทึกได้เป็นค่าเฉลี่ยของ T_o ของโมเลกุลแป้งทั้งหมด ซึ่งแป้งที่นำมาใช้นั้นจะมีทั้งโมเลกุลแป้งที่อุณหภูมิเริ่มเกิดการสุก สูงและต่ำกว่าค่า T_o ที่บันทึกได้จากเครื่อง DSC หากว่าอุณหภูมิที่ใช้ในการแอนนีลใกล้กับ T_o เฉลี่ยของแป้งแล้ว โมเลกุลแป้งใดก็ตามที่มีค่าอุณหภูมิที่เริ่มเกิดการสุกต่ำก็จะเกิดการสุกก่อนนั่นเอง อนึ่ง การใส่เอนไซม์ไปในแป้งที่แอนนีลที่อุณหภูมิสูงจะช่วยให้ง่ายต่อการเกิดการสุก (Gelatinization) ของแป้งโดยการลด ΔH และเพิ่มปริมาณเม็ดแป้งที่ถูกทำลาย สำหรับในส่วนของการแอนนีลที่อุณหภูมิต่ำจะไม่ทำให้เกิดทั้งการเปลี่ยนแปลงของ ΔH ขณะที่เกิดการเปลี่ยนแปลงของเม็ดแป้งที่ถูกทำลายเล็กน้อย ตัวอย่างแป้งที่ผ่านการพ่นแห้งทุกชนิดจะนำไปทำการตอกเม็ดยาและเปรียบเทียบคุณสมบัติของเม็ดยา ซึ่งจากผลที่ได้พบว่าแป้งแอนนีลมันสำปะหลังและแป้งข้าวเจ้าย่อยด้วยเอนไซม์พ่นแห้งให้คุณลักษณะของเม็ดยาที่ดีเยี่ยม เช่น ได้ค่าความแข็งของเม็ดยาที่สูง ทั้งนี้ความแข็งที่เพิ่มขึ้น สืบเนื่องมาจากผลของน้ำตาลโมเลกุลเล็ก ๆ ที่ได้จากแป้งที่ถูกย่อยด้วยเอนไซม์ โดยแป้งเหล่านี้จะไปมีผลต่อการเพิ่มขึ้นอย่างมากของแป้งที่ถูกทำลายหรือแป้งสุก เมื่อเปรียบเทียบกับแป้งที่ไม่ผ่านการดัดแปร ซึ่งแป้งดัดแปรชนิดใหม่นี้มีแนวโน้มที่ดีในการที่จะนำไปทำเป็นสารเพิ่มปริมาณในเม็ดยาในอุตสาหกรรมการผลิตยาเม็ดต่อไป

182 หน้า ISBN 974-04-6099-2

CONTENTS

CONTENTS
(continued)

CONTENTS
(continued)

CONTENTS
(continued)

CONTENTS
(continued)

CONTENTS
(continued)

LIST OF TABLES

LIST OF TABLES

(continued)

LIST OF TABLES

(continued)

LIST OF FIGURES

LIST OF FIGURES

(continued)

LIST OF FIGURES

(continued)

LIST OF FIGURES

(continued)

LIST OF FIGURES

(continued)

LIST OF FIGURES

(continued)

LIST OF FIGURES

(continued)

LIST OF ABBREVIATIONS

α	Alpha
&	And
ANOVA	Analysis of variance
AOAC	Association of Official Analytical Chemists
cm	Centimeter
DP	Degree of Polymerization
e.g.	Exempli gratia (Latin), for example
et al.	Et alii (Latin), and others
ed.	Edition
ed. (eds.)	Editor, editors, edited by
g	Gram
h	Hour
i.e.	Id est (Latin), that is
J	Joule
kg	Kilogram
kN	Kiloneuton
kV	Kilovolt
m	Meter
µm	Micrometer
mA	Milliampare
mg	Milligram
min	Minute
ml	Milliliter
mm	Millimeter
mM	Millimolar
Mw	Molecular weight

LIST OF ABBREVIATIONS

(continued)

nm	Nanometer
N	Neuton
p. (pp.)	Page (pages)
ppm	Part per million
rpm	Revolutions per minute
s	Second
SD	Standard deviation
SPSS	Statistical Package for the Social Sciences
v/v	Volume by volume
w/v	Weight by volume
w/w	Weight by weight
w.t.	Wet weight
/	Per
%	Percent
^{0}C	Degree of Celsius

CHAPTER I
INTRODUCTION

The tapioca and rice starch is an important carbohydrate, which are produced in Thailand. However, theirs price in the world market is low when compared to starches from other sources. Therefore, it is of interest to add value by finding other uses. In this present work, the potential of tapioca and rice starches for use as filler in pharmaceutical tablets is investigated. The starch, *United States Pharmacopoeia* (*USP*) grade, may be obtained from either the grain of corn, rice, or wheat, or from tubers of tapioca or potato (United States Pharmacopoeia Convention, 2000). Native starch possesses many desirable filler properties. It is as dry, white, odorless, tasteless, insoluble and neutral, however, it has poor flowability make it unsuitable for use in direct compression formulation and low compressibility to make tablet of sufficient hardness (Atichockudomchai et al., 2001; Bos et al., 1987; Visavarungroj & Remon, 1992).

Direct compression is widely used method for tablet manufacturing. The advantages of this method over wet granulation have been well documented (Li & Peck, 1990; Sheth et al., 1989). To be an ideal excipient for direct compression, the material should possess the attributes of flowability and compressibility. There have been many researchers attempt to modify starch to improve its compressing and flow properties including pregelatinized starch (Bolhuis & Chowhan, 1996; Karr et al., 1990; Sheth, 1987), crosslink gelatinized high amylose starch (Dumoulin et al., 1998; Ispas-Szabo et al., 2000; Le bail et al., 1999; Lenaerts et al., 1991), spray dried starch (Bos et al., 1992; Mitrevej et al., 1995; Mitrevej et al., 1996; Mitrevej & Varavinit, 1992) and acid modified starch (Atichokudomchai et al., 2001; Atichokudomchai & Varavinit, 2003; Puchongkavarin et al., 2003).

Structures of starch granule are described as concentric layers (growth rings) of amorphous and semi-crystalline regions. In the semi-crystalline growth ring, the crystalline parts contain the double helices of the outer chains of amylopectin and the

amorphous parts contain amylopectin branch points and amylose (Jenkins et al., 1994). The current model of the molecular composition and arrangement of the surface is based on Lineback's " hairy billard ball" model (1986), in which the granule surface is not smooth but characterized by protruding chains. These chains are suggested to be ends of amylose chain and amylopectin clusters (Baldwin et al., 1997, 1998; Stark & Lynn, 1992). Because of the tight packing of the amylopectin chains, the granule surface is relatively impenetrable to large molecules such as amylases. However, it is well establish unequivocally that α-amylase can enter to the cavity center of granule which contains a large proportion of the reducing ends of starch molecules and shows less organized than the rest of the granule (Blanshard, 1987), via the pores or channels existing in some starches (Fannon et al., 1992, 1993; Huber & BeMiller, 1997).

Enzyme reaction from α-amylase with starch granules occurs via several steps: diffusion to the solid surface, adsorption (prerequisite step for subsequent catalytic activity) and finally catalysis. Initial hydrolysis in the case of most starch granule is superficial depending on the type of starch. In general, enzymes either erode the entire granule surface or sections of it (exocorrosion) or digest channels from selected points on the surface towards the center of the granule (endocorrosion) (French, 1984; Gallant et al., 1992).

Both annealing and partially gelatinization altered the hydrolysis pattern of starch granules as observed by Wang et al. (1997) and Lauro et al. (2000) respectively. By changing the granular structure of starch, physical and chemical treatments also affect its enzymatic susceptibility. The increased susceptibility of partially gelatinized barley starch granules to α-amylolysis correlates with the decrease in the gelatinization enthalpy (Lauro et al., 1993). The final products of α-amylase were maltotriose, maltose, as well as glucose. The latter product usually obtained at higher concentration of enzyme (Hanrahan & Caldwell, 1953; Roberts & Whelan, 1960; Walker & Whelan, 1960).

The major purpose of this study is to improve the compactability and tablet properties of spray dried tapioca and rice starches prepared by combined the effect from preheat treatment and enzyme treatment. Further objectives of this study were to determine the chemical compositions and characteristics of modified starches as well as ascertain the effect of partial gelatinization on the granular structure and thus on the

hydrolysis of large tapioca starch and small rice starch granules. The structural and morphological changes in starch granules that affect from those two combining techniques were also observed.

CHAPTER II
LITERATURE REVIEW

1. Starch

Starch is polymeric carbohydrate composed of anhydroglucose units and is extracted in granular form from the organ of certain plants. The word “starch” may be derived from Anglo-Saxon “stearc” and has the meaning of strength or stiffness.

The starch granule is nature’s chief way to store energy in green plants over long times. The granule is well suited to this role, being insoluble in water and densely pack, but still accessible to the plant’s metabolic enzymes. It is found in the leaves of green plants in the plastids where it is synthesized. Starch also synthesized in the amyloplasts of seeds, grains, roots, and tubers of many plants. Starch serves as the major carbohydrate food for many species of animals, bacteria, and molds. Therefore, it is a link for these organisms to the energy to the sun. Starch is the predominant carbohydrate in all the major foods used by man; for example, rice, wheat, beans, maizes, tapiocas and potatoes.

1.1. Rice starch

Rice is a short-lived plant, belonging related to the grass family and has been one of the most commonly used grain products since ancient times. There are two cultivated species of rice, *Oryza sativa* L. and *Oryza glaberrima* Steud. Asian cultivated rice, *O. sativa* is distributed throughout tropical, subtropical and temperate climates of the world, while African cultivated rice, *O. glaberrima* is endomeric to west Africa.

Rice is very nutritious grain, especially brown rice. It has high fiber, vitamin B, carbohydrate, protein, etc. It has no gluten, so it is non-allergic. It is one of the leading food crops of the world, the stable food of over half the world’s population. About 90% of the world rice crops is produced and consumed in East, Southeast and South Asia (Juliano, 1985; Whistler et al., 1984). It is well known that rice grains exhibit

distinct physicochemical properties depending on their cultivars, and cooking properties. These properties have been utilized and selected by people living in different parts of the world.

1.1.1. Chemical compositions

The physicochemical properties of rice starch was shown in Table 1

1.1.2. Morphology

Rice starch was one of the smallest starch granules of the commercial cereal starches, varying in size from 3 to 10 micron in mature grain (Figure 1). Mean granular size varies from 3 to 8 (Jane et al., 1994). Only one set of starch granules is produced in the developing rice grain, and starch accumulation mainly increases in granular size (Briones et al., 1968). They are very angular (usually five-sided), frequency aggregated into large clusters owing to the steeping or drying conditions used during manufacture, and have a centric hilum and low birefringence. Starch granules of rice are irregularly shaped, polyhedral or polygonal granules that could be characterized as “sharp stones”.

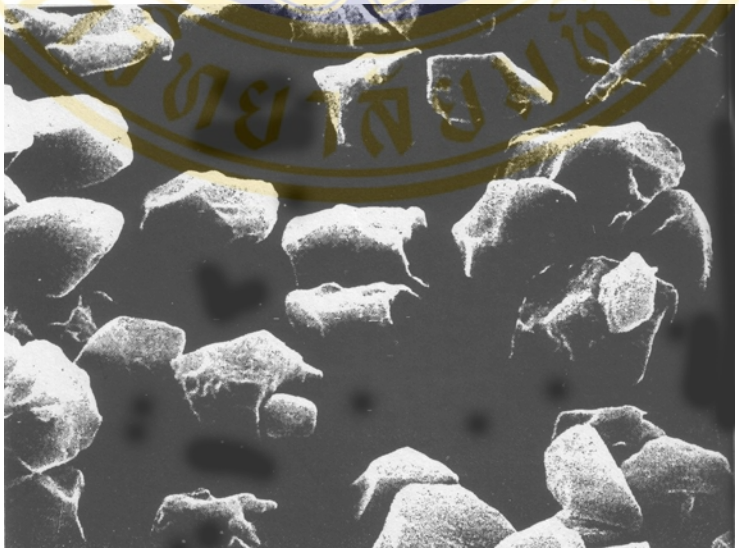

Figure 1 Rice starch granule with magnification 5000x (Whistler, BeMiller & Paschall, 1984).

Table 1 The physicochemical properties of rice starch

Property	Rice starch
Fat content (%)	0.8
Protein content (%)	0.45
Ash content (%)	0.5
Phosphorus content (%)	0.1
DP amylose	900-1,100
DP amylopectin	4,700-12,800
Swelling power	19
Solubility (%)	18
Kofler gelatinization temperature range (^{0}C)*	68-74-78
Crystallinity (%)	38

*The Kofler gelatinization temperature is the temperature at which the starch granules loss their polarization crosses.

1.1.3. Utilization

Rice starch contains tiny granules with a narrow size distribution, which makes it ideally suitable for using in many applications.

1. Using as cosmetic dusting powder.
2. Using as textile stiffening agent.
3. Using as fat mimetic in foods.
4. Using in paper industry
5. Less frequency used in the pharmaceutical industry
6. High purity rice starch with low surface protein-lipid contamination is desired for uses as a starting material for chemical modification, fermentation and industrial application.

1.2. Tapioca starch

Tapioca starch is available from large tuberous root of cassava or tapioca or manioc of family Euphorbiaceae. Its botanical name is *Manihot utilissima* Pohl or *Manihot esculenta* Crantz (Whistler et al., 1984; Duke, 1985). It is produced in Thailand, Brazil, the Philippines, Nigeria, Malaysia and Angola. Cassava is the term usually applied in Europe and in the United States to the roots of plant but tapioca is the name given to the processed products of cassava. The cassava plant is a semi-shrubbery perennial that grows under cultivation to a height of 2-4 m. The leaves are large and palmate, ordinary with 5-7 lobes, borne on a long slender petiole. The roots or tubers radiate from the stem just below the surface of the ground. Feeder roots growing vertically from the stem and from the storage roots penetrate the soil to a depth of 50-100 cm. The growing period can vary from 10-18 months. Tubers are cut from the stems and must be used within 48 hours to prevent loss of starch by enzymic changes and rot.

Tapioca is one of the most important starchy tubers in tropical zones, with 167 million tons of fresh tuber and roots produced annually all over the world (FAO, 1994). In industry, tapioca starch can take place with less manufacturing and reduced storage costs. These results of tapioca starch give a competitive advantage over the used of potato starch in many application. Modified starches are developed to archive desirable products.

1.2.1. Chemical composition

The chemical composition of cassava roots differs depending on variety, soil type, climate and age of the root. A typical root analysis would indicate 70 % moisture, 24 % starch, 2 % fiber, 1 % protein, 3 % fats, minerals and sugar. Young roots, under 10 months, have a low starch content whereas roots over 24 months are woody and difficult to handle. The physicochemical properties of tapioca starch was shown in Table 2.

Table 2 The physicochemical properties of tapioca starch

Property	Tapioca starch
Fat content (%)	0.1
Protein content (%)	0.1
Ash content (%)	0.2
Phosphorus content (%)	0.01
DP amylose	3000
DP amylopectin	2×10^6
Swelling power	71
Solubility (%)	48
Kofler gelatinization temperature range (^{0}C)*	59-64-69
Crystallinity (%)	38

*The Kofler gelatinization temperature is the temperature at which the starch granules loss their polarization crosses.

The root starch, for example tapioca starch, contains a very small percentage of lipids and proteins compared with cereal starches such as corn starch, rice starch and wheat starch. The small amount of lipids, which are predominantly free fatty acids, decreases the problems of rancidity on storage whereas the small amount of protein causes the loss of meaty flavor, odor and tendency to foam.

1.2.2. Morphology

Granules of tapioca starches are varying in shape. They may be round, egg-shaped, cap-shape, truncated and irregularly shaped. Hila are centric, sometimes slightly fissured. In addition, SEM shows that fractured sides are often dimpled and have a more textured appearance than the outer surface. The granule size is intermediate size with varying from 5 to 25 micron (Jane et al., 1994) (Figure 2).

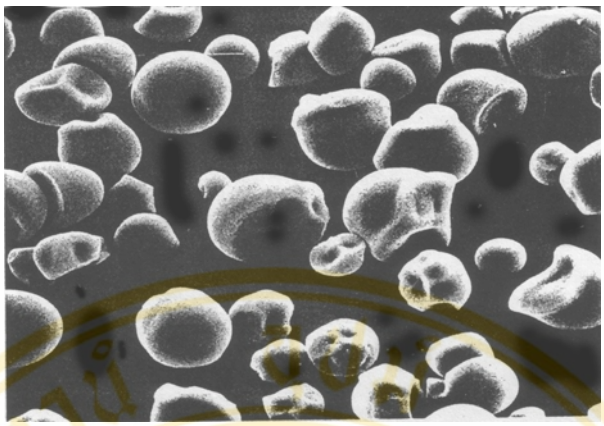

Figure 2 Tapioca starch granule with magnification 1500x (Whistler, BeMiller & Paschall, 1984)

1.2.3. Utilization

Tapioca starch is a typical root starch. The use is mainly in the production of food products, adhesives, alcohol and animal fodder. In pharmaceutical, tapioca starch is used as tablet binder and tablet disintegrant.

2. Molecular structure of starch

The two components of starch are amylose, the linear α(1-4) linked glucan, and amylopectin, a α(1-4) linked glucan with α(1-6) branch points. Intermediate component and several minor components such as lipids, proteins and phosphates are also present within the granule but at low concentrations (French, 1984).

2.1. Amylose

Amylose is an almost linear macromolecule (Manner, 1989; Matheson, 1990; Murugesan et al., 1993 & Curá et al., 1995) composed of glucose monomers bound predominantly by α-1,4 linkages (Figure 3) but slightly branched and the branches were α-1,6 glucosidically linked. Amylose covers a range of degrees of polymerization (DP), from about 200 to over 6,000 glucose unit (Swinkels, 1985) with molecular weight is about 10^6. The ratio of amylose to amylopectin is found depending upon the source of the starch. The amylose content may vary from trace amounts to 80 % of the total starch. When it is less than 2 %, the starches are referred to as waxy. Amylo-maize starch may contain up to 80 % amylose (Bean, 1992).

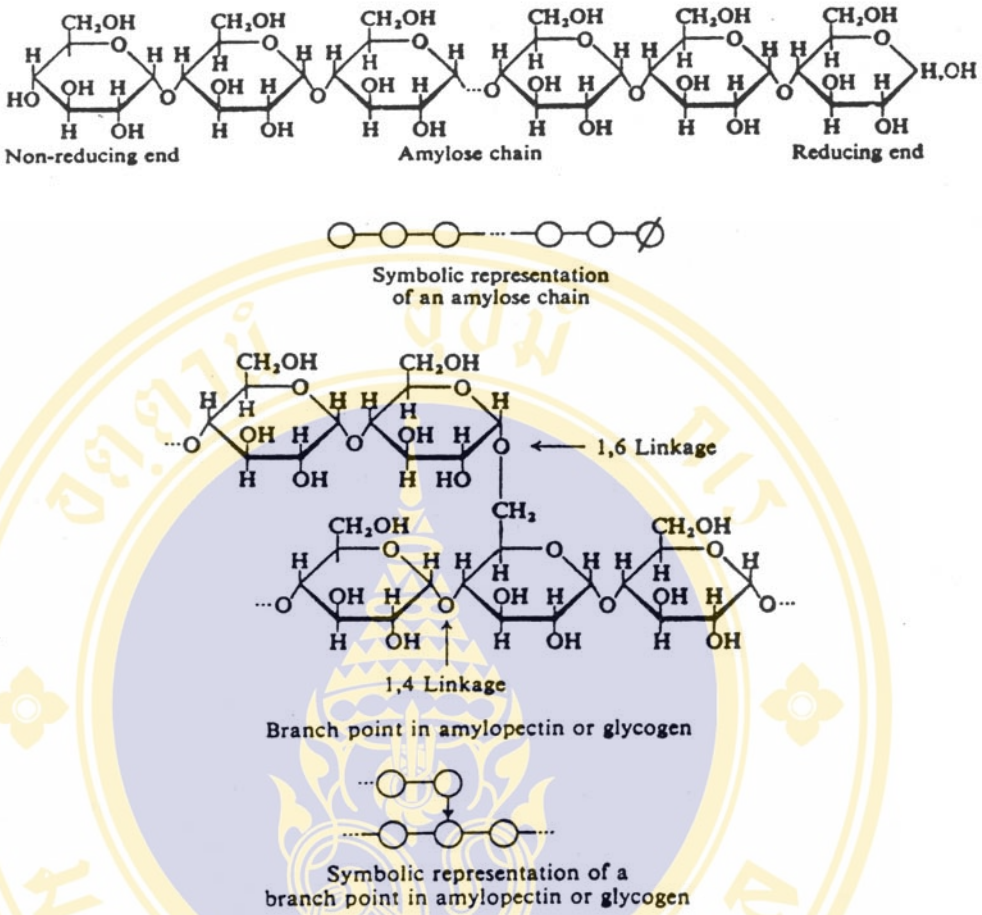

Figure 3 Chemical structure of the amylose (top) and amylopectin (bottom) chains and their symbolic representations

In normal starch granules amylose molecule are present. However, the localisation of amylose has proved more difficult to determine. Research using enzyme treated granules provided evidence that amylose fraction in maize starch granules is located within the amorphous region interspersed between the crystalline amylopectin granule rings (Helbert et al., 1996). It was shown by cross-linking the components of granular starch that amylose is found next to amylopectin molecules rather than forming bundles with other amylose molecules (Jane et al., 1992). Except for high-amylose (Tester et al., 2000), the amylose is generally believed to be amorphous inside the granules. The two-directional backbone offers a room for amylose, where it could be found completely inside the amorphous lamella together with the amorphous chains of amylopectin (Figure 4) (Other amylose molecules, e.g.

those involved in lipid complexation are allocated to amorphous 'growth rings'). It was shown by Jerkins and Donald (1995) that the thickness of the amorphous lamella decreases and the crystalline lamella increases (retaining the 9 nm repeat distance) in the presence of amylose.

Further studies in maize, pea and barley starch granules (Jerkins & Donald, 1995) revealed that amylose molecules disrupt the structural order of amylopectin clusters. This was support by model from Tamaki et al. (1997). They deduced that amylose penetrates several crystal regions of amylopectin and part of amylose is incorporated to the crystal region like as pearl string, which pearl is crystal and string is amorphous, and heat treatment brings about drastic movement at string, then the string is disrupted and pearl is liberated. Amylose could also be partly involved in double helixes with amylopectin short chains in the crystalline regions (Blanshard, 1987; Buleon, 1998). Moreover, amylose chains could be involved in amylose-lipid complexes, though it is rarely detected in native starches (Buleon, 1998).

Recently, Seguchi et al. (2003) were proposed that amylose plays a role in the maintenance of the structure of the starch granule. This is in agreement with the results of Tester and Morrison (1990) that starch granule swelling is promoted by amylopectin and prohibited by amylose.

Figure 4 The two-directional backbone model in a normal starch, where the amylose (thick wave-line) is found together with the amorphous chains of amylopectin (A: Amorphous region; C: Crystalline region)(Bertoft, 2004)

2.2. Amylopectin

Amylopectin, one of starch main constituents poses an enormous value, is one of the worlds highest molecular mass (molecular weight 10^7-10^9) and complicated biopolymers. Amylopectin is a large, branched macromolecule with glucose monomers bound via both α-1,4 linkages (DP 12-70) and interlink by α-1,6 linkages as shown in Figure 3.

The main features of amylopectin are now established after sequential analysis of the macromolecules, For instance, by using pullulanase or isoamylase (which are debranching enzymes), three or more population of chains are obtained. They are short chains, S (average DP 12-20), long chain, L (average DP 40-45), and chains with an average DP more than 60 (Gallant et al., 1992).

X-ray crystallography and microscopy studies have revealed the amylopectin framework within the starch granule to be crystalline and organise in separated concentric ring as seen in cross-section (French, 1984). Amylopectin molecules are oriented perpendicular to the ringed structure and to the outer surface of the starch granule. That is, they are aligned along an imaginary axis extending from the hilum of the granule radially towards the edge of the granule.

There are three types of chains presented in amylopectin (A, B and C). The A chains are the chains that are linked to the B and C chains through the reducing group by an α-1,6 linkage and do not have any other chains attached, The B chains are similarly linked but carry one or more A chains or other B chains. The C chain is the only chain of the molecule which has a free reducing group, The ratio of A chain to B chain is one method used to characterize the structure of amylopectin (Atwell et al., 1980; Manners & Matheson,1981).

According to the cluster model of amylopectin proposed by Hizukuri (1986)(Figure 5), amylopectin chains can be fractionated into B_3, B_2, B_1 and A chains. A chains carry no chain, and B chains carry at least one or more A or B chains. A and B_1 chains are localized to one cluster, B_2 chains span two clusters and B_3 chains span three cluster. A single cluster displays the double helical structure, forming the crystallinity of starch granules. The length of the crystalline region is 6 nm, which corresponds to the length of 18 glucose residue (Ball et al., 1996). Unit-chains with DP 6-17, which mainly comprise A chains, would give rise to a single cluster of

amylopectin. Recently, Bertoft (2004) was introduced the new model of amylopectin structure. The structure is a two-directional backbone model, in which the clustered chains are standing in one direction, with their external parts forming the crystalline lamella, and the long B-chains are found in a perpendicular direction as shown in Figure 4. A major feature of the two-directional model is that the entire long B-chains are amorphous.

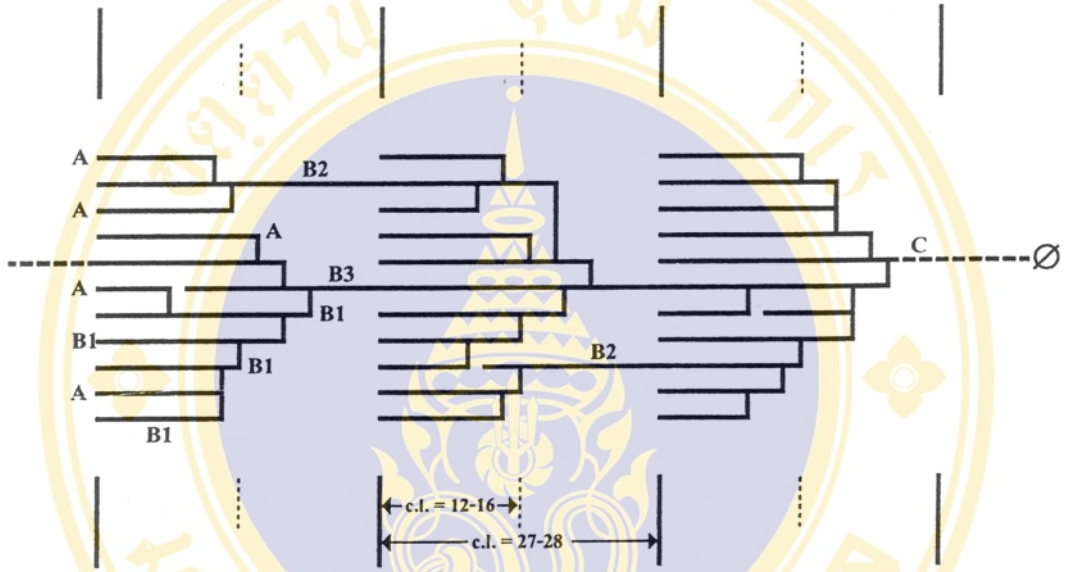

Figure 5 Cluster model of amylopectin (Hizukuri, 1986)

In native starch granules, the amylopectin is partially crystalline. The side chains of the amylopectin are arranged in a double helical conformation and by this yield an ordered structure. The crystallinity of starch can be examined by X-ray diffraction methods. X-rays, focused on a powdered starch preparation, scatter in a pattern determined by the crystalline structure of the starch. Its X-ray diffractogram, A-, B- or C- type is characteristic for each type of starch depending on the botanical origin. Imberty et al (1988) and Imberty and Perez (1988) refined the model for the double helical structure of A- and B-type starch, respectively (Figure 6). In general, the starches from cereals are regarded as of A-type. Electron diffractograms, recorded from micron-sized, needle-shaped crystals, revealed a unit cell of the crystalline part of these starch polymorphs, two left-handed, parallel-stranded helices are crystallized in the monoclinic space group B2. The unit cell contains of 12 glucose residues, which

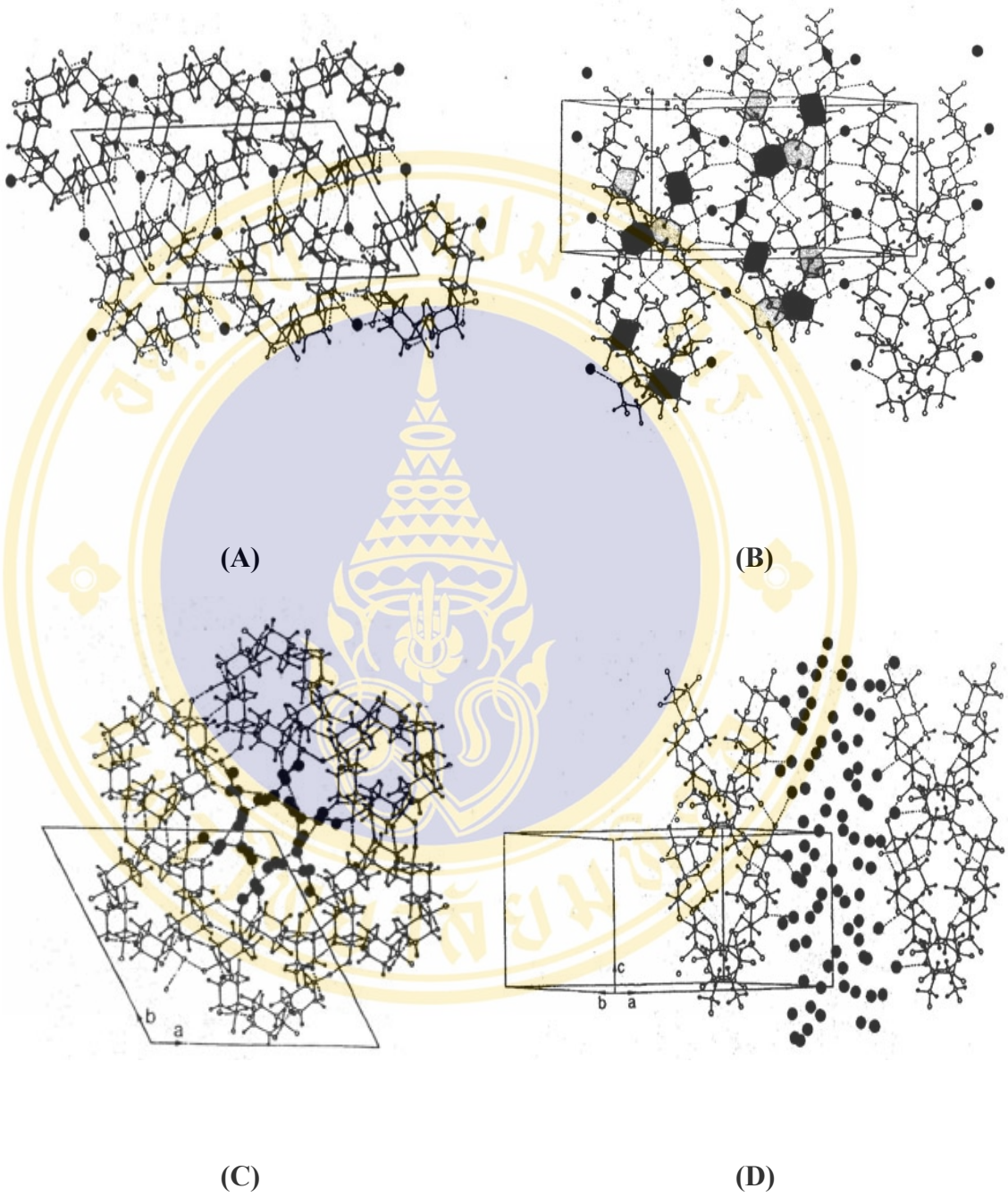

Figure 6 Model for the two starch polymorphs A-type (A, B) and B-type (C, D); A, C are top views and B, D are longitudinal views. Close circles represent water molecules (Imberty et al., 1988; Imberty and Perez, 1988).

are presented four water molecules between the helices. In the starches from roots and tubers the double helices are crystallized in the hexagonal space group P61. Such conformation is called B-type. B-type polymorph consists of a unit cell in which 12 glucose residues are located in left-handed parallel-stranded double helices.

If we compare the three dimensional order of the double helices, in type B a channel of approximately the same diameter as that of the double helix is found in the center of the hexagon. These channels filled with water. In contrast to A-type starch, thirty-six water molecules can be located in the unit cell, i.e. six per maltose unit. The two residues in the asymmetric unit differ only slightly; the O-6 groups are all gauche-gauche. Otherwise, the double helices in B and A starch are essentially identical, including the same inter-strand hydrogen bonding. The double helices are connected through a network of hydrogen bonds that leaves a channel in the center of the hexagonal arrangement of six double-helices. The water molecules are located in fixed positions within this channel; half are hydrogen bonded to the amylose chains and the other half to other water molecules. In legume starches, known as C-type, A-type and B-type polymorphs exist in varying portions (Sarko & Wu, 1978; Gernat et al., 1990).

2.3. Intermediated component

Many reports have indicated the presence of a material having properties different from those of amylose and amylopectin so called the intermediate component (Lansky et al., 1949; Peat et al., 1952; Wolff et al., 1955). The intermediate components displayed iodine-binding affinity and by a beta-amylolysis limit between those of amylose and amylopectin. Lansky et al. (1949) reported that maize starch contained 5-7 % of the intermediate component. Erlander and French (1958) also reported the presence of a component with a lower molecular weight than amylopectin in waxy-maize starch. Many reports also suggest the presence of an intermediate component in high amylose starch (Bank et al., 1974; Colonna & Mercier, 1984; Dias & Perlin, 1982; Greenwood & Mackenzie, 1966; Whistler & Doane, 1961). Dias and Perlin (1982) studied the intermediate component (amylopectin C) by using high field ^{13}C NMR. They claimed that the intermediate component has a chain length that is 20-25 % shorter than that of normal amylopectin.

2.4. Minor component

The interaction of the minor components, such as lipids and protein, with amylose and amylopectin, can also influence the properties and molecular architecture of the granule. Lipid-bound amylose is present within the amorphous regions of the granule (Morrison et al, 1993) where the lipid (lysophospholipid and free fatty acid) is immobilised within the α-glucan helices. These amorphous regions are predicted to have a rubbery consistency, which acts as a shock absorber, if the granule is subjected to compression (Morgan et al., 1995). Water absorption studies have also indicated lipid and amylose interaction within the granule contributing to inhibit of swelling when the granule is hydrated and heated (Tester & Morrison, 1990).

3. Localisation of amylose and amylopectin in different environment

A general model of amylose and amylopectin localisation from three starches containing 0-70 % amylose has been proposed by Atkin et al. (1999) (figure 7). The amylopectin forms closely packed concentric layers in dry waxy maize starch granules (0 % amylose), which expands on hydration with granule swelling. These concentric layers of amylopectin form the framework for the majority of different starch granules. Potato starch granules reveal the effect of a low concentration of amylose (21 %) within the granule. The amylose is localised in separate concentric layers which alternate between the amylopectin layers that form the granule framework. On hydration, the granule swells and the layers expand, reducing the amorphous amylose concentration as the encapsulating volume of the layers increased was observed and amylose is also lost by leaching out of the granule. The amylomaize granules are composed of 70 % amylose polymers and increased separation between the amylose and amylopectin is observed in these granules. With hydration the amylose is diluted, and as no granule swelling occurs, it is presumed that amylose has leached out from the granule through the thinning granule surface.

The disruption of hydrated potato starch granules by heating clearly showed the movement of starch polymers out of the granule, resulting in complete loss of central polymers and disruption to the outer layers.

In general, the starch granule appears to be composed of a crystalline amylopectin framework with a separate amorphous amylose component. It is possible

for amylose to phase separate within the aqueous environment of the granules in situ after synthesis due to incompatibility with the ordered amylopectin layers, resulting in the compartmentalisation of the two carbohydrates. As the amylose proportion increases, the separation between amylose and amylopectin appears to increase and becomes more distinct. However, amylose that presence in the crystallites may be unable to phase separate as it becomes trapped between amylopectin units, interfering with the packing order and subsequently the amylopectin layers with trapped amylose require less energy to disrupt (Atkin et al.,1998).

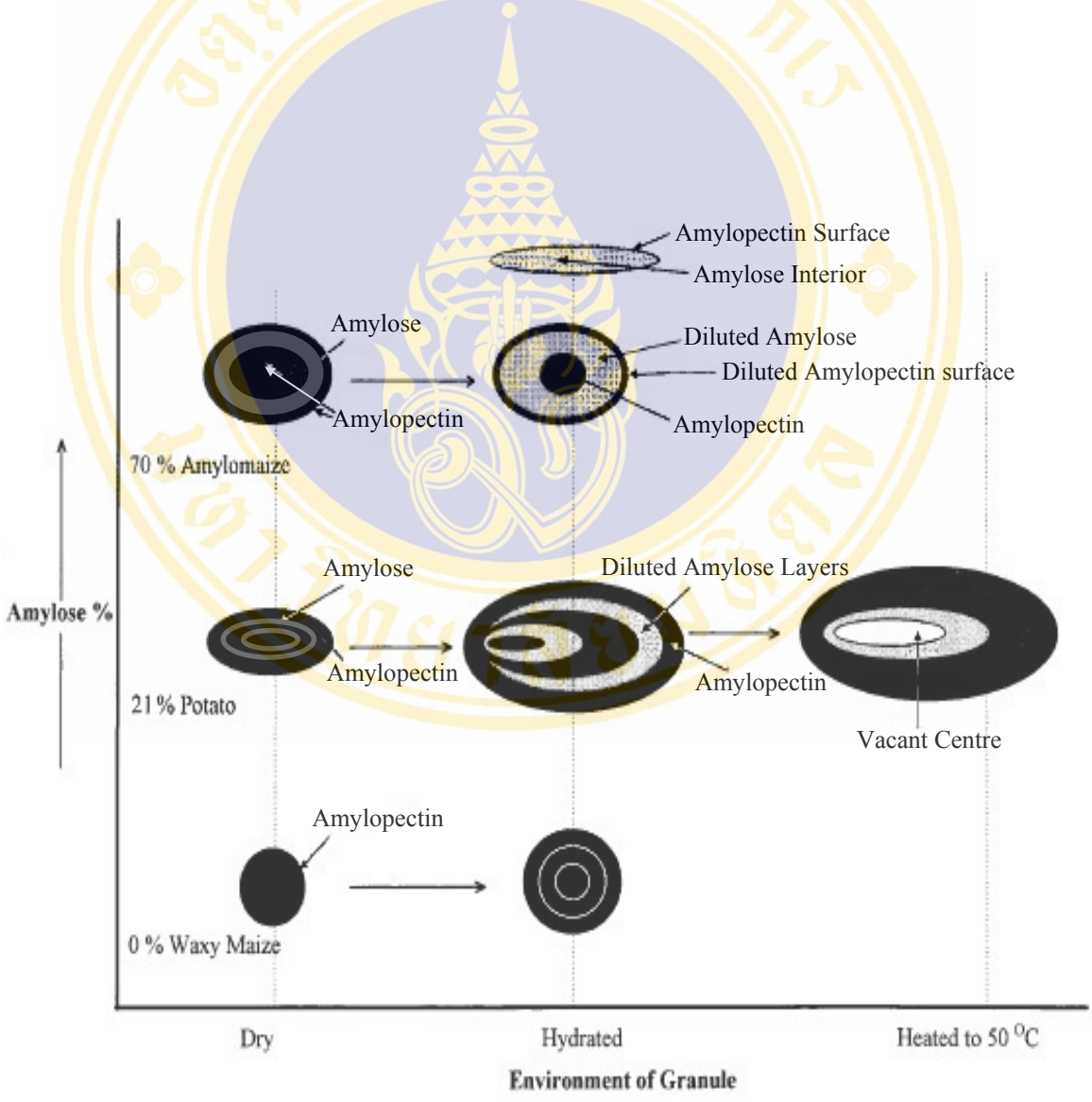

Figure 7 Proposed model of amylose and amylopectin localisation within a range of granules in different environments (Atkin et al., 1999).

4. Crystalline structure of starch granule

The starch granule organization is very complicates and depends strongly on the botanical origin. Despite several decades of investigation on the crystalline ultrastructure of starch, many questions remain unresolved such as the respective contribution of amylose and amylopectin to crystallinity, the distribution of ordered and unordered areas in the granule, the size distribution of crystalline areas or the organization of mixed A- and B-type granules (Buleon et al., 1998). Starch granules are usually believed to consist of alternating 120-140 nm thick amorphous and semi-crystalline layers. It is the regular orientation of the amorphous and crystalline regions that give the granule its characteristic birefringent pattern, known as the maltese cross observed in the polarizing microscope (French, 1984). Considerable evidence now supports the finding that the semi-crystalline layers consist of a regular alternating amorphous (branched regions and amylose) and crystalline (double helices) lamellae embedded in a background region (Figure 8) as reviewed by French (1984). This cluster model has been extended (Blanshard, 1987) to incorporate the presence of amylose molecules in the amylopectin rings as well as in the amorphous rings in the granule.

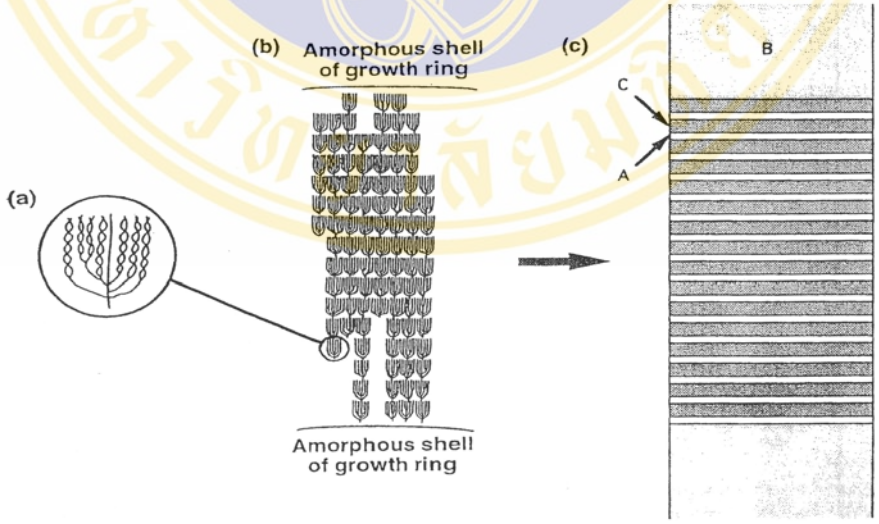

Figure 8 a) A single amylopectin cluster with double helix formation. b) Schematic representation of the arrangement of amylopectin molecules within a semi-crystalline growth ring. c) The structure may be modelled in terms of a lack of lamellae alternating in electron density (crystalline region (C) and amorphous region (A), emmbedded in a background region (B) (Jenkins et al., 1993).

It is now widely accepted that the amylopectin molecule is the crystalline component in granules, with the short, branched chains forming local organizations (French, 1984). This concept is compatible with cluster models for amylopectin proposed by French (1984), Robin et al. (1974), and Manners and Matheson (1981). Extensive enzymatic studies (Manners, 1989) suggest that the branching chains have lengths ranging between 9-20 glucose residues.

A simplified super-helix model based on Hizukuri's structure (1986) is presented in Figure 9A. The super-helix is a cooperative structure build up of several individual "pie shaped lamellae motifs" of amylopectin molecules. The amorphous lamellae between these motifs form a backbone for the double helices. The double helices are lined up close together to form the left-handed crystalline lamellae (Waigh et al., 1999). The direction of the clustered chains and of the individual amylopectin molecules follows that of the super-helix axis.

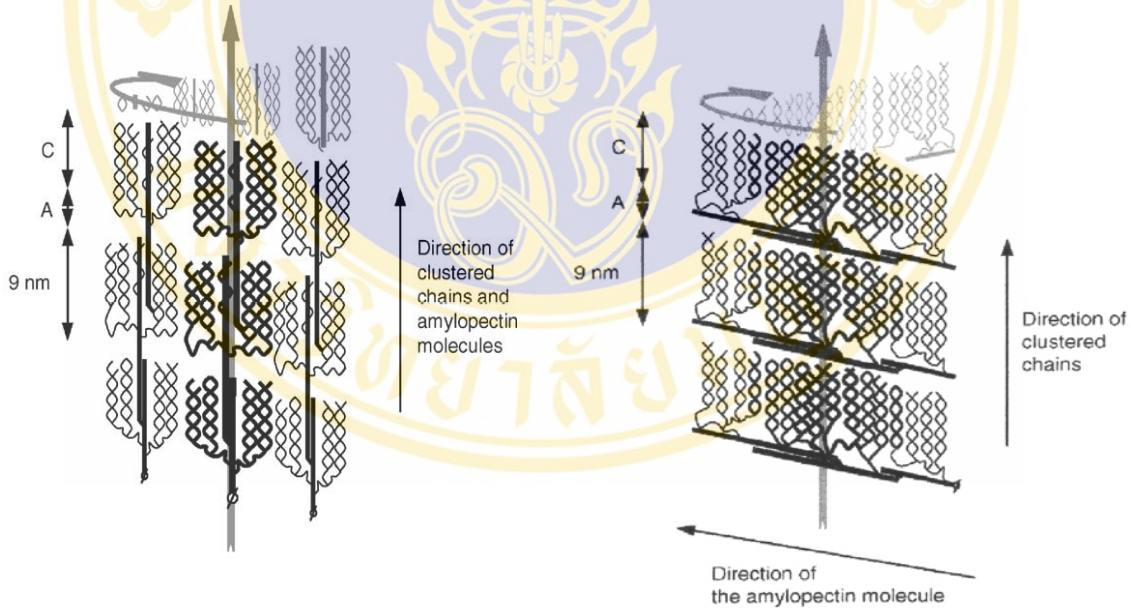

(A) **(B)**

Figure 9 A) The super-helix based on the cluster model by Hizukuri (1986) is a cooperative structure formed by several individual amylopectin molecules. The axis and the turns of the super-helix are indicated by grey arrows. B) The super-helix based on the two-dimensional backbone model is formed by a single amylopectin molecule (Bertoft, 2004)

Small-angle X ray diffraction (Blanshard et al., 1984) and electron microscopy (Kassenbeck, 1978; Yamaguchi et al., 1979) have revealed a periodicity (sum of the sizes of one amorphous and one crystalline lamellae) in the granule ranges from 9-10 nm that can be explained by stacks of thin crystalline lamellae as proposed in the cluster model of amylopectin. This was supported by the electron micrographs of granule fragments with a rippled structure, the ripples being separated by the same 10 nm distance (Oostergetel & van Bruggen, 1989). The results are interpreted as alterations of crystalline regions with amorphous zones in which the 1- 6 branch points occur. The lamellae are believed to represent the crystalline (side chains double helixes clusters with DP ranging between 15- 18) and the amorphous regions (branching regions) of the amylopectin molecules, according to the model of Robin et al (Gallant et al., 1997; Buleon et al., 1998) (Figure 10). The super-helix model based on Bertoft (2004) was introduced recently. This super-helix model was adapted from the two-directional backbone model (Figure 4) by simply twisting it into the helix (Figure 9B). The crystalline lamella is structurally similar to the cooperative alternative, but the amorphous lamella is build up of a true backbone formed by the long chains of the amylopectin. The direction of the clustered chains is still similar to the super-helix axis, but the direction of the amylopectin molecule follows the turns of the super-helix. It is temping to suggest that a single macromolecular super-helix is identical to the units of blocklets observed by atomic force microscopy (Baldwin et al., 1998 & Gallant et al., 1997).

From recent investigations by atomic force microscopy, it was concluded that crystalline and amorphous domains within the starch granule are organized in larger structures, which were called ‘blocklets’. The size of these blocklets varies from 20 to 500 nm and depends on the botanical origin of starch and the location within the granule (Gallant et al, 1997) (Figure 11).

5. Modified starch

Each starch types has it owns characteristic in both physicochemical properties and morphology. The characteristic in native starch somehow is not suitable for applying in the industrial application. The way to meeting the satisfaction is to modify starch.

Modified starch is defined as the product that was obtained from starches, for example, tapioca, corn, potato, wheat and rice. The characteristic of these starches was changing in chemical and/or physical properties from the native, either by thermal treatment, chemical reagents and/or enzyme. The modified starch was then archived for appropriate using in industries.

In order to characterize the structure properties of modified starch, there are many techniques to investigate the change after modification. A pictorial representation of the length scales within starch granules together with techniques used for their quantification are presented in Figure 12.

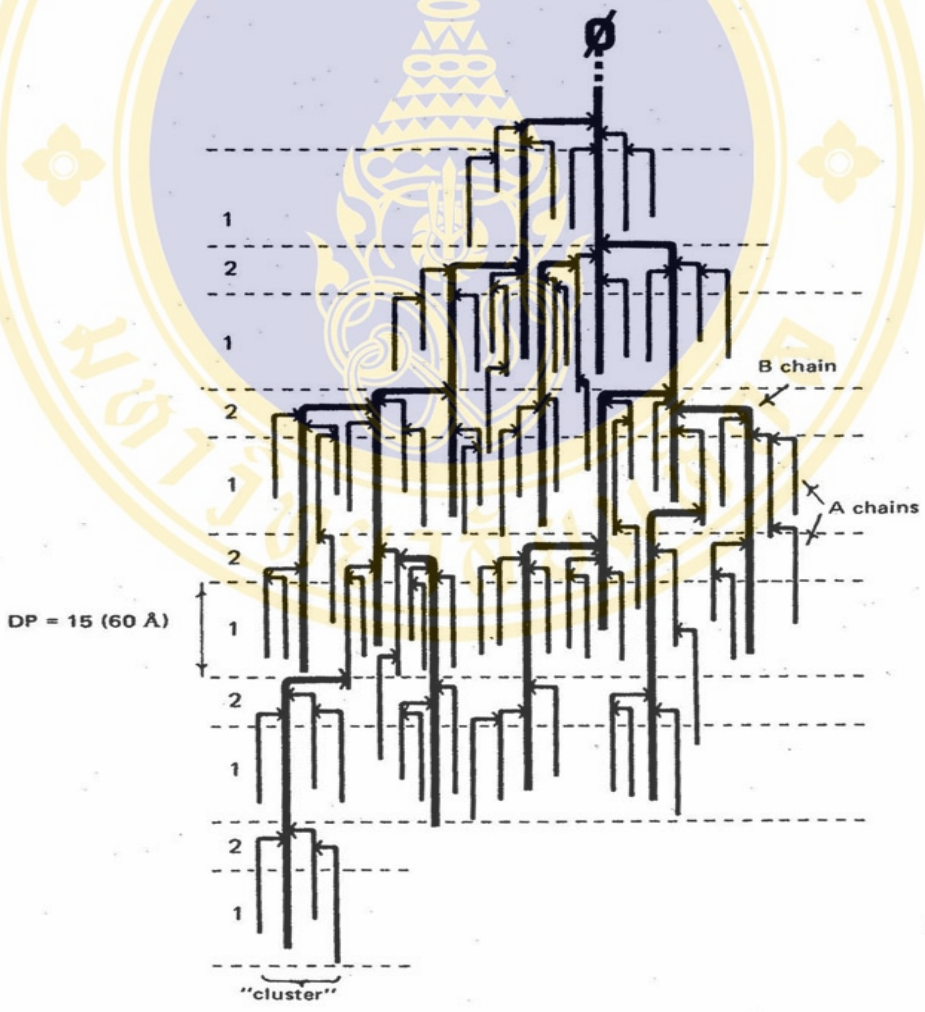

Figure 10 Scheme of macromolecular organization of amylopectin in native starch, the cluster organization showing crystalline (1) and amorphous (2) lamellae (Robin et al, 1974)

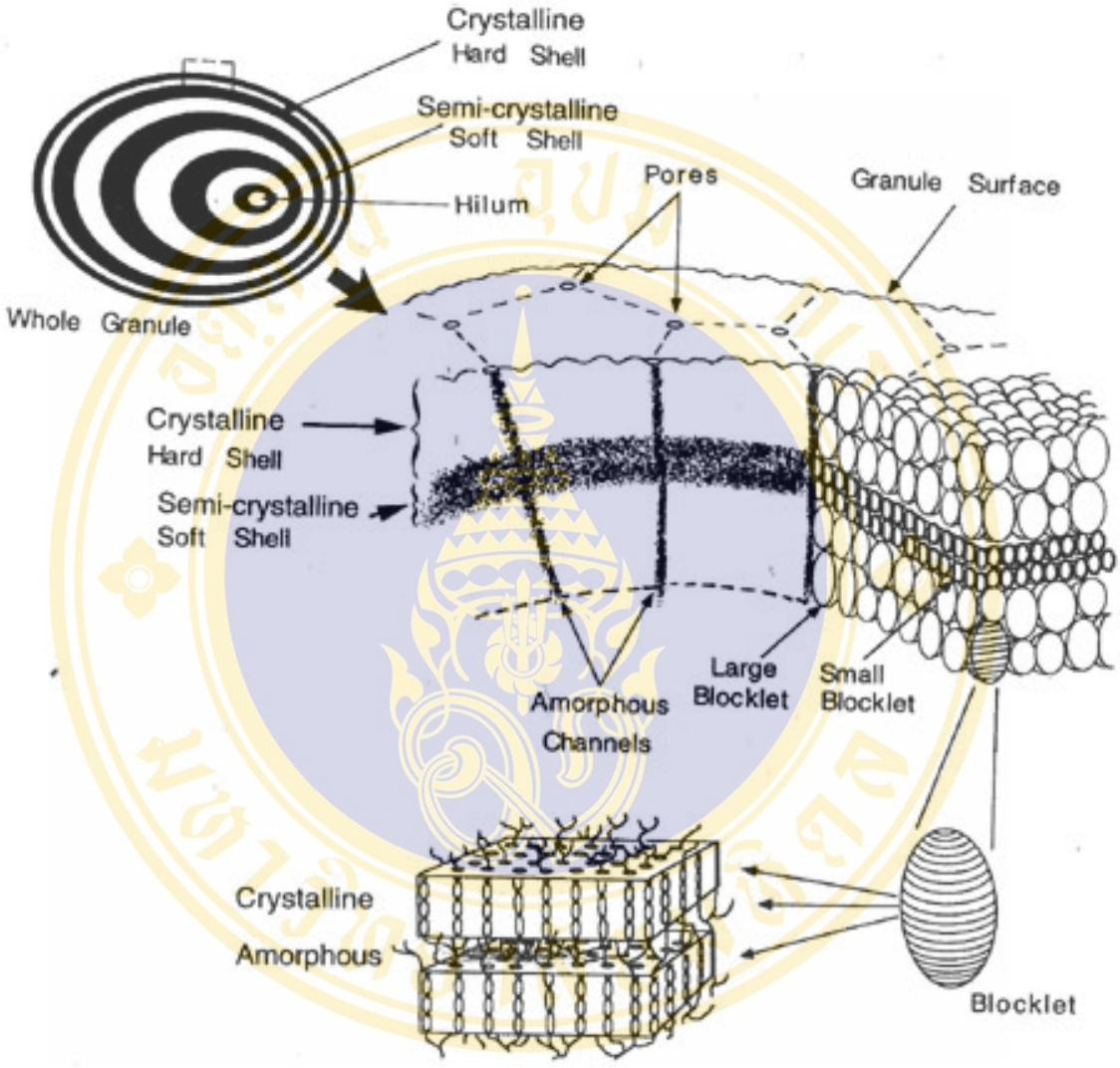

Figure 11 Blocklet structure of the starch granule (Gallant et al, 1997)

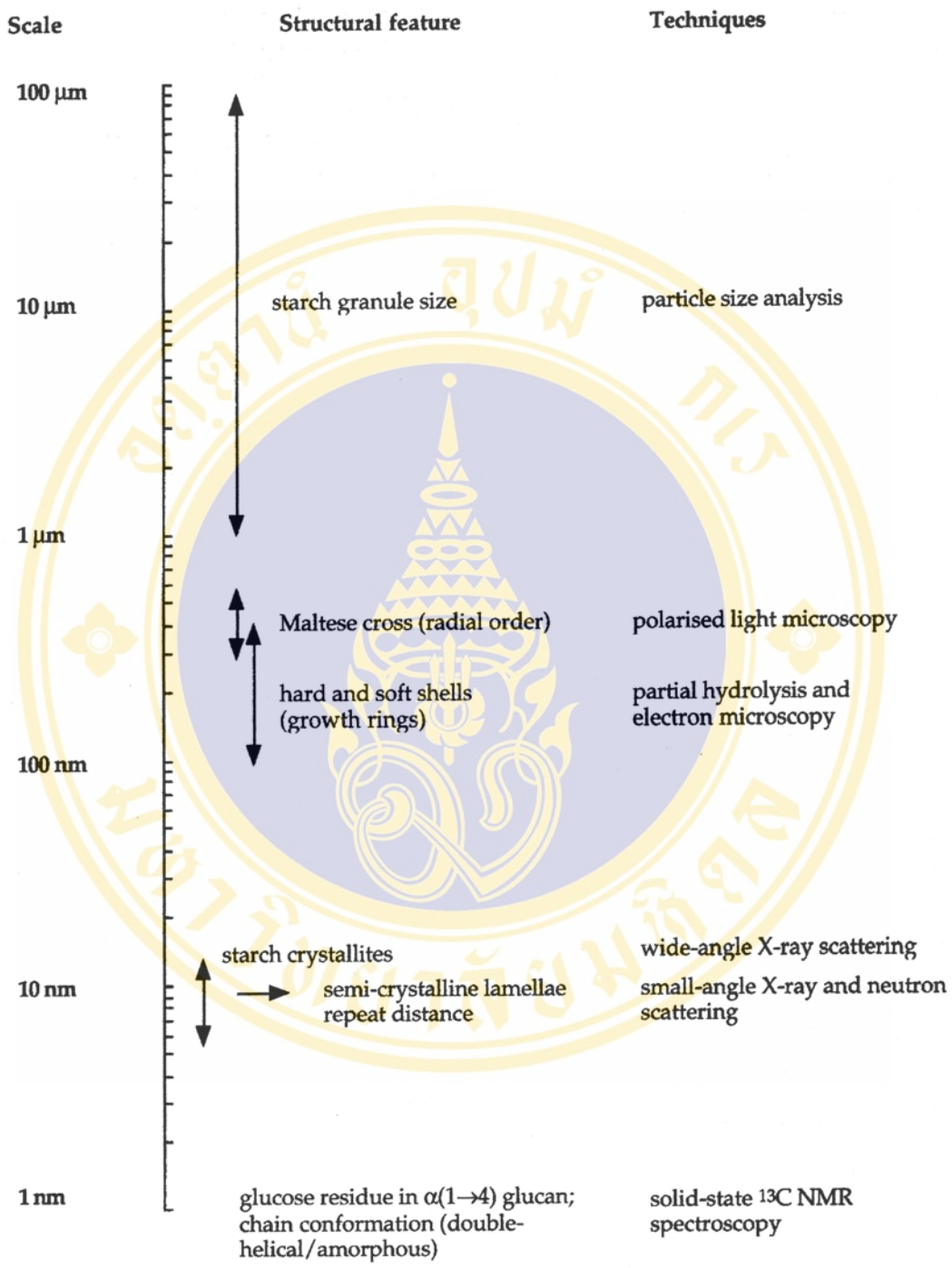

Figure 12 A pictorial representation of the length scales within the starch granule together with techniques used to characterise the structural features (adapted from Gidley, 1998)

6. Enzymatic-modified starch

6.1. Properties of the α-amylase

Bacterial α-amylase (E C 3.2.1.1.), being an endo-enzyme, catalyzes hydrolysis of 1,4 α-glucosidic linkages located in the inner regions of the starch molecules in amylose, amylopectin and related oligosaccharides, causing their fission into smaller dextrin molecules. This enzyme does not hydrolyze the 1,6-α-branch points in amylopectin, but can bypass them (Outtrup & Norman, 1984). All α-amylase investigated so far are calcium-metallo enzyme and contributes to the stability of the tertiary structure. The calcium ion(s) imparts resistance against effect of pH, temperature, and proteolysis (Stein & Fisher, 1958). The number of calcium ions per molecule of enzyme varies. Usually there are one or two gram-atoms per mole of enzyme that are very tightly bound and a number (1 to 10) more loosely bound (Stein et al., 1964; Hsiu et al., 1964). The pH- activity curves are usually broad with optima between 6 and 8.

Thermostable α-amylase is a group of α-amylase that can catalyze the reaction at high temperature. Most of Thermostable α-amylase from a strain identified as a member of the Bacillus family. Initial characterisation (Outtrup & Norman, 1984) reveal that it produced maltose in the α-configulation as the final reaction product from starch, was most effective at 60-70 ^{0}C at pH 4.5-5.5, degraded amylopectin to a greater extent than β-amylase and hydrolysed cyclodextrins.

6.2. Factors effect on amylolysis of starch granule

The action of α-amylase on native starch granules has been shown to affect by the granule structure. In particular, the amylose/amylopectin ratio, crystal type, average molecular weight of the components and the presence of lipids and protein (Williamson et al., 1992), and reaction conditions and enzyme specificity (Yook & Robyt, 2002). Marsden and Gray (1986) and Franco et al. (1988) have postulated that α-amylase initially hydrolyzes the amorphous regions of the granule. However, Williamson et al.(1992) have shown by studies on “A” type and “B” type spherulitic polycrystalline amylose (degree of polymerization ~20) that “A” type spherulites retain their crystallinity after partial hydrolysis by α-amylase from *Aspergillus Oryzae*. Whereas, “B” type spherulites show a reduction in their level of crystallinity.

Although dissolved or gelatinized forms of natural starches react rapidly towards α-amylase, reaction rates of raw or granular forms are much slower and vary according to the source of starch. Due to their different botanical origin, susceptibilities to amylolysis of starches are quite different. Cereal starches are generally more susceptible to enzymatical hydrolysis than starches extracted from roots, tubers and fruits (Rasper et al., 1974; Leach & Schoch, 1961). So that no fragments remain as seen in the cereal starch (Gallant et al., 1972). Moreover, even in a group of tropical tuber starches are quite different in susceptibility in amylolysis (Delpeuch & Favier, 1980 & Gallant et al., 1982). Namely, potato starch is found to be much more resistant to amylolysis than many other starches (Rasper et al., 1974). However, as soon as the hydrolysis reaches the internal of potato starch granules, hydrolysis proceeds very rapidly. Conversely, cassava starch is as susceptible as the main cereal starches. Leach and Schoch (1961) found the following order of increasing resistance of granules towards α-amylase: waxy maize < tapioca < waxy sorghum < sorghum < ordinary corn < wheat < rice < sago < arrowroot < potato < high-amylose corn.

Effect of particle size on enzymatic hydrolysis of native starch and starch food is expressed in terms of available surface area per mass for enzymatic action both in vivo and in vitro. Specific surface area of substrate rather than concentration of substrate seems to be a most important factor for a better understanding of the initial stage of enzymatic hydrolysis of native starch granules. Also starches that naturally have a porous surface were more susceptible to digestion as a result of accessibility to hydrolytic enzyme molecules to the granule interior (Helbert et al., 1996; Huber & Bemiller, 1997). However, Kong et al. (2003) suggest that pores present in maize granules appeared not to affect the initial stage of hydrolysis significantly but clearly played an important role for digestion after an initial stage.

The effect of starch granule size on enzymatic susceptibility has been studied by various authors (MacGregor & Balance, 1980; Meredith, 1981; Eliasson & Karlsson, 1983; MacGregor & Morgan, 1984; Franco & Ciacco, 1992), and many of them have observed that smaller starch granules underwent more hydrolyzation than larger ones, regardless of botanical sources. Properties such as gelatinization, X-ray diffraction and amylose content also vary, depending on starch granule diameter

(MacGregor & Balance, 1980; Franco & Ciacco, 1992). Franco and Ciacco (1992) also reported a basic difference in the mode of action of enzymes on small and large commercial corn and cassava starch granules. Enzymatic attack on the large granules at slower rate proceeds by pinholes on the surface and surface corrosion, mainly at the radial axis and then the enzyme apparently hydrolyses the granule from the inside. In the early stages, both the crystalline and the amorphous parts of the large granules are equally attacked, resulting in solubilisation of both amylopectin and free amylose. whereas for small ones, the enzymatic action was restricted to the surface and was characterized by an erosion accompanied by solubilization of the granules. These results suggest that the components of small and large starch granules differ structurally from one another.

6.3. Mode of enzyme action

The susceptibility and mode of enzyme action depend on the starch source and enzyme system. Differences in susceptibility are not only described in terms of degree of hydrolysis but also in the mode of attack and the products of hydrolysis.

For enzymic action on polymeric substrates, three distinct mechanisms are possible: Single chain, Multichain or single attack, and multiple attack (Figure 13).

In the single-chain mechanism, once enzyme forms an active complex with the substrate, it catalyzes a reaction in a “zipper” fashion toward one end of the substrate and does not form an active complex with another substrate until it comes to the end of the first substrate.

The multichain process is the classical random attack in which the enzyme catalyzes the hydrolysis of only one bond per encounter.

In the multiple-attack mechanism, once the enzyme forms a complex with the substrate and produces the first cleavage, the enzyme remains with the one of the fragments of the original substrate and catalyzes the hydrolysis of several bonds before it dissociates and forms a new active complex with another substrate molecule.

It was proposed that α-amylases have a multiple attack mechanism (Robyt & French, 1967). The direction of multiple attack is from reducing end toward the non-reducing end as determined for porcine pancreatic α-amylase by Robyt and French (1970): i.e., after the first cleavage, the fragment with the new non-reducing end

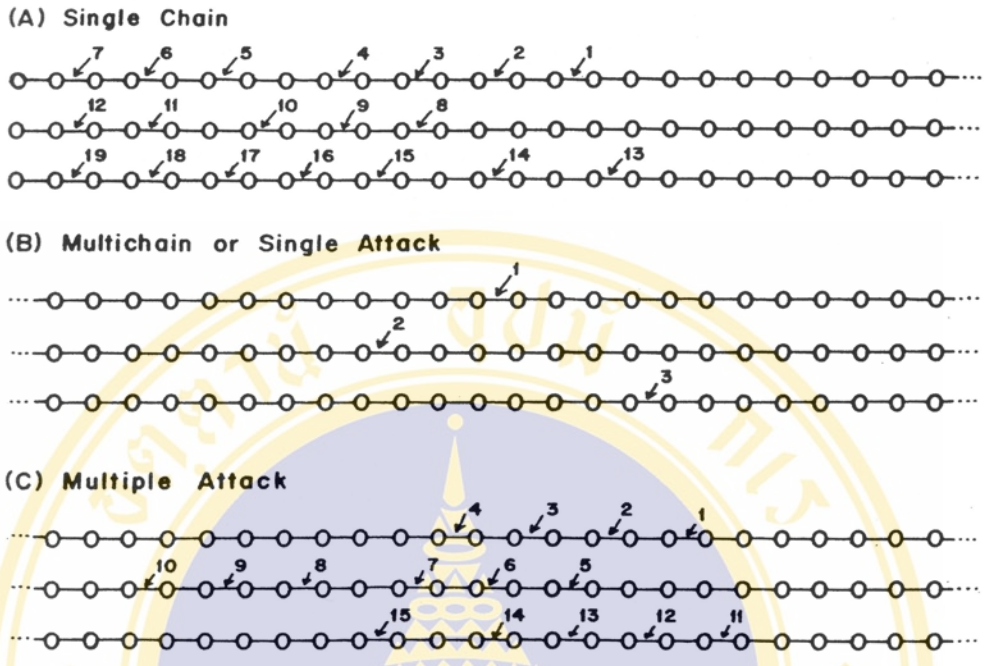

Figure 13 Types of attack pattern for endo amylases. Each type represents the action of a single enzyme molecule. The arrows represent the catalytic hydrolysis of a glycosidic bond; the numbers indicate the sequence of each catalytic event. The direction of multiple attack is toward the non reducing end as determined for porcine pancreatic α-amylase by Robyt and French (1970)

dissociates from the active site while the fragment with the newly formed hemiacetal reducing end remains associated with the active site and repositions itself to give another cleavage and the formation of maltose or maltotriose (Figure 14).

This mechanism is consistent with the observed rapid decrease in iodine color and the formation of low-molecular-weight maltodextrins (Robyt & French, 1967). For an equal drop in blue value (e.g. 50%), the different α-amylases give different percents of conversion to apparent maltose (Figure 15). These differences in reducing value may be interpreted as differences in the amount of multiple attack that occurs per encounter of enzyme and substrate. Further, during early stages of α-amylase action, a set of specific, low-molecular-weight oligosaccharides are found (Robyt & French, 1967; 1963; Walker, 1965). Therefore, it was conclude that the action of α-amylase is not random as was previously believed.

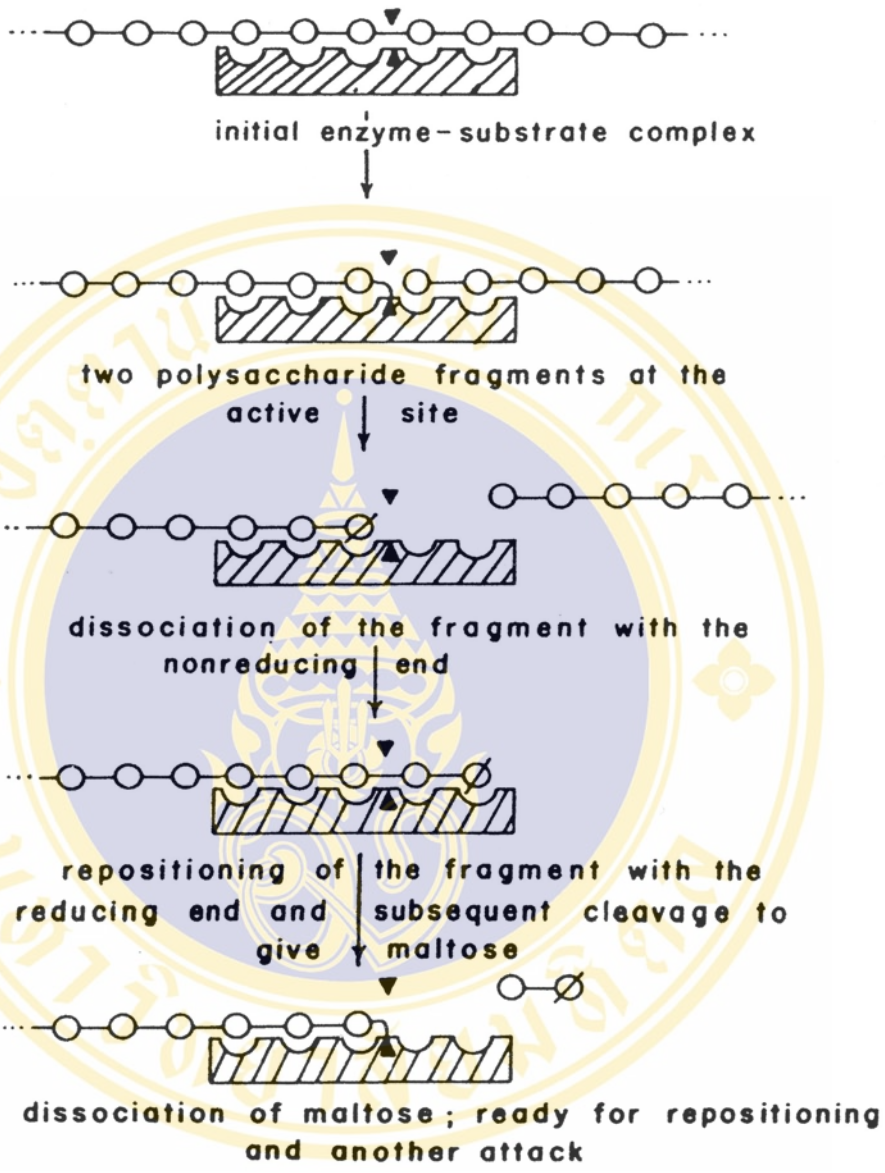

Figure 14 Sequence of events at the active site for multiple attack by an endo-acting enzyme. The active site is pictured here with five binding subsites and the catalytic groups located between the second and third subsites; ▲and ▼represent the catalytic groups; O represents a glucosyl unit; Ø, a reducing glucose unit; and —, an α-D-(1→4) glucosidic bond.

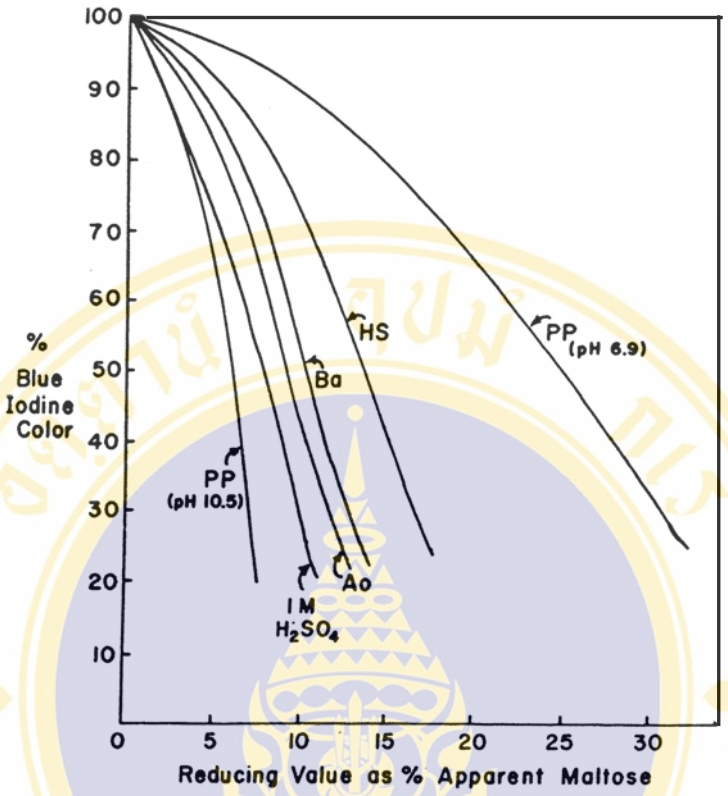

Figure 15 Blue iodine color vs. reducing value for the action of porcine pancreatic α-amylase (PP) at pH 6.9, human salivary α-amylase (HS) pH 6.9, *Bacillus amyloliquefaciens* α-amylase (Ba) at pH 6, *Aspergillus oryzae* α-amylase (Ao) at pH 5.5, 1 M Sulfuric acid at 600, and (PP) at pH 10.5 on amylose. Data in part from Robyt and French (1967).

6.3.1. Action on linear substrates

α-amylase catalyze an essentially random hydrolysis of non-terminal (1→4) α-D-glucosidic linkages in amylose. However, Enzyme action on maltosaccharides is not entirely random. It's may be altered by some specificity requirement. With low concentrations of enzyme, a first stage of α-amylolysis is reached when maltose and maltotriose in the molar ratio of about 2.4 to 1 are the products. Higher concentrations of enzyme cause a further, slow hydrolysis (second stage), resulting in the degradation of maltotriose into maltose and D-glucose (Walker & Whelan, 1960 & Hanrahan & Caldwell, 1953). Maltose is not a substrate, maltotriose is only slowly attacked, and maltotetraose is readily hydrolyzed.

Data for three α-amylases are shown in Figure 16; the specificities of pig pancreatic and *A. oryzae* α-amylases are probably similar to that of salivary α-amylase (Whelan, 1960). With high concentrations of enzyme, D-glucose is a product.

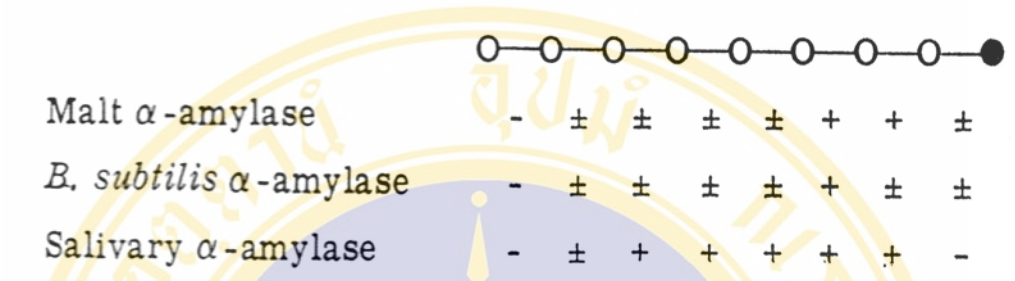

Figure 16 Hydrolysis of linear substrate by α-amylase. (Key: O—, (1→4) α-linked α-D-glucose residue; ●, reducing group; —, no hydrolysis; ±, slow hydrolysis; +, rapid hydrolysis.) Data from Bird and Hopskin (1954).

6.3.2. Action on branched substrates

The action of α-amylases on amylopectin, like that on amylose, can be considered into two stages (Whelan, 1960). In the first, maltose (42%), maltotriose (28%), and a series of oligosaccharides of degree of polymerization (DP) greater or equal to 5 are produced from amylopectin by salivary α-amylase (Walker & Whelan, 1960; Hanrahan & Caldwell, 1953 & Roberts & Whelan, 1960), whereas, with higher concentrations of enzyme, the products are maltose, D-glucose, and oligosaccharides of DP greater or equal to 4. The nature of these oligasaccharides, which contain one or more terminal (1 → 6) α-D-glucosidic linkages, depends on the enzyme source.

From the structures of the smallest oligasaccharides produced at the second stage of amylolysis, it is evident that certain (1 → 4) –linkages adjacent to the inter-chain linkage are resistant. These are shown in Figure 17. The action of pig pancreatic and *A. oryzae* α-amylases again appear to be identical with that of the human salivary α-amylase (Whelan, 1960).

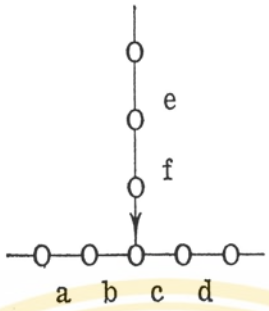

Segment of amylopectin or glycogen near an inter-chain linkage

Source of α-amylase	Smallest oligosaccharide[130]	Action on linkages a b c d e f
Saliva	6^3-α-D-glucosylmaltotriose	+ + - - + +
Malt	6^2-α-D-glucosylmaltose	+ + - + + +
B.subtilis	6^2-α-D-maltosylmaltotriose	+ - - + + -

Figure 17 Action of α-amylase on (1 → 4) –linkages adjacent to the inter-chain linkage. (Key: O—, (1→4) α-linked α-D-glucose residue; ●, reducing group; —, no hydrolysis; ±, slow hydrolysis; +, rapid hydrolysis.) Data from Bird and Hopskin (1954).

6.4. Mechanism of enzyme hydrolysis

The initial stage of enzyme action on substrate is formation of the enzyme-substrate complex. Adsorption of α-amylase from *Bacillus subtilis* on the spherulitic starch particles, which are essentially resistant to α-amylolysis at 25 ^{0}C, was found to be a prerequisite step for hydrolysis (Leloup et al., 1991).

The α-amylases were so named because the product of enzyme action are in the α-D form, that is, there is retention of configuration at C-1 of D-glucose. Three possible mechanisms have been suggested to explain the retention of configuration in these circumstances. These are: a front-side displacement (Thoma et al., 1963; Koshland, 1954), a double displacement (Thoma et al., 1963; Mayer & Larner, 1958; 1959; Halpern & Leibotwiz, 1959 & Koshland, 1954) and the stereospecific hydration of the carbonium ion (Mayer & Larner, 1958; 1959).

In the front-side displacement (a type of S_N2 mechanism), the C-1—O—C-4′ bond breaks simultaneously with the formation of the new C-1—OH bond. The possible role of amino acid side-groups in the enzyme is shown in Figure 18a. In the double-displacement mechanism, which involves two S_N2 substitutions, the C-1—O C-4′ bond breaks, and an enzyme-substrate complex is formed; the enzyme-substrate bond is then hydrolyzed to give the products (Figure 18b.). In the third mechanism (a S_N1 substitution), the ring-oxygen atom becomes protonated, and the C-1—O bond breaks; the enzyme then guides the water molecule stereospecifically to one side of the carbonium ion, and the products are formed as in Figure 18c.

6.5. Morphology of enzymatic-modified starches

The morphological changes induced by amylolysis have been largely explored (Fuwa et al., 1977; 1979; Gallant et al., 1972; 1973). Enzymes cause surface alterations and degrade the external part of the granule by exocorrosion. According to Yamada et al. (1995), the some extra weak region to enzymatic attack may exist along radial direction to center in granule. When endocorrosion occurs, the internal part of the granule is corroded through small pores by which enzymes penetrate the granule (Gallant et al., 1972; 1973) into the center then enlarges the pore. Hydrolysed granules exhibit successive internal layers, which correspond to alternate area with strong and weak susceptibilities inside the granules.

It is well known that porous granule is formed from native starch of many species by amylase treatment (Whistler et al., 1984). Leach and Schoch (1961) suggested that cereal starches had porous structures accessible to enzymes. Sreenath (1992) was proposed that with α-amylase treatment, the corn starch granule showed many pits or pores with more or less same size. However, some granules with larger pits were also observed. The point of attack (pores or pits) due to α-amylolysis may be at random or at some susceptible parts such as less crystalline or less dense regions of starch grain (Novo enzyme information, 1985). Raw, uncooked corn starch was partially digested with α-amylase to obtain pitted or porous starch granules, which could find useful applications in food, cosmetics and pharmaceutical industries (Guibot & Mercier, 1985).

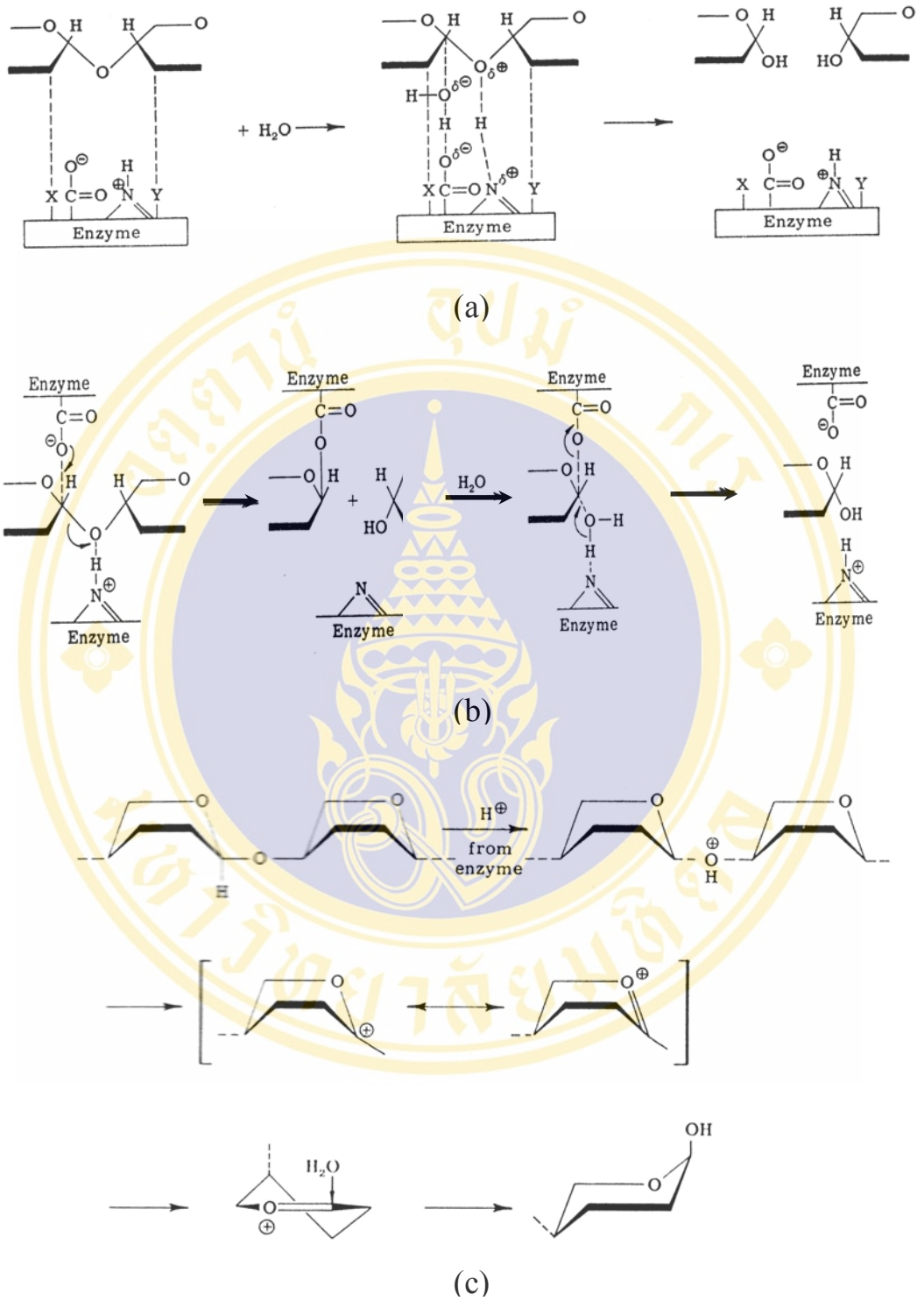

Figure 18 Suggested mechanism for α-amylase action. (a. Front-side displacement, where X and Y are substrate-binding groups, and N≤ represents part of an imidazolium ring; b. double displacement; and c. stereospecific hydration of a carbonium ion.) (Greenwood and Milne, 1968)

The presence of holes may effect the properties of the starch (Whistler et al., 1959; Fannon et al., 1992), and has implications for the internal structure of the starch granule. Whistler and Spencer (1960) suggested that chemical reactivity of corn starch granules was greatest at the granule surface and at the cavities, indicating that both cavities and surfaces could be important sites of chemical and enzymic attack. This has been highlighted in the recent work of Fannon et al. (1992) where large surface pores (upto 100 nm) were reported. It has been postulated that these pores may link with the interior granule cavity (Fannon et al., 1992; Whistler & Spencer, 1960; Whistler & Turner, 1955) and allow very large molecules, including enzymes, direct access to the granule interior. Baldwin et al. (1994) has hypothesized that the hylum of the granule, which is also where the Maltese cross is centered, is the weakest point of the internal structure and hence it is here that holes form when internal stress are set up during drying.

The observation from Yamada et al. (1995) induce a speculation that amylose would not be reached out of starch granule with amylase treatment, and it remain in the residual part at the same extent to amylopectin, and amylose may be homogeneously distributed in both crystal and amorphous region of starch granule.

7. Characterization of enzymatic-modified starches

7.1. Wide-angle X-ray diffraction

X-ray diffraction is a technique used to determine the existence of different material structures and phases in a sample, based on their characteristic diffraction behavior under X-ray irradiation of a known wavelength, i.e. each structure or phase will only diffract an incident X-ray at a specific set of incident angles, which can be measure. In addition to structural and phase analysis, other applications for X-ray diffraction include semi-quantitative phase analysis, relative degree of crystallinity measurement, particle size analysis, film thickness and stress analysis.

The starch granule contains both crystalline and amorphous regions, and each starch granule has its own degree of crystallinity with its own unique energy characteristics. The stability of the crystalline regions has been related to the conformation of starch chains in the amorphous regions (Marshant & Blanshard, 1978).

As mention above, X-ray diffraction can give information about the relative amounts of crystalline and amorphous phases. Following Nara et al (1978) method, if typical diffractometer tracings are examined, one see peaks from the crystals and a background from the amorphous or gel phase. By integrating the X-ray scattering intensity separately over the peaks and over the background, a number is obtained which can be interpreted as the X-ray crystallinity.

The X-ray diffractogram showing the crystalline and amorphous areas is displayed in Figure 19 (Komiya & Nara, 1986). A_c and A_a were the areas of crystalline and amorphous portions in the X-ray diffractogram, respectively. Relative crystallinity was given as A_c/A_t, that is $A_t = A_c + A_a$. Determining by this method, native starch granules were reported to have the relative crystallinity varying from 15% to 45% (Zobel, 1988).

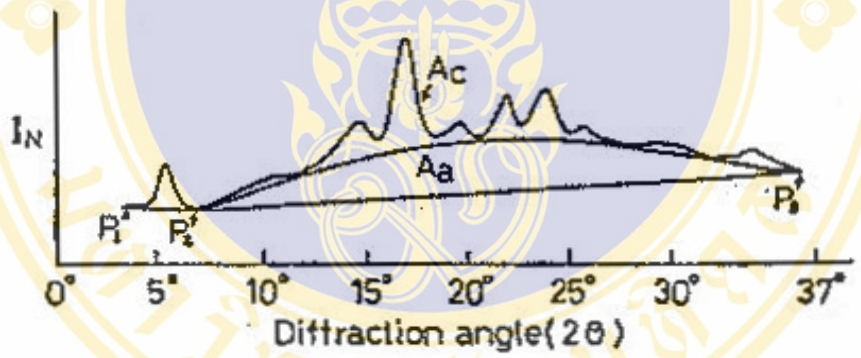

Figure 19 Suggested X-ray diffractogram of potato starch. A_c and A_a indicate the crystalline and amorphous portions in the X-ray diffractogram, respectively (Komiya & Nara, 1986).

Native starch granules can yield X-ray diffraction patterns, as classified to A, B, and C pattern as shown in Figure 20, with generally of low quality, with cereal starch typically giving A-type patterns, and tuber starch usually yielding B diagrams. Starch gives numerous other diffraction patterns, usually after a laboratory modification. If some traces of V pattern associated with complexed lipids may be ignored, the A and B pattern are considered to characterize native starch. The C pattern of native starch is now thought to be a combination of A and B patterns (Sarko

& Wu, 1978) but also occurs naturally, e.g. smooth-seeded pea starch and various bean starch. Retrograded starch, of considerable importance to starch industries also gives a B diffraction pattern.

The main difference between A and B types is that the former adopt a close-packed arrangement with water molecules between each double helical structure, while the B-type is more open, there being more water molecules, essentially all of which are located in a central cavity surrounded by six double helices (Wu & Sarko, 1987; Imberty & Pérez, 1988; Imberty et al., 1988)

Hizukuri (1985) and Hizukuri et al (1983) studied the distribution of chain lengths in the amylopectins of starches and found that there is a close relationship between the weight-average chain lengths of the amylopectins and crystal type of starch granules. Short chain lengths display A-type crystallinity, while long chain lengths show B-type crystallinity and intermediate chain length is associated with C-type crystallinity.

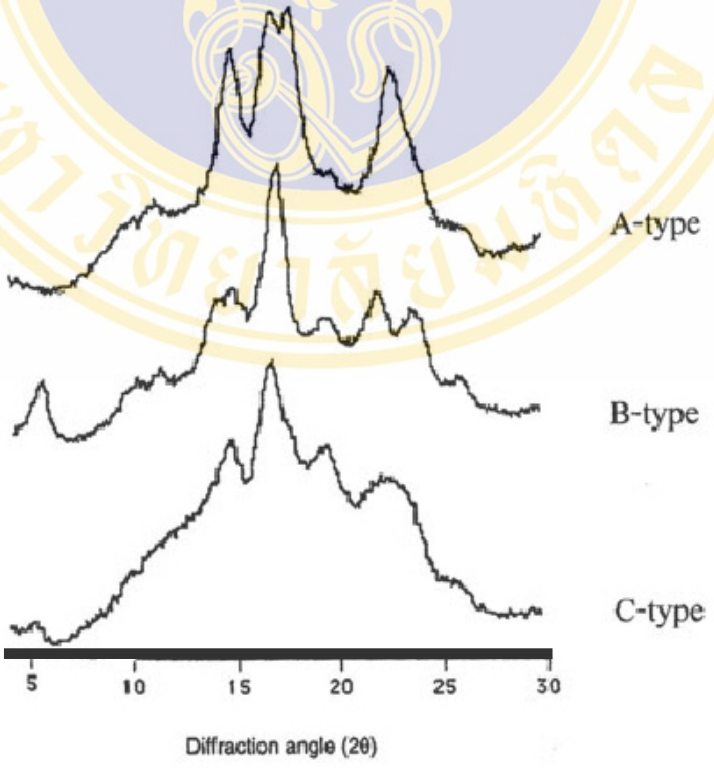

Figure 20 X-ray diffractograms of A-, B- and C-type starch. (Adapted from Cheetam & Tao, 1998)

Yamada et al. (1995) has studies on amylase treatment on maize starch. Amylase treated sample (50 % digestion) exhibited the same pattern of peak in X-ray diffractogram. In case of more digested one (76 % digestion) the peak is entirely changed, that is, almost peaks are disappeared. This indicates that amylase did not selectively attack amorphous region but both crystal and amorphous one, Furthermore, it looks attack rather crystal than amorphous region in final digestion stage. This unchanged of X-ray diffraction pattern was also supported by Tamaki et al. (1997) and Franco et al. (1998).

7.2. Differential scanning calorimetry

Differential Scanning Calorimetry (DSC) is a technique for monitoring changes in physical or chemical properties of material as a function of temperature by detecting the heat changes associated with such a process. It provides the method for obtaining the temperature range of gelatinization and the endothermic heat involved during the gelatinization of the starch (Bean, 1992). Melting of the crystalline structure of the starch granules during the gelatinization transition is an endothermic reaction, that is, it absorbs heat. This heat requirement is called enthalpy. (Bean, 1992). Recently, Cooke and Gidley (1992) have found that the melting enthalpy reflects the melting of double helices rather than the melting of the crystallinity or loss of X-ray crystallinity. Their analysis may explain a low X-ray crystallinity but high ΔH.

DSC is widely applied in the food industry to interpret water, starch, protein, lipid and carbohydrate interactions (Davis, 1994). Stevens and Elton (1971) appear to have been the first to apply DSC to the study of starch gelatinization. Since then, many investigators have used DSC to study starch and starch system.

When starch is heated in the presence of water, two endothermic transitions are observed by differential scanning calorimetry (DSC) (Donovan, 1979; Donovan & Mapes, 1980)

1. At high water:starch ratios, the low temperature endotherm is the only one observed. All the thermal events occur cooperatively due to full plasticization and the superposition of the swelling of the amorphous phase can promote the transformation of crystalline regions to amorphous regions by pulling the crystallites apart resulting in an irreversible melting of crystallites thus gives rise to a single endotherm. At a water

content lower than a certain ratio, the remaining crystallites melts at significantly higher temperatures and a shoulder peak forms a second endotherm (generally labelled as the G and M_1 edotherms) which shifts to a higher temperature as the water:starch ratio decreases.

2. At low water:starch ratios, water penetrates the amorphous regions and the granules start to swell. The swelling of the amorphous regions of the granule by imbibed water, "strip" starch chains from the surfaces of the order crystallites, effectively tearing the crystallites apart in the process known as gelatinization, giving rise to the first endotherm (the G endotherm disappears, leaving only the M_1 endotherm). At this temperature, the gelatinization temperature, the granules loses their birefringence and their X-ray diffraction pattern, which indicates that the ordered regions are being disrupted and material from the granules start to diffuse into the water. If sufficient water is present, all the crystallites might be pulled apart by the swelling, leaving none to be melted at higher temperatures.

The distribution of the amylopectin chain length is thought to be the primary factor that influences the starch gelatinization properties for the following reason. It has been speculated that the free end of the short chain of amylopectin gives rise to a single cluster, consisting of double helices (Manners, 1989). These double helices of amylopectin molecules from the molecular order and the crystallinity in the starch granule. Starches with higher gelatinization temperatures and gelatinization heats might be expected to display a stronger crystalline structure or more molecular order (Cooke & Gidley, 1992). The alteration in the crystalline regions in starch granules, which indicates a change in the distribution of the amylopectin chain length, appeared to influence the starch gelatinization properties.

It is concluded that, within the same botanical origin, an increase in short outer chains in amylopectin molecules reduces the efficiency of packing within the crystalline region of starch granules, resulting in lower T_o, T_p and ΔH. Consequently, starch gelatinization reflects the profile of the molecular architecture of amylopectin short chain but not by the proportion of crystalline region, which corresponds to the amylose-to-amylopectin ratio.

The advantages of DSC for studying thermal properties are as follows:1) it allows use of different water contents and heating rates, 2) transition temperatures and

enthalpy changes of the sample are obtain directly, 3) samples can be perfectly sealed for storage, and 4) it allows small sample size (Nakazawa et al.,1985).

Yamada et al., 1995 have shown that the gelatinization temperature (T_o), T_p, T_c and enthalpy (ΔH) values of DSC of amylase treated starches are almost the same with native samples.

7.3. Rapid Visco-Analyzer (RVA)

The Rapid Visco-Analyzer (RVA) was initially developed as a screening tool to measure α-amylase activity in flour. It has since been modified to include controlled heating and water-cooling features made the instrument more versatile and enable its use in characterization of starch pasting. However, the data for α-amylolysis of starch under observation on RVA is scanty. Jiang and Liu (2002) studied partially hydrolyzation of potato and high amylose corn starch by pancreatic α-amylase. The residues from hydrolyzed starches exhibited markedly decreased in peak viscosity and breakdown but final viscosity values did not show much change.

The RVA has many advantages over the traditional Brabender Visco-Amylograph including small sample size requirement, rapid running time, ease of operation, and provide good reproducibility for measuring starch pasting properites (Deffenbaugh & Walker, 1989; Haase et al., 1995; Panozzo & McCormick, 1993; Walker et al., 1988).

Heated starch granules in the presence of excess water undergo a process called gelatinization. The temperature at which gelatinization occurs is significance, and is followed closely by an increase of viscosity at the pasting temperature. This may be measured in the Rapid Visco-Analyzer (RVA) (Newport Scientific, 1998) as shown in Figure 21.

Irreversible granule swelling follows gelatinization causes a rapid rise in viscosity to a peak value (Peak viscosity as well as peak time). The viscosity indicates the water-binding capacity of the starch. As the shear and heating continues, then cause granule rupture and molecular alignment, which both lead to a “Breakdown” in viscosity to a “ holding strength” dependent on the starch source and test conditions.

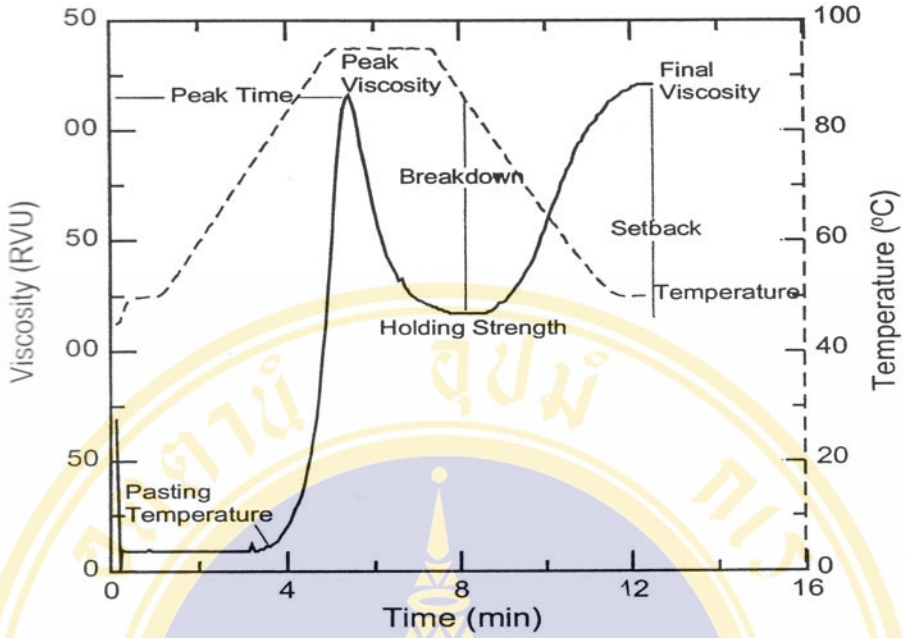

Figure 21 Typical RVA pasting curve showing the commonly measured parameters. (Newport Scientific Pty, Ltd., 1995)

The molecules comprising gelatinized starch begin to reassociate in an order structure through a process called retrogradation. In it initial phases, two or more starch chains may form a simple junction point which then may develop into more extensively orderd regions. Ultimately, under favorable conditions, a crystalline order appears. Thus give rises the final viscosity, which is parameter to define quality of products. It indicates the ability of material to form paste or gel after pasting (Figure 22). The final viscosity may or may not plateau depending on the starch and temperature used.

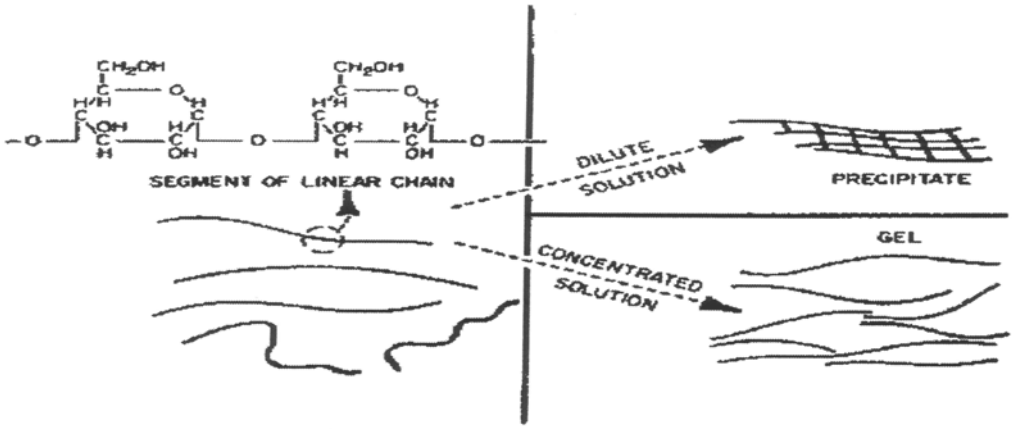

Figure 22 Amylose retrogradation (Solarek, 1986)

From the rheological viewpoint, retrogradation is related to setback (an increase in viscosity during cooling) in the pasting curve, where the starch commonly forms a gel. Large setback has been linked to the association of linear amylose molecules. The setback was correlated with texture of several products. High setback viscosity is also associated with syneresis during freeze-thaw cycles. The pasting properties of different type of starch was shown in Table 3

Table 3 Pasting properties of various types of starches determined by RVA (Newport Scientific Pty, Ltd., 1995)

Starch	Gel temp (^{0}C)	Peak viscosity	Breakdown	Setback	Paste type	Paste clarity
Wheat	52-65	Low	Low/ Moderate	Moderate/ High	Short	Opaque
Maize	62-72	Moderate	Moderate	High	Short	Opaque
Rice	61-78	Moderate	Low/ High	Moderate/ High	Short	Opaque
Tapioca	50-68	High	High	Low	Long	Clear
Potato	56-59	High	High	Moderate	Long	Clear
Sago	60-72	High	High	Low	Long	Clear

8. Hydrothermal treatment of starch

8.1. Annealing

8.1.1. Annealing in general

Annealing, defined as the heating of starch in excess water (or appropriate plasticiser) at temperature between glass transition temperature (T_g) and the onset temperature (T_o) of the native starch (or polymeric system) (Krueger et al., 1987; Larsson & Eliasson, 1991). It is recognised that annealing can be associated with partial gelatinization due to closely relationship of temperature ranges between annealing and gelatinization as shown in Figure 23. However, it is believed that annealing should be applied only where gelatinisation does not occur and hence T_o must not be exceed. In addition, according to this definition, the enthalpy of gelatinisation post-annealing cannot be less than for the native starch.

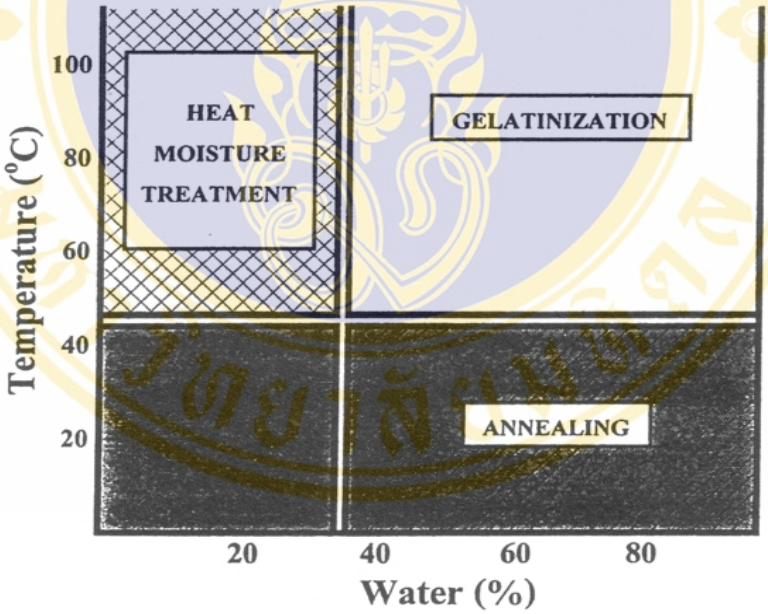

Figure 23 The relationship between annealing, gelatinization and heat moisture treatment (Eliasson and Gudmunddsson, 1996)

Sometimes, annealing type processes are confused with retrogradation. However, annealing of starch granule is a process that retains granular structure and original order. Retrogradation occurs as amorphous α-glucan chains form double helices and, perhaps eventually, aligns themselves in crystallites.

During annealing of starches, there are in essence two thermally driven processes which are intimately related and reflect the moisture content of the system – the elevation of T_g and the gelatinisation temperature (especially T_o). Low moisture causes elevation of (the relatively unplasticised) T_g of starches (Biliaderis, 1991; Biliaderis, 1992; Mizuno et al., 1998; Zeleznak & Hoseney, 1987) and model polymeric system (Bizot et al., 1997; Kalichevisky et al., 1992; Vodovotz & Chinachoti, 1998) which, in the case of starch, intimately reflects the increase in gelatinisation temperatures. Indeed, the elevation of T_g implies a more glassy state and hence reorganisation of amorphous regions.

The annealing process has important industrial implications. Starches may be deliberately annealed to impart novel processing characteristics. However, there are few commercial processes where annealing may be justified in terms of energy and time to generate starches with higher gelatinisation temperatures-especially when many inexpensive chemical process can be employed, over a short time frame, to selectively modify starch characteristics. Often annealing is achieved unintentionally. One example is the wet milling of maize when used to extract starch.

8.1.2. Annealing in structural molecular of starch granule

It has been difficult to define, at the molecular level, what happens to the internal structure of starch granules when they are annealed, Some authors have discussed the molecular event in terms of increasing granule stability (Hoover & Vasanthan, 1994), reorganising granule structure (Krueger et al., 1987) or lowering free energy (Blanshard, 1987). These terms do not, however, give readers a clear molecular picture associated with the reorganisations involved within granules when they are annealed. A number of authors have discussed annealing with more emphasis on the crystalline and amorphous domains. Crystallinity and crystalline “perfection” (optimisation of crystalline order) have been discussed in detail. Similarly, granular reorganisations have been discussed in terms of rigidity (Jacobs et al., 1995) and realignments and partial melting (Marshant & Blanshard, 1978; 1980). Others recognise the importance of interactions between, and mobility of, amorphous and crystalline region (Nazakawa et al., 1984; Stute, 1992) and the constituent amylose and amylopectin molecules (Knutson, 1990).

Testers et al. (1998)(working on wheat starches), have discussed annealing in the context of hydration and swelling of amorphous regions (temperature range between T_g and T_o), which facilitates ordering of double helices in crystalline regions. This ordering of double helices could be associates with minor optimisation of double helix length, although no additional double helical material is formed. The amorphous material post-annealing probably becomes more "glassy" (more rigid and less mobile) whereupon T_g is elevated. The constancy of double helix content pre- and post-annealing has also been shown by Jacob and Eerlingen (1998) for a range of starches (pea, potato and wheat).

The data from the study of NMR (Testers et al., 1999) and Wide angle X-ray scattering (Stute, 1992) are supported in the same general picture that annealing causes no significant increase in crystalline material formed within starch granules by either of two possible mechanisms: (i) formation of double helices (which need not necessarily be associated with existing crystalline domains) or; (ii) major increase in amount of crystallinity as a consequence of ordering of previously amorphous regions. Rather, the enhanced ordering of double helices, due to improved registration (alignment), with associated increase rigidity of amorphous regions, probably underlies the annealing process. In case of small angle X-ray scattering results from Jacobs et al (1998) showed that the repeat distances of the crystalline and amorphous lamellae remain unchanged (10.5 nm in wheat and 9.9 nm in potato), although there was an increase in peak intensity.

From many evidences of research above, it is believed that annealing represents the physical reorganization of starch granules (or appropriate polysaccharide matrices like amylose-lipid complexes) from the plasticisation of the amorphous lamellae and annealing of double helices is represented in Figure 24.

8.1.3. Effect of annealing to properties of starch granule

The annealing treatment causes drastic changes of the gelatinization characteristics. As the result of annealing, the gelatinization endotherms of annealed starches from various botanical origins show a shift of the endotherms to higher gelatinization temperature (especially T_o and T_p), the gelatinization temperature range (T_c-T_o) is narrowed and enthalpy of gelatinization is increased (Krueger et al., 1987;

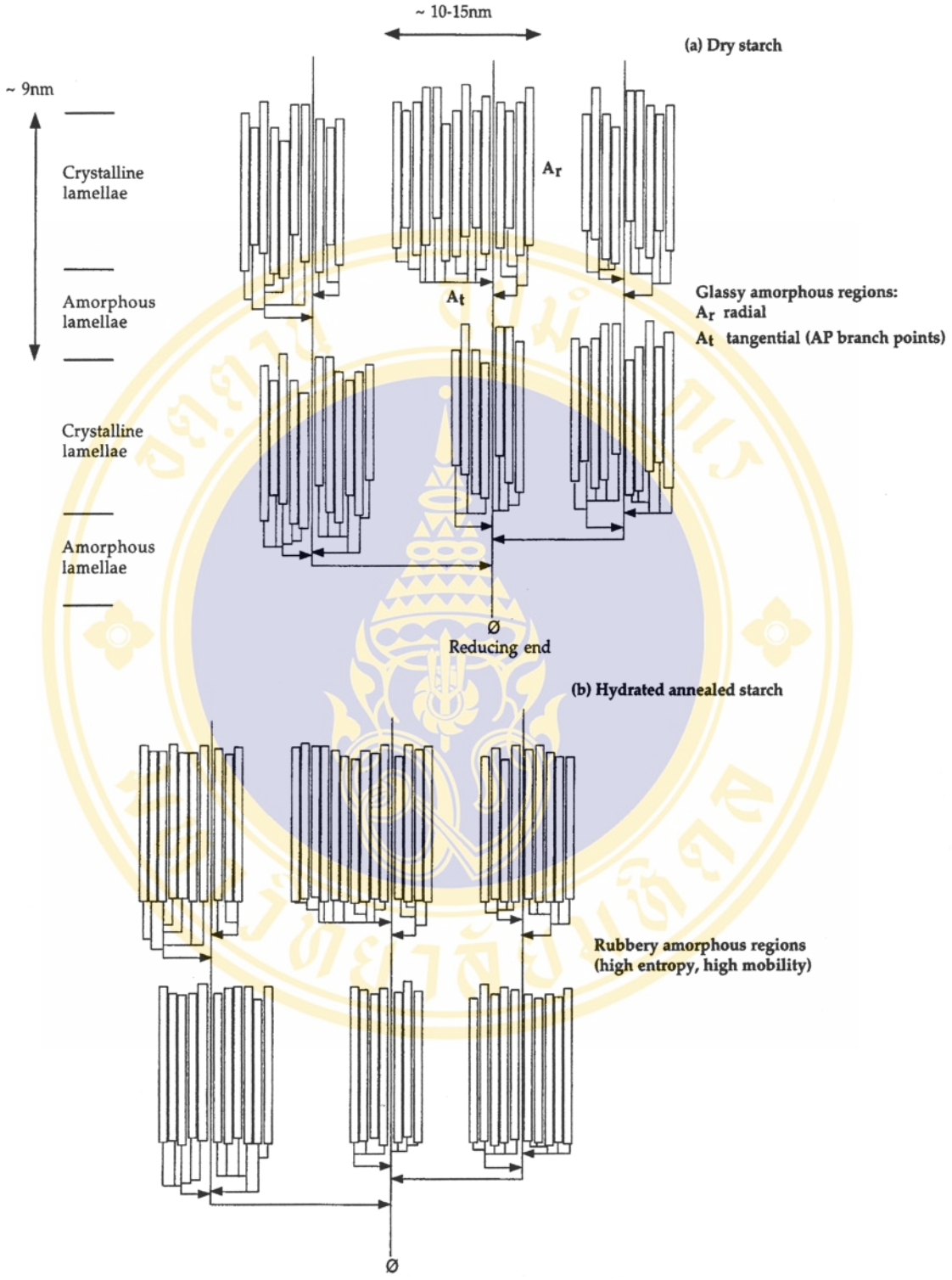

Figure 24 Pictorial representation of the effect of hydration and subsequent annealing on the semi-crystalline lamellae (amylopectin double helices are represented as rectangles): (a) dry starch with glassy amorphous regions; (b) hydrated annealed starch with rubbery amorphous regions (Adapted from Waigh et al., 1997).

Paredes-López et al., 1989; Knutson, 1990) or unchange (Larsson & Eliasson, 1991; Stute, 1992) (Figure 25). Annealing does not result in changes in the X-ray patterns (Gough & Pybus, 1971; Stute, 1992). Possible explanations for these phenomena include (i) crystallite growth or perfection (Larsson & Eliasson, 1991), or (ii) alterations of the coupling forces between crystallites and the amorphous matrix (Stute, 1992).

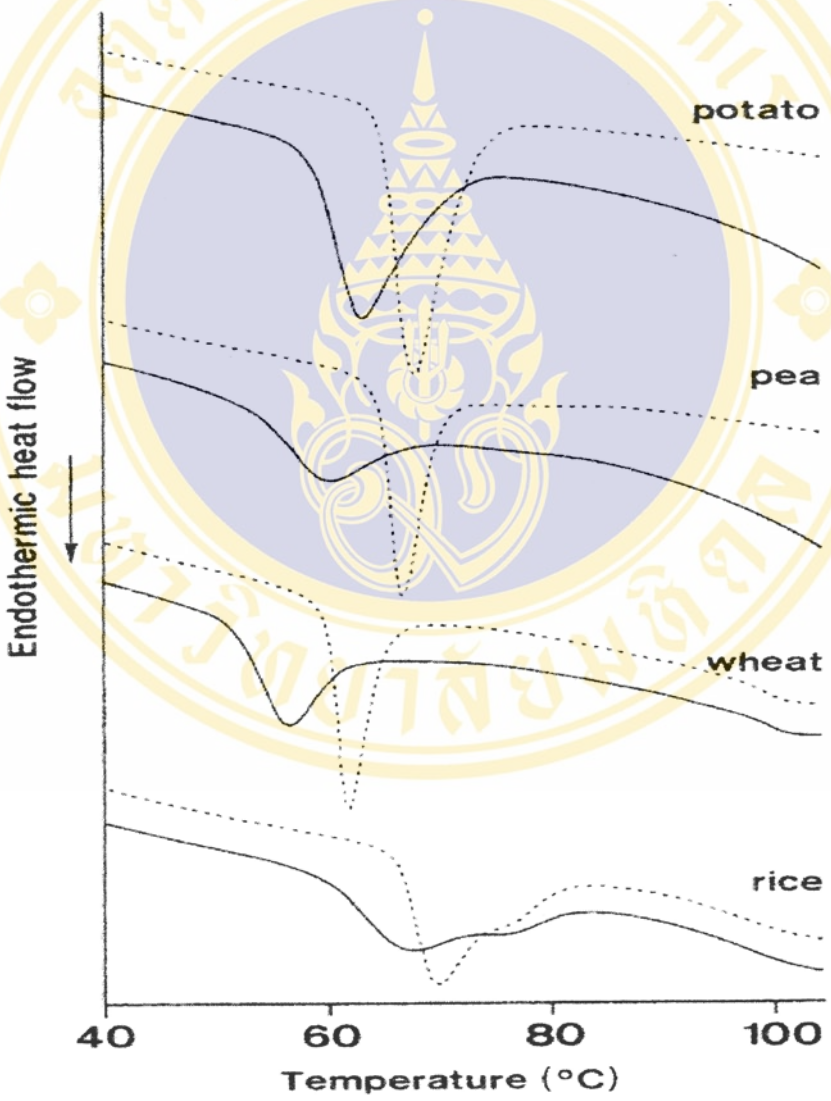

Figure 25 Differential scanning calorimetry patterns of native (—) and annealed (---) starch from various botanical origins (Jacobs et al., 1995).

According to some author (Hoover & Vasanthan, 1994), annealing causes no effect on granule dimensions or shapes, although early microscopic work indicated that wheat starch granule dimension increase after annealing (Gough & Pybus, 1971).

Annealing also affects the pasting properties of starches. With the Brabender visco-amylograph, Stute (1992) observed a higher onset temperature, a lower peak viscosity and a higher viscosity on cooling as a result of annealing of potato starch. The observations were ascribed to a reduced swelling power of the starch granules, resulting in as enhanced shear stability of the granules and, hence, a higher setback. Deffenbaugh and Walker (1989) and Jacobs et al. (1996) used the rapid visco-analyzer (RVA) to measure the effect of annealing. With this instrument, differences in pasting properties of native and annealed starches were detected. Thus, although the pasting properties measured with the RVA are altered by the annealing treatment, the observed effects depend on the source of the starch.

The annealing itself leads to little solubilisation of α-glucan (Testers et al., 1998). This is important as it shows that improved order is a genuine molecular event rather than a consequence of leaching amorphous α-glucan and hence "concentrating" crystalline material. The amylose must be more restricted from leaching out of the granules. Although at a given temperature post-annealing, the granules will swell less than un-annealed starches and this will be the primary restraint to leaching. This does, however, strengthen the view that there is molecular reorientation in the starch granule which makes the amorphous material more glassy with an elevated T_g.

8.2. Gelatinization

8.2.1. Gelatinization in general

Starch molecules have a large number of hydroxyl groups, which also tend to attract each other. As a consequence hydrogen bonds are directly formed between adjacent starch molecules or indirectly formed with water. Even though the hydrogen bonding forces are weak, there are so many such bonds in a starch granule that starch does not dissolve in cold water below its gelatinization temperature. This is of importance since it enables an easy extraction of starch granules from plant source in aqueous systems. Additionally, chemical modification can be performed in starch

suspension, which is subsequently purified by filtration, washing with water and drying.

Starch granules are generally insoluble in water below 50 ^{0}C. But can imbibe water reversibly; that is, they can swell slightly, and then return to their original size on drying. When starch granules are heated in an excess water, above 60 % of the total wet weight (w.t.), beyond a critical temperature (55-80 ^{0}C, depending on starch type). The hydrogen bonds which responsible for the structure integrity are weaken that allow the penetration of water which cause the hydration of the linear segment of the amylopectin. Starches from roots including the tapioca starch generally swell at lower temperatures and to greater extent than the common cereal starches because of high amount of weak hydrogen bonds in the structure which easily hydrate and highly swell. The granules absorb a large amount of water and swell to many times their original size until irreversible granule swelling was occurred. It undergoes an irreversible order-disorder transition called gelatinization as shown in Figure 26.

In the first stages of gelatinization the shorter micelles dissociate, while the longer micelles still persist to higher temperature and also gas bubbles develop in the central part of the starch granules and part of the amylose is solubilized and exuded (Sandstedt, 1955; Leach et al., 1959). Upon raising the temperature of a starch suspension, each individual granule gelatinizes quite sharply, not all the granules in the same suspension gelatinize at the same temperature, but rather over a range of 8-10 ^{0}C. That is to say, the gelatinization process of a starch suspension cannot be defined as to take place at certain temperature, but rather during a certain temperature range. On the whole, the smaller granules start to gelatinize at higher temperature (Whistler et al., 1984). Then starch granules undergo more or less intense swelling depending on water availability. The swelling of granules and the concomitant solubilization of amylose and amylopectin gradually improve digestibility and induce the loss of granular integrity and then may burst or rupture, themselves giving rise to a viscous solution when gelatinization is achieved (Leach et al., 1959).

Starch gelatinization is also affected by the solvent other than water, for example, liquid ammonia, formamide, formic acid, chloroacetic acids and dimethylsulfoxide. These solvents disrupt hydrogen bonding within the starch granule by forming soluble complexes with starch. Furthermore, some chemicals can decrease or increase starch gelatinization temperature. Salts, such as, sodium chloride and sodium sulfate as well as sugar are used to raise the gelatinization temperature of starches being derivatized. In addition, the amylose-lipids complexes in cereal starches inhibit granule swelling that is increasing in pasting temperature (Whistler et al., 1984).

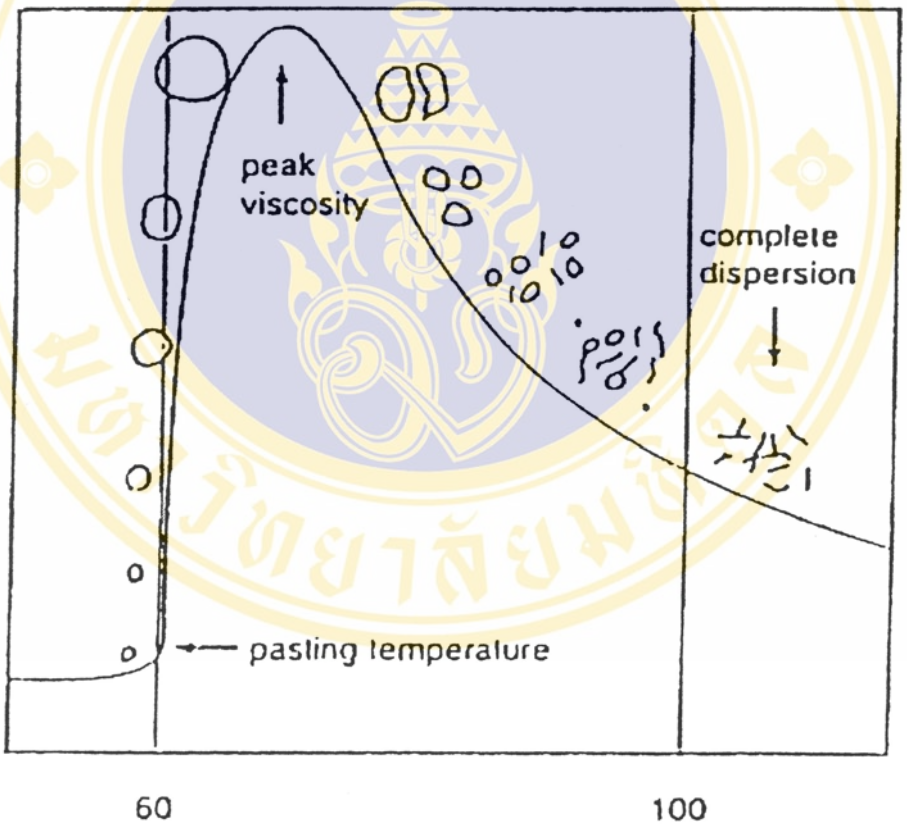

Figure 26 Swelling, disruption and dispersion of a starch granule during gelatinization process (Sanders, 1996).

8.2.2. Gelatinization in structural molecular of starch granule

Gelatinization is a term used to describe the molecular events associated heating starch in water. Starch is converted from a semi-crystalline, relatively indigestible form to (eventually) an amorphous (readily digestible) form. This gelatinization process (in excess water) is believed to involve primary hydration of amorphous regions around and above T_g, with an associated glassy-rubbery transition. Perhaps the relatively large amorphous growth ring type regions are the primary amorphous regions to hydrate, followed by amorphous lamellae "sandwiched" between the crystalline lamellae. The water induces a transition of the amorphous regions from a rigid glassy state to a mobile rubbery state, which in turn facilitates the hydration, and dissociation of double helices in crystallites. The dissociation of the crystallites begins after T_g of amorphous regions, and at this temperature (T_o), limited dissociation of amylopectin double helices (most of which are in crystallites) is associated with limited swelling of granules.

This in turn facilitates molecular mobility in the amorphous regions (with reversible swelling) which then provokes an irreversible molecular transition. This irreversible step involves dissociation of double helices (most of which are in crystalline regions) limited by the geometric size of the lamellae as discussed by Matveev et al. (1998) and Cooke and Gidley (1992), and expansion of granules as the polymers (and granule interstices) hydrate. The onset temperature (T_o) of DSC reflects the initiation of this process, which is follow by a peak (T_p) and conclusion (T_c). After T_c, all amylopectin double helices have dissociated as shown in Figure 27, although swollen granule will be retained until more extensive temperature and shear have been applied. Beyond approximate 95 ^{0}C a molten (unordered) state of viscous-flow amorphous gel is formed.

In addition, the application of heat was shown to cause "breakdown" of the amylopectin layers in the granule, starting from the granule center and progressing centrifugally towards the granule surface, leading to the formation of starch granule ghosts (Atkin et al., 1998; Atkin & Abeysekera & Robards, 1998).

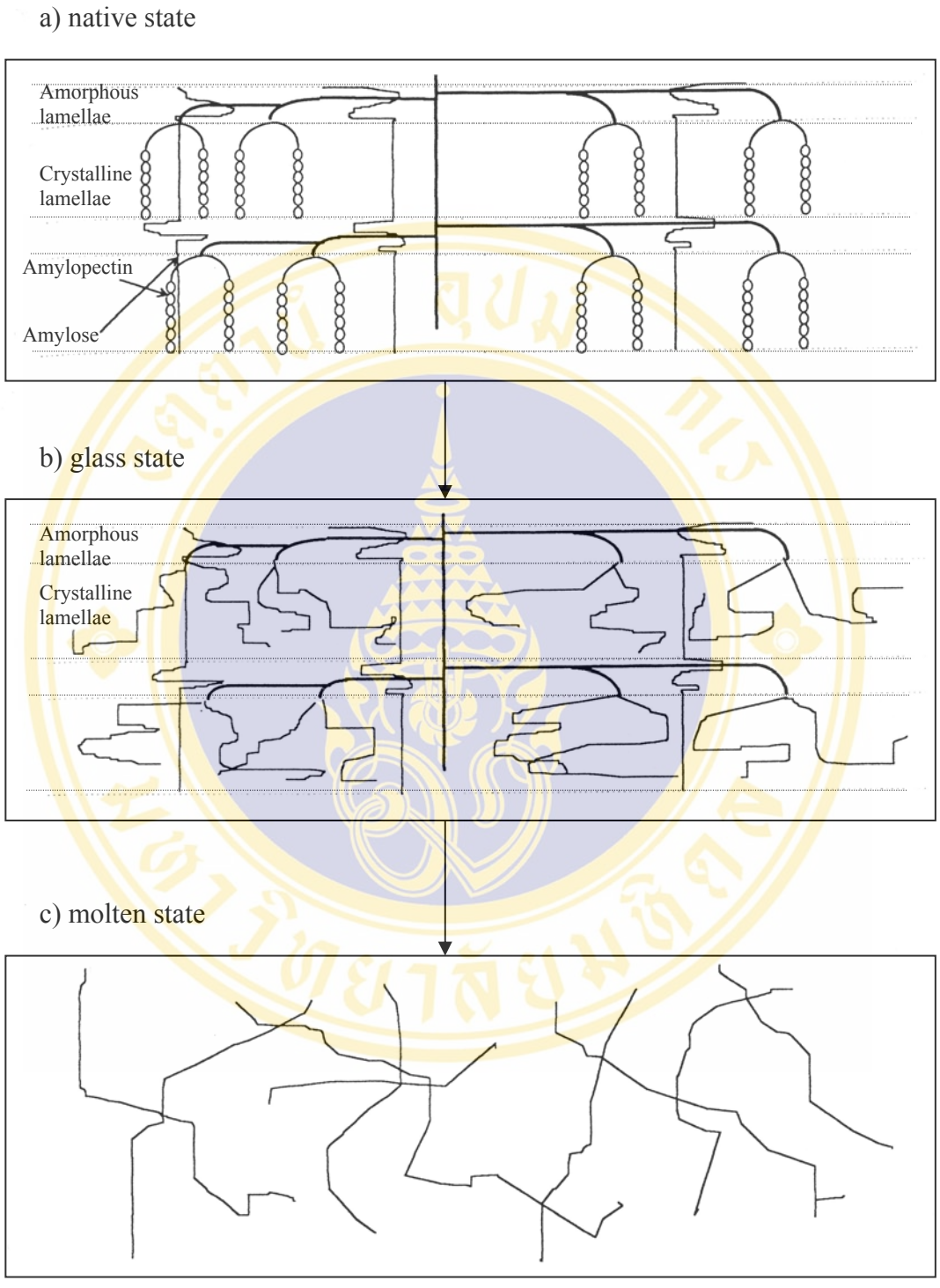

Figure 27 Schematic presentation of the melting process of native starches, (a) native (ordered) state, (b) glass state, and (c) molten (unordered) state. (Mateev et al., 1998)

8.2.3. Effect of gelatinization to properties of starch granule

The transition state in gelatinization process can be characterized by an endothermic process in differential scanning calorimetry (DSC), although it could involve the following two stages (Steven & Elton, 1971): Cleavage of existing hydrogen bonds (endothermic) and formation of new bonds (involving water) to give a less ordered structure (exothermic). Gelatinization induces loss of birefringence observed using polarized light microscopy and a disappearance of the crystalline X-ray diagram.

9. Effect of hydrothermal treatment on α-amylolysis of enzymatic-modified starches

Certain studies have indicated that annealed wheat, barley and sago starches are more easily hydrolysed by α-amylase than native starches (Gough & Pybus, 1971; Lorenz & Kulp, 1984; Wang et al., 1997).

Wang et al. (1997) was suggested that the degree of amylolysis be increased after annealing and the granule degradation pattern also altered from the un-annealing starch – from surface erosion to preferential digging of the internal regions of the granule (Figure 28). Section of the hydrolysed granule residues revealed that enzymes attacked from one point on sufficiently annealed granules, and that after extensive hydrolysis, only an empty shell remained.

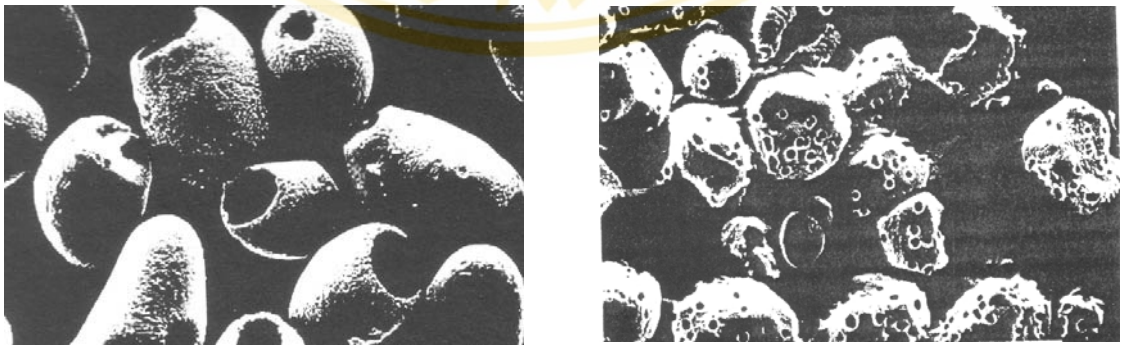

(A) (B)

Figure 28 Starch granules treated with glucoamylase and Thermamyl (A) with annealing (B) without annealing (Wang et al., 1997).

This has, however, been contradicted by other research on wheat, lentil and potato starches (Hoover & Vasanthan, 1994; Kuge & Kitamura, 1985), although small starch granule (oat) have been reported to be much more easily hydrolysed post-annealing (Hoover & Vasanthan, 1994). However, the rate of α-amylase hydrolysis for different starches follows two distinct phases: an initial rapid then subsequent slow phase. Annealing alters the extent of hydrolysis of these different phases as a function of botanical origin. During the second phase of hydrolysis, annealed wheat and pea starches are more resistant to α-amylase hydrolysis whilst the inverse was true in potato starch (Jacobs & Eerlingen, 1998). Although, the botanical origin of starch is important with respect to hydrolytic pattern, the surface area to volume ratio is probably of more significance than the actual plant source. It is also possible that the annealing process creates pores or fissures which alter the pattern of amylase hydrolysis from surface to internal erosion (Wang et al.,1997). Hence, although amorphous and crystalline lamellae become more ordered, accessibility to the amorphous regions by enzymes is facilitated.

Annealing can be conducted in the presence of amylase to selectively hydrolyse amorphous regions and the possibility of novel products with unique gelatinisation and swelling characteristics (Stoof et al., 1997; 1998). Both potential starch and glucose syrup products are possible using this general approach.

Lauro et al. (2000) studied the effect of partial gelatinization on α-amylolysis of barley starch granules. Partial gelatinization changed the hydrolysis pattern of large barley starch granules; the pinholes typical of α-amylase-treated large starch granules could not be seen (Figure 29). The lack of pinholes suggests that changes in the granule surface structure occurred during partial gelatinization. Moreover, the increased susceptibility of partially gelatinized barley starches granules to α-amylolysis correlates with the decrease in the gelatinization enthalpy (Lauro et al., 1993).

The gelatinization starch, which followed by α-amylase treatment, was observed by Bertoft et al. (2000). As gelatinized, the amylopectin of starch was easily hydrolyzed into small dextrin by the α-amylase. Moreover, long internal chain segments that are easily attacked by the enzyme were no longer present.

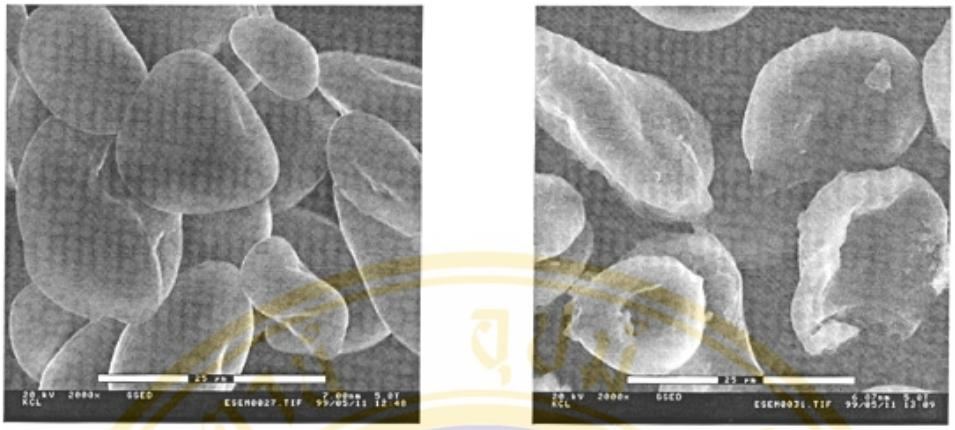

(A) (B)

Figure 29 Effect of α-amylase on partially gelatinized barley starch granules: (A) reference sample, (B) hydrolysis residue. (Lauro et al., 2000)

10. Starches as fillers for direct compression process in pharmaceutical industry

One of the most commonly used excipients in compressed tablets is starch since it can be used as filler, binder, disintegrant or lubricant in tablet formulation (Rubinstein, 1988). When incorporated into formulations starch exerts a favourable influence on dissolution rate of active medicament in a tablet (Underwood, 1972).

10.1. Direct compression

Compress tablets are defined as solid-unit dosage form made by compaction of a formulation containing the drug and certain fillers or excipients selected to aid in the processing and properties of the drug product.

Compressed tablets are the most widely used of all pharmaceutical dosage forms for a number of reasons. They are convenient, easy to use, portable and less expensive than other oral dosage forms. They deliver a precise dose with a high degree of accuracy. Tablets can be made in a variety of shapes and sizes limited only by the ingenuity of the tool and die maker (i.e. round, oval, capsule-shape, square, triangular, etc.).

However, most drugs cannot be compressed directly into tablets because they lack the bonding properties necessary to form a tablet. The powder drugs, therefore,

require additives and treatment to confer bonding and free-flowing properties on them to facilitate compression by a tablet press.

Compressed tablets may be prepared by wet granulation, dry granulation, or direct compression process, the step of three compressing tablets was shown in Table 4.

The most preferred and economical tableting method, direct compression, requires only four steps from weighing, mixing the dry components, admixing the lubricant and compressing the mixture into tablets as shown in Table 4 and Figure 30. Usually, the excipients include filler, disintegrant and lubricant (Sheth et al., 1987).

Table 4 Steps in the production of tablet by wet granulation, dry granulation and direct compression.

Wet granulation	Dry granulation	Direct compression
1. Weighing	1. Weighing	1. Weighing
2. Mixing	2. Mixing	2. Mixing
3. Preparing binder solution	3. Preparing slug by precompression	
4. Moistening		
5. Wet screening		
6. Drying		
7. Dry screening	4. Dry screening	
8. Admixing disintegrant, lubricant	5. Admixing disintegrant, lubricant	3. Admixing disintegrant, lubricant
9. Compressing	6. Compressing	4. Compressing

To the pharmaceutical manufacturer, the direct compression method provides advantages in that it requires a lesser investment in equipment and space, lower operating cost in terms of labor and power, eliminating of granulation process and variability in granulation (Mendes & Roy, 1978). The elimination of wet and dry

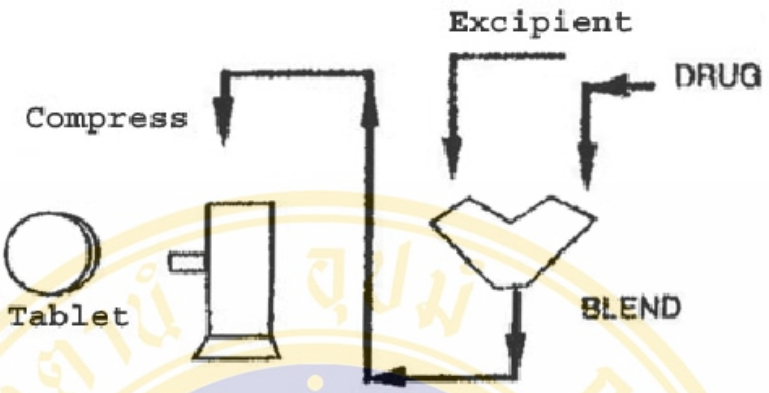

Figure 30 Direct compression tablet

granulation step increases the stability of drugs that can degrade by mechanical, moisture and/or heat. Another advantage of direct compression is that the tablets generally disintegrate into primary particles, rather than into granules. The increase surface area for dissolution may in the fast drug release for some drugs and some drug products. For the majority of tablet formulations, the efficiency of the disintegrant is strongly dependent on the nature of the filler-binder (Van Kamp et al., 1986).

The direct compression process also has a number of limitations. Tablets containing a high dose of an active ingredient that has poor compactability, poor flow properties, and/or low bulk density cannot be prepared by direct compression, because filler-binders have a limited dilution potential, and tablet size and weight are limited. However, if an active ingredient is more compressible and flowable, a greater proportion can be carried successfully by a filler-binder.

The direct compression process generally involves mixing a drug substance with excipient prior to compaction, Because of different in density of the drug substance particles and excipient particles, direct compression blends are subject to segregation transferring steps from the mixer to drum, tote bins, hoppers, and so on. The procedure of sampling for analysis must be well defined so that it does not introduce the major error in determining homogeneity of the powder blend. Segregation during the handling of the powder blend before compression and during sampling is a major disadvantage of the direct compression method. Careful

consideration must be given to particle size distribution and density of the drug substance and excipients. However, many low-dose drug substances are reduced in particle size in order to obtain uniform dosage or to obtain a large effective surface area in the dosage form for rapid dissolution (Bolhuis & Chowhan, 1996).

Another disadvantage of direct compression is Most direct compression fillers are produced in the United States or Europe, thereby cost of the filler in some region may be high, as compared to the binders and fillers used in wet granulation. Thus the direct compression technique may not offer any economical advantage over the wet granulation product (Mitrevej et al., 1996).

10.2. Fillers

Fillers, also called diluents or bulking agents, are inert materials that are added to a formulation to increase the bulk of the tablet so that the formulation becomes suitable for compression. Such materials are primarily used in instances in which the active ingredient is of the high potency or low-dosage variety (Sheth, 1987; Mendes & Roy, 1979).

The most important requirements for directly compressible filler are listed below (Sheth, 1987; Bolhuis & Chowhan, 1996).

1. The material should have high compressibility and high flowability
2. It should be physically inert, colorless and tasteless.
3. It should have high stability without any physical or chemical change on aging and should be stable to air, moisture and heat.
4. It should be compatible with all types of active ingredients.
5. It should be relatively inexpensive.
6. It should not interfere with the biological availability of active ingredients.

The first tablet filler for direct compression was introduced in late 1950's. Over the past 30 years, several direct compression fillers have been developed. The products are based, among others on starch, cellulose, inorganic calcium salts, lactose and other sugars (Bos et al., 1992). Two main parameters are taken into account during the development of the direct compression filler, i. e., flowability and compressibility. Good flowability ensures uniformity in die fill and thus uniformity in tablet weight. It also facilitates blending of fine powders encountered in direct

compression blends. Moreover, the fillers should yield tablets of adequate hardness without applying excessive compression force (Shangraw, 1989; Bolhuis & Chowhan, 1996). Tablets produce from new filler must then be evaluated for such parameters as hardness (crushing strength), friability and disintegration or dissolution (Mendes & Roy, 1979).

Most all of the classic tablet fillers have been modified in one way or another to provide fluidity and compressibility. In viewing the scanning electron photomicrographs of the various direct compression filler-binders, one is taken with the fact that none of the products consist of individual crystals instead, all of them are actually minigranulations or agglomerations that have been formed in the manufacturing process by means of cocrystallization, spray drying, etc. The resulting material thus is able to deform plastically in much the same manner as the larger particle size granules formed during the traditional wet granulation process. The key to making any excipient or drug directly compressible thus become obvious and the possibility of making all tablets by direct compression appears to be within the scope of present technology.

10.3. Modified starches as direct compression fillers

In pharmaceutical manufacturing, starch is employed as the common stuffing material to form pills and tablets by making use of its aggregating property.

Starch is naturally occurred filler. Its advantages are that it is white, insoluble, neutral and non-reactive. However, it is not widely used as a filler in compressed tablets because it has compressibility too poor to make tablet of sufficient hardness and also tends to expand after compression (Sheth, 1987). There have been many attempts to modified starch to improve its compressing and flow properties. Special starch products, which are accepted in direct compressible quality, are subjected to modifications as described below.

10.3.1. Pregelatinized starch

Pregelatinized starch is a starch that has been chemically and/or mechanically process to rupture all or part of the granules in the presence of water and subsequently dried. Similar to regular starch, pregelatinized starch is a multi-purpose excipient. It

can also be used as filler, binder and disintegrant. Its binding properties are slightly greater than starch when it used in place of starch as starch paste (Karr et al., 1990). Starch® 1500 (Colorcon Ltd.) is pregelatinized starch prepared from corn starch that has received wide spread acceptances in directly compressible quality. It is prepared by subjecting corn starch to physical compression or shear stress in high-moisture conditions causing an increase in temperature and a partially gelatinization of some starch granules. It consists of both individual and aggregated starch granules bonded to the gelatinized starch (Bolhuis & Chowhan, 1996). Although pregelatinized starch will readily compact by itself, it does not form hard compacts. Moreover, its flow properties are poor when compared with other fillers, so its filler potential is considered minimal and not generally used without combining with other fillers (Sheth, 1987).

10.3.2. Spray dried starch

In an evaluation of several native starches, rice starch was proved to have much better compaction properties than potato, maize and tapioca starch. However it exhibited worst flowability, cause by its fine particle size as compared to the other starches (Bos, 1987). Recently, modified rice starch was introduced (Mitrevej & Varavinit, 1992). Modified rice starch is produced by spray-dried modification of rice starch and is composed of aggregates of rice starch spherical grains. Since rice starch posses small particle size and polygonal shape; upon spray drying, the rice starch grains can easily form spherical aggregates. The spray dried rice starch had been proved to exhibit excellent flowability and good compactibility (Bos et al., 1992; Mitrevej et al., 1995; Mitrevej et al., 1996). It should have gained greater popularity than it happens to be. The fact is that the rice starch, as a starting material, itself is not widely available.

On the contrary, tapioca starch is believed to be in excess of demand in Thailand due to the enormous cultivation of cassava. Any modified forms of tapioca starch should be more feasible in commercial aspect than those of rice starch, unless rice starch has to be sufficiently available. Since tapioca starch grains have one flat side and smooth surface, the spraying process can not produce aggregates of tapioca starch. At present, research on the spray dried modified tapioca starch is being

conducted. The tapioca starch is modified such that the starch grains are able to be cohere and form suitable size aggregate upon spray drying. The preliminary evaluation indicate the possibility of producing tapioca starch for the direct compression purpose.

Spray drying involves atomization of an aqueous solution or suspension into a spray, contact between spray and hot air in a drying chamber resulting in moisture evaporation and recovery the dried product from the air. Because of the spherical nature of liquid particles after evaporation of water, the resulting spray-dried material consists of porous, spherical agglomerates of solid particles that are fairly uniform in size. The particle size distribution of the spray-dried material is controlled by the atomization process and the type of drying chamber (Bolhuis & Chowhan, 1996). The spherical nature of the agglomerated granules, resulting from spray drying, improves the flowability of rice starch. So far, there is no report on the success of using other spray-dried starches as the tablet filler.

10.3.3. Cross-linked gelatinized high amylose starch

When starch is treated with multifunctional reagents, such as phosphorus oxychloride, epichlorohydrin and sodium trimetaphosphate, cross-linking occurs. The reagent introduces intermolecular bridges or cross-links between molecules, thereby reinforcing hydrogen bonds holding starch chains together (Rutenberg & Solarek, 1984). Cross-linking of gelatinized high amylose starch was introduced a few years ago as an excipient for controlled drug release (Lenaerts et al., 1991). It is prepared by gelatinizing high amylose starch, then cross-linking with epichlorohydrin (Dumoulin et al., 1998; Le Bail et al., 1999). It was found that covalent cross-linking of gelatinized high amylose starch at the suitable degree can increase the hardness of the tablets (Ispas-Szabo et al, 2000). The authors explained that the maximal value of cross-linking of gelatinized high amylose tablet hardness was a result of maximal stabilization of the system by both covalent and hydrogen bonding when the polymeric chains rearranged after compression. So far, cross-linking in the granular state has never been studied as a method for the tablet filler preparation.

10.3.4. Acid modified spray-dried starches

Puchongkavarin et al. (2003) was proposed that the higher order structure of acid modified waxy rice starch used as fillers in tablet compression. This was in agreement with Atichokudomchai et al. (2001) and Atichokudomchai and Varavinit (2003) which modified tapioca starch by acid treatment. Hydrolyzed waxy rice starch with 6 % (w/v) Hydrochloric acid solution at room temperature will increase relative crystallinity, whereas decrease in amylose content and decrease (Puchongkavarin et al., 2003) or unchanged (Atichokudomchai et al., 2001) in median particle size of granular starches, due to acid attack. This was resulted in pronounced crushing strength and produced longer disintegration time, which contrast with friability of the tablets. The appearance of exo-corrosion distributed over the surface of acid-modified starches was observed under Scanning Electron Microscope (SEM). The highly crystalline and spherically agglomerating granules of the produced starch modifications demonstrated substantial improvements in functional properties and could therefore be employed as alternative tablet fillers in the relevant pharmaceutical industry.

CHAPTER III
MATERIALS AND METHODS

1. Materials

1.1. Starches

Native tapioca starch and native rice starch were kindly supplied by Cho Heng Rice Vermicelli Factory Co. Ltd., Nakornpathom, Thailand.

1.2. Enzyme

Termamyl 120L type LS (a thermostable *Bacillus licheniformis* α-amylase, product of Novo Nordisk-industri A/S, Denmark) was donated, by Cho Heng Rice Vermicelli Factory Co. Ltd., Nakornpathom, Thailand, for this investigation.

1.3. Chemicals and reagents

Glacial acetic acid, calcium chloride dihydrate, glycerol, iodine, sodium hydroxide, sulphuric acid and magnesium stearate were purchased from Merck KGaA. Darmstadt, Germany. All chemical reagents are analytical grade. Silver nitrate was purchased from Fisher Scientific, UK. Potassium Iodide was procured from BDH Laboratory Supplies, England. Ethanol, potato amylose (Type III, product number A0512) was obtained from Sigma Chemical Co., St. Louis MO, USA and the damaged starch assay kit was purchased from Megazyme International Ireland Ltd., Ireland.

1.4. Instruments

The general laboratory equipments were used throughout this study and also some special instruments were employed in this study including a Mobile Minor Spray Dryer (Type 2627, Rotary atomizer, Gea-Niro, Copenhagen, Denmark), sieve size 40 and 200 mesh sifter (Laboratory Test Sieve, Endecotts Ltd., England), Bruker

Advance X-ray powder diffractometer (D-8 type, Bruker, Karlsruhe, Germany), Laser diffraction spectrometer (Malvern instruments Ltds, Melvern, UK), sample dispersion accessory unit (Hydro 2000S), Fluorescent light microscope (Olympus BX 51) with camera set (Olympus DP 12), JOEL JSM-5410LV microscope (JOEL, Tokyo, Japan), Rapid Visco-Analyzer (Series 4V, Newport Scientific Pty. Ltd, Warriewood, Australia), Differential Scanning Calorimeter (DSC6, Perkin Elmer, Norwalk, CT), single punch rotary tablet machine (Type N3B. Narongkarnchange. Bangkok, Thailand), electronic hardness tester (Schleuniger Model 4M Dr Schleuniger Co.,Switzerland), Roche type friabilator (Narongkarnchang, Thailand), USP disintegration apparatus (Hanson Model QC 24, Hanson Research Corp., USA), thermostatted water bath (GFL, Germany), hot air oven (Model SLM 400-800 Memmert, Universal, Germany), moisture analyzer (MA 30-000V2, Sartorius Ao Gottingen, Germany), spectrophotometer (Genesys 20, Thermospectronic, USA), micro-pipettors; 100, 500, 1000 and 5000 microlitre (Gilson Pipetman, France), bench centrifuge (Sigma 2-5 D-37520 Osterode an Harz, Germany) and centrifuge (Sorvall RC 3B Plus, Sorvall Instruments, Dupont, USA).

2. Methods

2.1. Preparation of spray dried native tapioca starch (SNT)

Native tapioca starch 900 g (dry basis) (Choheng Co., Ltd. (Thailand)) was suspended with agitation in distilled water 3000 ml to obtain 25 % (w/w) solid content of solution. The suspended solution was subjected to spray drying (Centrifugal type Mobile Minor Spray Dryer type 2627, Rotary atomizer, Gea-Niro, Copenhagen, Denmark) at an inlet temperature of 160 °C and an outlet temperature of 60 °C. The spray dried native starch was sieved through a 200-mesh sifter, then the remaining starch on the 200-mesh sifter was again passed through 40-mesh sifter to obtain spray dried native tapioca starch.

2.2. Preparation of spray dried annealed tapioca starch at higher temperature (SANT-H)

Native tapioca starch 900 g (dry basis) was suspended in distilled water 3000 ml with 500 ppm of calcium chloride to obtain 25 % (w/w) solid content of suspension. The solution was heated in water bath at 60 °C for 90 min and spray dried by inlet temperature 160 °C and an outlet temperature of 60 °C following by screening size as previously describe in SNT to obtain spray dried annealed tapioca starch at higher temperature.

2.3. Preparation of spray dried annealed tapioca starch at lower temperature (SANT-L)

900 g (dry basis) of native tapioca starch was suspended in distilled water 3000 ml to obtain 25 % (w/w) solid content of solution. The suspended solution was heated with agitation in water bath in annealing temperature range to minimize the partial gelatinization effect, which was at 55 °C and subjected to spray drying at an inlet temperature of 160 °C and an outlet temperature of 60 °C. The spray dried annealing tapioca starch was obtained by sieved through a 200-mesh sifter, then the remaining starch on the 200-mesh sifter was again passed through 40-mesh sifter.

2.4. Preparation of spray dried combined annealing and enzymatic hydrolyzed tapioca starch (SANET)

Native tapioca starch 900 g (dry basis) was suspended in distilled water 3000 ml with 500 ppm of calcium chloride to obtain 25 % (w/w) solid content of suspension. The suspension was heated in water bath at 60 °C for 90 min. Since the temperature used in this study nearly onset temperature of starch from tapioca starch (63 ^{0}C). Thermostable alpha-amylase has been used to retain their activity at higher temperature. The enzyme hydrolysis of tapioca starch was performed at various reaction time (15, 30 and 60 min) by adding 0.5 % (v/w) Termamyl (NOVO industry) into the suspension. The modified starch was then subjected to spray drying by inlet temperature 160 °C and an outlet temperature of 60 °C following by screening size as stated earlier from SNT to obtain spray dried combined annealing and enzymatic hydrolyzed tapioca starch.

2.5. Preparation of spray dried native rice starch (SNR)

900 g (dry basis) native rice starch (Choheng Co., Ltd. (Thailand)) was suspended in distilled water 3000 ml to obtain 25 % (w/w) solid content of solution. The suspension was heated in water bath at 70 °C for 150 min, and spray dried with inlet-air at 160 °C and outlet-air at 60 °C to obtain spray dried native rice starch.

2.6. Preparation of spray dried annealed rice starch at higher temperature (SANR-H)

900 g (dry basis) native rice starch was suspended in distilled water 3000 ml with 500 ppm of calcium chloride to obtain 25 % (w/w) solid content of suspension. The suspension was heated in water bath at 70 °C for 150 min, and spray dried by inlet temperature 160 °C and an outlet temperature of 60 °C to obtain spray dried annealed rice starch.

2.7. Preparation of spray dried annealed rice starch at lower temperature (SANR-L)

900 g (dry basis) of native rice starch was suspended in distilled water 3000 ml to obtain 25 % (w/w) solid content of solution. The suspended solution was heated with agitation in water bath in annealing temperature range to minimize the partial gelatinization effect, which was at 65 °C and subjected to spray drying at an inlet temperature of 160 °C and an outlet temperature of 60 °C to obtain spray dried annealed rice starch at lower temperature.

2.8. Preparation of spray dried combined annealing and enzymatic hydrolyzed rice starch (SANER)

Native rice starch 900 g (dry basis) was suspended in distilled water 3000 ml with 500 ppm of calcium chloride to obtain 25 % (w/w) solid content of suspension. The suspension was heated in water bath at 70 °C for 150 min. Since the temperature used in this study nearly onset temperature of starch from rice starch (73 ^{o}C). Thermostable alpha-amylase has been used to retain their activity at higher temperature. The enzyme hydrolysis of rice starch was performed at various reaction

time (15, 30 and 60 min) by adding 0.5 % (v/w) Termamyl (NOVO industry) into the suspension. The modified starch was then subjected to spray drying at inlet and outlet temperatures of 160 and 60 °C, respectively. The final product was obtained as spray dried combined annealing and enzymatic hydrolyzed rice starch.

2.9. Proximate analysis

Quantitative determinations of moisture, protein, lipid and ash contents were performed according to AOAC (1990).

2.10. Amylose content of starch

Amylose content was analyzed by following the iodine affinity method (Knutson, 1986).

2.11. Damaged starch analysis

Damaged starch was determined using AACC standard method 76-31 based on the method of Evers and Stevens (1985) and Gibson et al. (1991, 1993) with the damaged starch assay kit from Megazyme. A slurry of starch was incubated at 40 ^{0}C before the addition of α-amylase. The reaction was then terminated by dilute sulphuric acid (0.2 % v/v) and the slurry incubated further at 40 ^{0}C for 10 min with amyloglucosidase. Glucose was detected using a glucose oxidase/peroxidase reagent.

2.12. Granule morphology

2.12.1. Light and Polarization light microscopy

Starch granule was dispersed in a 1:1 (v/v) glycerol-water mixture to minimize evaporation and granule movement in the field (Hall & Sayre, 1970; Wivinis & Maywald, 1967) and observed in a fluorescent light microscope (Olympus BX 51) with camera set (Olympus DP 12) under light field. The birefringence of starch granules was observed under the polarized light.

2.12.2. Scanning electron microscopy (SEM)

The starch sample was mounted on SEM stubs with double-sided adhesive tape and coated with gold. Scanning electron micrographs were taken using a JOEL JSM-

5410LV microscope (JOEL, Tokyo, Japan). The accelerating voltage and the magnification are given on the micrograph.

2.13. Size distribution of the spray dried starches and the starch granules

The size distribution of the spray dried native, annealed with partially gelatinized and enzymatic hydrolyzed starches were measured by suspending the spray-dried starch sample in the range between the “obscuration” bar in the solution of 99 % ethanol as a dispersant. The starch suspension was stirred at 3500 rpm in sample dispersion accessory unit (Hydro 2000S) and immediately passed through a laser diffraction spectrometer (Malvern instruments Ltds, Melvern, UK). The granular size distribution of the starches was measured by suspending the starch granules in distilled water. After that the starch suspension was stirred at 3500 rpm while sonicated for 10 minutes in sample dispersion accessory unit and suddenly passed through the laser diffraction spectrometer. The volumetric weighted means of all samples were recorded.

2.14. Pasting properties measurement by Rapid Visco-Analyzer (RVA)

A Rapid Visco-Analyzer (Series 4V, Newport Scientific Pty. Ltd, Warriewood, Australia) was employed to investigate the pasting properties of native, preheat treatment and preheated enzymatic-modified starches. In this assay, 2.5 g (dry basis) of starch sample and 25 ml of distilled water were mixed in aluminum can with paddle. The heating and cooling cycles were programmed in the following manner of Batey, Curtin and Moore (1997). The starch suspension was held at 60 °C for 2 min, heated from 50 °C to 95 °C at a rate of 5.83°C/min over 6 min, held at 95 °C for 4 min, cooled down to 50 °C at a rate of 11.25 °C/min over 4 min and held at 50 °C for 4 min.

To determine the RVA pasting properties of starch without the effect of alpha-amylase, the water was replaced with the same volume of a solution of 12 mM silver nitrate. This was achieved by reducing the water volume by 2.0 ml and adding 2.0 ml of 10 % (w/v) silver nitrate solution for native and modified tapioca starch samples. In

case of native and modified rice starch, the volume was replaced by adding 3.0 ml of 10 % (w/v) silver nitrate solution while reducing the water volume by 3.0 ml.

2.15. Gelatinization properties

Gelatinization properties of native, annealed, annealed wih partially gelatinized and annealed with partial gelatinized enzymatic hydrolyzed starches were analyzed using a Differential Scanning Calorimeter (DSC6, Perkin Elmer, Norwalk, CT). Starch sample was suspended in distilled water with a starch to water ratio of 1:2. Each starch suspension was then transferred to an aluminum pan (Perkin Elmer) and hermatically sealed. Following equilibration at room temperature for 1 h, the samples were heated from 20 to 100 °C at 10 °C/min. An empty pan was used as the reference and the DSC was calibrated using indium. All measurements were done at least in triplicate. The onset (T_o), peak (T_p) and conclusion (T_c) temperatures and the melting enthalpy (ΔH) in J/g of dry starch were recorded.

2.16. X-ray powder diffraction measurements

The X-ray diffraction pattern was recorded with a copper anode X-ray tube (Cu-K_α radiation, wavelength = 1.542 A) using a Bruker Advance X-ray powder diffractometer (D-8 type, Bruker, Karlsruhe, Germany). The 100% relative humidity starch powders were packed tightly and kept the smooth surface in sample holders. Each sample was exposed to the X-ray beam at 30 kV and 30 mA. The scanning region of the diffraction angle (2θ) was from 5-30 °C, scan rate 1.2 °/min, step interval 0.04 with a count time of 1.0 s. The sollet and divergence slit was 1 °. The receiving slit was 0.6 ° and anti-scattering slit was 1 °. The rotary speed of the sample holder was 30 min^{-1}. The water content in starch samples was determined by drying at 130 °C for 1 h both before and after measurement.

2.17. Determination of the relative crystallinity

The relative crystallinity of starch samples was quantitatively estimated by the method of Nara and Komiya (1983). A smooth curve of the baseline below the peaks was computer-plotted on the diffractogram. The crystalline portion was assigned to the area above the smooth curve (upper diffraction peak area), while the lower area

situated between the smooth curve and a linear baseline, which connected the peaks at 2θ from 5 °C to 30 °C was taken as the amorphous region. The upper diffraction peak area and total diffraction area over the diffraction angle (2θ) from 5 °C to 30 °C were integrated. The ratio of upper area to total diffraction was calculated as the relative crystallinity.

2.18. Preparation of tablets

Plain filler of tablet was prepared by mixing 99.5 % starch and 0.5 % magnesium stearate (as lubricant) in a V-blender. The mixture was compressed with 8mm a flat-face-beveled-edge punch on a single punch rotary tablet machine (Type N3B. Narongkarnchange. Bangkok, Thailand), which had been equipped with resistance strain gauges and strain amplifier (Kyowa, model DPM-712B, Kyowa Co., Ltd., Japan) according to Wray et al. (1976) to monitor compression and ejection forces. The calibration has been described in detail previously (Salpeakar & Augsbuger, 1974). A single station was used only to help minimize tooling errors. The same circular, flat-faced punches with a die of 8 mm diameter and 300 mg target weight, was used throughout the study.

2.19. Tablet properties

2.19.1. Hardness

The crushing strength of tablets was determined with an electronic hardness tester (Schleuniger Model 4M Dr Schleuniger Co.,Switzerland). All crushing strengths values reported were given as means of ten determinations.

2.19.2. Friability

The friability of approximately 3 grams of tablets was conducted in a Roche type friabilator (Narongkarnchang, Thailand) (Sjokvist & Nystrom, 1991).

2.19.3. Disintegration time

Six tablets from each compression force were tested for their disintegration time (Sheh et al., 1980) using USP disintegration apparatus (Hanson Model QC 24, Hanson Research Corp., USA) and water as immersion fluid. The mean disintegration time and standard deviation of six tablets were calculated.

2.20. Statistical analysis

All measurements were performed in triplicate at least, and the average values were presented in respective table. Analysis of variance (ANOVA) was performed by Turkey's HSD test ($P < 0.05$) using statistical software SPSS 9.0 for Windows (SPSS Inc., Chicago, Illinois, USA).

CHAPTER IV
RESULTS

1. Chemical properties

1.1. Proximate analysis

The proximate analysis (%moisture content, %protein, %fat and %ash) of SNT, SNR, SANET, SANER, SANT-H and SANR-H were compared and shown in Table 5.

Protein and ash content of SANET were significantly increased ($P \leq 0.05$) in comparison with SANT-H and SNT. However, increasing of the hydrolysis time did not show the significantly different ($P > 0.05$). Fat content was constancy with the hydrolysis times. Carbohydrate content of SANT-H in this study is 88.69 % which is not significantly different ($P > 0.05$) when compared to SNT (88.53 %) and SANET range between 89.47 % to 89.70 %.

Protein and ash contents of SANER were significantly increased ($P \leq 0.05$) with the hydrolysis time, while fat content was not changed after the enzymatic treatment. However, increasing of the hydrolysis time did not show the significant different ($P > 0.05$). The range of carbohydrate content of SANER is varied from 88.39 % to 88.77 %, whereas SNR and SANR-H show 87.66 % and 87.95 % of carbohydrate content, respectively.

Table 5. Proximate composition (%) [1] of SNT, SNR, SANT-H, SANR-H, SANET and SDEHR as a function of time: 15 min, 30 min and 60 min.

Starch type	Reaction time(min)	Moisture	Ash	Protein[2]	Fat	Carbohydrate
SNT		11.27 ± 0.20 ^{a}	0.14 ± 0.01 ^{c}	0.01 ± 0.01 ^{b}	0.05 ± 0.01 ^{a}	88.53 ± 0.19 ^{b}
SANT-H		11.03 ± 0.06 ^{a}	0.24 ± 0.01 ^{b}	0.01 ± 0.00 ^{b}	0.04 ± 0.01 ^{a}	88.69 ± 0.06 ^{b}
SANET	15	9.99 ± 0.11 ^{b}	0.26 ± 0.01 ^{a,b}	0.07 ± 0.02 ^{a}	0.04 ± 0.00 ^{a}	89.65 ± 0.10 ^{a}
	30	10.15 ± 0.07 ^{b}	0.27 ± 0.02 ^{a,b}	0.08 ± 0.00 ^{a}	0.04 ± 0.01 ^{a}	89.47 ± 0.08 ^{a}
	60	9.93 ± 0.13 ^{b}	0.25 ± 0.01 ^{a}	0.08 ± 0.00 ^{a}	0.05 ± 0.00 ^{a}	89.70 ± 0.13 ^{a}
SNR		10.58 ± 0.21 ^{a}	0.65 ± 0.01 ^{c}	1.04 ± 0.01 ^{d}	0.08 ± 0.01 ^{a}	87.66 ± 0.21 ^{c}
SANR-H		10.45 ± 0.06 ^{a,b}	0.70 ± 0.01 ^{b}	1.03 ± 0.01 ^{d}	0.06 ± 0.01 ^{a}	87.95 ± 0.03 ^{c}
SANER	15	9.33 ± 0.10 ^{c}	0.74 ± 0.01 ^{a}	1.09 ± 0.01 ^{b}	0.07 ± 0.01 ^{a}	88.77 ± 0.10 ^{a}
	30	9.40 ± 0.33 ^{c}	0.75 ± 0.01 ^{a}	1.06 ± 0.00 ^{c}	0.07 ± 0.01 ^{a}	88.54 ± 0.57 $^{a, b}$
	60	9.72 ± 0.09 ^{b,c}	0.72 ± 0.00 ^{b}	1.11 ± 0.01 ^{a}	0.06 ± 0.01 ^{a}	88.39 ± 0.08 $^{a, b, c}$

[1] Data with the same superscript in the same column are not significantly different ($P > 0.05$) by Tukey's HSD[a] test. All data represent mean ± SD of three determinations.

[2] Conversion factor (f) = 5.70 for tapioca starch and rice starch. (http:// www.starch.dk/isi/applic/tapiocafarma.htm & Puchongkavarin et al., 2003)

1.2. Amylose content

The changes in amylose content of SNT, SNR, SANT-H, SANR-H as well as SANET and SANER at different time periods of hydrolysis were shown in Table 6. This revealed the presence of considerable proportion of straight chain fractions, mainly the linear (amylose) component in the starches. % Amylose content in both SANT-H (31.78 %) and SANR-H (30.25 %) were significantly decreased ($P \leq 0.05$) when compared to SNT (33.58 %) and SNR (31.02 %) which was consequently from mild acid hydrolysis of amylose due to the presence of acidity of distilled water (pH 5.5) that used throughout in the study. Compared to the results reported by Hizukuri (1988), Oates (1996) and Ramesh et al. (1999), our results were somewhat higher. However, this result is in the range as observed by Atichokudomchai and Varavinit (2003) for native tapioca starch. Amylose content in both of SANET and SANER were also significantly decreased ($P \leq 0.05$) after the enzymatic hydrolysis of the starches. In case of SANER, the amylose content was gradually decreased by the increasing of hydrolysis time. However, for the extension of enzymatic hydrolysis time for the SANET was not changed in amylose content too much.

Table 6. Amylose content (%) [1] of SNT, SNR, SANT-H, SANR-H, SANET and SDEHR as a function of time: 15 min, 30 min and 60 min.

Starch type	Reaction time(min)	Amylose content[2]
SNT		33.58 ± 0.23 [a]
SANT-H		31.87 ± 0.08 [b]
SANET	15	25.17 ± 0.04 [c]
	30	25.05 ± 0.04 [c]
	60	23.26 ± 0.12 [d]
SNR		31.02 ± 0.04 [a]
SANR-H		30.25 ± 0.09 [b]
SANER	15	23.35 ± 0.05 [d]
	30	23.66 ± 0.08 [c]
	60	22.95 ± 0.05 [e]

[1] Data with the same superscript in the same column are not significantly different ($P > 0.05$) by Tukey's HSD[a] test. All data represent mean ± SD of three determinations.

[2] Amylose content determined as apparent amylose by iodine binding affinity without removal of free and bound lipids.

2. Morphological properties

2.1. Tapioca starch

The micrographs under light and cross polarized field of SNT, SANT-H and SANET at 60 ^{0}C were performed on the same area of starch granule samples in order to assess the size and birefringence observation as shown in Figure 31. SNT showed varying size and shape in tapioca starch granule. The round, truncated and bell shapes were observed. The 'Maltese cross' (the characteristic dark cross seen on starch granules when viewed under polarizing light, and the point at which the hilum is centred) of starch granule was also presented in Figure 31A and 31D. The micrographs of SANT-H were shown in Figure 31B and 31E. There was not different in shape and size of SANT-H when compared to SNT. Both starch granules of SNT and SANT-H displayed birefringence with a typical "Maltese cross" indicating crystalline order. Micrograph of SANET was shown in Figure 31C and 31F. Some intact granules show a reduced intensity or coverage by the Maltese cross. Many of granule starches were cracked, fissured, broken and fragmented which also retain some birefringence. The hole from endocorrosion and granule surface erosion was caused by enzyme attack. The center of Maltese cross was expanded which often retained a residual birefringence at their edge due to the disappearance of internal region of starch granule by endocorrosion. Gross damage (explode) that appears leave only the outer layers of the granule which was observed by almost totally absent of birefringence still rarely observed. It is clear that the peripheral region of the granule had been more resistant to α-amylase than the interior of the granule. The remaining were rough surface and also the present of small granule inside the large one that exhibited the change in the Maltese cross under polarized light.

SEM has also been used to study the granule morphology. Starch granules from different botanical origins differ in morphology. SEM images of native granular tapioca starch (NT) and native spray dried tapioca starch (SNT) were clearly shown in Figure 32A and 32B. NTS had irregular, round, compound and truncated shapes with diameters ranging from 5 to 25 μm. The truncated area is characterized by flat, convex or concave pyramidal surfaces. The surface of most of the starch granules was smooth without observable pores or fissures while SNT exhibited the spherical shape as a result from aggregation of various size of NT packing together during spray drying.

It was found that the different sizes and shapes of granule from tapioca starch were agglomerate as shown in Figure 33A. Each starch granules was aggregated to form agglomerated starch with clearly observed under higher magnification (Figure 33D). Moreover, the surface of granule was not smooth but a little bit rippled and no evident of the pore formation. The fusion of each starch granules of SANT-H together was observed and shown in Figure 33B and 33E. For SANET, five characteristics combinable types of the starch granule were exhibited (smooth gel-like surface, surface erosion, hole, caving and fragment) and the fusion of granule starch by surface gelatinization are shown in Figure 33C and 33F.

SEM micrographs of SANET at various hydrolysis times (15 min, 30 min and 60 min) are shown in Figure 34. Granules subjected to extended hydrolysis exhibited the same pattern of hydrolysis (surface erosion and caving). At the hydrolysis time of 15 min, the surface erosion and hole deepening into inner part of the starch granule from endocorrosion by amylolysis were also observed with surface gelatinization as shown in Figure 34A and 34B. For 30 min of hydrolysis time, the α-amylolysis was preferentially occurred at the interior of starch granule, leaving a deep round hole on the starch granule surface and some granule exhibited surface erosion with caving. The degree of surface gelatinization seemed to be increased as shown in Figure 34C and 34D. The extremely damaged of starch granule was exhibited in 60 min of hydrolysis time (Figure 34E and 34F). The hole was disappeared, the granule was hydrolysed to become a broken shell (the outer layer of the starch) or fragment, some fragments fused each other and some were fused with non-hydrolysed granule, probably due to the caving action of enzymes. The degree of attack on individual granules in all hydrolysis time was very different. Whereas some granules were extensively attack, others were apparently completely intact.

Moreover, major population of the SANET at any hydrolysis times showed the binding together among the starch granules of the starch agglomeration (Figure 35). This binding of granules of the agglomerated starch will lead to the larger size of the agglomeration as observed from the particle size diameter while the spherical agglomerated forms were the minor population.

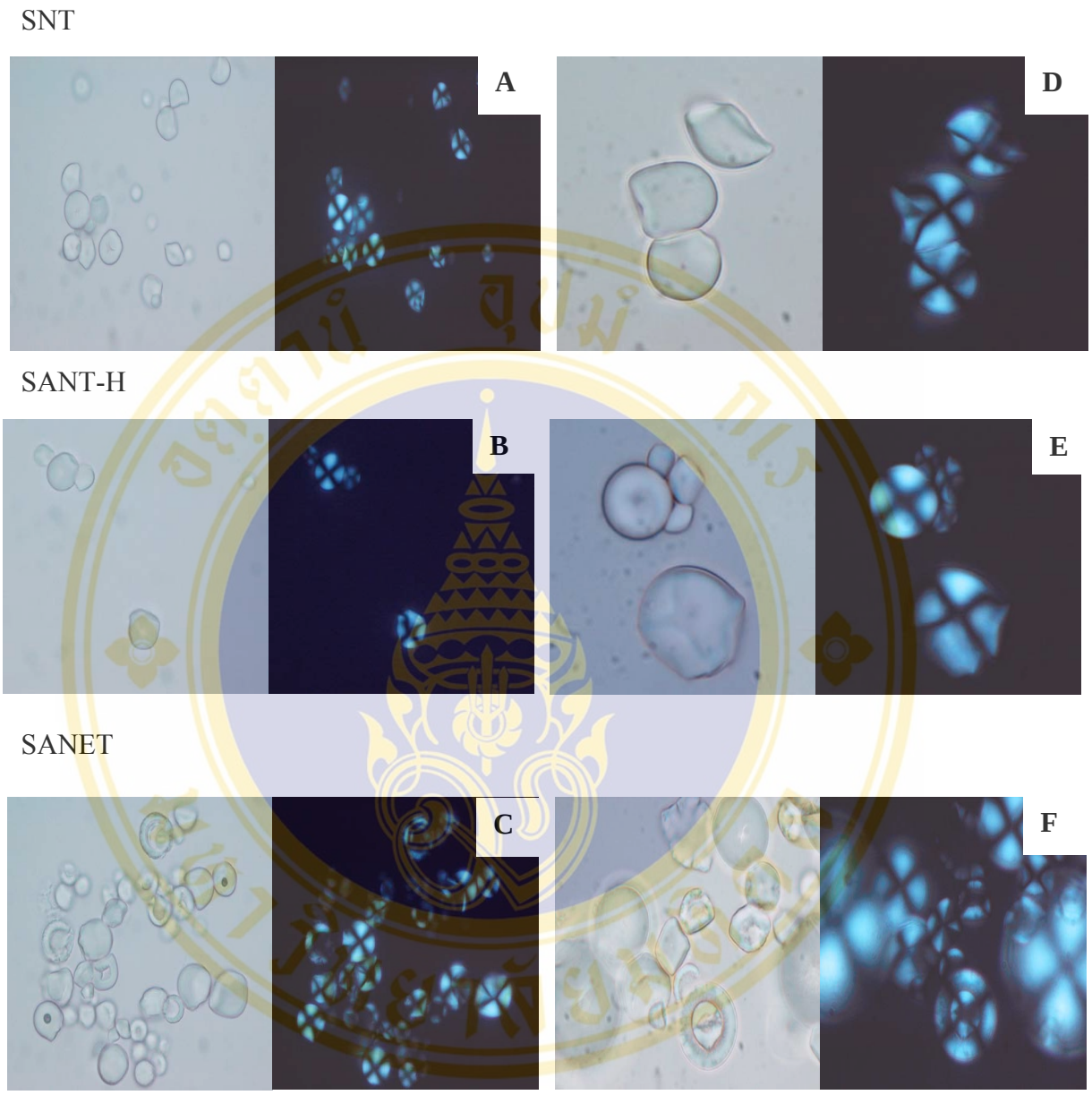

Figure 31. Micrographs of spray dried tapioca starch observed under neutral and cross-polarized lights by light microscope (magnificent 400x for A-C; magnificent 1000x for D-F).

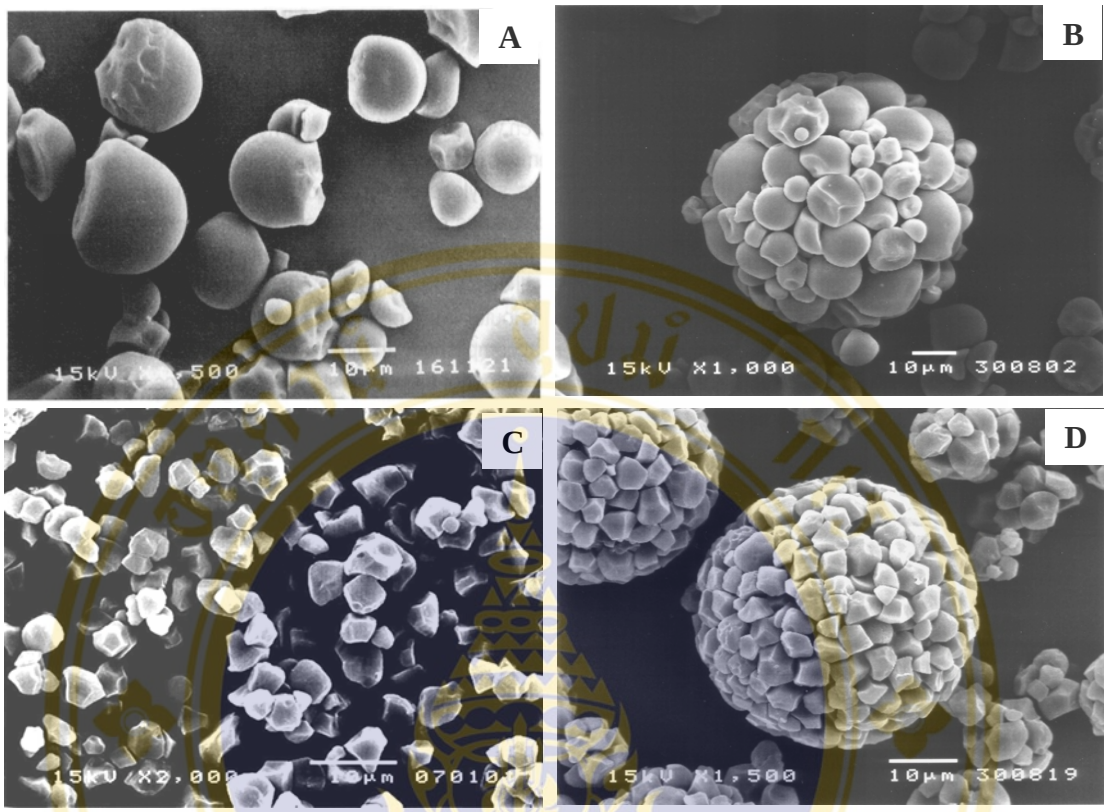

Figure 32. SEM (magnification 1000x, 1500x and 2000x) of NT (A), SNT (B), NRS (C) and SNR (D)

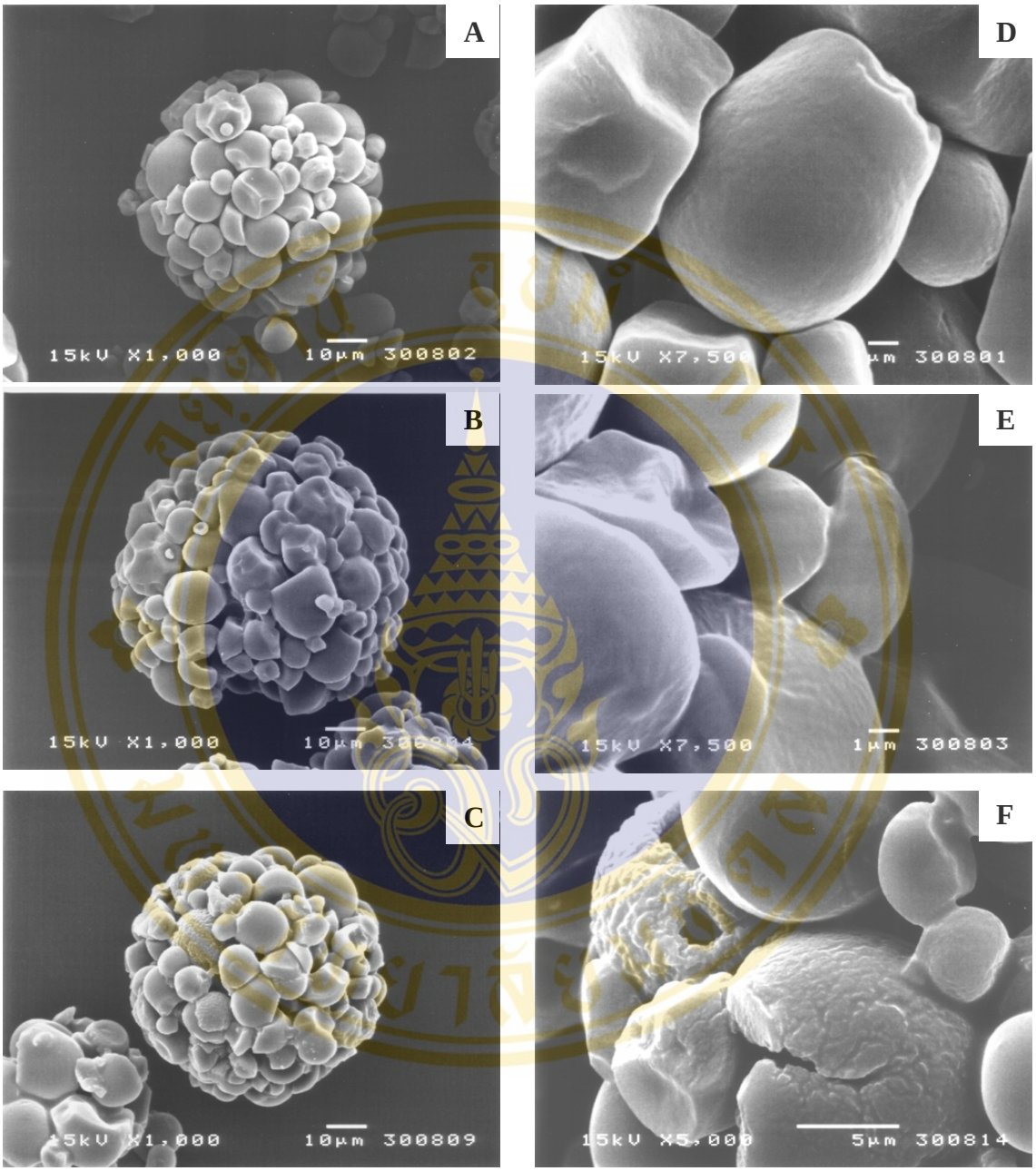

Figure 33. SEM (magnification 1000x, 5000x and 7500x) of SNT (A and D), SANT-H (B and E) and SANET (C and F).

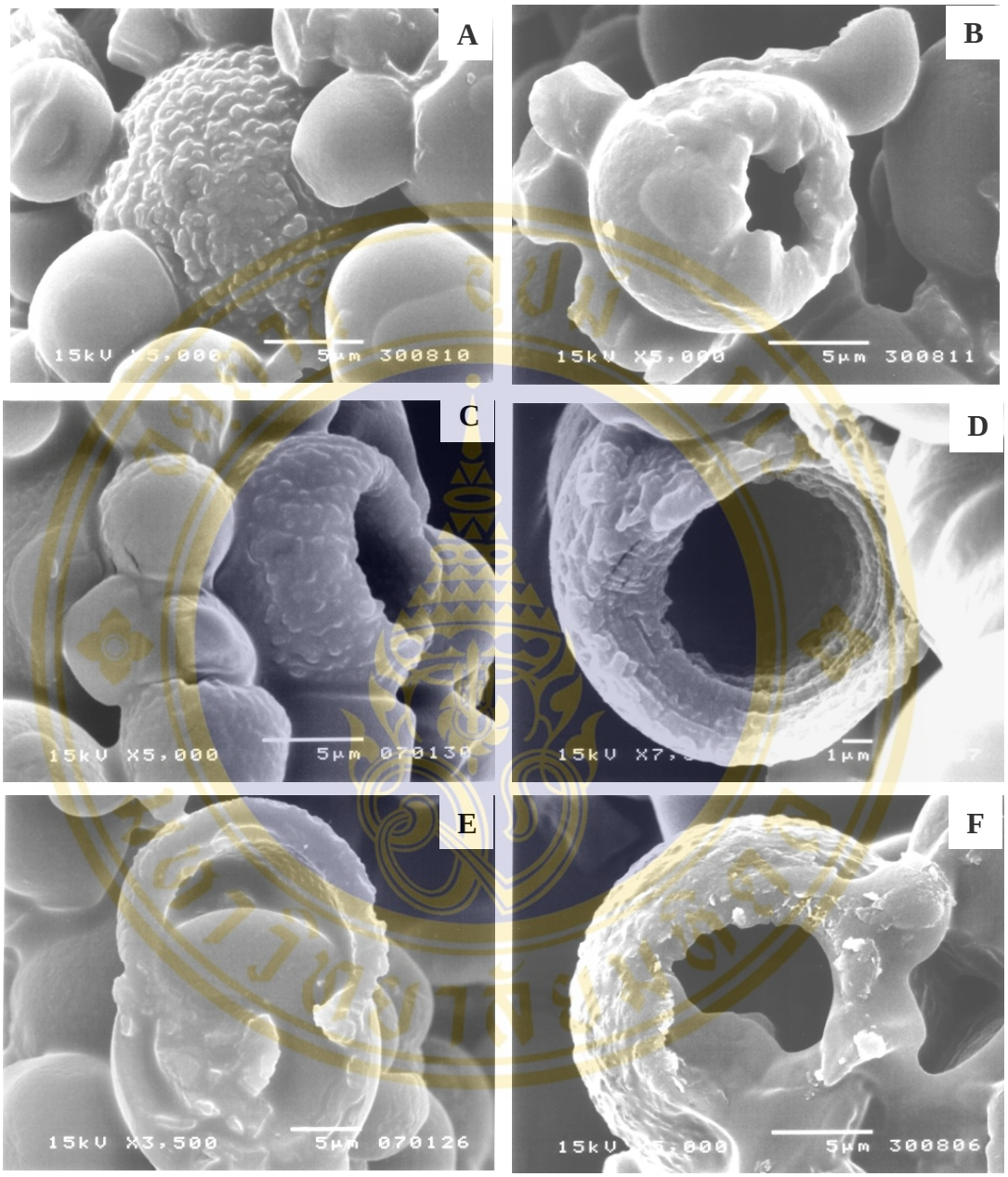

Figure 34. SEM (magnification 3500x, 5000x and 7500x) of SANET at 15 min (A and B), 30 min (C and D) and 60 min (E and F).

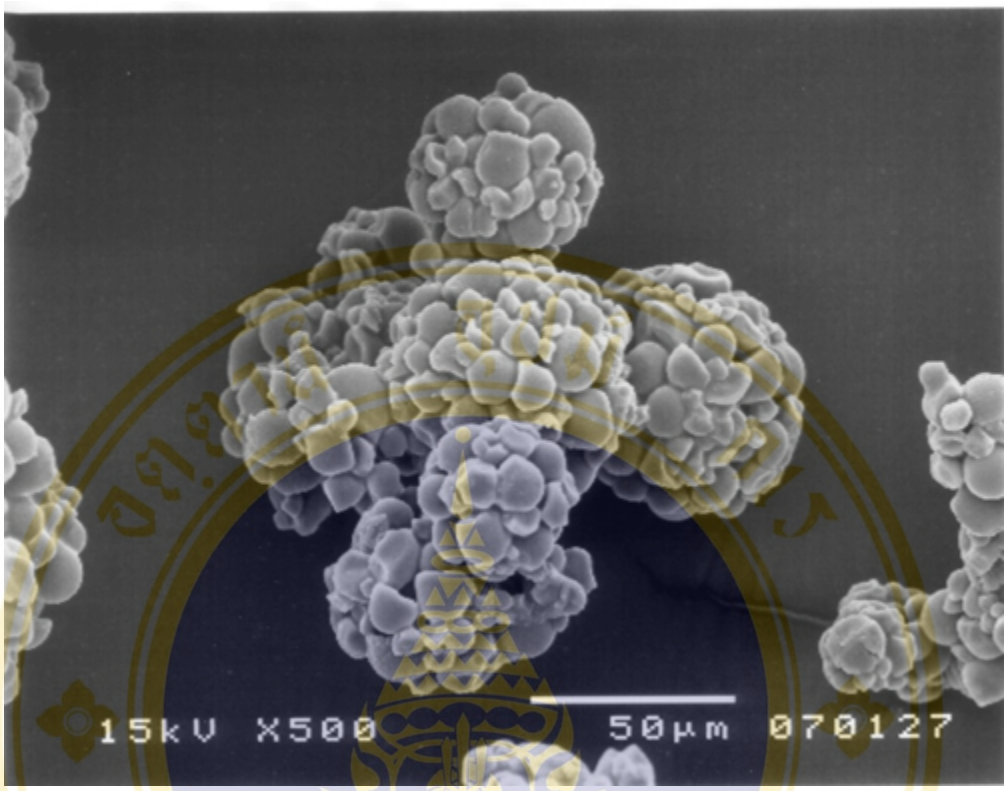

Figure 35. SEM (magnification 500x) of SANET at 30 min hydrolysis time.

2.2. Rice starch

The micrographs under light and cross polarized field SNR, SANR-H, SANER at 70 ^{0}C are shown in Figure 36.

SNR showed irregularly, polyhedral and polygonal shapes is typical for this starch. The flower-type “Maltese cross” of rice starch granules was also presented in Figure 36A2. The micrographs of SANR-H were shown in Figure 36B1 and 36B2. The regular starch granules of SNR and SANR-H displayed the typical “Maltese cross”. The shape, size and also the Maltese cross of SANR-H were not different when compared to SNR. Micrographs of SANER were shown in Figure 36C1 and 36C2. Many of granular starches were cracked and fragmented while some were intact. The hole from endocorrosion and granule surface erosion by enzyme attack was also observed. The Maltese cross under polarized light was depended on the remaining shape from enzyme attack which is appears in the non-hydrolyzation area.

SEM images of native granular rice starch (NR) and native spray dried rice starch (SNR) are clearly shown in Figure 32C and 32D. NR had polygonal, compound and polyhedral shapes with diameters apparently smaller than 10 μm which was classified to small granule starch and this value is in the range reported by Jane et al. (1994). The surfaces of individual starch granules were mostly smooth without observable pores. However, small, rough and damaged areas can also be found. Agglomerates of SNR photographed exhibited the spherical shape.

SEM images of SNR, SANR-H and SANER are shown in Figure 37. The agglomerate native rice starch, introduced by spray dryer, is shown in Figure 37A. Each small starch granules was aggregated to form perfectly agglomerated starch with clearly observed under higher magnification (Figure 37D). Surfaces of rice granules were smooth with some shallow indentations and no evident of the pore formation. Some granule represented the disc-like pressing on the surface of rice starch and the number of depressions varied from granule to granule. Partially surface gelatinization led to the fusion of each starch granules together with alter the surface of rice starch granules as shown in Figure 37B and 37E. None of shallow indentations and small disc-like pressing was observed on the surface of SANR-H. For SANER, four characteristics combinable types of the starch granule from enzymatic hydrolysis were

exhibited (smooth gel-like surface, surface erosion, pore and hole), the fusion among the starch granules is shown in Figure 37C and 37F.

SEM micrographs of SANER at various hydrolysis times (15 min, 30 min and 60 min) are shown in Figure 38. At the hydrolysis time at 15 min, pores were rarely observed. Surface erosion and hole from endocorrosion by amylolysis were also observed with surface gelatinization as shown in Figure 38A. After 30 min of hydrolysis time, pore and hole from α-amylolysis were occurred which increasing in frequency of surface erosion observation. The degree of surface gelatinization at 30 min of hydrolysis time was increased as shown in Figure 38B. The extremely surface gelatinization of starch granule was clearly observed after 60 min of hydrolysis time (Figure 38C). Plenty of holes with the presence of pore were also observed. All hydrolysis time, however, shown some rice starch granules were still intact with no evidence of α-amylase attack.

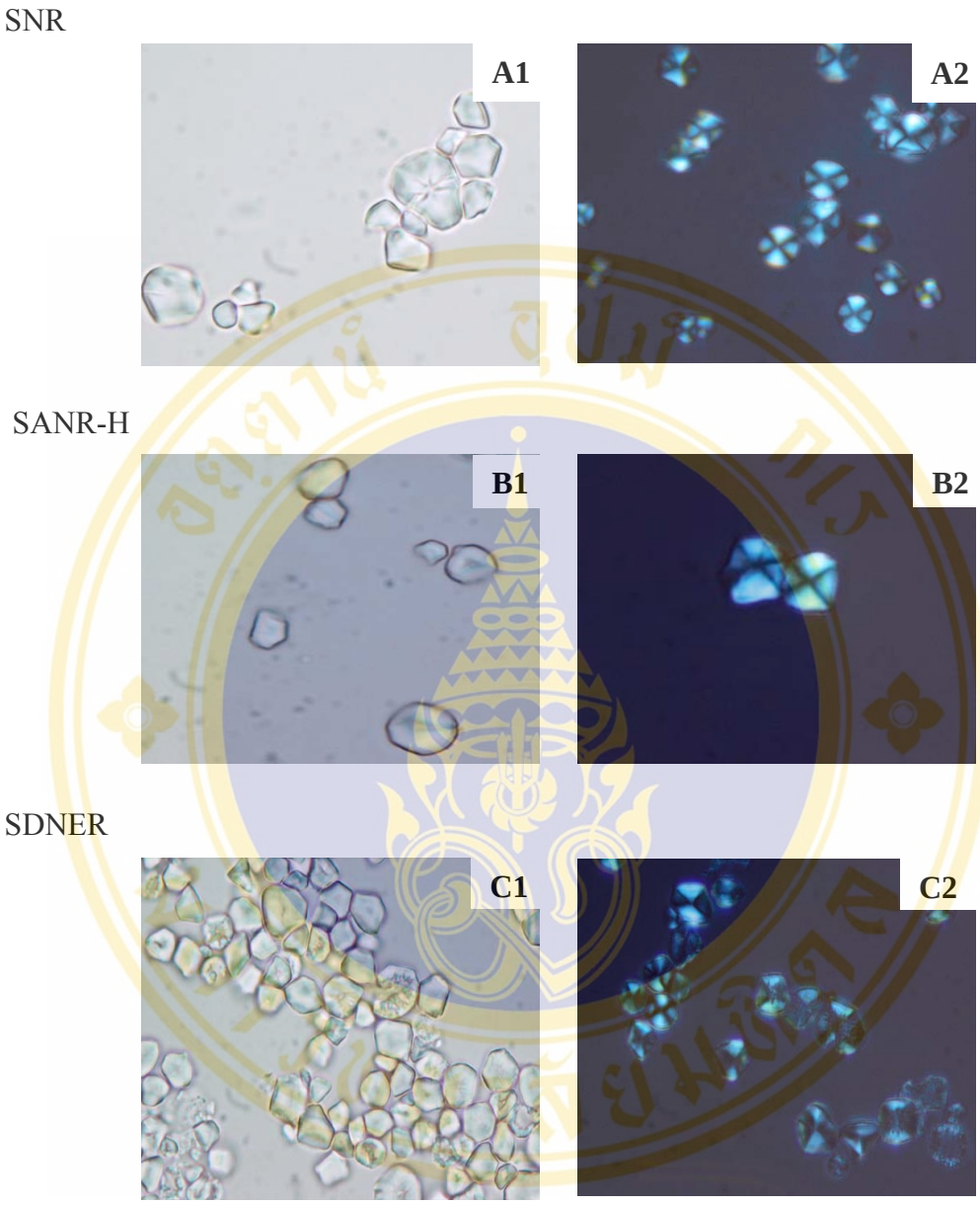

Figure 36. Micrographs (magnificent 1000x) of spray dried rice starch observed under neutral and cross-polarized lights by light microscope.

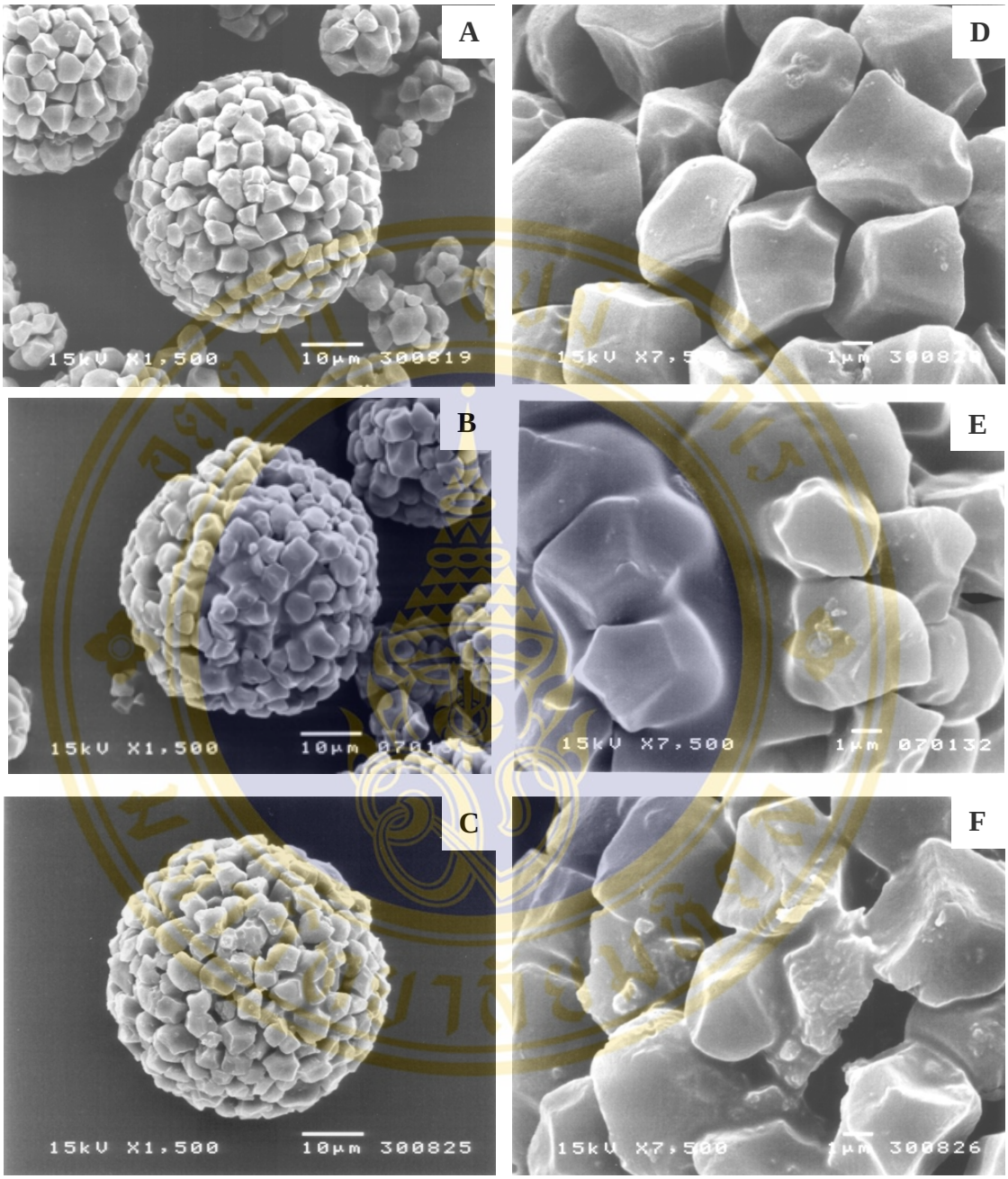

Figure 37. SEM (magnification 1000x and 7500x) of SNR (A and D), SANR-H (B and E) and SANER (C and F).

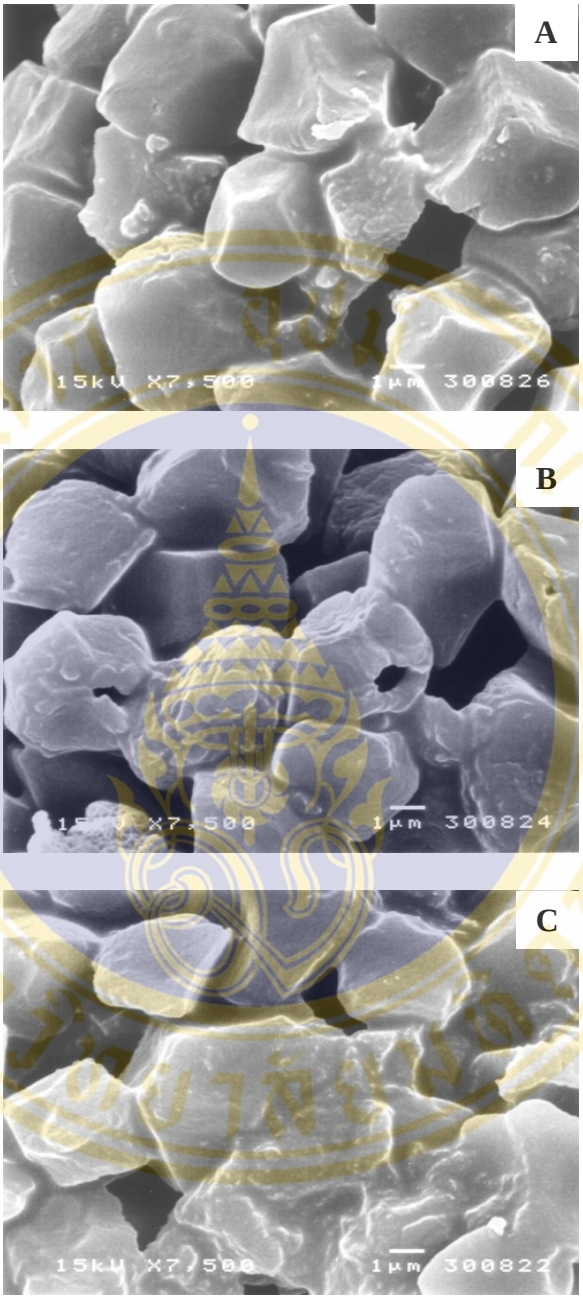

Figure 38. SEM (magnification 7500x) of SANER at 15 min (A), 30 min (B) and 60 min (C).

3. Particle size distribution

3.1. Tapioca starch

The particle size distribution pattern of SNT exhibited the boarder curve that is related to the higher span value (2.90) while SANT-H, SANET at 15 and 30 min hydrolysis time (SANET-15 and SANET-30) shows the shoulder curve at the lower region of the particle size (Figure 39 A-E). The median particle size of SNT, SANT-H and SANET at various hydrolysis times (15 min, 30 min and 60 min) with the median diameter of 77.35 ± 0.60, 149.54 ± 0.10, 143.18 ± 0.32, 154.66 ± 0.55 and 181.14 ± 0.68 μm, was obtained respectively. It was demonstrated that partial gelatinization of tapioca starch provided the increasing of the median particle size of agglomerated form obtained by spray drying process. Increasing of enzymatic hydrolysis time was also increased the particle size as illustrated in Figure 35. The granule size distributions pattern were measured and shown in Figure 39 F-J, all of the granular starch exhibited the same particle size distribution pattern. The particle size distribution range of the granular NT is from 8.49 ± 0.19 to 21.45 ± 0.30 μm while those of the granular ANT-H is range from 8.25 ± 0.03 to 27.77 ± 0.13 μm. The median diameter (d (v 0.5)) of NT (13.63 ± 0.05 μm) is not much different from ANET while ANT-H value (15.34 ± 0.05 μm) slightly higher than those NT and ANET. However, increasing hydrolysis time does not affect the median particle size.

The partial gelatinized enzymatic hydrolysis of tapioca starch did not much more affect the median particle sizes on the granular size but greatly effect on the agglomerated form of tapioca starch. However, the partial gelatinized starch (SANT-H) increased the median particle sizes of both the granular and agglomerated form when compared to the native tapioca starch.

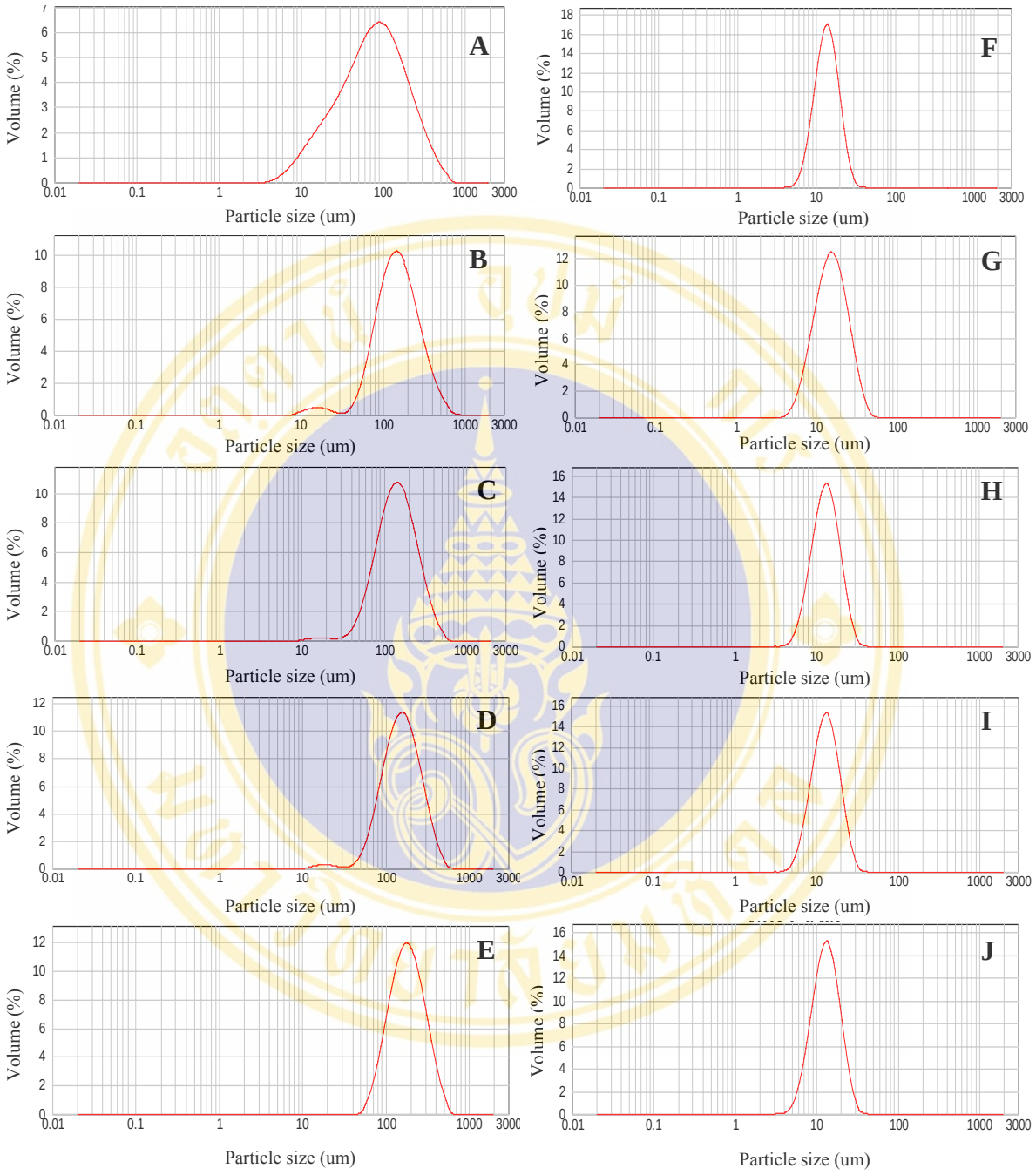

Figure 39. Volumetric particle size distributions of agglomerated (A-E) and granular (F-J) tapioca starches; SNT (A, F), SANT-H (B, G), SANET at 15 min (C, H), 30 min (D, I) and 60 min (E, J).

3.2. Rice starch

The particle size distribution pattern of SANR-H shows the shoulder curve at the upper region of the particle size (Figure 40 A-E). The median particle size of SNR, SANR-H and SANER at various hydrolysis times (15 min, 30 min and 60 min) with median diameter of 40.57 ± 0.00, 39.65 ± 0.08, 58.76 ± 0.05, 68.84 ± 0.39 and 64.51 ± 0.27 μm, was obtained respectively. It was demonstrated that partial gelatinized rice starch did not increase the median diameter (d (v 0.5)) of agglomerated form by spray drying process but it clearly increased in volume weight mean diameter size d (4,3) (59.05 ± 1.83 μm) in comparison with SNR. However, the SANER provided larger diameter of the median particle size in comparison with the SNR and SANR-H.

The agglomerated rice starch could be broken into individual granules by sonicating in distilled water and the granule size distributions were shown in Figure 40 F-J. All of the granular rice starches exhibited the same particle size distribution pattern. The particle size distribution of the granular NR was ranged from 3.68 ± 0.00 to 8.55 ± 0.00 μm while those of the granular of the SANR-H was ranged from 4.63± 0.03 to 12.68 ± 0.05 μm. The median diameter of granule of SNR (5.65 ± 0.00 μm) was not much different from the granule of SANER while the granule of SANR-H value (7.78 ± 0.04 μm) seems to slightly higher than those of the granule from SNR and SANER.

The partial gelatinized enzymatic hydrolysis did not effect on the granular size rice starch however it was more affect to the agglomerated rice starch. Whereas only partial gelatinized rice starch increased the particle sizes of the granular starch but slightly decreased the agglomeration when compared to SNR.

It is obvious that partial gelatinization would greatly affect on the increasing of median particle size of agglomerated tapioca starch than rice starch.

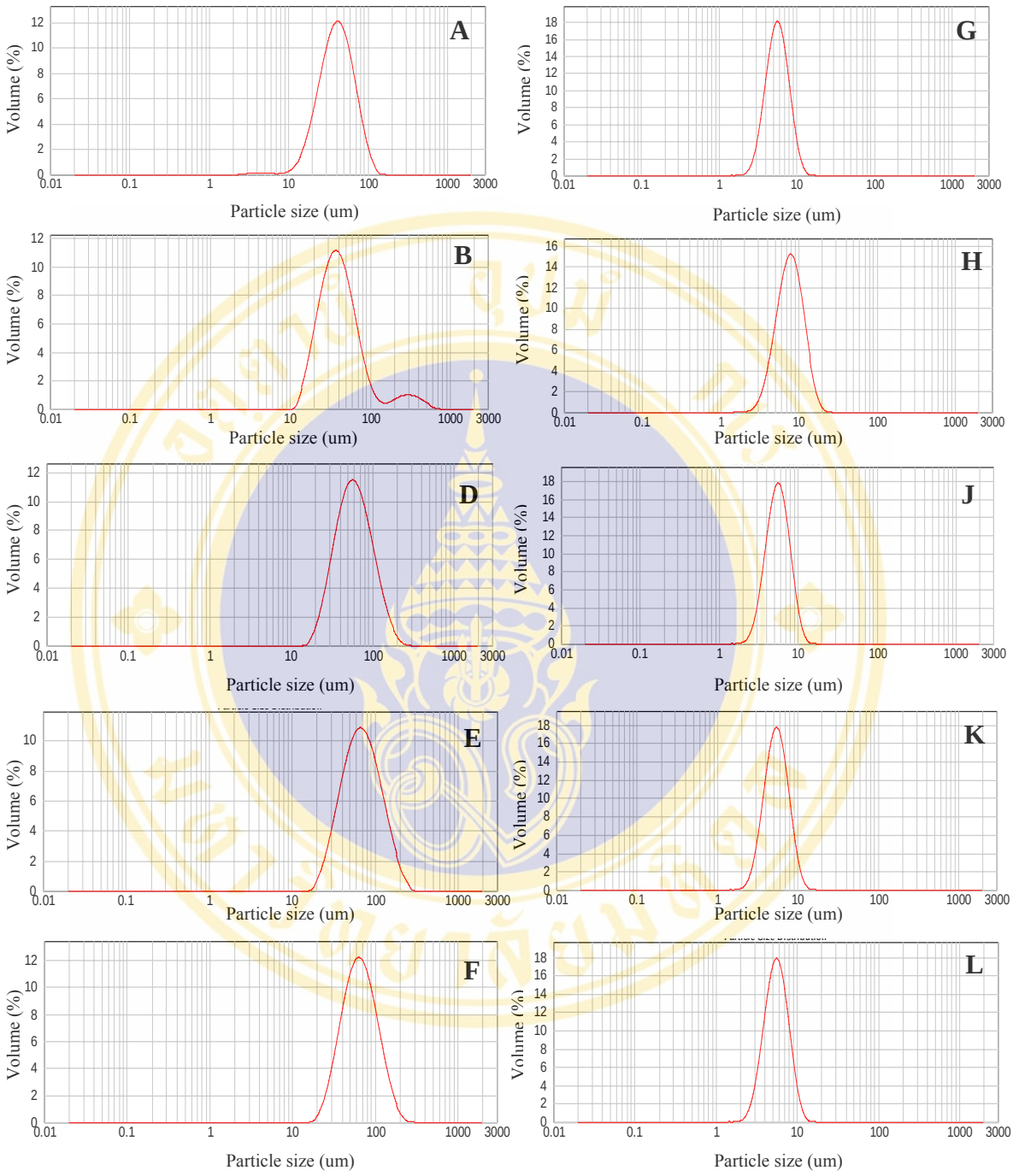

Figure 40. Volumetric particle size distributions of agglomerated (A-F) and granular (G-L) rice starches; SNR (A, F), SANR-H (B, G), SANER at 15 min (C, H), 30 min (D, I) and 60 min (E, J).

4. Thermal properties (DSC)

4.1. Tapioca starch

Onset (T_o), peak (T_p), conclusion (T_c) temperatures and gelatinization enthalpy (ΔH) of SNT, SANT-H, SANT-L and SANET at various hydrolysis times (15 min, 30 min and 60 min) were evaluated from DSC thermogram as shown in Table 7. SANT-L exhibited the significantly increased ($P \leq 0.05$) of T_o, T_p and T_c in comparison with SNT. All T_o, T_p, T_c of SANT-H were also significantly increased ($P \leq 0.05$) when compared to SNT. At this temperature, the temperature increase (ΔT, which respect to the SNT) was in the following order: $T_o > T_p > T_c$. This corresponded to 5.38 > 2.80 > 1.20 ^{0}C for SANT-H. The increasing of enzymatic hydrolysis time of SANET was also increase T_o, T_p, T_c when compared with SNT, SANT-L and SANT-H.

The quantum of heat flow recorded in term of energy to gelatinized SANT-L and SANT-H was not significantly differed ($P > 0.05$) from SNT. However, SANT-L showed significantly increased ($P \leq 0.05$) in ΔH when compared to SANT-H. The narrowing of the gelatinization range of SANT-L and SANT-H was again due to the shift of onset temperature (T_o) to a higher temperature with conclusion temperature (T_c) being slightly affected. However, significantly decreasing ($P \leq 0.05$) in temperature range ($T_c - T_o$) was also found in enzymatic hydrolysis at 60 ^{0}C with lowest value in 60 min hydrolysis (11.63 ± 0.02 ^{0}C). The increasing susceptibility of SANET to α-amylolysis correlates with the decreasing of ΔH ($r^2 = 0.7814$) as shown in Figure 41. The decrease of ΔH, which extended in hydrolysis time, would correlate with the present of increasing ($r^2 = 0.6624$) in the degree of damaged starch in the SANET samples.

Table 7. Endothermal properties [1] (T_o, T_p, T_c and gelatinization enthalpy) of SNT, SANT-L, SANT-H, SANET at various hydrolysis times.

Starch type	Reaction time (min)	T_o (^{0}C)	T_p (^{0}C)	T_c (^{0}C)	ΔH (J/g)	Temperature range (T_c-T_o) (^{0}C)
SNT		65.39±0.13 ^{e}	71.48±0.39 ^{e}	82.19±0.04 ^{d}	15.26±0.38 ^{a,b}	16.80±0.09 ^{a}
SANT-L		67.39±0.12 ^{d}	72.23±0.08 ^{d}	83.13±0.16 ^{c}	15.73±0.15 ^{a}	15.74±0.21 ^{b}
SANT-H		70.77±0.08 ^{c}	74.28±0.08 ^{c}	83.39±0.06 ^{c}	14.68±0.51 ^{b}	12.61±0.14 ^{c}
SANET	15	74.77±0.18 ^{b}	78.38±0.24 ^{b}	87.40±0.28 ^{b}	11.98±0.19 ^{c}	12.63±0.10 ^{c}
	30	75.06±0.02 ^{b}	78.70±0.09 ^{a,b}	87.81±0.07 ^{a}	10.66±0.30 ^{d}	12.75±0.05 ^{c}
	60	75.76±0.01 ^{a}	79.17±0.00 ^{a}	87.38±0.02 ^{b}	10.14±0.01 ^{d}	11.63±0.02 ^{d}

[1] Data with the same superscript in the same column are not significantly different ($P > 0.05$) by Tukey's HSD^a test. All data represent mean ± SD of three determinations.

4.2. Rice starch

The endothermal properties of SNR, SANR-L, SANR-H and SANER at various hydrolysis times (15 min, 30 min and 60 min) were evaluated from DSC thermogram (Table 8). The gelatinization temperatures (T_o), T_p and T_c of SANR-L, SANR-H and SANER were significantly increased ($P \leq 0.05$) when compared to SNR. At this temperature, the temperature increase (ΔT, which respect to the SNR) was in the following order: $T_o > T_p > T_c$. This corresponded to 5.76 > 3.11 > 0.83 ^{0}C for SANR-H. As a consequence the range ($T_c - T_o$) was significantly reduced ($P \leq 0.05$) from 12.30 to 7.38 ^{0}C. These trends were also observed in SANR-L as compared to SNR. However, the increasing of enzymatic hydrolysis time was not changed the gelatinization temperature (T_o), T_p and T_c.

SANR-L showed constancy ΔH (13.53 J/g) while SANR-H provided significantly lower ($P \leq 0.05$) ΔH (11.74 ± 0.19 J/g) when compared to SNR (13.44 ± 0.06 J/g). Significantly decreasing ($P \leq 0.05$) of gelatinization enthalpy was also found in 60 min enzymatic hydrolysis at 70 ^{0}C with lowest value (9.81 ± 0.24 J/g). However, the correlation between hydrolysis time of SANER and ΔH was weak ($r^2 = 0.4560$) as shown in Figure 41. The higher degree of partially gelatinization which observe by linearly increasing in degree of damaged starch of SANER ($r^2 = 0.8170$) may influences in decreasing of ΔH of rice starch samples with the extension of hydrolysis time.

Table 8. Endothermal properties [1] (T_o, T_p, T_c and gelatinization enthalpy) of SNR, SANR-L, SANR-H, SANER as a function of hydrolysis times.

.

Starch type	Reaction time (min)	To (^{0}C)	Tp (^{0}C)	Tc (^{0}C)	ΔH (J/g)	Temperature range (Tc-To) (^{0}C)
SNR		72.84±0.17 ^{d}	78.33±0.10 ^{e}	85.15±0.04 ^{d}	13.44±0.06 ^{a}	12.30±0.13 ^{a}
SANR-L		75.53±0.10 ^{c}	79.34±0.09 ^{d}	85.71±0.25 ^{c}	13.53±0.04 ^{a}	10.18±0.03 ^{b}
SANR-H		78.60±0.09 ^{b}	81.44±0.19 ^{c}	85.98±0.26 ^{c}	11.74±0.19 ^{b}	7.38±0.17 ^{c}
SANER	15	83.81±0.10 ^{a}	86.29±0.10 ^{a}	89.74±0.16 ^{a}	10.03±0.32 ^{c}	5.93±0.06 ^{d}
	30	83.54±0.43 ^{a}	85.62±0.10 ^{b}	89.13±0.09 ^{b}	11.19±0.40 ^{b}	5.59±0.35 ^{d}
	60	83.80±0.09 ^{a}	86.11±0.11 ^{a}	89.36±0.26 ^{a,b}	9.81±0.24 ^{c}	5.56±0.18 ^{d}

[1] Data with the same superscript in the same column are not significantly different ($P > 0.05$) by Tukey's HSD[a] test. All data represent mean ± SD of three determinations.

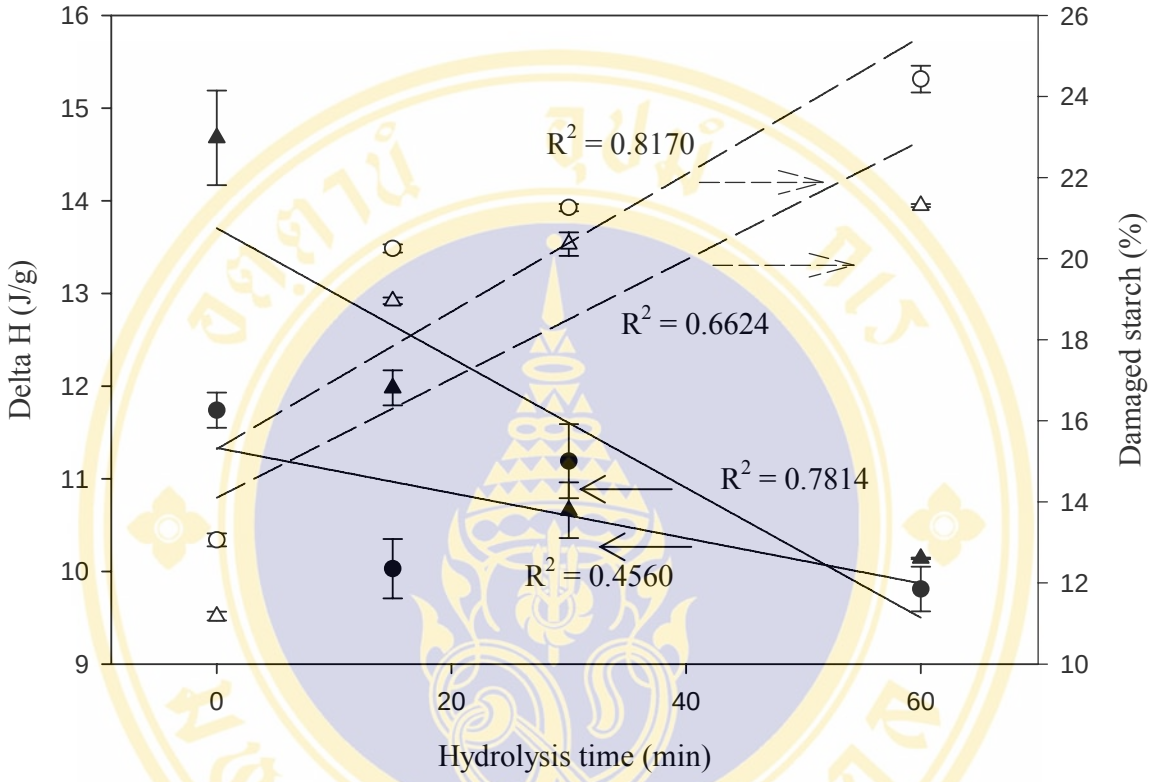

Figure 41. Relationship between gelatinization enthalpy (ΔH) (—) and damaged starch (---) as a function of hydrolysis times of SANET (σ, Δ) and SANER (λ, O)(SANT-H and SANR-H are at 0 min).

5. Crystallinity

5.1. Tapioca starch

X-ray diffraction pattern of SNT, SANT-H and SANET as a function of time: 15 min, 30 min and 60 min showed the A-type crystallinity pattern as shown in Figure 42 with no obviously different pattern among samples. They showed strong reflection (2θ) at 15 ^{0} and 23 ^{0} and unresolved doublets at 17 ^{0} and 18 ^{0}. However, the peak intensity of SANET looks sharper at 17 ^{0}, 18 ^{0} and 23 ^{0} when compared to SNT. The effect of moisture content of starches on the relative crystallinity were neglected since the moisture content of all starches were ~11 %. From Nara and Komiya method, calculated relative crystallinity (%) of SANET was significantly decreased ($P \leq 0.05$) when compare to SNT and SANT-H. SANT-H (35.70 ± 1.79 %) provided a significantly decrease ($P \leq 0.05$) on % relative crystallinity in comparison with SNT (38.81 ± 0.22 %). The observed % relative crystallinity of SNT is in the range that observed by Atichokudomchai and Varavinit (2003) and Zobel (1988). The enzymatic hydrolysis product (SANET) provided also the decreasing of relative crystallinity by significantly decreased with the increasing of hydrolysis time ($r^2 = 0.8560$) as shown in Figure 44. This was accounted for the remaining of the relative crystallinity after the enzymatic treatment of tapioca starch. In contrast, the percentage of damage starch is increased ($r^2 = 0.6624$) after the extension of enzymatic reaction time. The decreasing of the percentage of relative crystallinity was due to the increasing of the degree of starch gelatinization after prolong hydrolysis (increasing of damage starch).

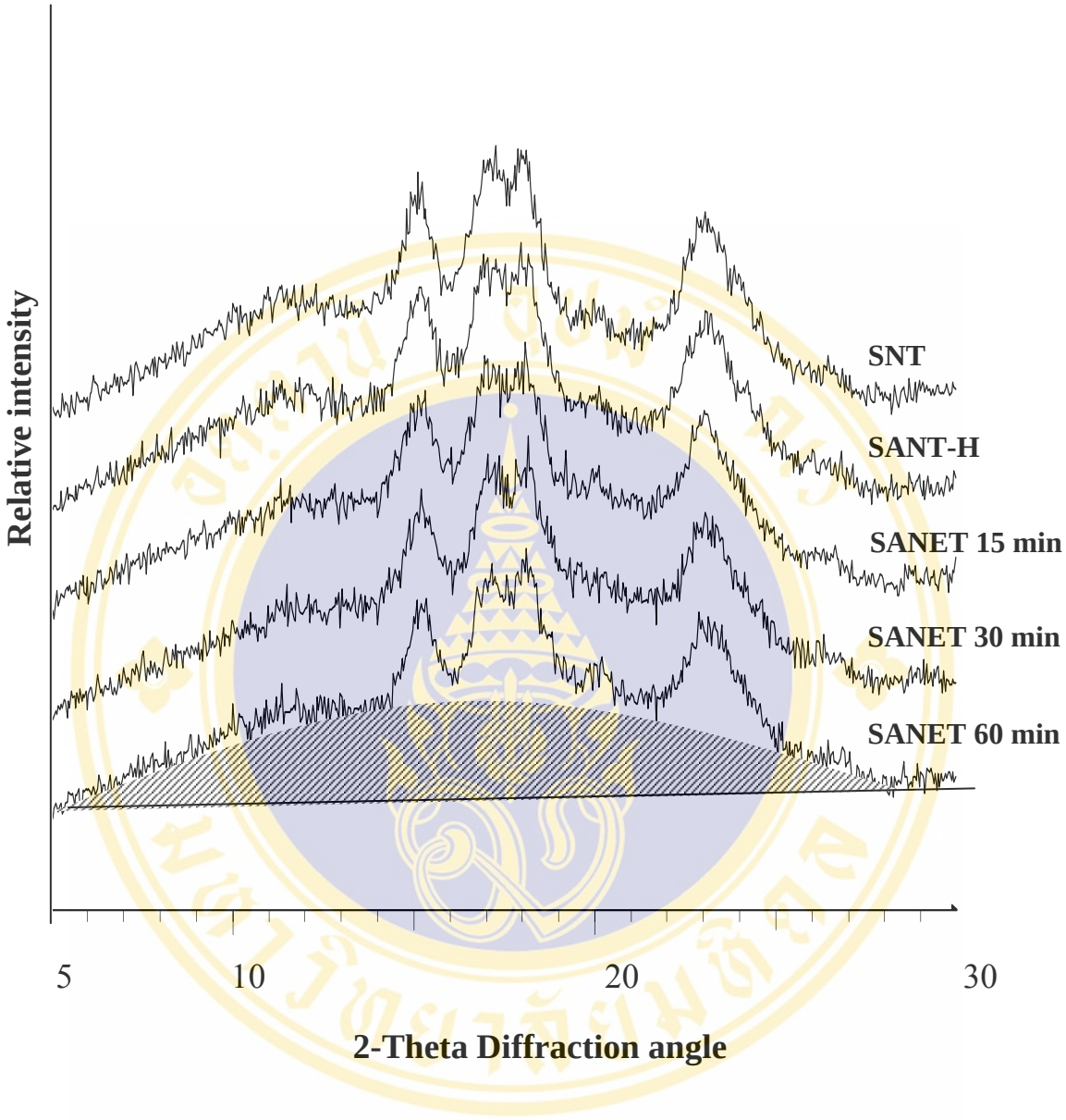

Figure 42. X-ray diffraction pattern of SNT, SANT-H and SANET at various hydrolysis times.

5.2. Rice starch

The A-type crystallinity pattern with strong peak at 2θ about 15^0 and 23^0 and unresolved doublets at 17 ^{0} and 18 ^{0} from X-ray diffraction pattern of SNR, SANR-H and SANER at various hydrolysis times (15 min, 30 min and 60 min), was shown in Figure 43. No obviously different pattern among samples was observed. However, the peak intensity of SANER looks clearly sharper at 17 ^{0}, 18 ^{0} and 23 ^{0} when compared to SNR. The effect of moisture content of starches on the relative crystallinity were neglected since the moisture content of all starches were not different (~11 %). Relative crystallinity (%) of SANER was significantly decreased ($P \leq 0.05$) in comparison with SNR and SANR-H. However, SANR-H (37.08 ± 0.84 %) provided a significantly lower ($P \leq 0.05$) in percentage of relative crystallinity than SNR (45.39 ± 0.68 %). The extension of enzymatic hydrolysis time also decreased linearly of the percentage of relative crystallinity ($r^2 = 0.7811$) as shown in Figure 48. It was accounted for the remaining of the relative crystallinity of rice starch after the enzymatic treatment. The relationship between relative crystallinity and percentage of damaged starch of SANER with various hydrolysis times are also shown in Figure 44. The increasing of hydrolysis time decrease the relative crystallinity which lead to a higher degree of gelatinization (high damage starch) ($r^2 = 0.8170$).

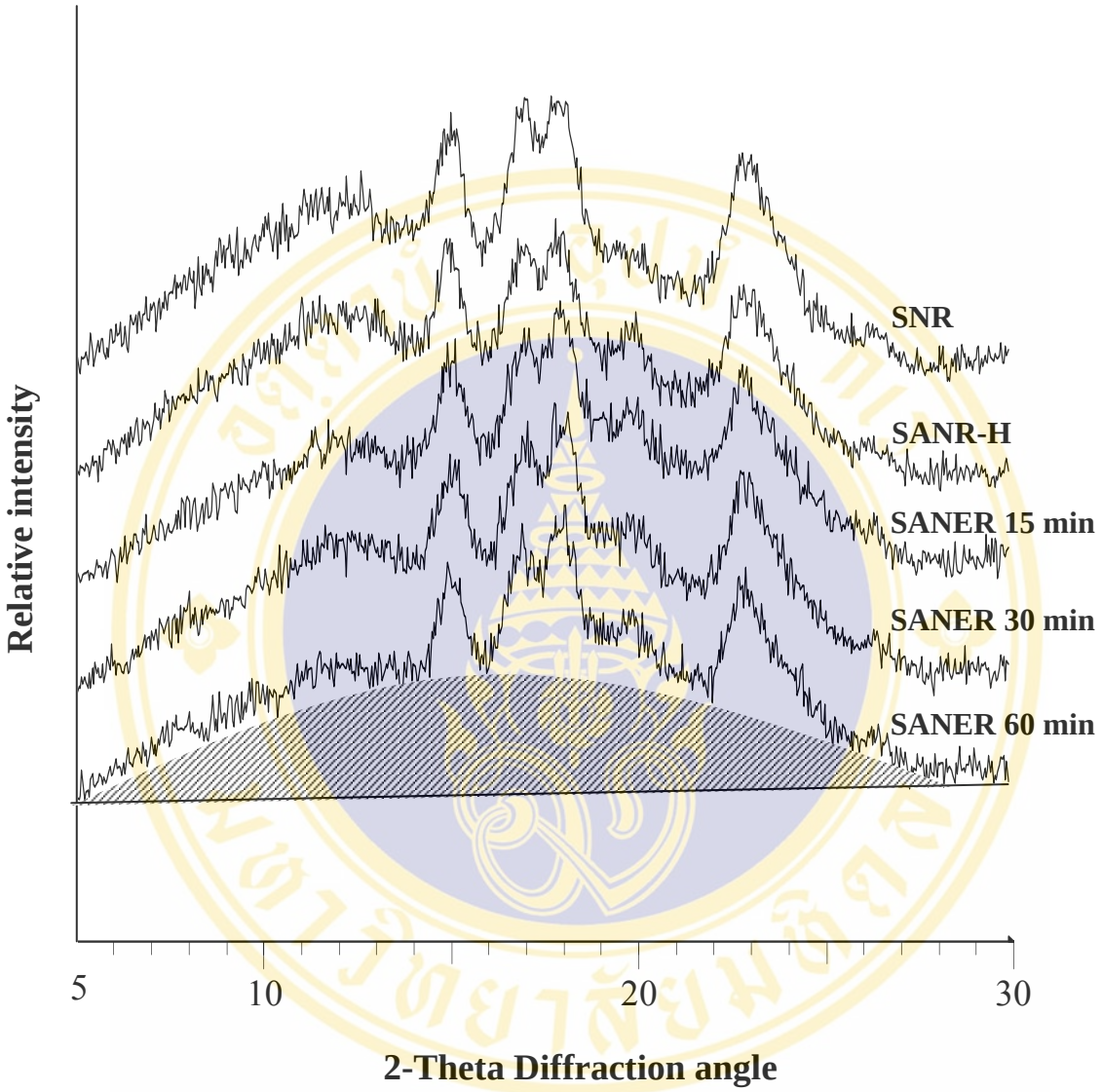

Figure 43. X-ray diffraction pattern of SNR, SANR-H and SANER at various hydrolysis times.

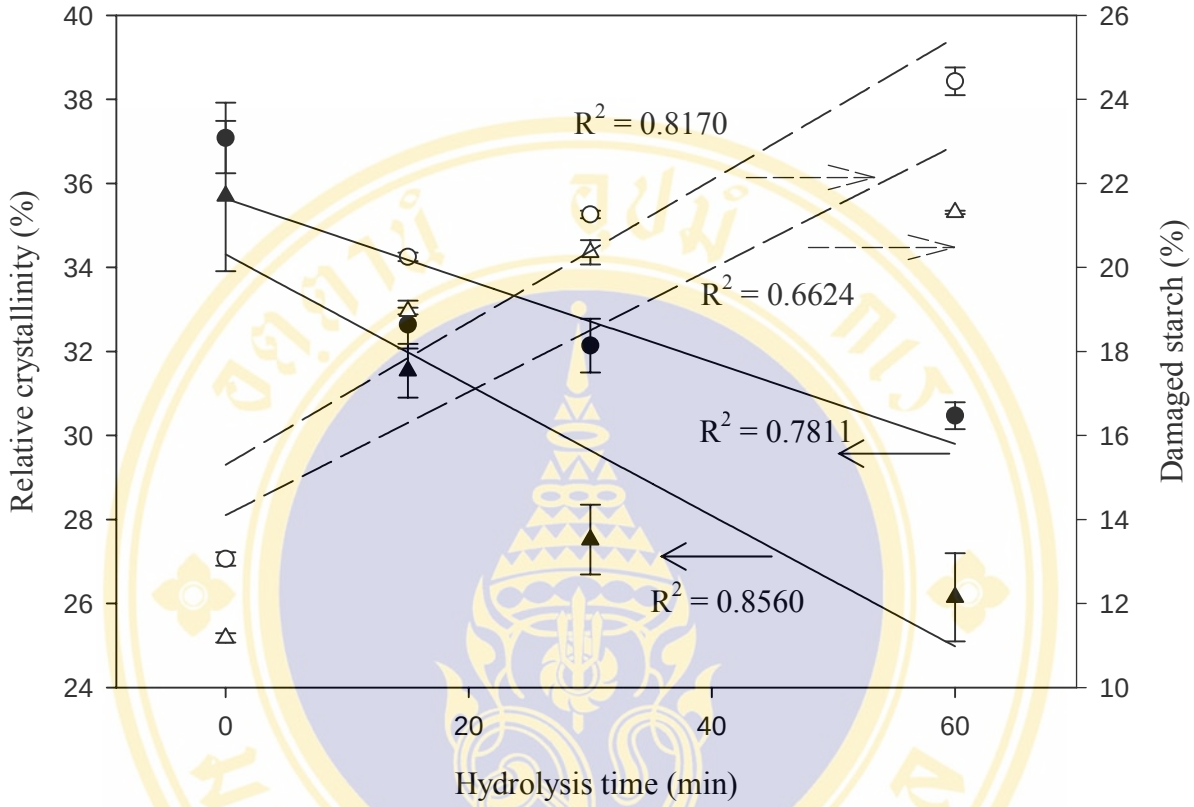

Figure 44. Relationship of percentage of relative crystallinity (—) and damaged starch (---) as a function of hydrolysis time of SANET (▲, Δ) and SANER (●, O) (SANT-H and SANR-H are at 0 min).

6. Utilization of spray dried enzymatic hydrolyzed starches as a direct compression fillers

6.1. Tablet properties

The spherical agglomerates of the enzymatic hydrolyzed tapioca and rice starches at 60 ^{0}C and 70 ^{0}C, respectively, were used as tablet direct compression filler. The plain filler tablets were prepared by mixing filler and 0.5 % magnesium stearate (lubricant) and then pressed into tablets by rotary tablet machine. The resulted tablets were determined for the crushing strength, percent friability, and disintegration time.

6.1.1. Tapioca starch

Enzymatic modification of tapioca starch at 60 ^{0}C (SANET) markedly increases the tablet hardness in comparison with SNT, SANT-L and SANT-H as presented in Figure 45. The maximum crushing strength of SANET with 30 min of hydrolysis time was 162.80 ± 0.78 N at 10.0 kN compression force and also at this hydrolysis time exhibited the highest crushing strength. At 60 min of hydrolysis time also exhibit the high value of crushing strength but this would decrease after 6.0 kN compression force. However, neither SANT-L nor SANT-H improved the crushing strength of the tablets.

The disintegration time from various compression of SNT, SANT-L, SANT-H and SANET at various hydrolysis times were graphically shown in Figure 46. SANT-H exhibit the highest disintegration time at any compression forces. SANT-L and SNT showed the minimum in disintegration time with lower than a minute. From the disintegration profile of SANET**,** it revealed that the disintegration time was progressively increased while increasing in compression force.

Tablet friability values are shown in Figure 47. In general, the friability decreased with the increase in compression force. The effect was more pronounced at lower compression forces. SNT showed the highest in percentage of friability (36.63 %) when compared to SANT-L, SANT-H and SANET. In case of 15 min and 60 min hydrolysis times of SANET showed the zero value of percentage friability at any compression forces. In overall, the percentage friability of SANET is very small when comparing to SNT.

In preliminary, it could be concluded that combined partial gelatinization with enzyme treatment could provide the properties of tapioca starch for preparing tablet with high crushing strength, low disintegration time and friability.

6.1.2. Rice starch

Generally, spray dry rice starch provided an agglomerated form and yield a high crushing strength when compare to tapioca starch. This was probably due to the very specific properties of rice starch.

Enzymatic modification of rice starch at 70 ^{0}C (SANER) increased the tablet hardness when compared to SNR, SANR-L and SANR-H as shown in Figure 48. The maximum crushing strength of SANER was also obtained from 30 min of hydrolysis time, which is 145.14 ± 0.45 N at 10.0 kN compression force. However, crushing strength profile of SANER at 15 and 30 min of hydrolysis times provided nearly the same. Inversely, At 60 min of hydrolysis time exhibited the poor compactability. However, Both SANR-L and SANR-H did not improve the crushing strength of tablets when compares to SNR.

The disintegration time profiles of tablets are shown in Figure 49. SANR-H exhibited the higher disintegration time (5.71 ± 0.28 min) when compared to SNR which providing the minimum disintegration time (1.80 ± 0.16 min). SANR-L also showed higher disintegration time than SNR at any compression forces. From the disintegration profile of SANER, it revealed that highest disintegration time was obtained from SANER at 15 min of hydrolysis time while the lowest was obtained from 60 min of hydrolysis time. Disintegration time of SANER exhibited higher value than that obtained from SANET.

Tablet friability values of SNR, SANR-L and SANR-H showed lower value in percentage friability. Tablet profiles at various hydrolysis times of SANER are also graphically illustrated in Figure 50. All of the SANER values at various reaction times showed the small values of the percentage friability. However, it was not correlated with the compression forces.

In preliminary, it could be concluded that combined partial gelatinization with enzyme treatment of rice starch could provided better properties of the tablet than the SNR, SANR-L or SANR-H did.

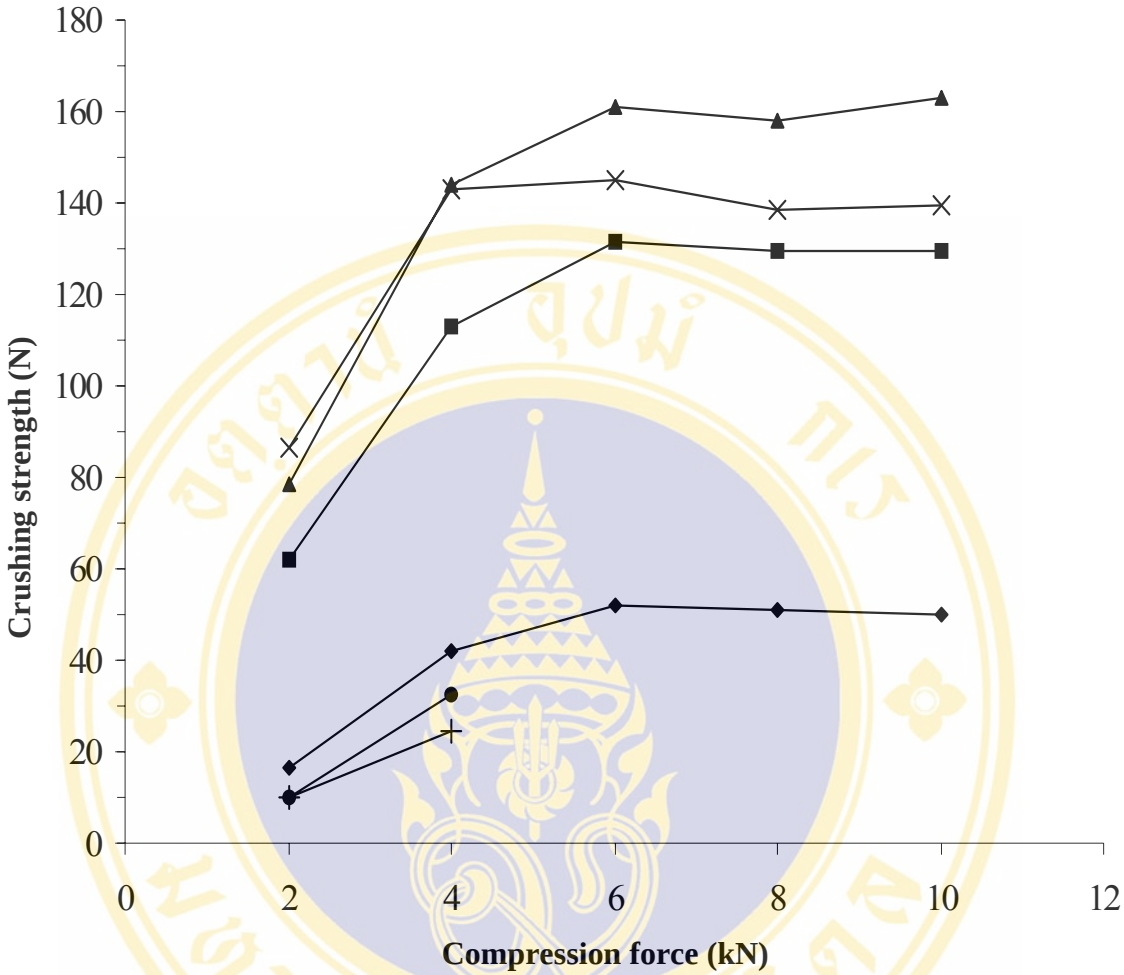

Figure 45. Crushing strength (N) as a function of compression forces (kN) of plain filler tablets lubricated with 0.5% magnesium stearate preparing from SNT (●), SANT-L (+), SANT-H (♦) and SANET at various hydrolysis times. (■ = 15 min, ▲ = 30 min and x = 60 min). SNT and SANT-L were capping after tablet pressing.

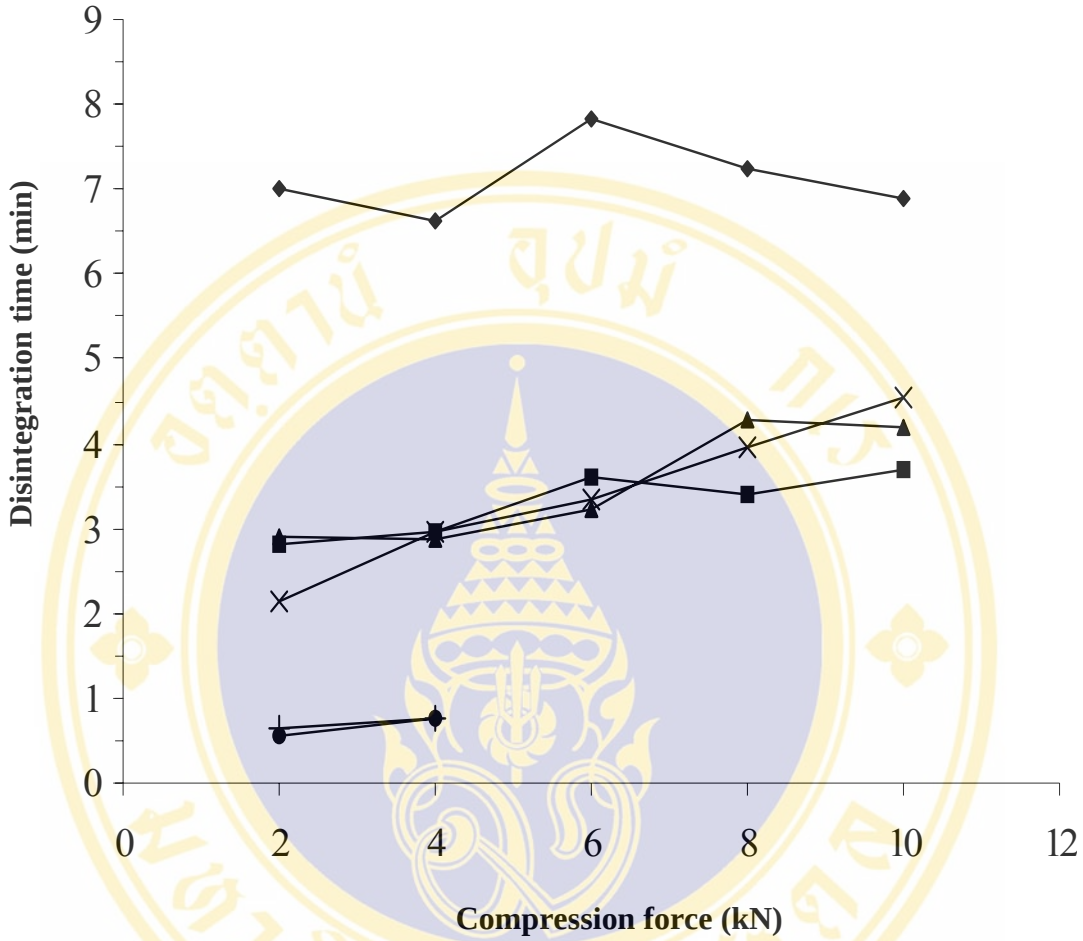

Figure 46. Disintegration time (min) as a function of compression forces (kN) of plain filler tablets lubricated with 0.5% magnesium stearate preparing from SNT (●), SANT-L (+), SANT-H (♦) and SANET at various hydrolysis times. (■ = 15 min, ▲ = 30 min and x = 60 min). SNT and SANT-L were capping after tablet pressing.

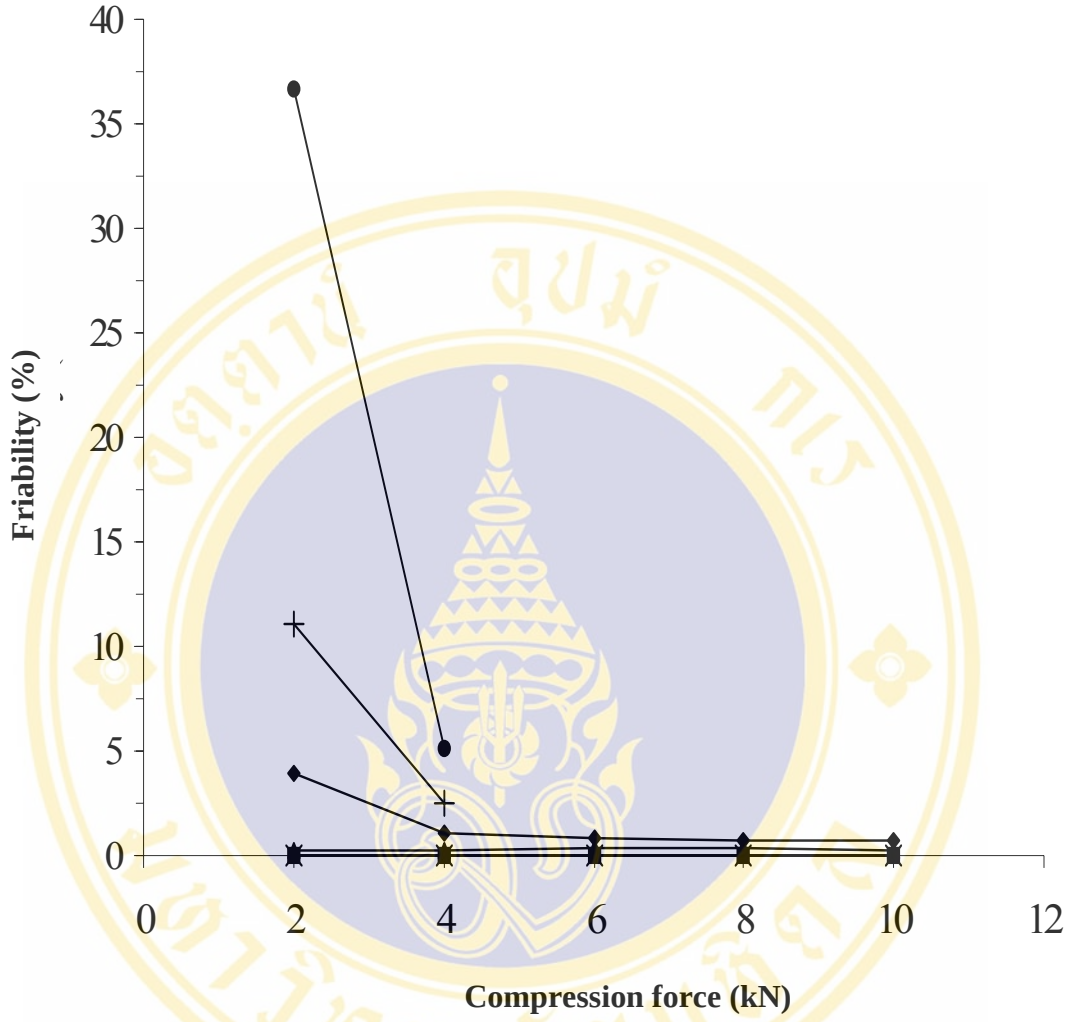

Figure 47. Friability (%) as a function of compression forces (kN) of plain filler tablets lubricated with 0.5% magnesium stearate preparing from SNT (●), SANT-L (+), SANT-H (♦) and SANET at various hydrolysis times. (■ = 15 min, ▲ = 30 min and x = 60 min). SNT and SANT-L were capping after tablet pressing.

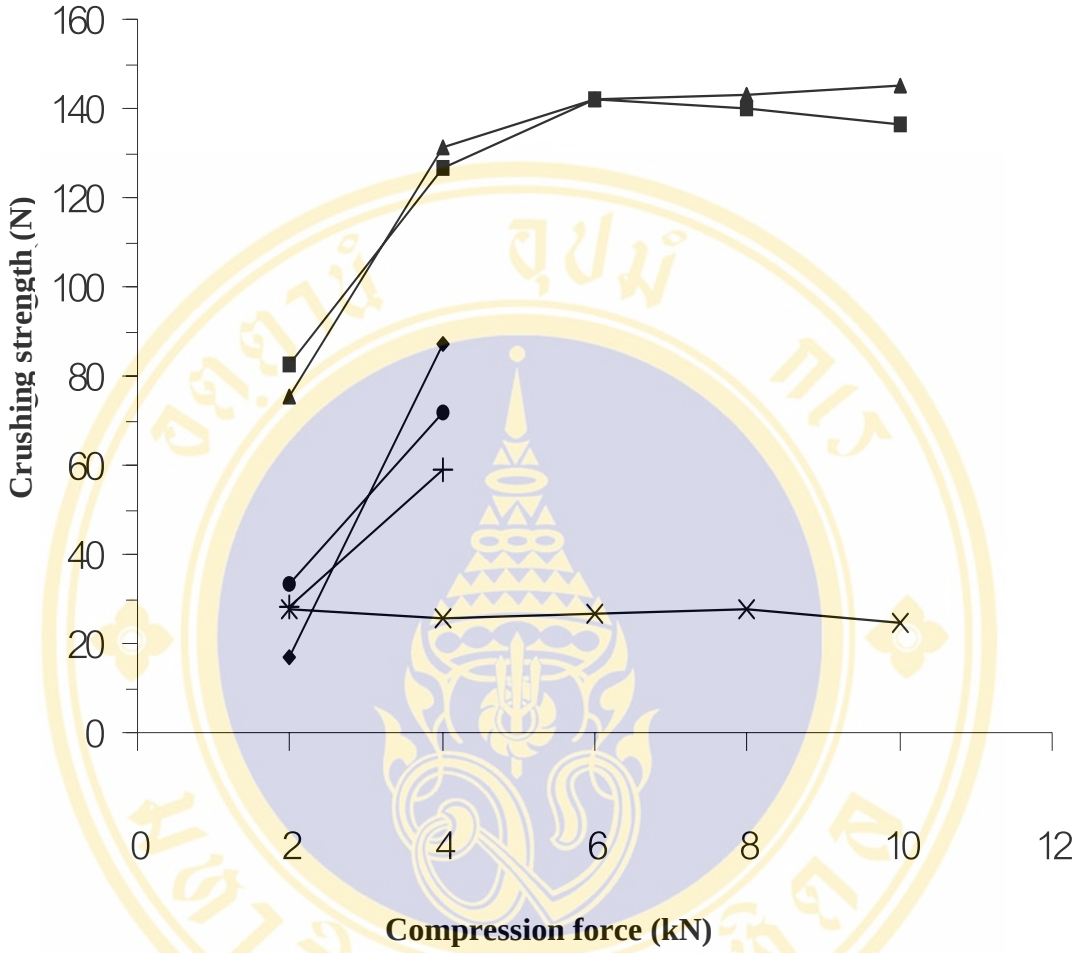

Figure 48. Crushing strength (N) as a function of compression forces (kN) of plain filler tablets lubricated with 0.5% magnesium stearate preparing from SNR (●), SANR-L (+), SANR-H (♦) and SANER at various hydrolysis times (■ = 15 min, ▲ = 30 min and x = 60 min). SNR, SANR-L and SANR-H were capping after tablet pressing.

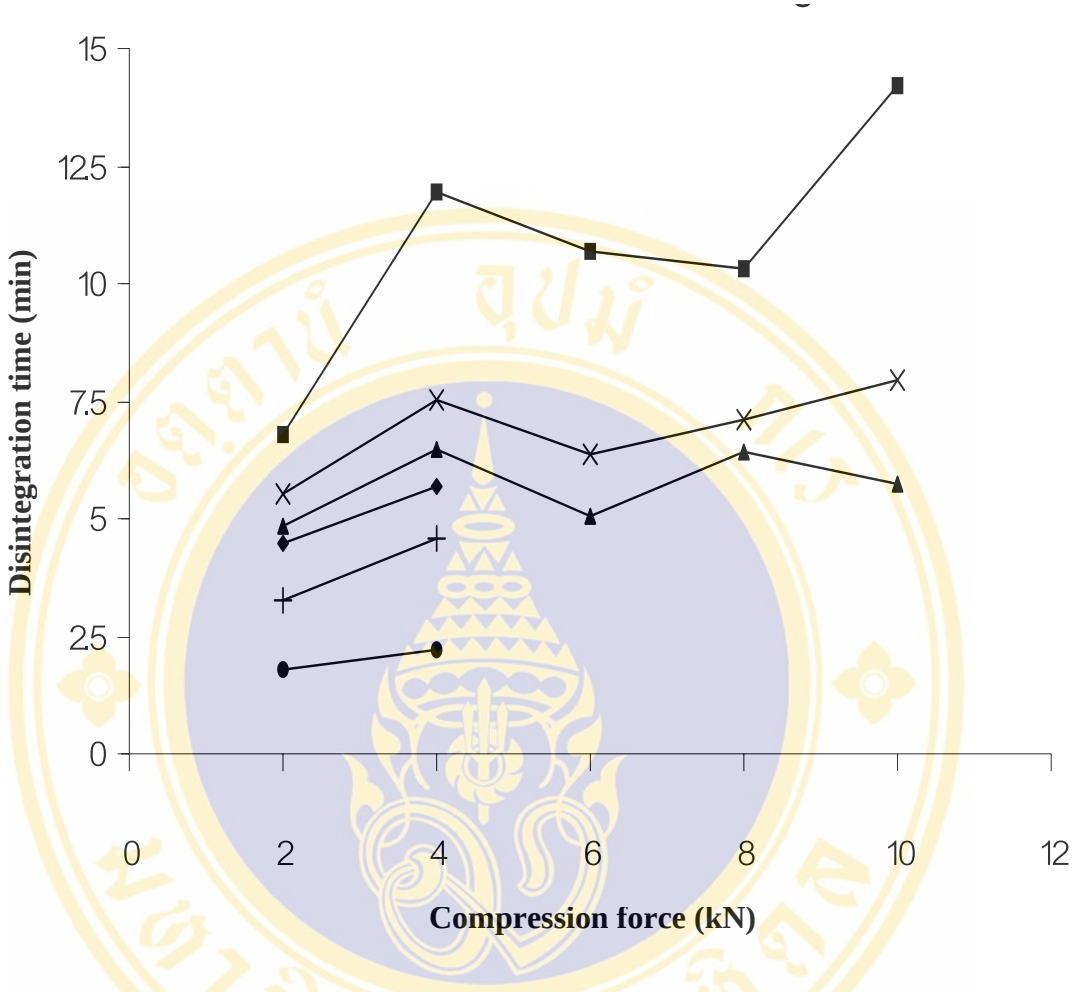

Figure 49. Disintegration time (min) as a function of compression forces (kN) of plain filler tablets lubricated with 0.5% magnesium stearate preparing from SNR (●), SANR-L (+), SANR-H (♦) and SANER at various hydrolysis times (■ = 15 min, ▲ = 30 min and x = 60 min). SNR, SANR-L and SANR-H were capping after tablet pressing.

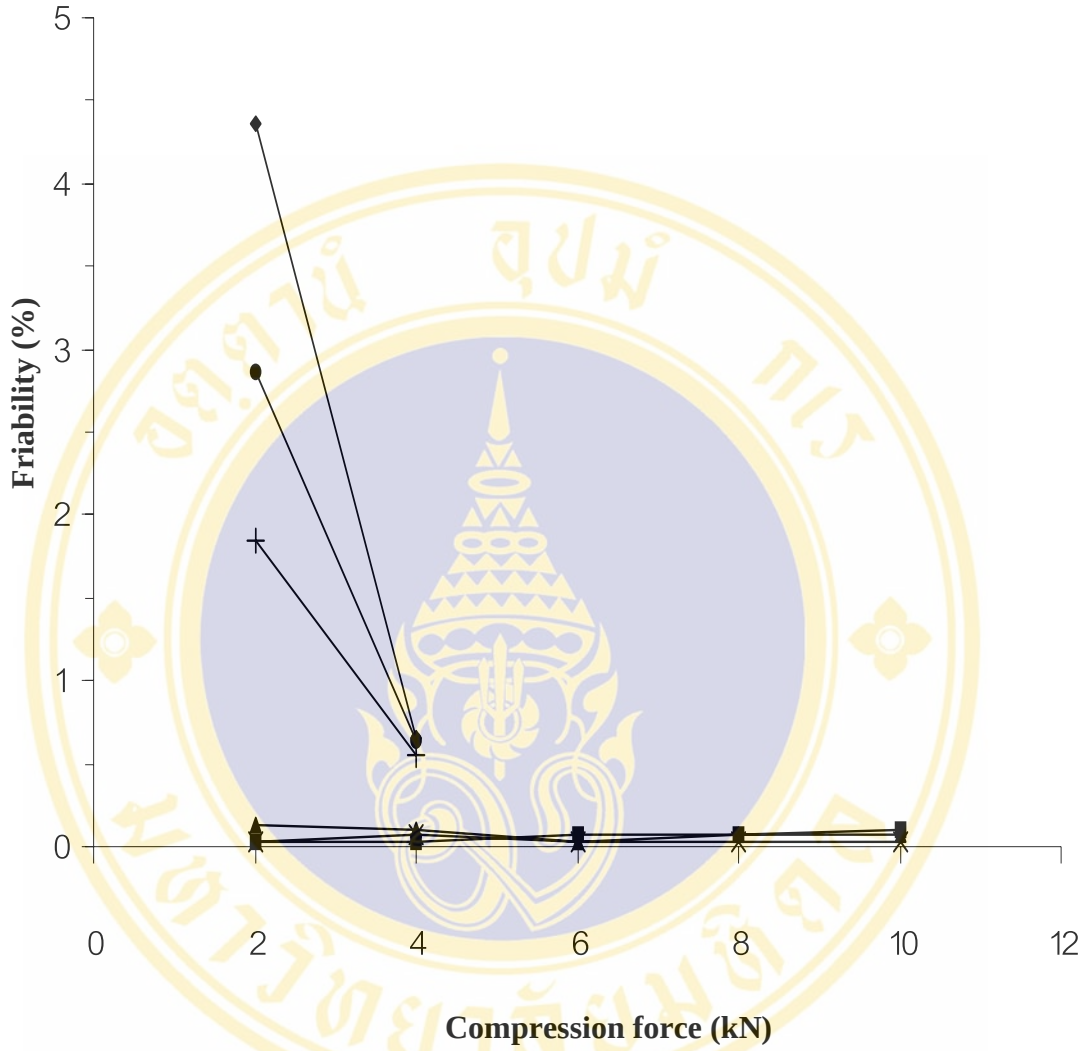

Figure 50. Friability (%) as a function of compression forces (kN) of plain filler tablets lubricated with 0.5% magnesium stearate preparing from SNR (●), SANR-L (+), SANR-H (♦) and SANER at various hydrolysis times (■ = 15 min, ▲ = 30 min and x = 60 min). SNR, SANR-L and SANR-H were capping after tablet pressing.

6.2. Comparative study of SANET-30 and SANER-30 with other commercial compression fillers.

From the study, SANET and SANER at 30 min hydrolysis times (SANET-30 and SANER-30) were suitable to be very good tablet filler for direct compression process. It was of interest to compare their tablet properties with those of similar fillers existing in the market. The selected fillers for this study were microcrystalline cellulose (MCC), pregelatinised starch (PS), lactose (L), Era-Tab, Era-Tab SP, SANET-30 and SANER-30. These plain fillers were physically mixed with 0.5 % magnesium stearate as lubricant.

Figure 51 shows the crushing strength (N) at various compression forces (kN) of the tablets of SANET-30 and SANER-30 with those of commercial tablet fillers. MCC showed the highest compactability among the fillers tested while the poorest was L. It should be noted that L and PS provided almost the same identical hardness profiles. SANET-30 and SANER-30 gave better compactability profile than Era-Tab and Era-Tab SP.

The disintegration times of all fillers are shown in Figure 52. Era-Tab SP and MCC provided lower disintegration time than the others at any compression force tested. Era-Tab and L came next, which showed almost the same disintegration time. The disintegration time of SANET-30 was in the range of 2.90 to 4.27 min while SANER-30 was 4.85 to 6.48 min and the highest disintegration time was PS. It should be mentioned that even though PS and L provided almost identical tablet hardness, the disintegration time of PS was greater than that of L.

The friability data are graphically presented in Figure 53. Era-Tab SP exhibited lower of percentage friability, which was almost identical with MCC, SANET-30 and SANER-30. Era-Tab provided lower friability at higher compression forces whereas PS and L possessed the highest friability value.

Table 9 showed the comparative study of tablets properties of SANET-30 and SANER-30 compare with commercial fillers at 4.0 kN compression force. The MCC showed the highest tablet hardness followed by SANET-30, SANER-30 and Era-Tab SP. PS and Era-Tab provided same compactability which came next and the lowest crushing strength was L.

The order of disintegration time from the highest to the lowest was shown in the following order: PS > SANER-30 > SANET-30 > Era-Tab > L > MCC > Era-Tab SP.

PS and L show almost the same highest value in friability at 4.0 kN compression force. The next was Era-Tab, which was 3.14 % followed by Era-Tab SP (0.45 %), SANET-30 (0.27 %) and MCC (0.12 %). SANER-30 showed the lowest value in percentage of friability when compare to other fillers.

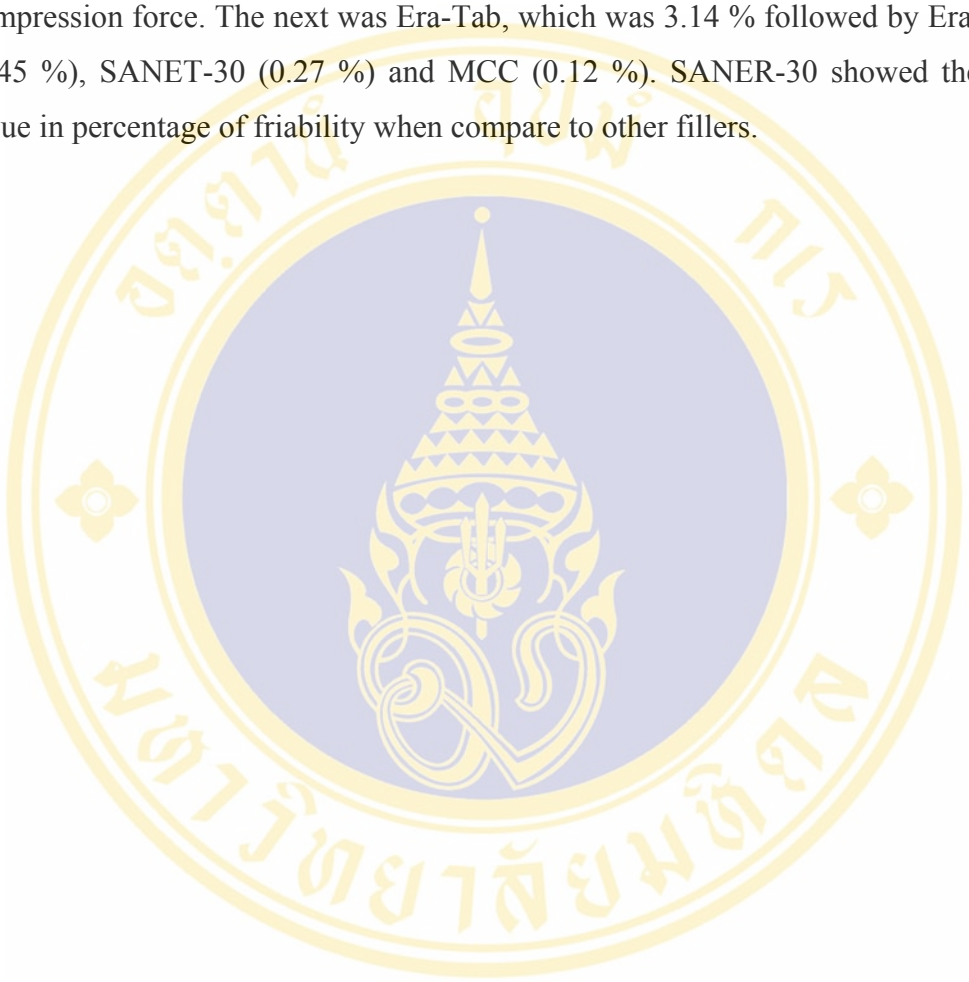

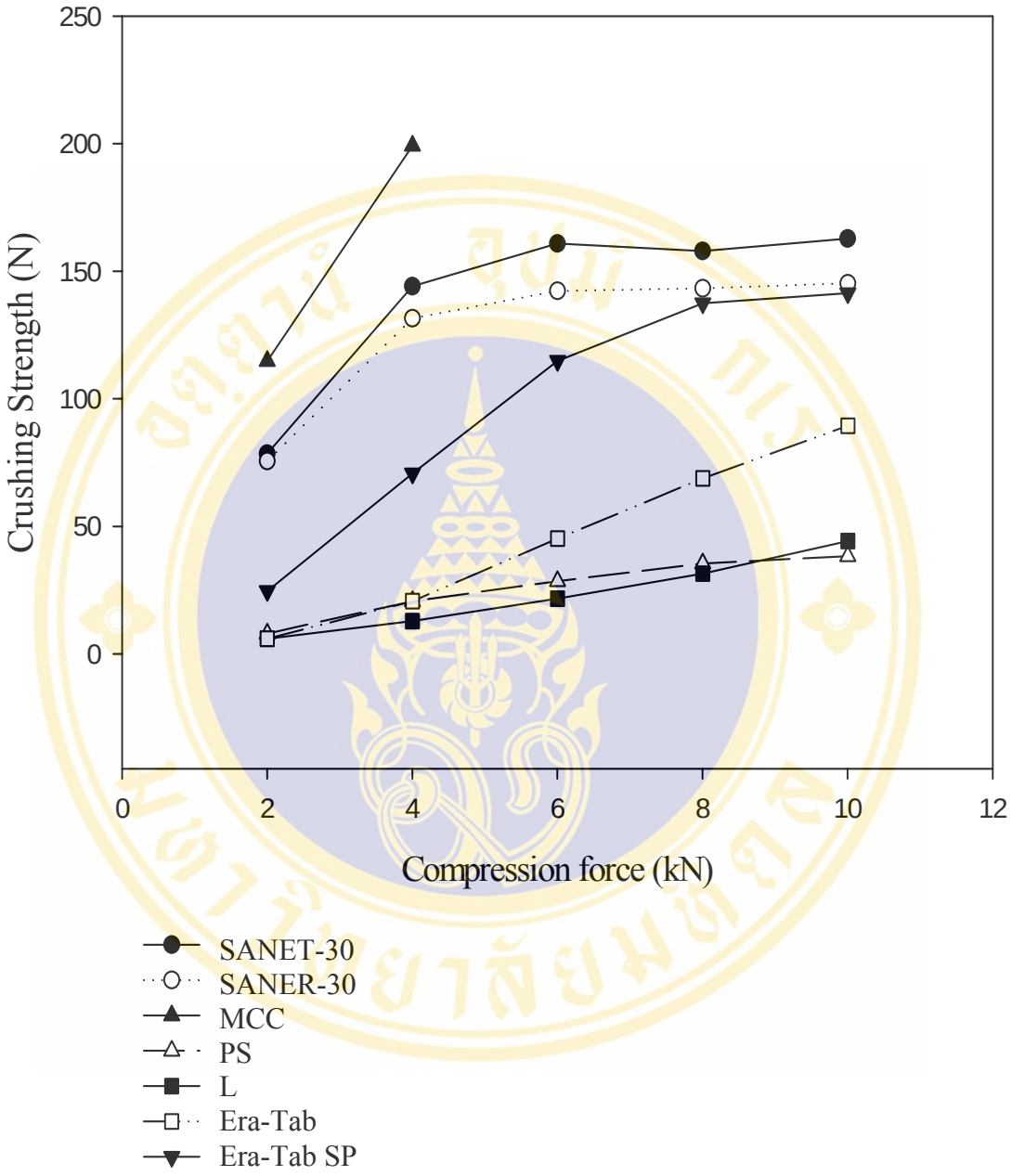

Figure 51. Tablet hardness (N) as a function of compression forces (kN) of plain filler tablets lubricated with 0.5% magnesium stearate preparing from SANET-30, SANER-30 comparing with those from some commercial fillers, i. e., MCC, PS, L, Era-Tab and Era-Tab SP.

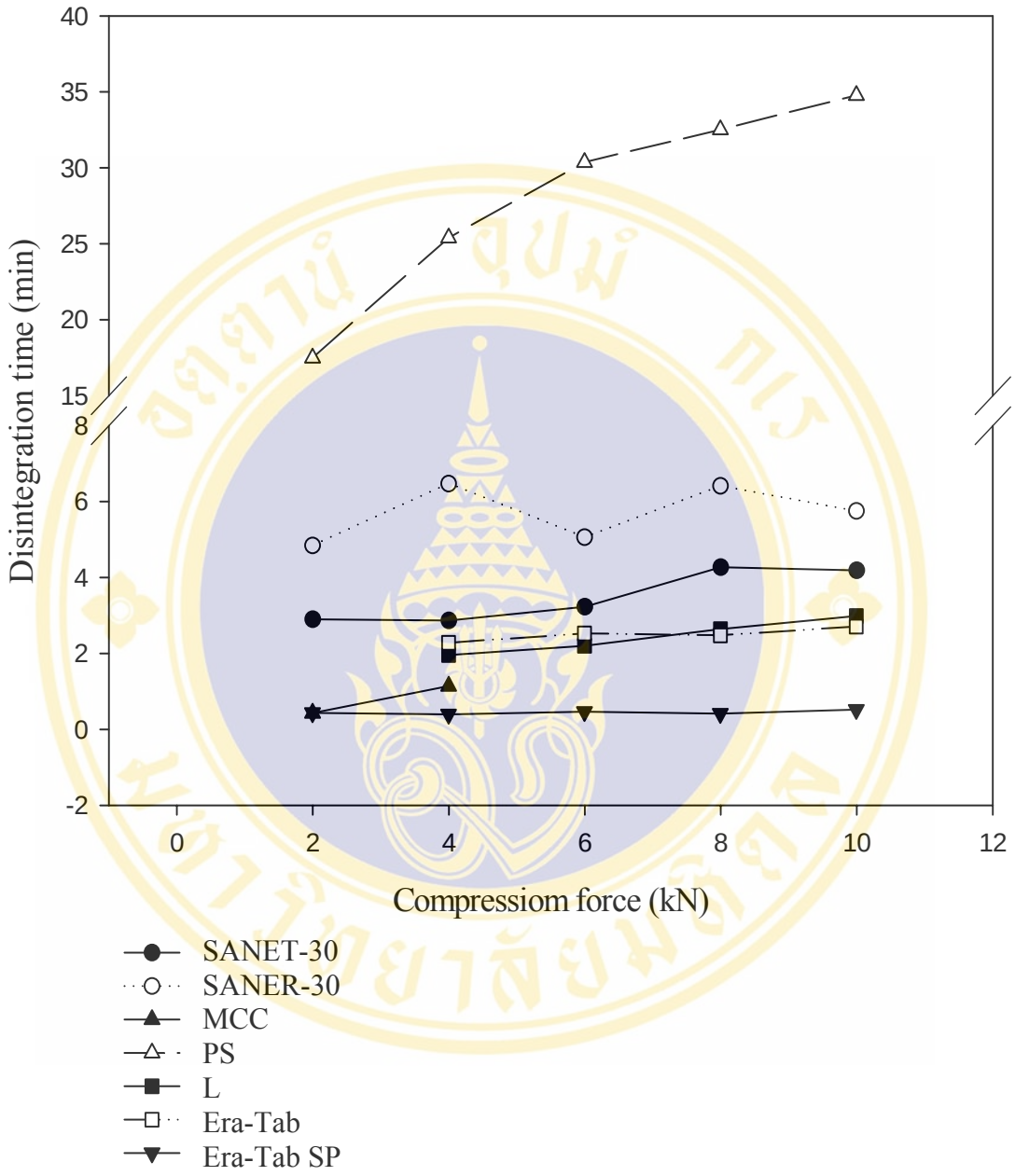

Figure 52. Disintegration time (min) as a function of compression forces (kN) of plain filler tablets lubricated with 0.5% magnesium stearate preparing SANET-30, SANER-30 comparing with those from some commercial fillers, i. e., MCC, PS, L, Era-Tab and Era-Tab SP.

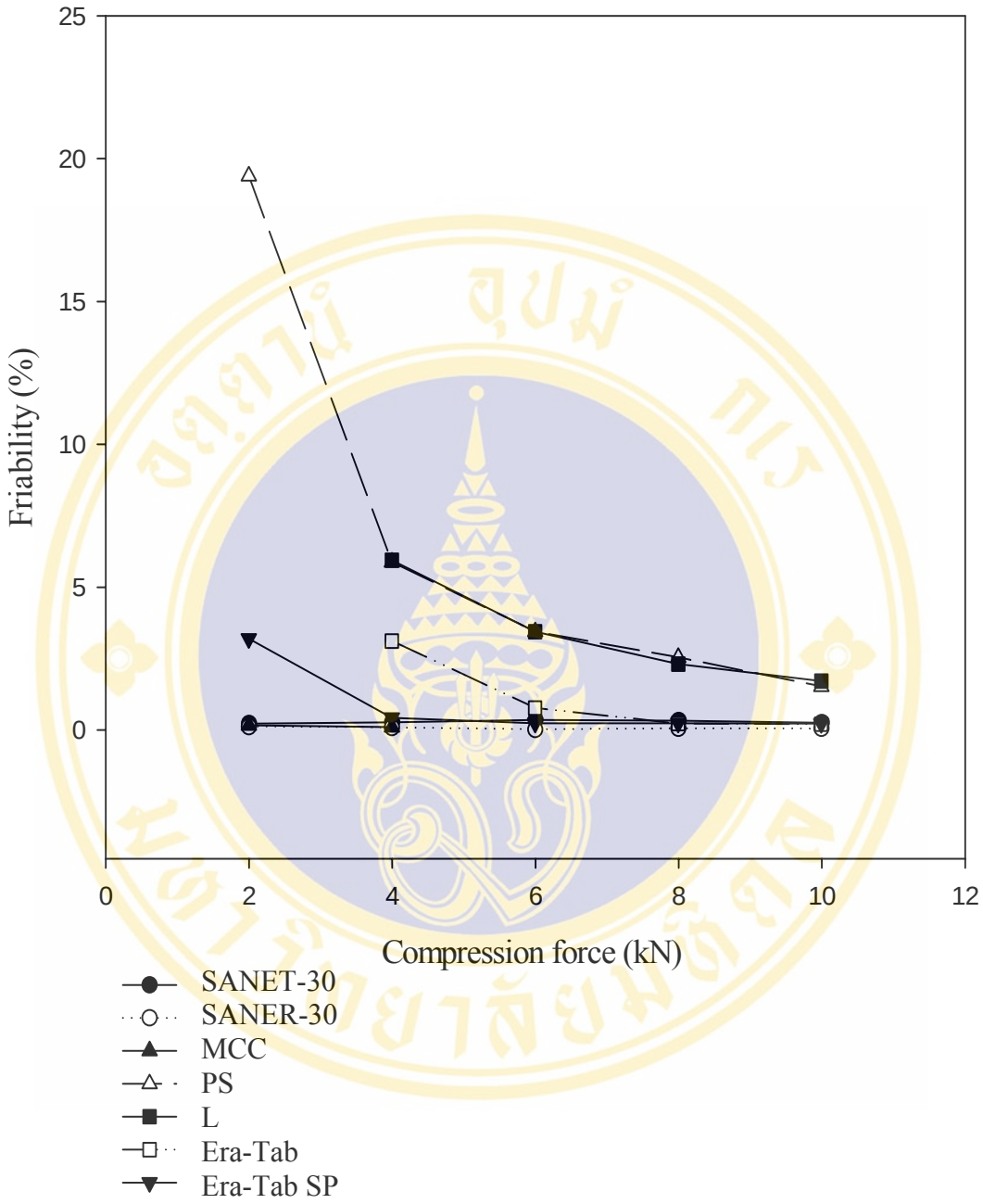

Figure 53. Friability (%) as a function of compression forces (kN) of plain filler tablets lubricated with 0.5% magnesium stearate preparing SANET-30, SANER-30 comparing with those from some commercial fillers, i. e., MCC, PS, L, Era-Tab and Era-Tab SP.

Table 9. Tablet properties of SANET-30 and SANER-30 comparing with those of the commercial tablet fillers, i. e., microcrystalline cellulose (MCC), pregelatinised starch (PS), lactose (L), Era-Tab and Era-Tab SP at 4.0 kN compression force.

Type	Tablet properties		
	Crushing strength [N]	Disintegration time [min]	Friability [%]
SANET-30	144.16	2.87	0.27
SANER-30	131.41	6.48	0.10
MCC	199.08	1.15	0.12
PS	20.59	25.42	5.90
L	12.75	1.97	5.96
Era-Tab	20.59	2.29	3.14
Era-Tab SP	70.61	0.41	0.45

CHAPTER V
DISCUSSION

1. Chemical properties

From Table 5, the increasing in protein content of SANET compared with SNT and SANT-H was due to the addition of thermostable α-amylase into the starch slurry for the enzymatic hydrolysis before spray drying. This trend was also archived in case of SANER when compared to SNR and SANR-H. The low ash content in SNT (0.14%) and SNR (0.65%) indicated that the starches were relatively free of hydrated fine fibers, which are derived from the cell wall enclosing. However, the addition of 500 ppm of calcium chloride using as the cofactor of α-amylase in SANET was responsible for increasing of the ash content. The higher ash content of SANT-H when compared to SNT was due to the addition of calcium chloride into the starch slurry. The high ash content, which was produced from high concentration of calcium chloride, was also observed in SANER and SANR-H. The starches were generally characterized by a low lipid or fat content (<1%). It is recognized that cereal starches also contain significant amounts of lipids (Swinkels, 1985). Heat can cause rapid alteration of the granule surface, restructuring the molecular architecture. This rearrangement possibly causes separation of the lipid component from the carbohydrate, leading to concentration of lipid within the outer layers (Atkin et al., 1998). Nevertheless, the enzymatic hydrolysis was not influent the fat content in both SANET and SANER when compared to their spray dried native starches.

Normally, amylose content of rice is greater or equal to tapioca (Jane et al., 1999; Hizukuri, 1988). The higher amylose content of SNT than SNR may be due to the higher proportion of long branch chain that could bind iodine and inflate the iodine affinity (Table 6).

The decreasing of amylose content which was affected by heat treatment from partial gelatinization would lead to the amylose leaching out of the starch granule.

Smaller amylose molecules near the surface can be leached out of the granule (Jane & Shen, 1993), into the external solution as a result of the water exchange from the external into the internal components of the granule, leaving the amylopectin, as well as granule crystallinity, largely intact (Zobel, 1992). However, according to many authors (Autio, 1990; Gallant et al., 1997; Valentudie et al., 1995) amyloses that lived inside the starch granules are preferentially leached out of the granules throughout the pores. In addition, the leaching process does not proceed to completion; there is always some amylose that is perhaps embedded or trapped by amylopectin crystallites which does not leach out easily. However, the decreasing of amylose content from SNR to SANR-H was not changed as much. This was due to the annealing effect which caused little solubilisation of α-glucan (Testers et al., 1998). The annealing process itself improved order is a genuine molecular event rather than a consequence of leaching amorphous α-glucan and hence "concentrating" crystalline material. As leachate is primarily (amorphous) lipid free amylose according to the definition of Morrison et al., (1993), the amylose must be more restricted from leaching out of the granules. This trend was also true in case of SANT-H in comparison with SNT (Table 6).

It is suggested that in a recent study (Tester & Morrison, 1990) that enzyme resistance in starch granules is generated by aggregation of amylose helices localised in the granule. Amylose is though to cause disruption to the crystallites, which form the amylopectin layer (Jenkins & Donald, 1995). The decreasing in amylose content (Table 6) due to amylose leaching from partial gelatinization would profitable offering for α-amylase to easily hydrolyse the starch residue after preheating.

The description for the pronounceable decreasing of amylose content of SANET and SANER is possible from most of the amylose chains embedded in the amorphous regions was preferentially hydrolyzed by α-amylase. Hydrolysis of starches with α-amylase occurred granule by granule, not uniformly throughout the granule population. Moreover, those amylose chains that leach out would be expected to exhibit the greater susceptibilities to hydrolysis. In addition, It is well known that (partial) gelatinization greatly lower the resistance of starch to enzymatic attack so the extension of hydrolysis time (also increasing in heating time's period) will increase the number of enzymatic hydrolyzed starch which would decrease in the amylose content.

This reducing trend in amylose content of residues from amylolysis was not only supported by Jiang and Liu (2002) but also Zhou et al. (2004) who postulated that in all legume starches, apparent amylose content decreased with hydrolysis time. However, The extent of the decreasing in amylose content between SANET and SANER was difference. Disruption of amylopectin crystallites by amylose and extent of starch damage (influenced by theirs amylose content, amylopectin chain and relative crystallinity) were also causative factors influencing the rate and extent of hydrolysis. Consequently, the differences in the extent of decrease in amylose content (SANET > SANER) reflect differences in the degree of accessibility of α-amylase to amylose chains within the amorphous domains of each starch granule types (Zhou et al., 2004).

2. Morphological properties

The size and shape of SNT and SNR under microscope did not different when compared to SANT-H and SANR-H. Clearly, however, small differences in size cannot be accurately quantified using microscopy and care should be placed on reliance upon this data. However, the other techniques such as particle size distribution analysis that can accurately quantify the size of starch granule will be discussed later.

The common starches are readily identifiable by using a polarizing light microscope to determine their size, shape, and position of the hilum (the botanical center of the granule) (Schoch & Maywald, 1967). It is noted by Atkin et al. (1999) that the hydration was intensified the birefringence of the dry starch granule. Thus, the investigation in this study of starch granules by the cross polarized was done under hydrate state. In general, gelatinization process induces loss of birefringence observed using polarized light microscopy. This is implied that the Maltese cross visible in SANT-H (Figure 31B and 31E) did not appear to be affected greatly by the partial heat treatment (annealing or partial gelatinization). Similarly, the existing of birefringence of SANR-H is indicated the unchange of crystalline order within rice starch granules in comparison with SNR due to the effect of partial heat treatment as observed in Figure 36A2 and 36B2. This was clear from the fact that the crystalline structure was preserved.

However the loss of some part of Maltese cross of SANET (Figure 31C and 31F) and SANER (Figure 36C1 and 36C2) was clearly observed under both light and polarized light fields. This was described by the occurring of endocorrosion or tunneling action of the α-amylase into the starch granule. The loss of birefringence initiates first at hilum and is associated with the formation of cavities in the central region of the granules which is facilitated by the presence of water, showing that the disorganization first affects at the less organized areas of the granule (Garcia et al., 1997). However, some starch granules that exhibited the surface erosion did not observe the change in birefringence. Moreover, not all of the starch granules that was hydrolyzed by enzyme. Some physically intact of starch granules from SANET (Figure 31C) and SANER (Figure 36C1) were still observed. This was suggesting an inherent structural heterogeneity in these starch granules which was confirmed a selective hydrolysis in which the enzyme possesses a "granule-by-granule" attack (Colonna et al., 1988; Leach & Schoch, 1961). The granules that have enough damage will hydrate partially in water, and the interference cross will fade as the granule swells. The most dramatic types of damage (broken and exploded); as hydration of the core ruptured the granule occur when areas within the granule swell, leaving the outer layers of the granule split but ostensibly intact (Figure 31C and 36F; Figure 36C1 and 36C2). The differentiation of the outer layers of the starch granule from the inner layers suggests a macroscopic model of granule structure comprising as outer layer, that is resistant to both damage and gelation and maintains the integrity of hydrated granules, covering a less resistant interior (Adler et al., 1994). In addition, all SNT, SANT-H and SANET were markedly observed the hole at the center of the intersection of the Maltese cross (Figure 31C). Quantification of the size of holes in rice starch samples was not possible with light microscopy because of their small size. However, holes were counted in the rice samples as observed by Baldwin et al. (1994). Some disarrangements had obviously occurred in the already less organized hilum because the granule center of the SANET and SANER was more disrupted.

In general, light microscopy method allows the optical sectioning of hydrated granules, exposing their interior and can not be expected to provide the detailed information that can be obtained with method such as SEM which is higher resolution and possible to determine a more detailed perspective on granule surface

characteristics and granule morphology without alterations due to hydration (Chmelik, 2001).

NT and NR (Figure 32A and 32C), after subjection to spray drying process, was in agglomerated spherical shapes particles of various size when compared with their native, which consisted of irregular shape aggregates. At ambient temperatures raw starch granules exist as individual particles that do not 'stick' to each other. This is mainly because raw starch granules have a highly ordered molecular structure and at room temperature, there is not enough energy to disrupt the structure even with the assistance of water. The tightly packed crystalline zone in raw starch granules prevents interactions between molecules from occurring.

A granular particle of spray dried starches was made up of a large number of starch grains attached together. During the spray drying process, the heat could induce partial gelatinisation of the surface of starch grains, resulting in the formation of solid bridges when water in a spraying droplet was evaporated; these solid bridges assisted starch particles in adhering together to form granular particles. By means of SEM photomicrographs at high magnification, the welding of starch grains at the contact regions could be observed. Unfortunately, SEM of SNT and SNR was not observed the stickiness of individual starch granules together (Figure 33D and 37D). However, spray drying did not cause damaged starch or at least slightly effect to the starch granules (SNT showed 0.31 % while SNR presented 1.04 %).

The fusion of each starch granules together as observed in SANT-H and SANR-H (Figure 33E and 37E) led by the surface gelatinization which occurring from partial gelatinization. Upon partial gelatinization, some part of crystalline structure of starch is disrupted if adequate energy is supplied. This leads to the break-up of hydrogen bonding between hydroxyl groups of starch molecules (French, 1984). Consequently, the hydroxyl groups are 'released' from the crystalline structure, and some free hydroxyl groups are "exposed" on or near the surface of the starch granules. If water molecules were available, a network of hydrogen bonding involving water would result in connecting those exposed or so-called "surface-active" hydroxyl groups on different starch granules. These new hydrogen bonds between starch and water molecules are formed replacing the original hydrogen bonding between starch molecular chains either inside or on the surface of the granules. These granules are

said to become ‘sticky’ because they are quick in forming inter-particle hydrogen bonding with neighboring particles, which finally turn the starch/water system into an inter-connected gel phase (Zobel, 1984). However, this was in accompanying with spray drying technique which also caused the surface gelatinization.

Heat damaged convert the large ordered regions (of the granule) into essentially disordered amorphous material that is freely accessible to external agents such as solvent water and amylolytic enzymes (Tipples, 1969). Further, Morrison et al. (1994) proposed that the amorphous, less resistant interior regions of the granule are protected by the integrity of ordered domains which form continuous concentric shells, with the surface of the granule being one of these resistant ordered shells. Thus they consider a reasonably perfect surface of ordered external chains of amylopectin to be impermeable to an enzyme, since the substrate sites for endo-acting amylases would be well buried and protected within the granule. We therefore postulated that, in SANT-H and SANR-H, granule surface damage due to heat processes leads to penetration of this outer more resistant layer, and is likely to have a significant contribution to the increase in hydration-enzyme susceptibility of starch granules following heat damage. In parallel, molecular leaching is increased as the pores of the surface increase in size, forming breaches in the outer surface of the granules due to swelling (Atkin et al., 1999).

From the SEM micrographs, it was clear that the very short time of enzymatic reaction in both SANET and SANER did affect the surface of starch granule. The patterns of enzymatic corrosion of both types of starches (tapioca and rice starch) are seem similar. Moreover, cassava starch is considered as susceptible as the main cereal starches (Leach & Schoch, 1961).

It is appropriate at this stage to give a brief description of the mechanism of α-amylase action, which would then enable a subsequent discussion later.

α-amylase has been shown to have five binding sites with the catalytic site located between subsites 2 and 3, with two subsites to the right and three subsites to the left of the catalytic site (Robyt & French, 1970). α-amylase catalyze hydrolysis of 1,4 α-glucosidic linkages in amylose, amylopectin and related oligosaccharides to give glucose (G1), maltose (G2), maltotriose (G3), maltotetraose (G4) and series of oligosaccharides of DP greater of equal to 5 and dextrin as products in a multiple

attack mechanism which depends on the concentration and time of enzymatic hydrolysis. The hydrolysis products of starch, such as maltodextrin, maltose, glucose and fructose have a wide applicability in textile, pharmaceutical (therapeutic tablet preparation) and food industries (Govindasamy et al., 1992; Mohan et al., 2005).

Normally, the granule surface is relatively impenetrated to large molecules such as amylases enter the granule through the pores or channels (Fannon et al., 1992) owing to the tight packing of the amylopectin chains.

During heating the slurry before enzymatic hydrolysis, as temperature is increased, the granule could swell further up to 200 % of the original diameter. The amorphous phase is the domain where water molecules diffuse and this organization gives the granule a porous structure. Nevertheless, the granule swelling of starch granules in this study was not fully exhibited due to the alteration of crystal structure via rearrangement of hydrogen bonds of starch granules by annealing (Hoover & Vasanthan, 1994). Pretreatment, by partial annealing in an excess of water can influence the relative susceptibility of the granule regions as described above. Initial adsorption of α-amylase which is prerequisite step for enzymatic attack occurred at the truncations of the granule surface. This truncated zone has proven to be particularly fragile and susceptible to enzymatic attack (Gallant et al., 1973) which then exhibited surface erosion or corrosion (Figure 34 and 38). Then the enzyme (~ 5-6 nm) (Morgan et al., 1995) attacked and passed through serpentine channels (Fannon et al., 1993; Huber & BeMiller, 2000) or surface pore opening (Fannon et al., 1992; Oostergetel and van Bruggen, 1993; Whister & Turner, 1955) that link the surface and inside of starch granules run through the most sensitive area in the center of starch granule (Baldwin et al. 1994) around the hilum which is believed to be the least organized region of the starch granule, since nucleation point for bubble formation in gelatinization, enzymic attack, chemical reaction and cavitation all originate there (Fuwa et al., 1978; Hoseney et al., 1978; Huber & BeMiller, 2000; Leach & Scoch, 1961; Whister and Spencer 1960; Whistler & Thornburg, 1957). The inside parts of the granule were more susceptible to enzyme action than their surface. It is also possible that the annealing process at higher temperatures creates pores or fissures which alter the pattern of amylase hydrolysis from surface to internal erosion (Wang et al., 1997). Hence, although amorphous and crystalline lamellae become more ordered,

accessibility to the amorphous regions by enzymes is facilitated. Then holes expanded mainly in the lateral direction, forming circular holes. After that the enzyme attacked the next layer of the granule, making the holes deeper (endocorrosion) that was observed in both SANET and SANER and finally granule crumble (Figure 34 and 38). This digestion process is almost the same as the digestion process reported by Haska and Ohta (1992).

The SEM-analysis showed that the extent of degradation of individual granules of SANET and SANER was very different (Figure 34 and 38). Some granules were extensively attacked whereas others still remained intact. The results obtained at any given stage of hydrolysis time will therefore only represent the average composition of a complex mixture of individual granules. They showed differences in solubility, enzymatic susceptibility and, they are not likely to be uniformly effected by heat. It is possible that the differences are due to variance in the development in the population that affected to varying in the amount of 'loose' material at their surface in different botanical sources, ages and sizes. The same was found for other starches (Bertoft et al, 1993; Manelius & Bertoft, 1996).

The sugars which were produced from enzymatic hydrolysis may be cooperated as additional starch grains binder. The hydrothermal treatment would bring partial gelatinization of surface of granule. In addition, spray drying did cause gelatinisation of starch, although this was restricted to less than 1 % (w/w) (Aticokudomchai et al., 2000) which was in agreement with our results that discussed above. The gelatinized starch and may be sugars held the starch grains together in spherical granules. The spherical shape of the granules comprised of agglomerated starch grains provides good flowability, which is essential in preparing tablets. However, the binding together among the starch granules of the starch agglomeration in case of SANT-H and SANET was probably due to the larger size of tapioca starch would easily stick to another starch granules and hence clusters of aggregates starch particles appear (Figure 35).

3. Particle size distribution

Starch granule size is a major key that affected to starch composition, gelatinization and pasting properties, enzyme susceptibility, crystallinity, swelling and

solubility. Moreover, several other factor, including amylose/amylopectin ratio and molecular weight and granule fine structure, are also influential. There are two aspects to determine the distribution of starch granule size. One is the impact of aggregation of the granules in a starch sample on the apparent granule size distribution. The other is the actual size distribution of individual granules.

Large spherical agglomerate particles, 30-80 μm in diameter, can be observed in spray dried sample, where the small granules cluster together to minimize surface area as observed in SNR, SANR-H and SANER (Figure 40A to 40E). This spherical agglomerate was also observed in SNT, SANT-H and SANET. However, it is a small population in case of SANT-H and SANET. Most of them are in the clusters of agglomerated granule binding together form as seen in Figure 35. That is enhanced the size of the spray dried tapioca starch samples (143.18-181.14 μm) (Figure 39B to 39E). The increasing in median size diameter of SANER after preheat and enzymatic treatment was corresponded to partial gelatinisation as observed by SEM (Figure 37 B and 37C). The photomicrographs revealed the composite particle consisting of rice starch grains forming a one-body particle. As previous describe, partial gelatinisation of starch grains might be responsible for binding rice grains together to form larger size of composite granular particles. Partial gelatinisation also had a pronounced effect on the shape of composite particles produced from SANET. When partial heating treatment was applied, in case of tapioca starch, composite particle not only provided the larger size of the particles but also produced more shape irregularity of the composite particles from binding together between agglomerated granules (Figure 35).

The larger agglomerate size powder that presented in both SANET and SANER indicated the ability in free flowing and can easily be transported by gravity discharge when preparing the tablet fillers. This is because inter-particle forces of attraction are small in comparison with gravitational force and in consequent cannot exert any appreciable influence (Jones, 1979).

Generally, granule size refers to the average diameter of the starch granules. For this, spherical granules are assumed, which is seldom correct. According to Lindeboom et al. (2004). NT granular from SNT is classified as medium granule size (10-25 μm) while NR granular from SNR as small granule size (5-10 μm). The particle

size distribution of NT and NR granular is in agreement as observed by SEM (Figure 32A and 32C).

The results from the enzyme degradation were slightly changed the median diameter (Figure 39 F-J for SANET and 40 F-J for SANER) of starch granules from SANET and SANER after prolong hydrolysis time when compared to their native starches indicated that the enzyme did not extensively hydrolyze or solubilize the starch granule to become smaller size of starch granules. Although some granule appeared the surface erosion and breaking the granules (Figure 34 for SANET and 37 for SANER). This was in agreement with partially hydrolyzed barley starch granules swelled more evenly as compared to their native starch granules that was observed by Lauro et al. (2000). Though enzymatic hydrolysis could not reduce the size of starch granules, the loss of starch on enzyme modification could be determined as damaged starch which will be discussed later.

The high median size d(v 0.5) of ANT-H and ANR-H (Figure 39G and 40G) was due to the high swelling of granule from the higher water absorption within the damaged area of starch granule. According to some author, in early microscopic work from Gough and Pybus, (1971) indicated that wheat starch granule dimension increased after annealing, although Hoover and Vasanthan (1994) was postulated that annealing caused no effect on granule dimensions or shapes.

4. Thermal properties (DSC)

From DCS thermal analysis of SNT, SNR, SANT-L, SANR-L, SANT-H, SANR-H, SANET and SANER, the sharp and well defined thermograms which give a relatively narrow temperature range (T_c - T_o), was observed in SANT-L and SANT-H (Table 7) and SANR-L and SANR-H (Table 8) when compared to SNT and SNR, indicating that melting is highly cooperative. Annealing before the onset of crystallite melting would lead to faster molecular relaxation in the amorphous regions of the starch granules and profound changes in the crystalline phase such as an increase crystal growth and/or perfection. In the DSC scans, this should translate to an increase in melting transition temperatures and a narrowing of gelatinization range as evidenced by the sharper melting endotherm observed by many researchers (Gough & Pybus, 1971; Knutson, 1990; Krueger et al., 1987; Larsson & Elisasson, 1991; Lund,

1984). Moreover, narrow peaks definitely are an indication for a better homogeneity of the sample, and in this case mean that the melting of the crystallites, the swelling and the hydration of the granules etc. is more homogenous in an annealed starch. However, the wider (T_c- T_o) exhibited by SNT and SNR suggests the presence of crystallites of varying stability. The differences in endothermic properties between SNT, SNR and SANET, SANER may be due to differences in granular structure and composition. SNT contain a significantly higher amylose content compared to SANET (Table 6). The amorphous regions of the starch granules swell by taking in water, resulting in cooperative melting of the crystalline regions within the granules (Donovan, 1979; Krueger & Walker, 1987). The SNT and SNR make cooperative melting difficult because they are apart from each other. Thus, SNT and SNR yielded broad, shallow thermogram.

T_o, T_p and T_c of SANT-L and SANR-L were significantly increased while ΔH was constancy after annealing process at 55 ^{0}C and 65 ^{0}C, respectively, when compared to their spray dried native starches. This changes were also observed in many researchers (Krueger et al., 1987; Paredes-López et al., 1989; Knutson, 1990; Larsson & Eliasson, 1991; Stute, 1992). Upon annealing in unrestricted water, the amorphous regions hydrate (and proceed through a glass transition) and allow amylopectin exterior chains-which are not optimally registered (packed together) or completely double-helical along their lengths (especially at the ends)-to optimise their helical associations and structure rather than facilitating formation of double helices. Hence, the number of double helices pre- and post annealing remain constant but registration is optimised (enhance the ordering of double helices in crystallites). These molecular events restrict ease of hydration of the starch granules during gelatinisation and elevate gelatinisation temperatures. Waigh et al. (2000) have postulated that two stages are involved during starch gelatinization in excess water. The first stage involves a slow side by side dissociation of helices and the second stage involves a rapid helix turns to coil transition. Cooke and Gidley (1992) have claimed that ΔH reflects primarily the loss of double helical order rather than loss of crystalline register. The larger ΔH values for SNT (Table 7), suggest that interactions (via hydrogen bonding) between double helices (that are packed in clusters) forming the crystalline region of the above starch are probably more extensive (due to longer

chains in amylopectin) than in SNR (Table 8). Consequently, the ΔH associated with dissociation and unraveling (hydrogen bonds are broken during both stages of gelatinization) and melting of the double helices would be of a higher order of magnitude in SDNTS.

'Annealing' of SANT-H and SANR-H at 60 ^{0}C and 70 ^{0}C, respectively, exhibited higher T_o and T_p values whereas T_c was relatively change a little when compared to their native starches as a result from the typical characteristic of annealing effect (Table 7 and 8). It is recognised that annealing can be associated with partial gelatinisation (Eliasson & Gudmunddsson, 1996). Annealing at temperature near the onset temperature of the native starches (T_o of native tapioca starch and rice starch are 63.09 ^{0}C and 72.89 ^{0}C, respectively) was cooperatively occurred the partial gelatinization. It is possibly that the starch granule can occurred in both annealing and partial gelatinization due to inherent structural heterogeneity in the starch granules. Because of T_o is the average onset temperature from all of the starch molecules, thus, some annealed starch granules exhibit the lower gelatinization temperature than the detecting T_o of native starches and some were higher than the observed T_o value. Thus those starch granules that showed lower gelatinization temperature than T_o of the native starches would occur the gelatinization at the annealing temperature that near the gelatinization temperature (the different between annealing temperature and gelatinization temperature is ~3 % in both SANT-H and SANR-H). However, partial gelatinization which was incorporated during preheating did not affect to the increasing of T_o, T_p and T_c values. This was confirmed by the study of Wolters et al. (1992) who demonstrated that T_o, T_p and T_c values did not change with increasing gelatinized/native potato starch ratio. Annealing of SANT-H and SANR-H also resulting in a decrease rather than constancy/increase of ΔH as anticipated for unrestricted annealing. This was also observed in the study of Lauro et al. (2000) and Tester et al. (2000). Although the ΔH of SANR-H decreased significantly due to the partial gelatinization, most of the granule structure and birefringence was preserved (Figure 31E and 36E). This was clearly evidence by the increasing of percentage of damage starch from native starches (0.31 % for SNT and 1.04 % for SNR) in comparison with SANT-H (11.18 %) and SANR-H (13.06 %) (Figure 41). This

annealing condition was the new properties that influent the increasing of T_o, T_p and T_c while ΔH was clearly decreased especially in case of rice starch.

The greatly enhanced increasing of T_o values of SANET (Table 7) and SANER (Table 8) in comparison with their native starches was mainly involved from combined annealing and enzymatic hydrolysis. Amylolysis may possibly play a role for increasing in T_o values by increasing the chance of cleavage of amylose chain that associated with the long branched chain in the amorphous region based on Bertoft's two-directional back bone model (2004). Thus, the amylose would freely liberated and the reorientation or reorganization of amorphous region was easily occurred according to annealing effect. As a consequence, the registration of double helices in crystalline regions was optimized when compared to only annealing effect from SANT-H and SANR-H. Hence, the higher temperature should be applied for melting the more ordering of crystalline structure. The ΔH of both SANET and SANER were decreased with the extension of hydrolysis time was attributed following 2 factors

(i) Partial gelatinization: Partial gelatinisation proceeds as the temperature is increased which is induces a transition of the amorphous regions from a rigid glassy state to a mobile rubbery state and in turn facilitates the hydration and dissociation of double helices in crystallites (Cooke & Gidley, 1992). This can proved by the presence of strong correlation of increasing (r^2 = 0.8170) in the degree of damaged starch in the SANET samples as shown in Figure 41. As mention in tapioca starch earlier, the higher degree of partial gelatinization which observed by increasing in degree of damaged starch (r^2 = 0.6624) may influences in decreasing of ΔH of rice starch samples (SANER) with the extension of hydrolysis time as shown in Figure 41. The assumption was clearly seen in ΔH value from SANR-H (11.74 J/g) when compared to SNR (13.44 J/g), which possibly affects from the smaller size of rice granules that imply the more heating can contact with the larger surface area per volume of rice starch granule. In addition, the study of Wolters et al. (1992) observed the decreasing of ΔH linearly with increasing gelatinized/native potato starch ratio.

(ii) Enzymatic hydrolysis: α-amylase is able to hydrolyze double helical structure in the granule crystallites from amylopectin side chains and retrogrades amylose (formed by hydrolyzed amylose chains). This would cooperated with the slight swelling of the amorphous region may render amorphous region more

susceptible to enzyme action, and hydrolysis of this region will expose the crystalline region to the enzyme. This mechanism may explain why the hydrolysis of the unprotected crystalline region is also improved. (Jacobs et al., 1998; Wang et al., 1997; Zhou et al., 2004).

Moreover, the percentage of damaged starch of SANET and SANER were increased from 0.31 % to 18.96-21.31 % in case of tapioca starch and 1.04 % to 20.25-24.43 % in case of rice starch when compared to spray dried native starches. Thus, these make the clear picture of the new properties of the modified starches which were increasing in T_o, T_p and T_c while decreasing ΔH due to partial gelatinization.

5. Crystallinity

Wide angle X-ray scattering provides information on the inter-atomic length scale, and hence (in case of starch) may be used to identified the crystalline polymorph of the amylopectin helices (Imberty et al., 1991)

There were no different of X-ray diffraction patterns among the SNT, SANT-H and SANET which revealed A pattern, a high solubility in water, as shown in Figure 42. The type X-ray pattern of tapioca starch was studied by many researchers (Gallant et al., 1982; Moorthy, 1994; Zobel, 1988) and were possesses “A” and “C” type X-ray pattern. “A” type X-ray pattern were found for all SNR, SANR-H and SANER (Figure 43), as is expected for most cereal starches (Badenhuizen, 1969). This is in agreement with reports from Tamaki et al. (1997) and Franco et al. (1998) and Zhou et al. (2004) that observed the unchanged of X-ray diffraction type after amylase treatment. It was shown by Hizukuri et al. (1983) that variations in the lengths within the group of short chains determine the type of crystallinity (A, B, C). They concurred that A-type starches contains shorter average chain lengths and a larger proportion of short chains than amylopectin fractions from B-type starches may also contribute to the formation of helices (ordered structure) (Gidley & Bulpin, 1987), and thus partial hydrothermal (annealing or partial gelatinization) and amylase treatment in this study is not basically changed molecular arrangement in residual granule (Gough & Pybus, 1971; Stute, 1992). These results indicate that the observed crystal types are inherent to the molecular properties of granular starches. However, the peak of X-ray diffraction pattern of amylase treated sample in the studied of Yamada et al. (1995)

was changed following with proceed of digestion. The sharper peak intensity of SANET and SANER at 17 ^{0}, 18 ^{0} and 23 ^{0} when compared to SNT and SNR (Figure 46 and Figure 47) was described by Yamada et al. (1995). Several researchers (Colonna et al., 1988; Lauro et al., 1999; Leach & Schoch, 1961) have shown that α-amylase did not selectively attack amorphous region but both crystal and amorphous one. This was based on the observation that α-amylolysis did not produce an increase in crystallinity. Furthermore, the crystal region may be more sensitive to amylase than amorphous one. Even though the α-amylase initially hydrolyzes the amorphous regions of the granule (Marsden & Gray, 1986; Franco et al., 1988).

The ability of α-amylase to hydrolyze the crystalline region has been explained (Colonna et al., 1988) as follows: each of the subsites of α-amylase is able to bind one glucose unit of the starch chain. When the substrate binds to the active site, it is distorted by the enzyme in the direction of the transition rate for catalysis by a strain at the glucosidic bond to be cleaved. This enables α-amylase to grasp onto portions of molecule, involved in the crystalline region, leading to an active disentanglement of the crystalline chains. Colonna et al. (1988) have shown by iodine binding studies, that there is no preferential hydrolysis of either amylose or amylopectin by α-amylase.

The lower relative crystallinity of SNT (38.81 %) could be attributed to its low amylopectin content and/or to a poorly organized crystalline structure when compared to SNR (45.39 %). It was noted that decreasing in degree of crystallinity from SANT-H and SANR-H when compared to SNT and SNR due to the partial gelatinization effect because of annealing causes no significant increase in crystalline material (Gough & Pybus, 1971; Stute, 1992; Tester et al., 1999). The process of heating has been shown to decrease the crystallinity of starch (Craig & Stark, 1984; Lelièvre, 1974). The extended hydrolysis time of SANET and SANER more pronouncedly decreased in the relative crystallinity which was supported by the report from Mohan et al. (2005). The decreasing of degree of crystallinity of combine heat treatment and enzymatic hydrolysis tapioca and rice starches was dominantly effected from partial gelatinization because of partial gelatinisation progressively uncoiling the double helices and converting some part of crystalline material to amorphous material as the holding temperature augmented (Figure 44). Moreover, gelatinization from progressive increasing temperature induces a disappearance of the crystalline X-ray

diagram due to the chain packing arrangements required to diffract X-ray are absent. This was in agreement of the results from the decreasing of gelatinization enthalpy (ΔH) from DSC (Figure 41) and increasing of percentage of damaged starch (Figure 41 and Figure 44) which indicated the higher degree of partial gelatinized starch with increasing hydrolysis time. In addition, α-amylase also responsible for the decreasing of the crystalline regions (Yamada et al., 1995) (although this was not strong as partial gelatinization) in the starch granule of SANET and SANER. This suggests that extensive hydrolysis effectively destroys and solubilize the crystalline areas of the granule. Nevertheless, the exact mechanism by which starch crystallites are degraded by α-amylase remains controversial. However, Williamson et al. (1992) have shown by studies on "A" type spherulitic polycrystalline amylose (degree of polymerization ~20) that "A" type spherulites retain their crystallinity after partial hydrolysis by α-amylase from *Aspergillus Oryzae*.

The granule size of starches may be influence to the occurring of the partial gelatinization. The smaller size of rice starch granule imply the higher surface area that improve the high frequency of contacting to the heating environment when compared to larger granule of tapioca starch which mean the higher possibility of partial gelatinization to occur. Thus, the higher decrease in percentage of relative crystallinity of SANR-H (8 % different from SNR) as compared to SANT-H (3 % different from SNT).

6. Utilization of spray dried enzymatic hydrolyzed starches as a direct compression fillers

The hot inlet air temperature (160 ^{0}C) in spray drying from this study are maximized to obtain the best thermal efficiencies without leading to product damage. However, low values of damaged starch from SNT and SNR is still observed in the presence study which may be posses either by starch extraction or spray drying processes. The outlet air temperature was relatively low (60 ^{0}C) to increase the possibility for particles to stick together with a degree of agglomeration is achieved. Agglomerated powder is formed having a moisture content that requires further moisture removal in the fluid bed.

6.1. Tablet properties

SNT and SNR exhibited low crushing strength (9.81-32.36 N for SNT; 33.34-71.59 N for SNR), although they are spherical particle forms. This indicated the spray-drying process had an effect on the shape of the particulate agglomerates by acts as a tool for particle engineering of the composite particles but not an effect on the compactability of starches (Limwong et al. 2004). Similarity, annealing process did not improve the tablet hardness. As a consequence, SANT-L and SANR-L showed lower values of hardness (Figure 45 and 48) which exhibited capping of tablets from the direct compression process at 6.0-10.0 kN as also observed in SNT and SNR. SANT-H and SANR-H also showed low values of crushing strength of tablets which implied that annealing with partial gelatinization that caused “stickiness” between pairs of granules still did not help for improving the crushing strength of the prepared tablets.

The increase in hydrolysis time in both SANET and SANER from 15 to 30 and to 60 min yielded the tablets with the increasing range of hardness (Figure 45 and 48). Except for SANER-60 which gave the lower values of crushing strength which possibly from the highly damage that was observed by damaged starch (24.43 %) and SEM micrographs (Figure 38C). The independence of compressibility from the compression force could be due to the property of the filler itself. Starch may completely undergo consolidation, hence increasing in the compression force did not conduce any more strength of the compact.

It was attempt to utilized the enzymatic modified tapioca and rice starch as tablet filler for the pharmaceutical industries. Since the price of tapioca and rice is rather low, the modification process is simple. The crystalline region is an ordered arrangement of double helical amylopectin structures. Upon spray drying, each droplet of the slurry would contain a large number of starch grains with damaged area and soluble sugar on the surface and also inside the starch granules. The dissolved fraction would blend and be an integral part of the agglomerates. After the water was removed, the tiny starch grains in each spray-dried particle was covered and held together. Upon compaction the bonding on the surface of starch particles was strongly introduced by surface gelatinization and sugar binding, thus improving the compactibility of the spray dried products. Base on the molecular structure of starch, embedded in the

amorphous regions, amylose has been proposed to disrupt the crystalline packing of amylopectin (Jerkins & Donald, 1995). Some amylose molecules, especially on the surface granule, were leached out from the granule due to swelling causes porous structure which affect from partial gelatinisation, then leaving the crystalline packing regions. However, the annealing affected the more rigidity and reorientation of the double helices in the crystallites. Hence increasing the order structure of the crystalline regions, even though some double helices were dissociated by heating and amylolysis. Thus, when applying the compaction force to the starch granules, the crystalline regions could be forced to become closely packed and so the intermolecular forces, i. e., van de waals forces and hydrogen bonding, increased, leading to more order arrangement within the starch granules. The stronger packing structure combine with the sticky surface due to the presence of surface gelatinisation from the effect of partial gelatinisation and binder dextrin from enzymatic hydrolysis that discuss above, resulted in an increase in the crushing strength of the tablet preparing from SANET and SANER as observed in Figure 45 and 48.

Normally the requirement for tablets that have better disintegration time should not more than 30 minutes. Spray dried native starches showed the good disintegration time which less than 1 min for SNT and around 2 min for SNR. Since most common disintegrants are natural polysaccharides of plant origin (Shangraw et al., 1980). Holstius and Dekay (1952) showed that various starches, i. e., arrowroot, corn, potato, rice, sorghum, tapioca and wheat starches yielded the tablet of different disintegration time. SANT-L exhibited the low disintegration time as closed to SNT value (Figure 46) while SANR-L showed a little bit longer disintegration time than SNR (Figure 49). This can referred that annealing process would not or at least minimized the occurrence of gelatinous layer due to heat damage. Thus, the properties of tablets prepared from SANT-L and SANR-L were the same as spray dried native starches. SANT-H and SANR-H showed longer disintegration time than those from spray dried native starches (SNT and SNR) (Figure 46 and 49). The gelatinous layer developing from damaged starch during partial gelatinization impedes the penetration of water into the tablet and thus prolongs the disintegration (Akande et al., 1991; Graf et al., 1982; Mitrevej et al., 1996; Van Kamp et al., 1986; Visavarungroj & Remon, 1990). However, treatment with enzyme in both SANET and SANER caused the lower in

disintegration time. This was possibly due to the producing of sugar and low molecular weight polysaccharide from amylolysis. Thus, those with highly soluble in water could enhance the solubility of the tablet in water. Consequently, SANET had lower disintegration time than in SANT-H (Figure 46). In contrast, SANER-15 obviously showed longer disintegration time than SANR-H. This could be possibly from the higher producible gelatinous layer at 15 min of hydrolysis than SANR-H. At 15 min of hydrolysis, the enzyme still not reached their optimum time for completely catalyzed to lower molecular weight polysaccharide. So the gel formation from partial gelatinized starch proportion might be higher than those soluble sugars at this hydrolysis time and yet might higher than SANR-H. At 30 min of hydrolysis time, caused an opposing effect on the disintegration time. The decreasing of disintegration time was obtained from higher producing of sugar and low molecular weight polysaccharides when immerse in water, although the solubilized sugar layer was formed (Figure 49). However, the delay disintegration time of SANET and SANER is observed when compared to SNT and SNR due to the effect of sugar which can solubilize, induce the viscosity and also form the barrier to obstruct the water penetration to break the tablet apart. This can implied that the gelatinous barrier from partial gelatinized starch had well effectiveness for preventing the water permeation into the tablets than sugar layer which produced from enzymatic hydrolysis.

Tablet hardness is not an absolute indicator of strength since some formulations, when compressed into very hard tablet, tend to cap on attrition, losing their crown portions. Therefore, another measure of tablet's strength, its friability is often measured.

With any given additives, the friability profiles agreed very well with the pressure hardness profiles. For example, without modification, the SNT would give as high friability values as compared to SANT-L and SANT-H, while SANET would give the low friability values. This trend was also agree well with spray-dried native and modified rice starches. It is obvious that the % friability of SANT-L and SANR-L is in the range between spray dried native starches and annealed with partial gelatinized starches. Thus, This can implied that the increasing of temperature would influent the tablet properties i.e. % friability. Both SANET and SANER showed the low % friability (Figure 47 and 50) which indicated the withstanding of mechanical

stress during handling in manufacture, packaging and shipping. However, in SANET at 15 and 60 min hydrolysis time showed zero value of percentage friability at any compression forces. This was possibly described by the absorb of water from moisture in the air into tablet due to the normally occurring hygroscopic property of starch granules, so the weight after test will equal to the beginning weight and zero values were obtained finally.

The shape of particle influences the rheological properties of the powder. Spherical particles usually have the greatest fluidity. However, highly fluid powder blends tend to facilitate segregation. SEM shows the surface roughness and stickiness of SANER and SANET (Figure 34 and 38), such surface structure results from the modification and aggregation of starch grains. Porous surface can trap or lock or even immobilized neighboring particles, thus minimizing the segregation.

According to the study of Puchongkavarin et al. (2003) which proposed that the relative crystallinity proved to be an important factor in tablet compression with agglomerated crystalline rice starch. This was oppose by our study that with spray dried enzymatic hydrolyzed starch did not improve the relative crystallinity. However, the tablet properties of SANER which prepared from rice starch also satisfied for use as filler in pharmaceutical industry. Moreover, this treatment can also use to modify tapioca starch to obtain a good tablet properties too. This can conclude that with this modification could make the starches (“A” type in this study) to obtain a good tablet characteristics for tablet filler prepared from direct compression pressing.

6.2. Comparative study of SANET-30 and SANER-30 with other commercial compression fillers.

From Figure 51-53, Among directly compressible fillers, microcrystalline cellulose (MCC) is the most compressible, forming strong compacts, that the hardness could not be measured by hardness tester at high compression force. However, because of the high cost and poor fluidity when compared with that of most other direct compression vehicles, it is generally not used as the only diluent in table formulations but is usually combined with other direct compression vehicles to improve the flowability and reduce the cost of the product.

Era-tab SP comes second with relatively high compactability, low disintegration time and % friability. The better tablet properties from Era-tab SP in comparison with Era-tab was due to the advance modifying of Era-tab SP from Era-tab which is a general agglomerated rice starch.

PS is able to swell in cold water without cooking. The properties of the pregelatinized starch are similar to those of parent starch (SNT) except for the high percentage of friability, since it is only a physical modified product. It may be modified to render it directly compressible and flowable in character. PS and L showed high percentage of friability indicated the less resistant to mechanical stress. Although PS and L exhibit almost identical tablet hardness, the disintegration time of L was smaller than PS. The discrepancy could be due to difference in solubility and water accessibility properties of those fillers (or may be difference in particle size) as discussed above.

SANET-30 and SANER-30 showed high compressibility, low percentage of friability and relatively low disintegration time. The presented of good tablet properties from those 2 spray-dried modified products due to the combination of advantages between (partial) gelatinized starch and enzymatic hydrolysis.

CHAPTER VI
CONCLUSION

The process of hydrothermal treatment (annealing/partial gelatinization) combine with the addition of thermostable α-amylase hydrolyzing tapioca and rice starches itself were not influent the proximate composition of the native starches. However, the change that was observed in proximate analysis of SANET and SANER were mainly due to the external factor (enzyme) that was added to the starch slurry. Both SANET and SANER showed significantly decreased in amylose content after prolong hydrolysis. This was accounted for the leaching of amylose out from the swollen and porous starch granules during partial gelatinization in the presence of α-amylase.

SEM showed the pattern of amylolysis, exocorrosion on the starch granule surface, the tunnel or endocorrosion and the solubilization, by slightly reduction of starch granular size in both SANET and SANER after prolong hydrolysis. The surface gelatinization provided the adhesion together of the starch granules and thus forming with the increasing of the agglomeration size which pronouncedly affected in case of SANET rather than SANER.

Annealing starches at lower temperature (SANT-L and SANR-L) led to increase T_o, T_p and T_c whereas ΔH was not different with respect to their native starches. However, the slightly increasing of damaged starch still observed. In addition, annealing tapioca (SANT-H) and rice (SANR-H) starches at temperature near gelatinization temperature (T_o) would gain the new properties which was due to the combination between annealing and partial gelatinization. The T_o, T_p and T_c were increased while ΔH was decreased. Moreover, addition of α-amylase for enzymatic hydrolysis into starch slurry would also responsible for the decreasing of ΔH. In addition, the increasing of damaged starch were obtained from those processing. Moreover, these events led to decreasing in relative crystallinity after prolong hydrolysis in both SANET and SANER without changing the “A” type X-ray patterns.

The correlation of the decreasing of relative crystallinity of starches was inversed proportional to the quantity of damaged starch. It is possibly to use spray dried starches with these properties to obtain a good tablet fillers properties, i.e., high tablet hardness, from the direct compression tablet when compared to spray dried native starches (SNT and SNR). The improving of crushing strength from those tablet fillers prepared from SDNET and SANER was responded from the presence of maltose or low molecular weight oilgosaccharide that derived from the enzymatic hydrolyzed starch granules. In addition, hydrolyzed starch would also influence the progressively increased in percentage of damaged starch in both SANET and SANER with respected to their spray dried native starch.

SANET-30 and SANER-30 exhibited highest compressibility in each type of starches and self-integration for use as the vehicle for direct compression tablet and can be potentially introduced as a new directly compressible excipient as compared to other commercial fillers available in the market.

BIBLIOGRAPHY

Adler, J., Baldwin, P. M. & Melia, C. D. (1994). Starch damage part 2: Types of damage in ball-milled potato starch, upon hydration observed by confocal microscopy. *Starch/Stärke*, *46*, 252-256.

Akande, O. F., Deshpande, A. V. & Bangudu, A. B. (1991). An evaluation of starch obtained from pearl millet-*Penniselum typhoides* as a binder and disintegrant for compressed tablets. *Drug Development in Industrial Pharmacy*, *17(3)*, 451-455.

AOAC (1990). *Anonymous: Official Method of Analysis* (15th ed.). Virginia, USA: The Association of Official Analytical Chemists

Atichokudomchai, N., Shobsngob, S., Chinachoti, P. & Varavinit, S. (2001). A study of some physicochemical properties of high-crystalline tapioca starch. *Starch/Stärke*, *53*, 577-581.

Atichokudomchai, N., Shobsngob, S. & Varavinit, S. (2000). Morphological properties of acid-modified tapioca starch. *Starch/Stärke*, *52*, 283-289.

Atichokudomchai, N. & Varavinit, S. (2003). Characterization and utilization of acid-modified cross-linked tapioca starch in pharmaceutical tablets. *Carbohydrate Polymers*, *53*, 263-270.

Atkin, N. J., Abeysekera, R. M., Cheng, S. L. & Robards, A. W. (1998). An experimentally-based predictive model for the separation of amylopectin subunits during starch gelatinisation. *Carbohydrate Polymers*, *36*, 173-192.

Atkin, N. J., Abeysekera, R. M. & Robards, A. W. (1998). The events leading to the formation of ghost remnants from the starch granule surface and the contribution of the granule surface to the gelatinisation endotherm. *Carbohydrate Polymers*, *36*, 193-204.

Atkin, N. J., Cheng, S. L., Abeysekera, R. M. & Robards, A. W. (1999). Localisation of amylose and amylopectin in starch granules using enzyme-gold labelling. *Starch/Stärke*, *51*, 163-172.

Atwell, W. A., Hood, L. F., Lineback, D. R., Marston, E. V. & Zobel, H. F. (1988). The terminology and methodology associated with basic starch phenomena. *Cereal Foods World*, *33*, 306-311.

Atwell, W. A., Milliken, G. A. & Hoseney, R. C. (1980). A note on determining amylopectin A to B chain ratios. *Starch/Stärke*, *32*, 362-364.

Autio, K. (1990). Rheological and microstructural changes of oat and barley starches during heating and cooling. *Food Structure*, *9*, 297-304.

Badenhuizen, N. P. (1969). *The Biogenesis of Starch Granules in Higher Plants. Appleton Century Crafts*. New York: Academic press.

Baldwin, P. M., Adler, J., Davies, M. C. & Melia, C. D. (1998). High resolution imaging of starch granules surfaces by atomic force microscopy. *Journal of Cereal Science*, *27*, 255-265.

Baldwin, P. M., Adler, J., Davies, M. C. & Melia, C. D. (1994). Holes in starch granules: confocal, SEM and light microscopy studies of starch granule structure. *Starch/Stärke*, *46*, 341-346.

Baldwin, P. M., Davies, M. C. & Melia, C. D. (1997). Starch granule surface imaging using low-voltage scanning electron microscopy and atomic force microscopy. *International Journal of Biological Macromolecules.*, *21*,103-107.

Ball, S., Guan, H. P., James, M., Myers, A., Keeling, P. Mouille, G., Bulleon, A., Colonna, P. & Preiss, J. (1996). From glycogen to amylopectin; A model for the biogenesis of the plant starch granule. *Cell*, *86*, 349-352.

Banks, W., Greenwood, C. T. & Muir, D. D. (1974). Studied on starches of high amylose content. Part XVII: A review of current concepts. *Starch/Stärke*, *26*, 289-300.

Batey, I. L., Curtin, B. M. & Moore, S. A. (1997). Optimization of Rapid-Visco Analyser Test Consition for Predicting Asian Noodle Quality. *Cereal Chemistry*, *74(04)*, 497-501.

Bean, M. M. & Setser, S. C. (1992). Polysaccharides, sugars, and sweeteners. In J. Bowers Ed., *Food theory and applications* (pp. 69-118). New York: Macimilian Publishing.

Bertoft, E. (2004). On the nature of categories of chains in amylopectin and their connection to the super helix model. *Carbohydrate Polymers*, *57*, 211-224.

Bertoft, E., Boyer, C., Manelius, R. & Avall, A. -K. (2000). Observation on the α-amylolysis pattern of some waxy maize starches from inbred line Ia453. *Cereal Chemistry*, *77(5)*, 657-664.

Bertoft, E., Manelius, R. & Qin, Z. (1993). *Starch/Stärke*, *45*, 215-220; 258-263.

Biliaderis, C. G. (1992). Structure and phase transitions of starch in food system. *Food Technology*, *46*, 98-109,145.

Biliaderis, C. G. (1991). In H. Levine & L. Slade (Eds.), *Water relationships in food* (pp. 251-273). New York: Plenum.

Bird, R. & Hopskin, R. H. (1954). *Biochemical Journal*, *56*, 86.

Bizot, H., Le Bail, P., Leroux, B., Davy, J., Roger, P. & Buleon, A. (1997). Calorimetric evaluation of the glass transition in hydrated, linear and branched polyanhydroglucose compounds. *Carbohydrate Polymers*, *32*, 33-50.

Blanshard, J. M. V. (1987). Starch granule structure and function: A physico-chemical approach. In F. Gaillard Ed., *Starch: Properties and potentials* (pp. 16-54). Chichester: John Wiley & Sons.

Blanshard, J. M. V., Bates, D. R., Muhr, A. H., Worcester, D. L. & Higgins, J. S. (1984). Small-angle neutron scattering studies of starch granule structure. *Carbohydrate Polymers*, *4*, 427-442.

Bolhuis, G. K. & Chowhan, Z. T. (1996). Material for direct compaction. In G. Alderborn & C. Nystrom (Eds.), *Pharmaceutical powder compaction technique* (pp. 419-500). New York: Marcel Dekker.

Bos, C. E., Bolhuis, G. K., Lerk, C. F. & Duinevekd, C. A. A. (1992). Evaluation of modified rice starch, a new excipient for direct compression. *Drug Development in Industrial Pharmaceutics*, *18*, 93-106.

Bos, C. E., Bolhuis, G. K., Van doorne, H. & Lerk, C. F. (1987). Native starch in tablet formulation: properties on compaction. *Pharm Weekblad Science Ed*, *9*, 274-282.

Briones, V. P., Magbanua, L. G. & Juliano, B. O. (1968). *Cereal Chemistry*, *45*, 351.

Buleon, A., Colonna, P., Planchot, V. & Ball, S. (1998). Starch granules: Structure and biosynthesis. *International Journal of Biological Macromolecules*, *23*, 85-112.

Chetaam, N. W. H. & Tao, L. (1998). Variation in crystalline type with amylose content in maize starch granules: an X-ray powder diffraction study. *Carbohydrate Polymers*, *36*, 227-284.

Chmelik, J. (2001). Comparison of size characterization of barley starch granules determined by electron and optical microscopy. Low angle laser light scattring and gravitational field-flow fractation. *Journal of Inst. Brewing*, *107*, 11-17.

Cooke, D. & Gidley, M. J. (1992). Loss of crystalline and molecular order during starch gelatinization: origin of the enthalpic transition. *Carbohydrate Research*, *227*, 103-112.

Colonna, P., Buléon, A. & Lemarié, F. (1988). Action of *Bacillus subtilis* α-amylase on native wheat starch. *Biotechnology and Bioengineering*, *31*, 895-904.

Colonna, P. & Mercier, C. (1984). Macromolecular structure of wrinkled- and smooth-pea starch components. *Carbohydrate Research*, *126*, 233.

Conversion factor for tapioca starch from http:// www.starch.dk/isi/applic/tapiocafarma.htm

Craig, S. A. S. & Stark, J. R. (1984). Molecular properties of physically damaged sorghum starch granules. *Journal of Cereal Science*, *2*, 203-211.

Curá, J. A., Jansson, P. E. & Krisman, C. R. (1995). Amylose is not strictly linear. *Starch/Stärke*, *47*, 207-209.

Davis, E. A. (1994). Thermal analysis. In S. S. Nielsen Ed., *Introduction to the Chemical Analysis of Food* (chapter 34, p. 505). Boston: Jones and Bartlett Publishing.

Deffenbaugh, L. B. & Walker, C. E. (1989). Comparison of starch pasting properties in the Brabender Viscoamylograph and the Rapid Visco-Analyzer. *Cereal Chemistry*, *66*, 493-499.

Delpeuch, F. & Favier, J. C. (1980). *Annaul Technological Agriculture.*, *29*, 53.

Dias, P. & Perlin, A. (1982). High field, ^{13}C-NMR spectroscopy of beta-D-glucans, amylopectin and glycogen. *Carbohydrate Research*, *100*, 103.

Donovan, J. W. (1979). Phase transitions of the starch-water system. *Biopolymer*, *18*, 263-275.

Donovan, J. W. & Mapes, C. J. (1980). Multiple phase transitions of starches and *Nägeli* amylodextrins. *Starch/Stärke*, *32*, 190-193.

Duke, J. A. (1985). *Handbook of medicinal herbs* (p. 293). Boca Raton, Florida: CRC Press Inc.

Dumoulin, Y., Alex, S., Szabo, P., Cartiler, L. & Mateescu, M. A. (1998). Cross-linked amylose as matrix for drug controlled release: X-ray and FT-IR structural analysis. *Carbohydrate Polymers*, *37*, 361-370.

Eliasson, A. C. & Gudmundsson, M. (1996). Starch: Physicochemical and functional aspects. In A. Eliasson Ed., *Carbohydrate in Food* (pp.431-503). New York: Marcel Dekker, Inc.

Eliasson, A. C. & Karlsson, R. (1983). Gelatinization properties of different size classes of wheat starch granules measured with Differential Scanning Calorimetry. *Starch/Stärke*, *35*, 130-133.

Erlander, E. R. & French, D. (1958). Dispersion of starch granules and the validity of light scattering results on amylopectin. *Journal of American Chemical Society*, *80*, 4413-4420.

Evers, A. D. & Stevens, D. J. (1985). Starch Damage. In Y. Pomeranz Ed., *Advances in Cereal Science and Technology* (Vol. VII, pp. 321-349). St. Paul Minesota: American Association of Cereal Chemists Inc.

FAO (1994): Food outlook: global information and early warning system on food and agriculture, n^0 10, Rome, 21-24.

Fannon, J. E., Hauber, R. J. & BeMiller, J. N. (1992). Surface pores of starch granules. *Cereal Chemistry*, *69*, 284-288.

Fannon, J. E., Shull, J. M. & BeMiller, J. N. (1993). Interior channels of starch granules. *Cereal Chemistry*, *70*, 611-613.

Franco, C. M. L., Preto, S. J. R. & Ciacco, C. F. (1992). Factors that affect the enzymatic degradation of natural starch granules. Effect of the size of the granules. *Starch/Stärke*, *44*, 422-426.

Franco, C. M. L., Preto, S. J. R., Ciacco, C. F. & Tavares, D. Q. (1998). The structure of waxy corn starch: Effect of granule size. *Starch/Stärke*, *50*, 193-198.

Franco, C. M. L., Preto, S. J. R., Ciacco, C. F. & Tavares, D. Q. (1988). Studies on the susceptibility of granular cassava and corn starches to enzymatic attack. Part 2. Study of the granular structure of starch. *Starch/Stärke*, *40*, 29-32.

French, D. (1984). Organization of starch granules. In R. L. Whistler, R. L. BeMiller & E. F. Paschall (Eds.), *Starch: Chemistry and Technology* (pp.183-247). Orlando, New York : Academic Press.

Fuwa, H., Nakajima, M. & Hamada, A. (1977). *Cereal Chemistry*, *54*, 203.

Fuwa, H., Sujimoto, Y. & Tanaka, T. (1979). *Carbohydrate Hydr. Research*, *70*, 233.

Fuwa, H., Sujimoto, Y., Tanaka, T. & Glover, D. V. (1978). Susceptibility of various starch granules to amylases as seen by scanning electron microscope. *Starch/Stärke*, *30*, 186-191.

Gallant, D. J., Bewa, H., Buy, Q. H., Bouchet, B., Szylit, O. & Sealy, L. (1982). On ultrastructural nutritional aspects of some tropical tuber starches. *Starch/Stärke*, *34*, 255.

Gallant, D. J., Bouchet, B. & Baldwin, P. M. (1997). Microscopy of starch evidence of a new level of granule organization. *Carbohydrate Polymers*, *32*, 177-191.

Gallant, D. J., Bouchet, B., Buleon, A. & Perez, S. (1992). Physical characteristics of starch granules and susceptibility to enzymatic degradation. *European Journal of Clinical Nutrition*, *46*, S3-S16.

Gallant, D. J., Derrien, A., Aumaitre, A. & Guilbot, A. (1973). Dégradation in vitro de l'amidon par le suc pancréatique. *Starch/Stärke*, *25*, 56-64.

Gallant, D. J., Mercier, C. & Guilbot, A. (1972). Electron microscopy of starch granules modified by bacterial α-amylase. *Cereal Chemistry*, *49*, 354-365.

Garcia, V., Colonna, P., Bouchet, B. & Gallant, D. (1997). Structural changes of cassava starch granule after heating at intermediate water contents. *Starch/Stä rke*, *49*, 171-179.

General picture of spray dryer and their components from http://www.niroinc.com/html/drying/fdspraychem.html

Gernat, Ch., Radosta, S., Damaschaun, G. & Schierbaum, F. (1990). Supermolecular structure of legume starches revealed by X-ray scattering. *Starch/Stärke*, *42*, 175.

Gibson, T. S., Al Qalla, H. & McCleary, B. V. (1991). An improved enzymatic method for the measurement of starch damage in wheat flour. *Journal of Cereal Science*, *15*, 15-27.

Gibson, T. S., Kaldor, C. J. & McCleary, B. V. (1993). Collaborative evaluation of an enzymic starch damage assay kit. *Cereal Chemistry*, *70*, 47-51.

Gidley, M. J. (1998). The 5th European Training Course on Carbohydrates. CRF: The Netherlands.

Gidley, M. J. & Bulpin, P. V. (1987). Crystalllisation of malto-oligosaccharide as models of the crystalline forms of starch: minimum chain-length requirement for the formation of double helices. *Carbohydrate Research*, *161*, 291-300.

Gough, B. M. & Pybus, J. N. (1971). Effect on the gelatinization temperature of wheat starch granules of prolonged treatment with water at 50 ^{0}C. *Starch/Stärke*, *23*, 210-212.

Govindasamy, S., Oates, C. G. & Wong, H. A. (1992). Characterization of changes of sago starch components during hydrolysis by a thermostable alpha-amylase. *Carbohydrate Polymers*, *18*, 89-100.

Graf, E. Ghanem, A. H. & Mahmoud, H. (1982). Studies on the direct compression 8. Role of liquid penetration and humidity on tablet formulation. *Pharmaceutical Industry*, *44*, 200-203.

Greenwood, C. T. & Mackenzie, S. (1966). Studied on starches of high amylose content. Part VI. The fraction of amylomaize starch: A study of the branched component. *Carbohydrate Research*, *3*, 7-13.

Greenwood, C. T. & Milne, E. A. (1968). Starch degrading and synthesizing enzymes: A discussion of their properties and action pattern. In M. L. Wolfrom & R. S. Tipson (Eds.), *Advances in carbohydrate chemistry* (Vol. 23, pp. 329-330). New York and London: Academic Press, Inc.

Guilbot, A. & Mercier, C. (1985). In Aspinall, G. O. Ed., *The polysaccharides* (pp. 33-60). London: Academic press.

Haase, N. U., Mintus, T. & Weipert, D. (1995). Viscosity measurements of potato starch paste with the Rapid Visco-Analyzer. *Starch/Stärke*, *47*, 123-126.

Hall, D. M. & Sayre, J. G. (1970). *Textile Research Journal*, *40*, 147.

Halpern, M. & Leibowitz, J. (1959). On the mechanism of the glucosidic bond cleavage in the enzymatic hydrolysis of starch. *Biochemica et Biophysica Acta*, *36*, 29.

Hanrahan, V. M. & Caldwell, M. L. (1953). *Journal of American Chemical Society*, *75*, 2191.

Haska, N & Ohta, Y. (1992). Mechanism of hydrolysis of the treated sago starch granules by raw starch digesting amylase from *Penicillium brunneum*. *Starch/Stärke*, *44*, 25-28.

Helbert, W, Schulein, M. & Henrissat, B. (1996). Electron microscopic investigation of the diffusion of *Bacillus licheniformis* α-amylase into corn starch granules. *Introduction to Journal of Biological Macromolecule*, *19*, 165-169.

Hizukuri, S. (1988). Recent advances in molecular structure of starch. *Journal of Japanese Society Starch Sciences*, *31*, 185.

Hizukuri, S. (1986). Polymodal distribution of the chain lengths of amylopectins and its significance. *Carbohydrate Research*, *147*, 342-347.

Hizukuri, S. (1985). Relationship between the distribution of the chain length of amylopectin and the crystalline structure of starch granules. *Carbohydrate Research*, *141*, 295-306.

Hizukuri, S., Kaneto, T. & Takeda, Y. (1983). Measurement of the chain length of amylopectin and its relevence to the origin of crystalline polymorphism of starch granules. *Biochemica and Biophysica Acta*, *760*, 188-191.

Holstius, E. A. & Dekay H. G. (1952). A statistical study of some disintegrating and binding agents in certain compressed tablets. *Journal of American Pharmaceutical Associated Science Ed*, *41(9)*, 505-509.

Hoover, R. & Sosulski, F. (1985). Studies on the functional characteristics and digestibility of starches from *Phaseolus vulgaris* biotype. *Starch/Stärke*, *37*, 181-191.

Hoover, R. & Vasanthan, T. (1994). The effect of annealing on the physicochemical properties of wheat, oat, potato and lentil starches. *Journal of food Biochemistry*, *17*, 303-325.

Hoseney, R. C., Zeleznak, K. J. & Yost, D. A. (1978). A note on starch gelatinization. *Starch/Stärke*, *38*, 407-409.

Hsiu, J., Fisher, E. H. & Stein, E. A. (1964). *Biochemistry*, *3*, 61.

Huber, K. C. & BeMiller, J. N. (2000). Channels of maize and sorghum starch granules. *Carbohydrate polymers*, *41*, 269-276.

Huber, K. C. & BeMiller, J. N. (1997). Visualization of channels and cavities of corn and sorghum starch granules. *Cereal Chemistry*, *74*, 537-541.

Imberty, A., Buleon, A., Tran, V. & Perez, S. (1991). Recent advances in knowledge of starch structure. *Starch/Stärke*, *43*, 375-384.

Imberty, A., Chanzy, H., Perez, S., Buleon, A. & Tran, V. (1988). The double helical nature of the crystalline part of A-starch. *Journal of Molecular Biology*, *201*, 36-378.

Imberty, A. & Pérez, S.(1988). A revisit to the three-dimensional structure of B-amylose. *Biopolymer*, *27*, 1205-1221.

Ispas-Szabo, P., Ravenelle, F., Hassan, I., Preda, M. & Mateescu, M. A. (2000). Structure properties relationship in cross-linked high-amylose starch for use in controlled drug release. *Carbohydrate Research*, *323*, 163-175.

Jacobs, H., Eerlingen, R. C., Clauwaert, W. & Delcour, J. A. (1995). Influence of annealing on the pasting properties of starches from varying botanical sources. *Cereal Chemistry*, *72*, 480-487.

Jacobs, H., Eerlingen, R. C. & Delcour, J. A. (1996). Factors affecting the visco-amylograph and rapid visco-analyzer evaluation of the impact of annealing on starch pasting properties. *Starch/Stärke*, *48*, 266-270.

Jacobs, H., Eerlingen, R. C., Spaepen, H., Grobet, P. J. & Delcour, J. A. (1998). Impact of annealing on the susceptibility of wheat, potato and pea starches to hydrolysis with pancreatin. *Carbohydrate Research*, *305*, 193-207.

Jacobs, H., Mischenko, N. Koch, M. H. J., Eerlingen, R. C., Delcour, J. A. & Reynaers, H. (1998). *Carbohydrate Research*, *306*, 1-10.

Jane, J.-l., Chen, Y. Y., Lee, L. F., McPherson, A. E., Wong, K. S., Radosavljevic, M. & Kasemsuwan, T. (1999). Effects of amylopectin branch chain length and amylose content on the gelatinisation and pasting properties of starch. *Cereal Chemistry*, *76*, 629-637.

Jane, J.-l., Kasemsuwan, T., Leas, S., Ames, I. A., Zobel, H., Darien, I. L. & Robyt, J. F. (1994). Anthology of starch granule morphology by Scanning Electron Microscopy. *Starch/Stärke*, *46*, 121-129.

Jane, J.-l. & Shen, J. (1993). Internal structure of the potato starch granule revealed by chemical gelatinisation. *Carbohydrate Research*, *247*, 279-29.

Jane, J.-l., Xu, A. Radosavliejevic, M. & Sieb, P. A. (1992). Location of amylose in normal starch granules. I. Susceptibility of amylose and amylopectin in cross-linking reagents. *Cereal Chemistry*, *69*, 405-409.

Jenkins, P. J., Cameron, R. E. & Donald, A. M. (1993). A universal feature in the structure of starch granules from different botanical sources. *Starch/Stärke*, *45*, 417-420.

Jenkins, P. J., Cameron, R. E., Donald, A. M., Bras, W., Cerbyshire, G. E., Mant, G. R. & Ryan, A. J. (1994). *Journal of Polymer Science Physicals Edu*cations, *32*, 1579-1583.

Jenkins, P. J. & Donald, A. M. (1995). The influence of amylose on starch granule structure. *Introduction to Journal of Biological Macromolecule*, *17*, 315-321.

Jiang, G & Liu, Q (2002). Characterization of residues from partially hydrolyzed potato and high amylose corn starches by pancreatic α-amylase, *Starch/Stärke*, *54*, 527-533.

Jones, T. M. (1979). The influence of excipients on the design and manufacture of tablets and capsules. *Drug and Cosmetic Industry*, *124(3)*, 40-104.

Juliano, B. O. (1985). Polysaccharide, Protein, and Lipids of rice. In B. O. Juliano Ed., *Rice: Chemistry and Technology* (pp.1-2). St. Paul, Minnesota, U.S.A: The American Association of Cereal Chemists, Inc.:

Kalichevisky, M. T., Jaroszkieiwcz, E. M., Ablett, S., Blanshard, J. M. V. & Lillford, P. J. (1992). *Carbohydrate Polymers*, *18*, 77-88.

Karr, J. L., Shiromani, P. K. & Brabiz, J. F. (1990). Binding efficiencies of starch NF and modified starches in formulations of poorly water soluble drugs. *Drug Development in Industrial Pharmaceutics*, *16(5)*, 821-835.

Kassenbeck, P. (1978). *Starch/Stärke*, *30*, 40-46.

Kim, J. M. & Lee, C. M. (1987). Effect of starch of textural properties of surimi gel. *Journal of Food Science*, *52*, 722-725.

Komiya, T. & Nara, S. (1986). Changes in crystallinity and gelatinization phenomena of potato starch by acid treatment. *Starch/Stärke*, *38*, 9-13.

Kong, B. -W., Kim, J. -I., Kim M. -J. & Kim, J. C. (2003). Porcine pancreatic α-amylase hydrolysis of native starch granules as a function of granule surface area. *Biotechnology progress*, *19*, 1162-1166.

Koshland, D. E. (1954). In W. D. McElroy & B. Glass (Eds.), *Mechanism of Enzyme Action* (pp. 612-614). Baltimore: Johns Hopkins Press.

Knutson, C. A. (1990). Annealing of maize starches at elevated temperatures. *Cereal Chemistry*, *67*, 376-384.

Knutson, C. A. (1986). A simple calorimetric procedure for determination of amylose in maize starches. *Cereal Chemistry*, *63*, 89-92.

Krueger, B. R., Knutson, C. A., Inglett, G. E. & Walker, C. E. (1987). A differential scanning calorimetry study on the effect of annealing on gelatinization behaviour of corn starch. *Journal of Food Science*, *52*, 715-718.

Krueger, B. R., Walker, C. E., Knutson, C. A. & Inglett, G. E. (1987). Differential scanning calorimetry of raw and annealed starch isolated from normal and mutant maize genotypes. *Cereal Chemistry*, *64*, 187-190.

Kuge, T. & Kitamura, S. (1985). *Journal of Japanese Society Starch Science*, *32*, 65-83.

Lansky, S., Kooi, M., & Schoch, T. J. (1949). Properties of the fractions and linear subfractions from various starches. *Journal of American Chemical Society*, *3*, 4066-4075.

Larsson, I. & Eliasson, A, -C. (1991). Annealing of starch at an intermediate water content. *Starch/Stärke*, *43*, 227-231.

Lauro, M., Forssell, P. M., Suortii, M. T., Hulleman, S. H. D. & Poutanen, K. S. (1999). α-amylolysis of large barley starch granules. *Cereal Chemistry*, *76*, 925-930.

Lauro, M., Poutanen, K. & Forssell, P. (2000). Effect of partial gelatinization and lipid addition on α-amylolysis of barley starch granules, *Cereal Chemistry*, *77(5)*, 595-601.

Lauro, M., Suortii, T., Autio,. K., Linko, P. & Poutanen, K. (1993). Accessibility of starch granules to α-amylase during different phases of gelatinization. *Journal of Cereal Science*, *17*, 125-136.

Le Bail, P., Morin, F. G. & Marchessault, R. H. (1999). Characterization of a crosslinked high amylose starch excipient. *International Journal of Biological Macromolecules*, *26*, 193-200.

Leach, H. W., McCowen, L. D. & Schoch, T. J. (1959). Structure of the starch granule I. Swelling and solubility patterns of various starches. *Cereal Chemistry*, *36*, 534-544.

Leach, H. W. & Schoch, T. J. (1961). Structure of the starch granule II. Action of various amylases on granular starches. *Cereal Chemistry*, *38*, 34-64.

Lelièvre, J. (1974). Starch damage. *Starch/Stärke*, *26*, 85-88.

Leloup, V. M., Colonna, P. & Ring, S. G. (1991). α-Amylase adsorption on starch crystallites. *Biotechnology and Bioengineering*, *38*, 127-134.

Lenaerts, V., Dumoulin, Y. & Mateescu, M. A. (1991). Controlled release of theophylline from cross-linked amylose tablets. *Journal of Controlled Release*, *15*, 39-46.

Li, L. C. & Peck, G. E. (1990). The effect of agglomeration methods on the micromeritic properties of a maltodextrin product, Maltrin 150™. *Drug Development in Industrial Pharmaceutics*, *16(9)*, 1491-1503.

Lim, S. T., Kasemsuwan, T. & Jane, J. (1994). Characterization of phosphorus in starch using 31P-NMR spectroscopy. *Cereal Chemistry*, *7*, 488-493.

Limwong, V., Suthanthavibul, N. & Kulvanich, P. (2004). Spherical composite particles of rice starch and microcrystalline cellulose: A new cocompressed excipient for direct compression. *AAPS PharmSciTech*, *5(2)*, 1-10.

Lindeboom, N., Chang, P. R. & Tyler, R. T. (2004). Analytical, biochemical and physicochemical aspects of starch granule size, with emphasis on small granule starches: A review. *Starch/Stärke*, *56*, 89-99.

Lineback, D. R. (1986). Current concepts of starch structure and its impact on properties. *Journal of Japanese Society Starch Science*, *33*, 80-88.

Lorenz, K. (1990). Quina (Chenopodium quina) starch: Physicochemical properties and functional characteristics.). *Starch/Stärke*, *42*, 81-86.

Lorenz, K. & Kulp, K. (1984). *Starch/Stärke*, *36*, 122-126.

Lund, D. (1984). Influence of time, temperature, moisture, ingredients and processing conditions on starch gelatinization. *CRC Critical Review Food Science Nutrition.*, *20*, 249-273.

MacGregor, A. W. & Ballance, D. L. (1980). Hydrolysis of large and small starch granules from normal and waxy barley cultivars by alpha-amylase from barley malt. *Cereal Chemistry*, *57*, 397-402.

MacGregor, A. W. & Morgan, J. E. (1984). Structure of amylopectins isolated from large and small starch granules of normal and waxy barley. *Cereal Chemistry*, *61*, 222-228.

Manelius, R. & Bertoft, E. (1996). The effect of Ca^{2+}-ions on the α–amylolysis of granular starches from oats and waxy-maizes. *Journal of Cereal Science*, *24*, 139-150.

Manners, D. J. (1989). Recent developments in our understanding of amylopectin structure. *Carbohydrate Polymers*, *11*, 87-112.

Manners, D. J. & Matheson, N. K. (1981). The fine structure of amylopectin. *Carbohydrate Research*, *90*, 99-110.

Marsden, W. L. & Gray, P. P. (1986). Enzymatic hydrolysis of cellulose in lingo cellulosic materials. *CRC Critical Review Biotechnology*, *3*, 235-276.

Marshant, J. W. & Blanshard, J. M. W. (1980). *Starch/Stärke*, *32*, 223-226.

Marshant, J. W. & Blanshard, J. M. W. (1978). Studies of the dynamics of the gelatinization of starch granules employing a small angle light scattering system. *Starch/Stärke*, *30*, 257-264.

Matheson, N. K. (1990). A comparison of the structures of the fractions of normal and high-amylose pea-seed starches prepared by precipitation with Concanavalin A. *Carbohydrate Research*, *199*, 195-205.

Matveev, Y. I., Elankin, N. Y., Kalistrova, E. N., Danilenko, A. N., Niemann, C. & Yuryev, V. P. (1998). Estimation of contributions of hydration and glass transition to heat capacity changes during melting of native starches in excess water. *Starch/Stärke*, *50*, 141-147.

Mayer, F. C. & Larner, J. (1958). Substrate cleavage points of α- and β-amyloses. *Biochemica et Biophysica Acta*, *29*, 465.

Mayer, F. C. & Larner, J. (1959). *Journal of Amercan Chemical Society*, *81*, 188.

Mendes, R. W. & Roy, S. B. (1979). Tableting excipients part III. *Pharmaceutical Technology*, *3*, 69-75.

Mendes, R. W. & Roy, S. B. (1978). Tableting excipients part I. *Pharmaceutical Technology*, *3*, 33-37.

Meredith, P. (1981). Large and small starch granules in wheat-Are they really different? *Starch/Stärke*, *33*, 40-44.

Mitrevej, A., Sinchaipanid, N. & Faroongsarng, D. (1996). Spray-dried rice starch: comparative evaluation of direct compression fillers. *Drug Development in Industrial Pharmaceutics*, *22*, 587-594.

Mitrevej, A., Sinchaipanid, N. & Palanuphap, S. (1995). Spray-dried rice starch for direct compression. *Thai Journal of Pharmaceutical Science, 19(3)*, 163-170.

Mitrevej, A. & Varavinit, S. (1988). Modified rice starch for direct compression. Presented before the Industrial Pharmacy Section of the 12th Asian Congress of Pharmaceutical Sciences, Federation of Asian Pharmaceutical Associaion, Bali, Indonesia.

Mitrevej, A., Varavinit, S. & Sinchaipanid, N. (1992). Comparative evaluation of direct compression fillers: Application of spray dried rice starch in tabletting, in recent developments in pharmaceutics and pharmaceutical technology, (pp.132-145). NUS-JSPS. Seminar, Chiba.

Mizuno, A., Mitsuiki, M. & Motoki, M. (1998). *Journal of Agricultural Food Chemistry*, *46*, 98-103.

Mohan, B. H., Gopal, A., Malleshi, N. G. & Tharanathan, R. N. (2005). Characteristics of native and enzymatically hydrolyzed ragi (*Eleusine coracana*) and rice (*Oryza sativa*) starches. *Carbohydrate polymers*, *59*, 43-50.

Moorthy, S. N. (1994). *Tuber crop starches*, Sreekariyam, Thiruvananthapuram, Kerala (pp.1-40). India: Center Tuber Crops Research Institute.

Morgan, K. R., Furneaux, R. H. & Larsen, N. G. (1995). Solid-state NMR studies on the structure of starch granules. *Carbohydrate Research*, *276*, 387-399.

Morrison, W. R., Tester, R. F. & Gidley, M. J. (1994). Properties of damaged starch granules. II. Crystallinity, molecular order and gelatinisation of ball-milled starches. *Journal of Cereal Science*, *19*, 209-217.

Morrison, W. R., Tester, R. F., Snape, C. E., Law, R. & Gidley, M. J. (1993). Swelling and gelatinization of cereal starches. 4. Some effects lipid-complexed amylose

and free amylose in waxy and normal barley starches. *Cereal Chemistry*, *70*, 385-391.

Murugesan, G., Shibanuma, K. & Hizukuri, S. (1993). Characterization of hot water-soluble-components of starches. *Carbohydrate Research*, *242*, 203-215.

Nakazawa, F., Noguchi, S., Takahashi, J. & Takada, M. (1985). Retrogradation of gelatinized potato starch studied by Differential Scanning Calorimetry. *Agriculture Biological Chemistry*, *49*, 953-957.

Nakazawa, F., Noguchi, S., Takahashi, J. & Takada, M. (1984). Thermal equalibrium state of starch-water mixture studied by differential scanning calorimetry. *Agriculture Biological Chemistry*, *48*, 2647-2653.

Nara, S. & Komiya, T. (1983). Studies on the relationships between water-saturated state and crystallinity by the diffraction method for moistened potato starch. *Starch/Stärke*, *35*, 407-410.

Nara, S. H., Mori, A. & Komiya, T. (1978). Study on relative crystallinity of moist potato starch. *Starch/Stärke*, *30*, 111-114.

Newport Scientific Pty, Ltd. (1998). Application Manual for the Rapid Visco Analyser (p. 123). Australia.

Newport Scientific Pty, Ltd. (1995). Operation Manual for the Series 4 Rapid Visco Analyzer (p. 93). Australia.

Novo enzyme information (1985). Novo Industri, Denmark.

Oates, C. G. & Powell, A. (1996). Bioavailability of carbohydrate material stored in tropical fruit seeds. *Food Chemistry*, *56*, 405-414.

Oostergetel, G. T. & van Bruggen E. F. G. (1993). The crystalline domains in potato starch granules are arranged in a helical fashion. *Carbohydrate polymers*, *21*, 7-12.

Oostergetel, G. T. & van Bruggen E. F. G. (1989). *Starch/Stärke*, *41*, 331-335.

Outtrup, H. & Norman, B. E. (1984). *Starch/Stärke*, *36*, 405-411.

Panozzo, J. F. & McCormick, K. M. (1993). The Rapid Viscoanalyzer as a method of testing for noodle quality in a wheat breeding programme. *Journal of Cereal Science*, *17*, 25-32.

Paredes-López, O., Schvenin, M. L., Hernández-López, D. & Carabez-trejo, A. (1989). *Starch/Stärke*, *41*, 205.

Peat, S., Pirt, S. J. & Whelan, W. J. (1952). Enzymatic synthesis and degradation of starch, part XV, beta-amylase and constitution of amylose. *Journal of Chemistry Society*, *3*, 705-713.

Puchongkavarin, H., Bergthaller, W., Shobsngob, S. & Varavinit, S. (2003). Characterization and utilization of acid-modified rice starches for use in pharmaceutical tablet compression. *Starch/Stärke*, *55*, 464-475.

Ramesh, M., Mitchell, J. R., Jumel, K. & Harding, S. E. (1999). Amylose content of rice starch. *Starch/Stärke*, *1*, 311-313.

Rasper, V., Perry, G. & Dutschaever, C. L. (1974). *Can. Inst. Food Science Technology*, *7*, 166.

Roberts, P. J. P. & Whelan, W. J. (1960). *Biochemical Journal*, *76*, 246.

Robin, J. P., Mercier, C., Charbonniere, R. & Guilbot, A. (1974). Lintnerized starches. Gel filtration and enzymatic studies of insoluble residues from prolonged acid treatment of potato starches. *Cereal Chemistry*, *51*, 389-406.

Robyt, J. F. & French, D. (1970). The action pattern of porcine pancreatic α-amylase in relationship to the substrate binding site of the enzyme. *Journal of Biological Chemistry*, *245*, 3917-3927.

Robyt, J. F. & French, D. (1967). Multiple attack hypothesis of α-amylase action: Action of porcine pancreatic, human salivary, and *Aspergillus oryzae* α-amylases. *Archives of Biochemistry and Biophysics*, *122*, 8-16.

Robyt, J. F. & French, D. (1963). Action pattern and specificity of an amylase from *Bacillus subtilis*. *Archives of Biochemistry and Biophysics*, *100*, 451-467.

Rubinstein, M. H. (1988). Tablets. In M. E. Aulton Ed., *Pharmaceutical: the science of dosage from design* (pp. 304-321). New York: Churchill Livingstone Inc.

Rutenberg, M. W. & Solarek, D. (1984). Starch derivatives: Production and uses. In R. L. Whistler Ed., *Starch chemistry and technology* (pp. 311-388). New York: Academic Press.

Salpeakar, A. M. & Augsbuger L. L. (1974). Magnesium Lauryl Sulfate in Tableting: effect on Ejection Force and Compressibility. *Journal of Pharmaceutical Science*, *63*, 289.

Sanders, J. P. M. (1996). Starch manufacturing in the world. In Advanced Post Academic Course on Tapioca Starch Technology. Jan. 22-26 & Feb. 19-23, 1996. AIT Center, Bangkok.

Sandstedt, R. M. (1955). Photomicrographic studies of wheat starch II. Enzymatic digestion and granule structure. *Cereal Chemistry*, *32*, 17-47.

Sarko, A. & Wu, H. C. H.(1978). *Starch/Stärke*, *30*, 73-78.

Schoch, T. J. & Maywald, E. C. (1967). Industrial Microscopy of Starches. In R. L. Whistler, E. G. Paschall, J. N. BeMiller, & H. J. Roberts (Eds.*), Starch Chemistry and Technology* (2nd ed., pp. 675-689). New York: Academic Press.

Seguchi, M., Hayashi, M., Suzuki, Y., Sano, Y. & Hirono, H. Y. (2003). Role of amylose in the maintenance of the configuration of rice starch granules. *Starch/Stärke*, *55*, 524-528.

Shangraw, R. F. (1989). Compressed tablets by direct compression. In H. A. Lieberman, L. Lachman & L. B. Schwartz (Eds.), *Pharmaceutical dasage forms* (pp. 195-245). New York: Marcel Dekker Inc.

Shangraw, R. F., Mitrevej, A & Shah, M. (1980). A new era of tablet disintegrants. *Pharmaceutical Technology*, *Oct*, 48-57.

Sheh, B. B., Bandelin, F. J. & Shangraw, R. F. (1980). In H. A. Lieberman & L. Lachman (Eds.), *Pharmaceutical dosage forms: Tablets* (Vol. 1, p.153). New York: Marcel Dekker Inc.

Sheth, B., Bandelin, F. J. & Shangraw, R. F. (1989). Compressed tablets. In H. A. Lieberman & L. Lachman (Eds.), *Pharmaceutical dosage forms: Tablet* (Vol. 1, pp. 109-246). New York: Marcel Dekker Inc.

Sheth, B., Bandelin, F. J. & Shangraw, R. F. (1987). Compressed tablets. In G. M. A. V. Beynum & J. A. Roels (Eds.), *Starch conversion technology* (pp. 15-47). New York: Marcel Dekker Inc.

Sinthupinyo, T. (1997). Properties of glibenclamide/beta-cyclodextrin inclusion complexes prepared by spray drying technique. [M.S. thesis in pharmacy]. Bangkok: Faculty of graduate studies, Mahidol university.

Sjokvist, E. & Nystrom, C. (1991). Physicochemical aspects of drug release. XI. Tabletting properties of solid dispersions using xylitol as carrier material. *International Journal Pharmaceutical*, *67*, 139-153.

Solarek, D. B. (1986). Phosphorylated starches and miscellaneous inorganic esters. In O. B. Wurzburg Ed., *Modified starch: Properties and Uses* (pp.97-112). Boca Raton, FL: CRC press, Inc.

Sreenath, H. K. (1992). Studies on starch granules digestion by α-amylase. *Starch/Stärke*, *44*, 61-63.

Stark, J. R. & Lynn, A. (1992). Biochemistry of plant polysaccharides: Starch granules large and small. *Biochemical Society Transactions.*, *20*, 7-12.

Stein, E. A. & Fisher, E. H. (1958). *Journal of Biological Chemistry*, *232*, 867.

Stein, E. A., Hsiu, J. & Fisher, E. H. (1964). *Biochemistry*, *3*, 56.

Stevens, D.J. & Elton, G. A. H. (1971). Thermal properties of the starch/water system. Part I. Measurement of heat of gelatinization by Differential Scanning Calorimetry. *Starch/Stärke*, *23*, 8-11.

Stoof, G. Anger, H., Schmeidl, D. & Bergthaller, W. (1998). Hydrothermische behandlung von stärke in gegenwart von αamylase. Teil 4. Änderungen der eigenschaften von kartoffelstärke durck hydrothermisch-enzymatische behandlung. *Starch/Stärke*, *50*, 108-114.

Stoof, G. Anger, H., Schmeidl, D. & Bergthaller, W. (1997). *Starch/Stärke*, *49*, 225-231.

Stute, R. (1992). Hydrothermal modification of starches: the difference between annealing and heat/ moist treatment. *Starch/Stärke*, *44*, 205-214.

Swinkels, J. (1985). Sources of starch, its chemistry and physics. In G. M. A. V. Beynum & J. A. Roels (Eds.), *Starch conversion technology* (pp. 15-47). New York: Marcel Dekker Inc.

Tamaki, S., Teranichi, K., Hisamatsu, M. & Yamada, T (1997). Inner structure of potato starch granules. *Starch/Stärke*, *49*, 387-390.

Tester, R. F., Debon, S. J. J. & Karkalas, J. (1998). Annealing of wheat starch. *Journal of Cereal Science*, *28*, 259-272.

Tester, R. F., Debon, S. J. J. & Sommerville, M. D. (2000). Annealing of maize starch. *Carbohydrate Polymers*, *42*, 287-299.

Tester, R. F. & Morrison, W. R. (1990). Swelling and gelatinization of cereal starches. 1. Effects and amylopectin, amylose and lipids. *Cereal Chemistry*, *67*, 551-557.

Thoma, J. A., Wakim, J. & Stewart, L.(1963). Comparison of the active sites of alpha and beta amylases. *Biochemical and Biophysical Research Communications*, *12*, 350-355.

Tipples, K. H. (1969). The relation of starch damage to the baking performance of fluor. *Baker's Digest*, *42*, 28.

Underwood, T. W. & Cadwallader, D. E. (1972). Influence of various starches on dissolution rate of salicylic acid from tablets. *Journal of Pharmaceutical Science*, *61*, 239-243.

United States Pharmacopoeia Convention (2000). *United States Pharmacopoeia 24-National Formulary 19*. Rockville, MD: US Pharmacopoeia Convention, Inc; 2524-2525.

Valentudie, J. C., Colonna, P., Bouchet, B. & Gallant., D. J. (1995). Gelatinization of sweet potato, tania and yam tuber staches. *Starch/Stärke*, *47*, 298-306.

Van Kamp, H. V., Bolhuis, G. K., De boer, A. H., Lerk, C. F. & Lie, A. L. (1986). Role of water uptake on tablet disintergration: Design and improved method for penetration measurement. *Pharmaceutica Acta Helvetiae*, *61(1)*, 22-29.

Visavarungroj, N. & Remon, J. B. (1992). Starches and modified starches in tablet formulations. *Pharmaceutical Technological Int*, *4(1)*, 26-33.

Visavarungroj, N. & Remon, J. B. (1990). Crosslinked starch as a disintegrating agent. *International Journal of Pharmaceutics*, *62*, 125-131.

Vodovotz, Y. & Chinachoti, P. (1998). Glassy-rubbery transition and recrystallization during aging of wheat starch gels. *Journal of Agricultural and Food Chemistry*, *46*, 446-453.

Waigh, T. A., Donald, A. M., Heidelbach, F., Riekel, C. & Gidley, M. J. (1999). Analysis of the native structure of starch granules with small angle X-ray microfocusing scattering. *Biopolymers*, *49*, 91-105.

Waigh, T. A., Gidley, M. J., Komanshek, B. U. & Donald, A. M. (2000). The phase transformations in starch during gelatinisation: a liquid crystalline approach. *Starch/Stärke*, *52*, 165-176.

Waigh, T. A., Hopkinson, I., Donald, A. M., Butler, M. F., Heidelbach, F., & Riekel, C. (1997). *Macromolecules*, *30*, 3813-3820.

Waigh, T. A., Kato, K. L., Donald, A. M., Gidley, M. J., Clarke, C. J. & Riekel, C. (2000). Side-chain liquid crystalline model for starch. *Starch/Stärke*, *52*, 450-460.

Walker, G. J. (1965). *Biochemistry Journal*, *94*, 289.

Walker, C. E., Ross, A. S., Wrigley, C. W. & McMaster, G. J. (1988). Accelerated starch-paste characterization with the Rapid Visco-Analyzer. *Cereal Foods World*, *33*, 491-494.

Walker, G. J. & Whelan, W. J. (1960). The mechanism of carbohydrase action. 8. Structures of the muscle-phosphorylase limit dextrins of glycogen and amylopectin. *Biochemical Journal*, *76*, 264-268.

Wang, W. J., Powell, A. D. & Oates, C. G. (1997). Effect of annealing on the hydrolysis of sago starch granules. *Carbohydrate polymers*, *33*, 195-202.

Whelan, W. J. (1960). *Starch/Stärke*, *12*, 358.

Whistler, R. L., BeMiller, J. N. & Paschall, E. F. (1984). *Starch, Chemistry and Technology* (2nd ed., pp.469-476, 688). New York: Academic Press.

Whistler, R. L. & Doane, W. M. (1961). Characterization of intermediary fraction of high amylose corn starches. *Cereal Chemistry*, *38*, 251-257.

Whistler, R. L., Goatley, J. L. & Spencer, W. W. (1959). Effect of drying on the physical properties and chemical reactivity of corn starch granules. *Cereal Chemistry*, *36*, 84-90.

Whistler, R. L. & Spencer, W. W. (1960). Distribution of substituents in corn starch granules with low degrees of substitution. *Archives of Biochemistry and Biophysics*, *87*, 137-139.

Whistler, R. L. & Thornburg, W. L. (1957). Development of starch granules in corn endosperm. *Journal of Agricultural Food Chemistry*, *5*, 203-207.

Whistler, R. L. & Turner, E. S. (1955). Fine structure of starch granule sections. *Journal of Polymer Science*, *18*, 153-156.

Williamson, G., Belshaw, N. J., Seif, D. J., Noel, T. R., Ring, S. G., Cairns, P., Morris, V. J., Clark, S. A. & Parker, M. L. (1992). Hydrolysis of A and B type crystalline polymorphs of starch by α-amylase, β-amylase and glucoamylase I. *Carbohydrate polymers*, *18*, 179-187.

Wivinis, G. P. & Maywald E. C. (1967). In R. L. Whistler & E. F. Paschall (Eds.), *Starch: Chemistry and Technology* (Vol. II, p. 650). New York: Academic Press.

Wolff, I. A., Hofreiter, B. T., Watson, P. R., Deatherage, W. L. & MacMasters, M. M. (1955). The structure of a new starch of high amylose content. *Journal of America Chemistry Society*, *77*, 1654-1659.

Wolters, M. G. E., Cone, Z. W. & Cone, J. W. (1992). Prediction of degradability of starch by gelatinization enthalpy as measured by differential scanning calorimetry. *Starch/Stärke*, *44*, 14-18.

Wray, P. W., Vincent, J. G., Moller, F. W. & Jackson, G. J. (1976). Paper presented at The Industrial Pharmaceutical Section, (Aph A) Academy of Pharmaceutical Science, Dallas, meeting Apr., 25-29.

Wu, H. C. H. & Sarko, A. (1978). The double-helical molecular structure of crystalline B-amylose. *Carbohydrate Research*, *61*, 7-25; 27-40.

Yamada, T., Hisamatsu, M., Teranishi, K., Katsuro, K., Hasegawa, N. Hayashi, M. (1995). Components of the porous maize starch granule prepared by amylase treatment. *Starch/Stärke*, *46*, 358-361.

Yamaguchi, M., Kainuma, K. & French, D. (1979). *Journal of Ultrastructural Research*, *69*, 249-261.

Yook, C. & Robyt, J. F. (2002). Reaction of alpha amylases with starch granules in aqueous suspension giving products in solution and in minimum amount of water giving products inside the granule. *Carbohydrate Research*, *337*, 1113-1117.

Zeleznak, K. J. & Hoseney, R. C. (1987). *Cereal Chemistry*, *64*, 121-124.

Zhou, Y., Hoover, R. & Liu, Q. (2004). Relationship between α-amylase degradation and the structure and physicochemical properties of legume starches. *Carbohydrate Polymers*, *57*, 299-317.

Zobel, H. F. (1992). Starch granule structure. In R. J. Alexander & H. F. Zobel (Eds.), *Developments in Carbohydrate Chemistry* (pp. 1-36). St. Paul, Minnesota, USA: The American Association of Cereal Chemists.

Zobel, H. F. (1988). Starch crystal transformations and their industrial importance. *Starch/Stärke*, *40*, 1-7.

Zobel, H. F. (1984). Gelatinization of starch and mechanical properties of starch pastes. In R. L. Whistler, E. G. Paschall, & J. N. BeMiller (Eds.), *Starch Chemistry and Technology* (chap. IX, p. 285). New York: Academic Press, Inc.

APPENDIX

APPENDIX A

Spray Dry

1. Spray drying technology

(Sinthupinyo, 1997; http://www.niroinc.com/html/drying/fdspraychem.html)

1.1. Process

Spray drying is the most widely used industrial process involving particle formation and drying. It is highly suited for the continuous production of dry solid in either powder, granulate or agglomerate form from liquid feedstocks as solutions, emulsions and pumpable suspensions. Therefore, spray drying is an ideal process where the end-product must comply to precise quality standards regarding particle size distribution, residual moisture content, bulk density, and particle shape.

Spray drying offers significant versatility over other means of drying. This technique combined the synthesis, the drying and the agglomeration process into one step process with the advantage of reduction the preparation steps and saving times.

Spray drying combines multiple unit operations into one process consisting of

1. Evaporation of solvent (or water)
2. Creation of particles/granules
3. Separation of solid product

Spray dryer can handle only fluid materials such as fluid solution, slurries, and thin pastes. The fluid is dispersed as fine droplets into a moving stream of hot gas, where they evaporate rapidly before reaching the wall of the drying chamber. The product dries into a fine powder which is carried by the gas current and gravity flow in to a collection system.

The feed is delivered to the atomizer by gravity flow or by the use of a suitable pump. The rate of feed is adjust so that each droplet of sprayed liquid is completely dried before it comes in contact with the walls of the drying chamber and yet the resultant dried powder is not overheated in the drying process.

When the liquid droplets come into contact with the hot gas, they quickly reach a temperature slightly above the wet-bulb temperature of the gas. Evaporation of moisture from the droplets and formation of dry particles proceed under controlled temperature and airflow conditions. The surface liquid is quickly evaporated, and tough proceeds, the liquid in the interior of the droplet must diffuse through this shell. The diffusion of the liquid occurs at a much slower rate than those that transfer of heat through the shell to the interior of the droplet. The resultant buildup to heat causes the liquid below the shell to evaporate at a far greater rate than it can diffuse to the surface. The internal pressure causes the droplet to swell, and the shell becomes thinner, allowing faster diffusion. If the shell is nonelastic or impermeable, it ruptures, producing either fragment of budlike forms on the original sphere. Thus, spray-dried material consists of intact spheres, spheres with buds, ruptured hollow spheres or sphere fragments.

Separation of the solid product from the effluent gas is usually accomplished by means of a cyclone separator. It is referred to as the primary collector. The dried product collected at this point referred to as cyclone product. Product that reaches the walls of the drying chamber, referred as chamber product, is removed at the bottom of the chamber. This chamber product is usually coarser in size and subjected to heat longer the cyclone product. Powder is discharged continuously from the drying chamber. Operating conditions and dryer design are selected according to the drying characteristics of the product and powder specification.

1.2. Principles

Spray dryers can be considering to be made up of the following components: feed delivery system, atomizer, heated air supply, air disperser, drying chamber, solid-gas separator, system for exhaust air cleaning and product collection systems as shown in Figure 58. Widely varying drying characteristics and quality requirements of the thousands of products spray dried determine the selection of the atomizer, the most suitable airflow pattern, and the drying chamber design.

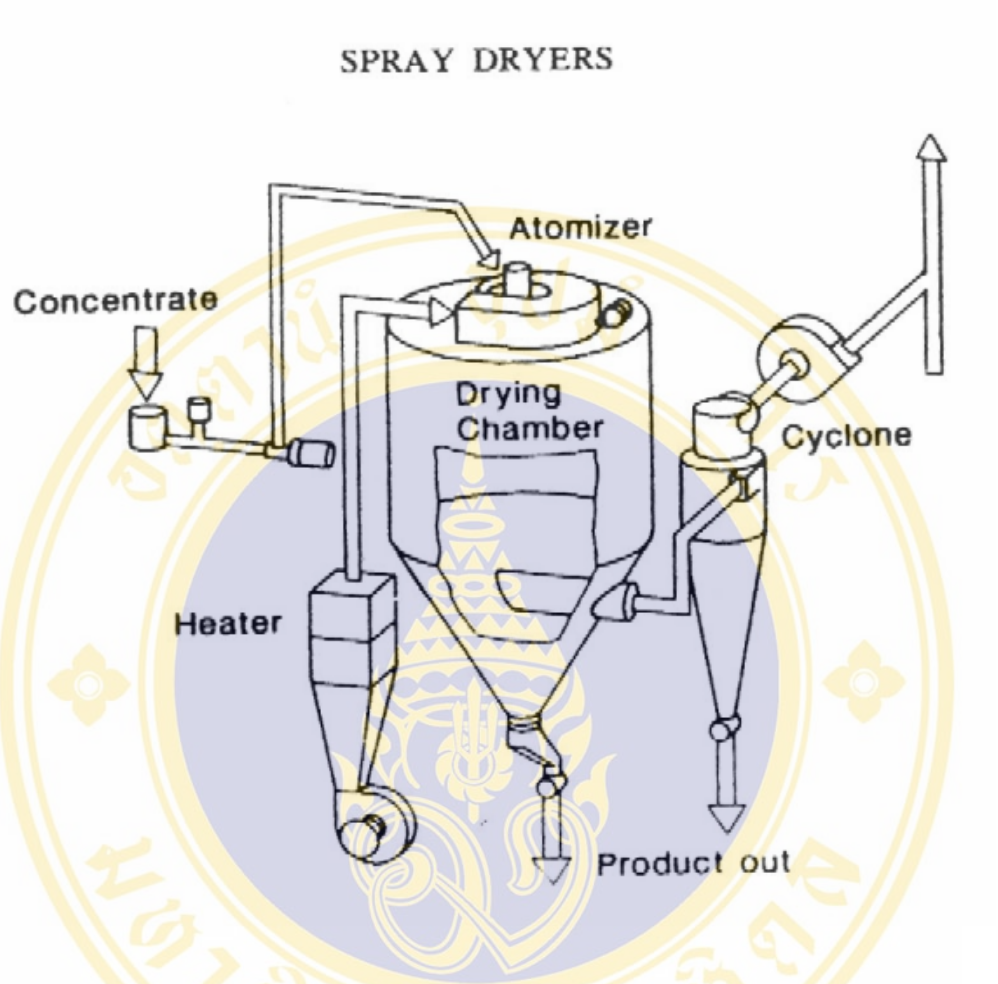

Figure 54. General picture of spray dryer and their components. (http://www.niroinc.com/html/drying/fdspraychem.html)

1.3. Atomization

The formation of sprays having the required droplet size distribution is vital to any successful spray dryer operation so that powder specifications can be met. Spray dryer atomizers is a high technology area and are consisted of three basic types: pneumatic (two-fluid) atomizers, pressure nozzles, and spinning disc atomizers.

1.4. Air flow

The initial contact between spray droplets and drying air controls evaporation rates and product temperatures in the dryer. There are three distinct modes of contact:

1.4.1. Co-current

Drying air and particles move through the drying chamber in the same direction. Product temperatures on discharge from the dryer are lower than the exhaust air temperature, and hence this is an ideal mode for drying heat sensitive products. When operating with rotary atomizer, the air disperser creates a high degree of air rotation, giving uniform temperatures throughout the drying chamber. However, an alternative non-rotating airflow is often used in tower or Filtermat-type spray dryers using nozzle atomizers with equal success.

1.4.2. Counter-current

Drying air and particles move through the drying chamber in opposite direction. This mode is suitable for products which require a degree of heat treatment during drying. The temperature of the powder leaving the dryer is usually higher than the exhaust air temperature. Countercurrent follow with these reason is not considering for application in food drying, as the driest particles will contact the hottest air, causing unacceptable heat damage in the product.

1.4.3. Mixed flow

Particle movement through the drying chamber experiences both co-current and counter-current phases. This mode is suitable for heat stable products where coarse powder requirements necessitate the use of nozzle atomizers, spraying upwards into an incoming airflow, of for heat sensitive products where the atomizer sprays droplets downwards towards an integrated fluid bed and the air inlet and outlet are located at the top of the drying chamber.

APPENDIX B

Particle size distribution

Table 10. Particle size distributions and volume weighted mean d (4,3) of particle size of SNT, SNR, SANT-H, SANR-H, SANET and SANER at various hydrolysis times.

Starch type	Reaction time (min)	d (v 0.1) [μm]	d (v 0.5) [μm]	d (v 0.9) [μm]	d (4,3) [μm]
SNT		18.40 ± 0.04	77.35 ± 0.60	242.68 ± 0.76	108.59 ± 0.84
SANT-H		70.31 ± 0.13	149.54 ± 0.10	322.14 ± 0.63	176.59 ± 0.26
SANET	15	68.61 ± 0.30	143.18 ± 0.32	289.52 ± 1.04	163.98 ± 0.31
	30	77.78 ± 0.18	154.66 ± 0.55	298.51 ± 0.52	173.70 ± 0.41
	60	96.50 ± 0.13	181.14 ± 0.68	339.12 ± 1.17	202.14 ± 0.57
SNR		20.78 ± 0.00	40.57 ± 0.00	74.34 ± 0.05	44.58 ± 0.02
SANR-H		20.74 ± 0.02	39.65 ± 0.08	90.02 ± 1.69	59.05 ± 1.83
SANER	15	30.75 ± 0.12	58.76 ± 0.05	116.09 ± 0.30	67.50 ± 0.03
	30	35.45 ± 0.90	68.84 ± 0.39	136.23 ± 1.86	78.85 ± 0.05
	60	34.91 ± 0.22	64.51 ± 0.27	121.22 ± 0.05	72.54 ± 0.18

Table 11. Particle size distributions and volume weighted mean d (4,3) of particle size of NT, NR, ANT-H, ANR-H, ANET and ANER at various hydrolysis times.

Starch type	Reaction time (min)	d (v 0.1) [µm]	d (v 0.5) [µm]	d (v 0.9) [µm]	d (4,3) [µm]
NT		8.49 ± 0.19	13.63 ± 0.05	21.45 ± 0.30	14.43 ± 0.02
ANT-H		8.25 ± 0.03	15.34 ± 0.05	27.77 ± 0.13	16.81 ± 0.17
ANET	15	7.92 ± 0.01	13.16 ± 0.00	21.32 ± 0.01	14.01 ± 0.03
	30	8.04 ± 0.18	13.12 ± 0.05	20.90 ± 0.29	13.92 ± 0.01
	60	8.00 ± 0.17	13.09 ± 0.03	20.90 ± 0.32	13.90 ± 0.03
NR		3.68 ± 0.00	5.65 ± 0.00	8.55 ± 0.00	5.93 ± 0.00
ANR-H		4.63 ± 0.03	7.78 ± 0.04	12.68 ± 0.05	8.30 ± 0.04
ANER	15	3.54 ± 0.04	5.48 ± 0.07	8.34 ± 0.10	5.76 ± 0.07
	30	3.52 ± 0.00	5.43 ± 0.01	8.27 ± 0.01	5.71 ± 0.01
	60	3.60 ± 0.00	5.55 ± 0.00	8.42 ± 0.00	5.82 ± 0.00

APPENDIX C

Pasting properties

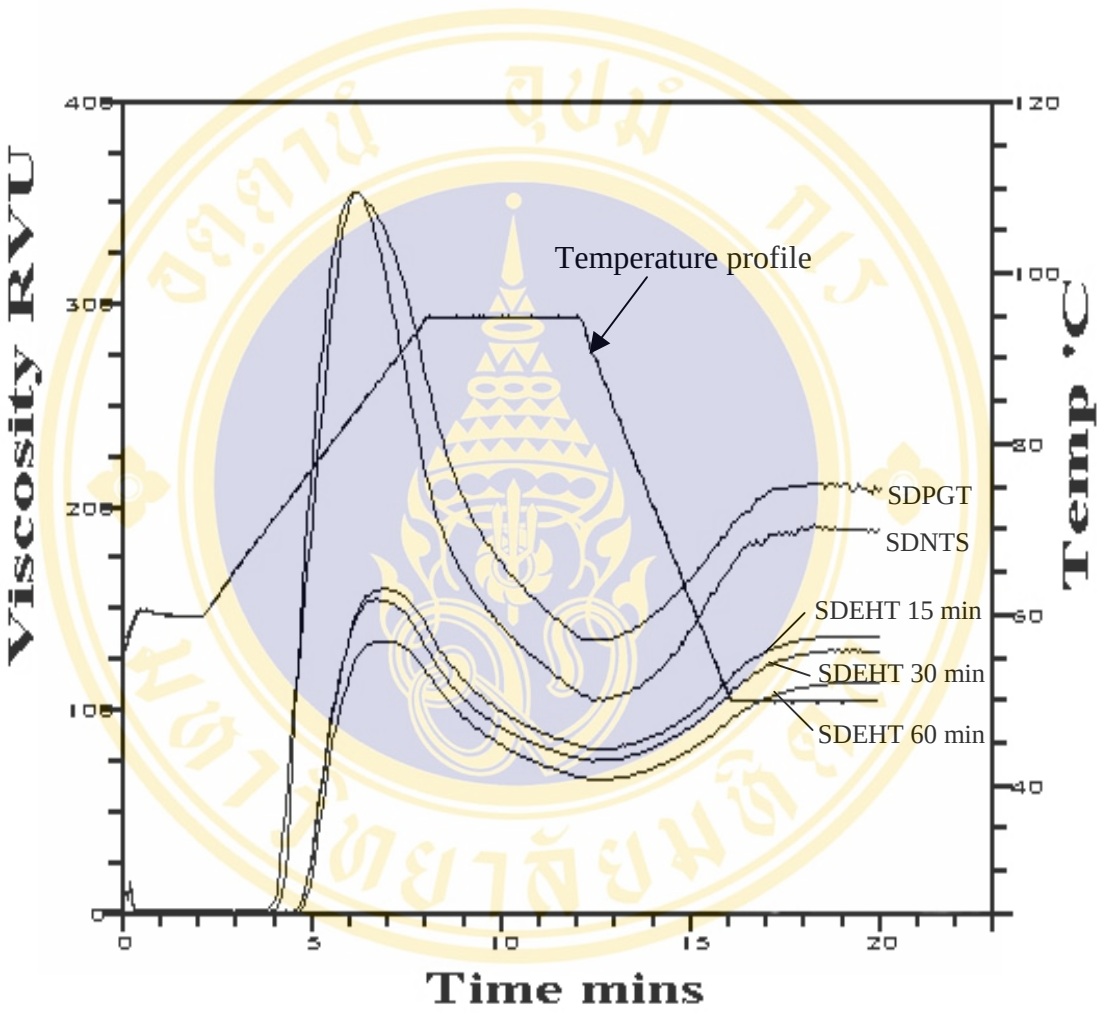

Figure 55. RVA pasting profile of SNT, SANT-H and SANET with varying hydrolysis times.

Table 12. Pasting properties[1] of SNT, SANT-H and SANET with various hydrolysis times: 15 min, 30 min and 60 min.

Starch type	Reaction time (min)	Pasting temp (^{0}C)	Pasting properties (RVU)				
			Peak	Trough	Breakdown	Final	Setback
SNT		69.63d (0.02)	356.21a (0.88)	109.79b (0.21)	246.42a (0.66)	188.13b (1.79)	78.33a (2.00)
SANT-H		70.33c (0.03)	354.64a (3.02)	137.53a (2.35)	217.11b (1.99)	210.31a (2.17)	72.78b (1.14)
SANET	15	74.05b (0.20)	159.13b (1.38)	81.84c (1.42)	77.29c (0.04)	134.50c (1.75)	52.67c (0.03)
	30	74.30a, b (0.40)	156.34b (1.42)	77.04d (0.04)	79.30c (1.38)	128.46c (0.13)	51.42c (0.08)
	60	74.63a (0.03)	136.14c (2.29)	67.22e (2.05)	68.91d (1.61)	111.86d (4.11)	44.64d (2.23)

[1] The experiments were done in triplicate. Numbers within parenthesis is standard deviation for three determinations. Mean with the same letter in each column are not significantly different ($P > 0.05$) by Tukey's HSD[a] test.

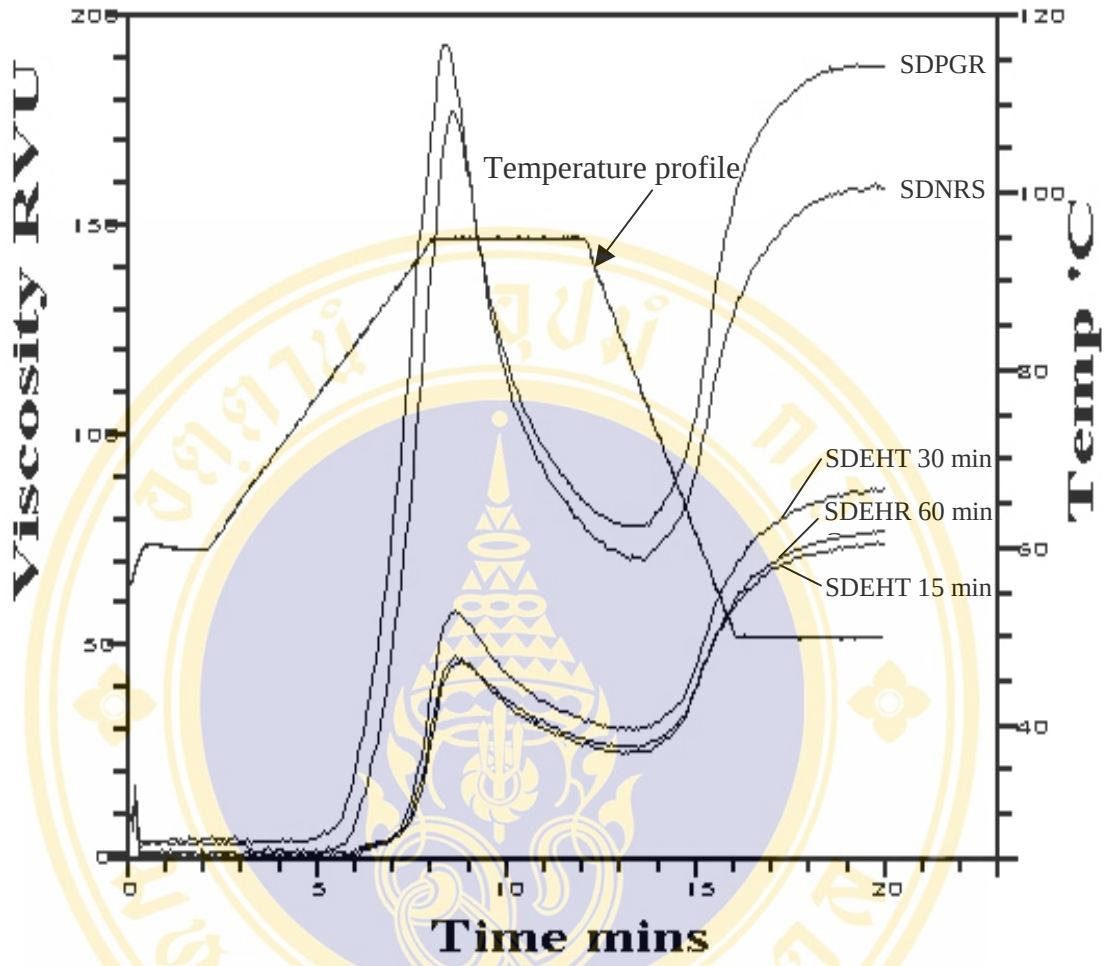

Figure 56. RVA pasting profile of SNR, SANR-H and SANER at various hydrolysis times.

Table 13. Pasting properties[1] of SNR, SANR-H and SANER at various hydrolysis times:15 min, 30 min and 60 min.

Starch type	Reaction time (min)	Pasting temp (^{0}C)	Pasting properties (RVU)				
			Peak	Trough	Breakdown	Final	Setback
SNR		81.23b (0.38)	196.03a (5.62)	71.89b (1.91)	124.14a (3.75)	162.06b (3.72)	90.17b (1.83)
SANR-H		83.42a (0.23)	176.92b (1.30)	76.81a (1.58)	100.11b (1.32)	186.92a (1.52)	110.11a (0.59)
SANER	15	83.75a (0.05)	47.56d (0.56)	24.78d (0.49)	22.78d (0.25)	74.08d (1.00)	49.30d (0.70)
	30	83.20a (0.25)	58.36c (0.77)	30.09c (0.52)	28.28c (0.42)	88.45c (1.29)	58.36c (0.98)
	60	83.83a (0.24)	46.33d (0.80)	25.94d (1.22)	20.39d (0.43)	74.06d (2.55)	48.11d (2.94)

[1] The experiments were done in triplicate. Numbers within parenthesis is standard deviation for three determinations. Mean with the same letter in each column are not significantly different ($P > 0.05$) by Tukey's HSD[a] test.

APPENDIX D

Differential Scanning Calorimetry

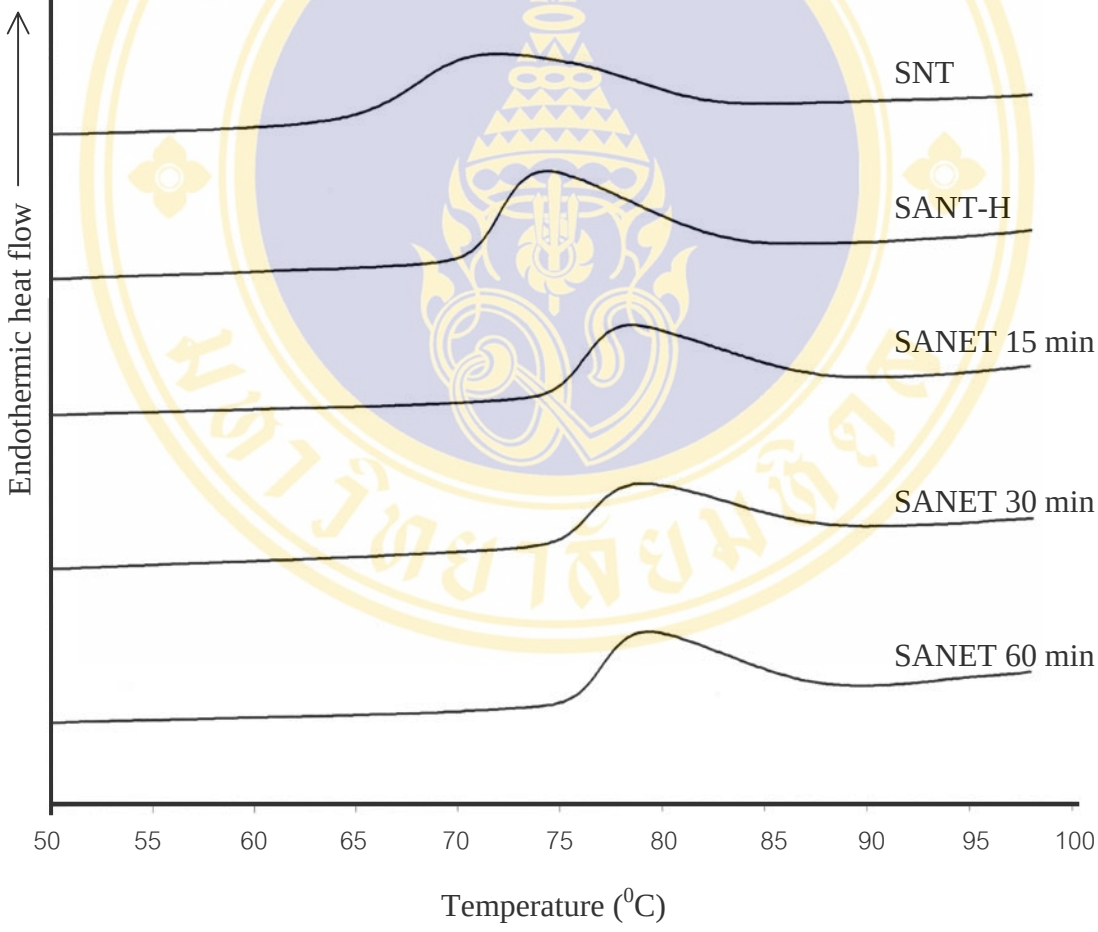

Figure 57. DSC thermogram of SNT, SANT-H and SANET at various hydrolysis times.

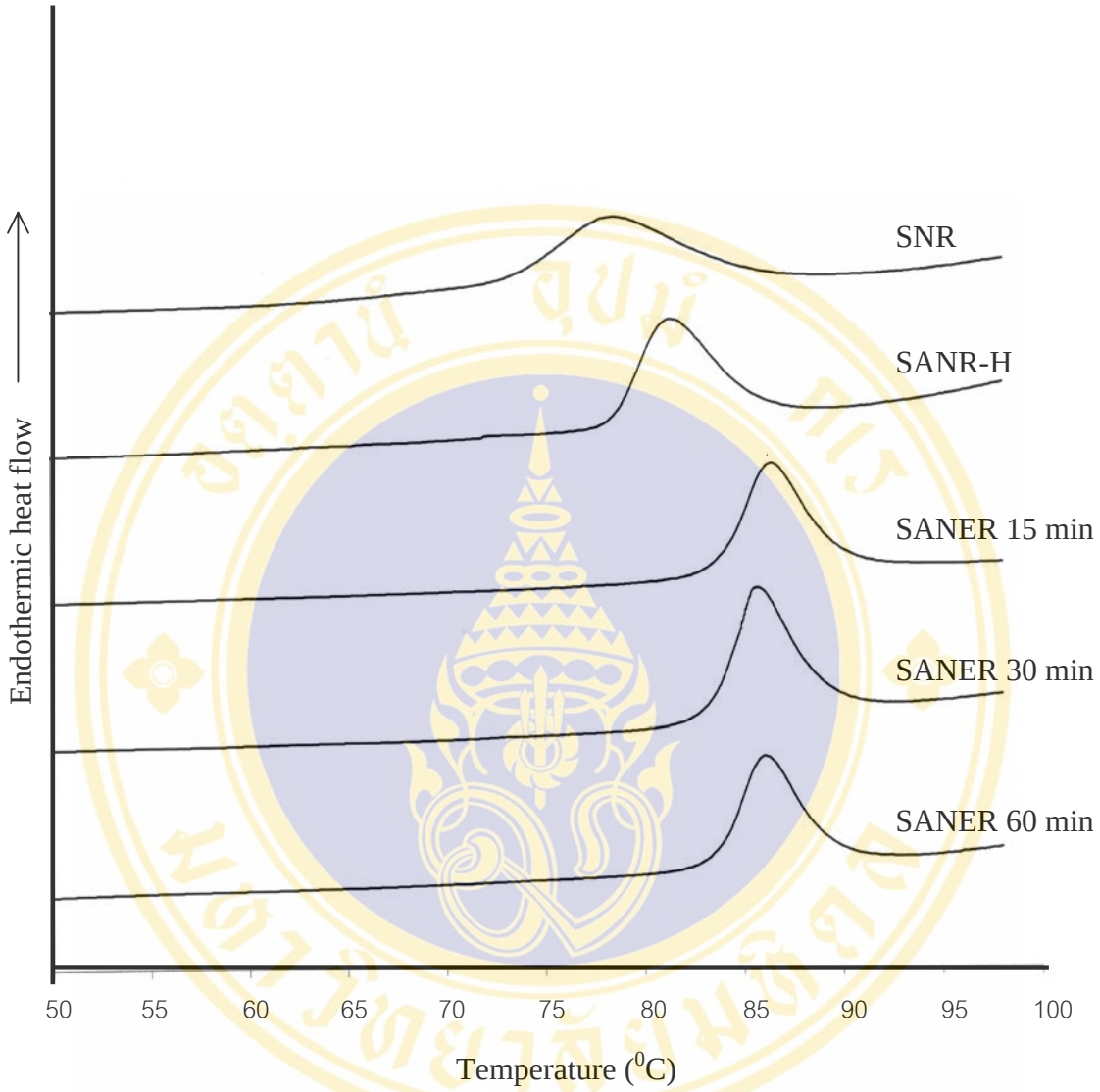

Figure 58. DSC thermogram of SNR, SANR-H and SANER at various hydrolysis times.

APPENDIX E

Relative crystallinity

Table 14. Relative crystallinity of SNT, SNR, SANT-H, SANR-H, SANET and SANER at various hydrolysis times[1].

Starch type	Reaction time (min)	Crystalline pattern	Relative crystallinity (%)[2]
SNT		A	38.81±0.22[a]
SANT-H		A	35.70±1.79[b]
SANET	15	A	31.54±0.64[c]
	30	A	27.52±0.83[d]
	60	A	26.15±1.05[d]
SNR		A	45.39±0.68[a]
SANR-H		A	37.08±0.84[b]
SANER	15	A	32.64±0.57[c]
	30	A	32.14±0.64[c, d]
	60	A	30.47±0.32[d]

[1] Moisture content of all starches approximately 11.0%

[2] Mean ± SD of three determinations. Data with the same superscript within the same column are not significantly different ($P > 0.05$).

APPENDIX F

Starch Damage

Table 15. Damaged starch (%) [1] of SNT, SNR, SANT-L, SANR-L, SANT-H, SANR-H and SANET and SANER as a function of time: 15 min, 30 min and 60 min.

Starch type	Reaction time(min)	Starch damage
SNT		0.31 ± 0.00 [f]
SANT-L		1.99 ± 0.06 [e]
SANT-H		11.18 ± 0.11 [d]
SANET	15	18.96 ± 0.08 [c]
	30	20.36 ± 0.29 [b]
	60	21.31 ± 0.04 [a]
SNR		1.04 ± 0.02 [f]
SANR-L		4.53 ± 0.20 [e]
SANR-H		13.06 ± 0.16 [d]
SANER	15	20.25 ± 0.10 [c]
	30	21.26 ± 0.09 [b]
	60	24.43 ± 0.33 [a]

[1] Data with the same superscript in the same column are not significantly different ($P > 0.05$) by Tukey's HSD[a] test. All data represent mean ± SD of three determinations.

APPENDIX G

Tablet Properties

Table 16. Crushing strength (N) as a function of compression forces (kN) of plain filler tablets lubricated with 0.5% magnesium stearate preparing from SNT, SANT-L, SANT-H and SANET at various hydrolysis times.

Compression force (kN)	Crushing strength (N)					
	SNT	SANT-L	SANT-H	Hydrolysis time (min) SANET		
				15	30	60
2.0	9.81±0.22	9.81±0.20	16.67±0.15	61.78±0.18	78.46±0.40	86.30±0.61
4.0	32.36±0.50	24.52±0.22	42.17±0.15	112.78±0.55	144.16±0.79	143.18±0.61
6.0	capping	capping	51.98±0.15	131.41±0.25	160.83±0.71	145.14±0.51
8.0	capping	capping	51.00±0.12	129.45±0.21	157.89±0.97	138.28±0.80
10.0	capping	capping	50.02±0.19	129.45±0.36	162.80±0.78	139.26±0.11

Note: Capping is the separation (or tendency toward separation) of a cavitation portion of the upper or lower surface of the tablet.

Table 17. Disintegration time (min) as a function of compression forces (kN) of plain filler tablets lubricated with 0.5% magnesium stearate preparing from SNT, SANT-L, SANT-H and SANET at various hydrolysis times.

Compression force (kN)	Disintegration time (min)					
	SNT	SANT-L	SANT-H	Hydrolysis time (min)		
				SANET		
				15	30	60
2.0	0.55±0.21	0.65±0.08	7.02±1.63	2.80±0.45	2.90±0.68	2.15±0.21
4.0	0.76±0.11	0.76±0.10	6.64±0.39	2.96±0.62	2.87±0.10	2.96±0.20
6.0	capping	capping	7.83±0.46	3.62±0.59	3.23±0.40	3.33±0.20
8.0	capping	capping	7.23±0.34	3.41±0.31	4.27±0.61	3.97±0.44
10.0	capping	capping	6.90±0.33	3.690±.65	4.19±0.62	4.55±0.63

Note: Capping is the separation (or tendency toward separation) of a cavitation portion of the upper or lower surface of the tablet.

Table 18. Friability (%) as a function of compression forces (kN) of plain filler tablets lubricated with 0.5% magnesium stearate preparing from SNT, SANT-L, SANT-H and SANET at various hydrolysis times.

Compression force (kN)	Friability (%)					
	SNT	SANT-L	SANT-H	Hydrolysis time (min)		
				SANET		
				15	30	60
2.0	36.63	3.93	3.93	0	0.23	0
4.0	5.1	1.09	1.09	0	0.27	0
6.0	capping	0.82	0.82	0	0.36	0
8.0	capping	0.69	0.69	0	0.33	0
10.0	capping	0.75	0.75	0	0.26	0

Note: Capping is the separation (or tendency toward separation) of a cavitation portion of the upper or lower surface of the tablet.

Table 19. Crushing strength (N) as a function of compression forces (kN) of plain filler tablets lubricated with 0.5% magnesium stearate preparing from SNR, SANR-L, SANR-H and SANER at various hydrolysis times.

Compression force (kN)	Crushing strength (N)					
	SNR	SANR-L	SANR-H	Hydrolysis time (min) SANER		
				15	30	60
2.0	33.34±0.20	28.44±0.23	16.67±0.21	82.38±0.45	75.51±0.31	27.46±0.20
4.0	71.59±0.31	58.84±0.44	87.28±0.53	126.51±0.74	131.41±0.58	25.50±0.10
6.0	capping	capping	capping	142.20±0.90	142.20±0.74	26.48±0.21
8.0	capping	capping	capping	140.24±0.82	143.18±0.50	27.46±0.17
10.0	capping	capping	capping	136.32±0.38	145.14±0.45	24.52±0.13

Note: Capping is the separation (or tendency toward separation) of a cavitation portion of the upper or lower surface of the tablet.

Table 20. Disintegration time (min) as a function of compression forces (kN) of plain filler tablets lubricated with 0.5% magnesium stearate preparing from SNR, SANR-L, SANR-H and SANER at various hydrolysis times.

Compression force (kN)	Disintegration time (min)					
	SNR	SANR-L	SANR-H	Hydrolysis time (min)		
				SANER		
				15	30	60
2.0	1.80±0.16	3.28±1.04	4.47±0.36	6.79±1.03	4.85±0.30	5.51±0.92
4.0	2.23±0.17	4.60±0.18	5.71±0.28	11.94±1.45	6.48±1.02	7.51±1.85
6.0	Capping	Capping	Capping	10.67±1.98	5.07±0.50	6.36±1.54
8.0	Capping	Capping	Capping	10.29±2.08	6.42±0.84	7.090±.76
10.0	Capping	Capping	Capping	14.23±1.87	5.76±1.04	7.95±1.76

Note: Capping is the separation (or tendency toward separation) of a cavitation portion of the upper or lower surface of the tablet.

Table 21. Friability (%) as a function of compression forces (kN) of plain filler tablets lubricated with 0.5% magnesium stearate preparing from SNR, SANR-L, SANR-H and SANER at various hydrolysis times.

Compression force (kN)	Friability (%)					
	SNR	SANR-L	SANR-H	Hydrolysis time (min) SANER		
				15	30	60
2	2.86	4.36	4.36	0.03	0.13	0.03
4	0.64	0.65	0.65	0.03	0.10	0.07
6	Capping	Capping	Capping	0.07	0.03	0.03
8	Capping	Capping	Capping	0.07	0.07	0.03
10	Capping	Capping	Capping	0.10	0.07	0.03

Note: Capping is the separation (or tendency toward separation) of a cavitation portion of the upper or lower surface of the tablet.

Table 22. Hardness (N) and friability (%) as a function of compression forces (kN) of plain filler tablets lubricated with 0.5% magnesium stearate preparing from SANET-30 and SANER-30 comparing with those from some commercial fillers, i. e., microcrystalline cellulose (MCC), pregelatinised starch (PS), lactose (L), Era-Tab and Era-Tab SP.

Compression force (kN)	Crushing strength (N)/ Friability (%)						
	SANET 30	SANER 30	MCC	PS	L	Era-Tab	Era-Tab SP
2.0	78.46 /0.23	75.51 /0.13	114.74 /0.18	7.85 /19.42	5.88 /eb	5.88 /eb	24.52 /3.22
4.0	144.16 /0.27	131.41 /0.10	199.08 /0.12	20.59 /5.90	12.75 /5.96	20.59 /3.14	70.61 /0.45
6.0	160.83 /0.36	142.20 /0.03	nd	28.44 /3.46	21.58 /3.46	45.11 /0.79	114.74 /0.26
8.0	157.89 /0.33	143.18 /0.07	nd	35.31 /2.56	31.38 /2.33	68.65 /0.25	137.30 /0.26
10.0	162.80 /0.26	145.14 /0.07	nd	38.25 /1.54	44.13 /1.73	89.24 /0.23	141.22 /0.25

eb is excessive breakage.

nd is not detectable.

Table 23. Disintegration time (min) as a function of compression forces (kN) of plain filler tablets lubricated with 0.5% magnesium stearate preparing from SANET-30 and SANER-30 comparing with those from some commercial fillers, i. e., microcrystalline cellulose (MCC), pregelatinised starch (PS), lactose (L), Era-Tab and Era-Tab SP

Compression force (kN)	Disintegration time (min)						
	SANET 30	SANER 30	MCC	PS	L	Era-Tab	Era-Tab SP
2.0	2.90	4.85	0.44	17.51	eb	eb	0.45
4.0	2.87	6.48	1.15	25.42	1.97	2.29	0.41
6.0	3.23	5.07	nd	30.40	2.21	2.54	0.48
8.0	4.27	6.42	nd	32.54	2.65	2.49	0.43
10.0	4.19	5.76	nd	34.80	3.00	2.72	0.53

eb is excessive breakage.

nd is not detectable.

BIOGRAPHY

NAME Mr. Prakan Leerapongnun

DATE OF BIRTH Aprial 17, 1980

PLACE OF BIRTH Lumpang, Thailand

INSTITUTIONS ATTENDED Mahidol University, Bangkok, 1998-2001:
Bachelor of Science (Biotechnology)
Mahidol University, Bangkok, 2002-2005:
Master of Science (Biotechnology)

STUDY & RESEARCH GRANT The Asian Development Bank (ADB)

HOME ADDRESS 184 Radburana Rd., Tumbon Phichai, Muang, Lumpang, 52000
Tel. 054-226-198, 02-526-5373 and 09-370-6078
Email: leeprakan@hotmail.com
leeprakan@yahoo.com